RHEOLOGICAL CHARACTERIZATION, AND THE DEVELOPMENT OF MOLECULAR ORIENTATION AND TEXTURE/DURING FLOW FOR A LIQUID CRYSTALLINE COPOLYMER OF PARA-HYDROXYBENZOIC ACID AND POLYETHYLENE TEREPHTHALATE

by

Georg Giuseppe Viola

dissertation submitted to the Faculty of the
Virginia Polytechnic Institute and State University
in partial fulfillment of the requirements for the degree of

DOCTOR OF PHILOSOPHY

in

Chemical Engineering

APPROVED:

D. G. Baird, Chairman

G. L. Wilkes

J. E. McGrath

G. B. Wills

J. N. Reddy

March, 1985
Blacksburg, Virginia

RHEOLOGICAL CHARACTERIZATION, AND THE DEVELOPMENT OF MOLECULAR ORIENTATION AND TEXTURE DURING FLOW FOR A LIQUID CRYSTALLINE COPOLYMER OF PARA-HYDROXYBENZOIC ACID AND POLYETHYLENE TEREPHTHALATE

by

Georg Giuseppe Viola

Abstract

It is generally agreed that the high physical properties arising in as-processed liquid crystalline materials are due to the high degree of molecular orientation which develops during the processing step. In order to more fully understand and predict such behavior, a constitutive equation describing the flow behavior of these materials would be useful. It has been suggested that in order to describe the rheology of liquid crystalline fluids such a constitutive equation would need to include molecular orientation effects. The purpose of part of this study has been to examine to usefulness of several constitutive equations for describing the steady and transient behavior of several liquid crystalline polymers. These include a copolyester of para-hydroxybenzoic acid and polyethylene terephthalate, and an anisotropic solution of 12 weight% Kevlar in 100% sulfuric acid. It was found that in the case of the copolyester system, the steady shear and dynamic viscosities were equal over certain temperature ranges. For this reason, the constitutive equation of Zaremba, Fromm, and DeWhitt (ZFD model) was used to predict the steady state behavior of the system studied. From knowledge of

either the steady shear or dynamic viscosity it was possible to predict both the steady state normal stresses (N1) and the storage modulus (G'). The model could not, however, predict the transient behavior of the systems studied. Ericksen's anisotropic fluid theory has been investigated in detail as it takes molecular orientation effects into account. Ericksen's theory can partially explain the transient behavior of the systems studied in terms of molecular orientation which develops during shear flow. However, wide angle x-ray scattering (WAXS) and scanning electron microscope (SEM) studies reveal that shear flow has little effect on the development of molecular orientation during flow. In addition, any orientation produced during flow may be lost within thirty seconds at the melt temperature. It appears that a disruption of texture is occuring during flow which may need to be incorporated into the theory of Ericksen.

Original Contributions

The author regards the following as his own original contributions in the present work:

1. Ericksen's theory is shown to predict stress overshoot behavior soley in terms of reorientation of the director. Wide angle x-ray scattering studies performed on specially prepared samples reveal, however, that the predictions of the theory are not entirely valid.

2. A method of qualitatively evaluating the material parameters in Ericksen's theory is presented. This method requires measurement of the value of N2, the secondary normal stress difference.

3. The constitutive theory of Zaremba, Fromm, and DeWhitt is shown to accurately correlate the steady shear behavior of the copolyester system studied. The theory cannot, however, predict the transient stress growth behavior.

ACKNOWLEDGEMENTS

It is a pleasure for the author to acknowledge the advice, help, and support of his major advisor, Dr. Donald G. Baird. This work would not have been completed except for his guidance and valuable suggestions. The author would also like to thank his advisory committee, Drs. G.L. Wilkes, G.B. Wills, J.E.McGrath, and J.N. Reddy for their help during the performance of this study.

Sincere thanks go to Dr. Ramesh Pisipati. The quality of this work would have suffered had it not been for his suggestions, and his willingness to spend long hours discussing data, and other problems facing this author. Deep appreciation goes to for her help in proofreading this work. The author would also like to thank for her patience and friendship throughout the course of this study. The author would like to express his gratitude to for keeping his spirits up during the most trying times of this work. To and the author leaves one IBM PC complete with a number of video games. The author also gives them his thanks for their patience and understanding. Finally, the author would like extend his deepest appreciation to his parents. It is doubtful whether this work would have been completed without their love, and encouragement.

CONTENTS

LIST OF FIGURES

CHAPTER ONE: INTRODUCTION

Certain organic materials exist which are capable of exhibiting a phase intermediate between that of a solid crystal and an isotropic liquid [1]. The term liquid crystal has been given to describe these systems [2]. The first part of this introduction will discuss the nature of the structure of the liquid crystalline state and the types of materials which exhibit liquid crystallinity. The next section will outline the importance of these materials including a summary of important industrial applications. A description of the molecular orientation present in these systems and the manner in which different flow fields can affect this orientation will follow. A brief discussion of the continuum theories available for these systems is included. The final section presents the research objectives of this dissertation.

1.1 DEFINITION OF LIQUID CRYSTALS

This section will deal with defining more clearly the nature of the liquid crystalline state. The term liquid crystal is often confusing as it combines the terms crystal and liquid which contradict each other. For this reason, these materials are often referred to as anisotropic fluids or mesophases. These terms will be used interchangeably throughout this chapter.

One important point to be made is that the ordering present in a liq-

uid crystalline mesophase is different from that of a solid crystal. In a solid crystal the molecules reside at fixed points in space as defined by the three-dimensional lattice structure of the cyrstal. The ordering present in a liquid crystal differs from that of a solid crystal in that there is no such rigid three-dimensional lattice structure. Rather, the molecules tend to reside in aggregates in which there is only short-range ordering of the molecules. Due to the lack of any rigid lattice structure, liquid crystals possess mechanical properties resembling those of fluids, such as flow under deformation [3].

Just as liquid crystals differ from solid crystals in their degree of molecular ordering, so too do they differ from isotropic liquids. Isotropic fluids can exhibit flow birefringence, but are not usually birefringent under static conditions. Liquid crystalline materials, however, are characterized by their ability to exhibit birefringence under static conditions. Such birefringence is due to molecular ordering present in the fluid at rest. In addition, whereas material parameters such as viscosity are independant of direction for isotropic fluids, these material parameters can be affected by the ordering of the molecules in the liquid crystalline state [4]. It is the anisotropic nature of liquid crystals, then, that sets them apart from isotropic liquids.

1.2 THE STRUCTURE OF LIQUID CRYSTALS

Low molecular weight organic materials displaying liquid crystalline

order have been known for nearly a century. It has only been within the past thirty years, however, that polymers exhibiting liquid crystallinity have been observed. In this section the structure of these polymers will be reviewed, as will be the physical make-up of the mesophases themselves.

Polymers exhibiting liquid crystalline order can exist in solution, in which case the term lyotropic is used, or within pure compounds which undergo a first order phase transition from solid to liquid crystal upon being heated, in which case the term thermotropic is used. In the case of the lyotropic systems, the materials can consist of aromatic amides dissolved in strong acid solvents. As the concentration of polymer in acid is increased the viscosity of the solution typically increases and goes through a maximum at a critical concentration, C*, which marks the onset of liquid crystallinity. At this critical concentration the solution becomes birefringent, being able to transmit polarized light. As the polymer concentration is further increased, the viscosity of the solution typically decreases due to favorable packing of the polymer molecules. If the polymer concentration is even further increased, the solution will become isotropic as the polymer molecules begin to interfere with each other and start to take up random positions. At this point the solution ceases to be birefringent, and the viscosity increases with polymer concentration.

For lyotropic materials, the onset of liquid crystallinity is a func-

tion of polymer concentration and temperature. In the case of thermotropic polymers, temperature is the main variable which determines the state of the polymer. Thermotropic polymers can consist of aromatic polyesters. As the temperature of a thermotropic system is raised the material undergoes a first order phase transition from solid to liquid crystal. This phase transition can usually be detected using differential scanning calorimetry (DSC). The mesophase is birefringent and remains capable of transmitting polarized light with increasing temperature until the transition to isotropic liquid occurs or the material degrades, whichever takes place first.

Besides the distinctions made between lyotropic and thermotropic systems, further distinctions are made depending on the molecular ordering exhibited in the liquid crystalline phase. The type of molecular ordering exhibited in a liquid crystalline phase depends heavily on molecular structure. Three basic molecular conformations have been identified which give rise to both lyotropic and thermotropic mesophase behavior. These conformations include: rigid rod-like molecules, helical molecules, and block-like molecules which can resemble soap molecules. Each molecular conformation tends to form a specific mesophasic type of which three major types exist: nematic, cholesteric, and smectic.

A schematic representation of the three major mesophasic types is given in Figure 1. The nematic mesophase is the lowest order mesophasic type. In pure compounds this mesophase consists of aggregates of

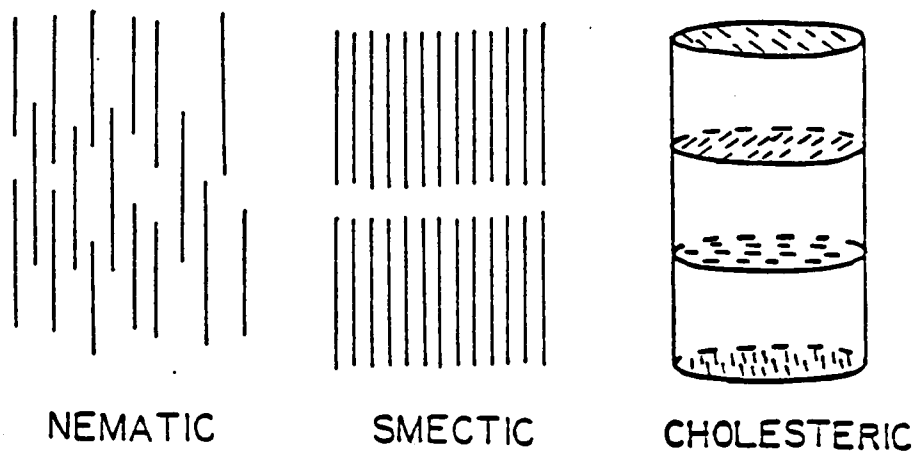

Figure 1.1 Schematic representation of the three mesophase types.

rod-like molecules. Within each aggregate the molecules tend to lie parallel to a common axis denoted by a unit vector, $\underline{n}$. There is no order as to the centers of gravity of the molecules in this mesophase. The molecules are free to slide over one another but maintain their relative orientations.

The cholesteric mesophase is closely related to the nematic mesophase and is also referred to as a twisted nematic or chiral nematic. In the cholesteric mesophase the molecules are arranged in layers. Each layer resembles a nematic mesophase with the molecules lying in the plane of the layer. Although $\underline{n}$ describes the preferred direction of the molecules in any one layer, $\underline{n}$ is not a constant throughout space and tends to vary periodically from layer to layer. Because of the periodicity of these layers cholesteric mesophases often exhibit Bragg scattering of light beams [5].

In the smectic (soaplike) mesophase the molecules reside in stratified layers separated by well defined distances which can be detected by x-ray scattering. Within each layer the molecules tend to lie along a direction perpendicular to the plane of the layer. Unlike the nematic mesophase, in the smectic mesophase there is ordering of the centers of gravity of the molecules and they are not free to slide over one another.

Having discussed the structures of the three major types of mesophases, it would now be instructive to discuss the different types of molecu-

lar structures capable of exhibiting liquid crystalline behavior. As stated earlier, these molecular conformations include: rigid rod-like molecules, helical molecules, and block-like molecules.

Molecules which are rod-like in solution or in the undiluted state tend to form either the nematic or cholesteric mesophase. The term rod-like not only includes molecules which are themselves rigid rods but also molecules which behave as helical coils. In appropriate solvents, molecules such as the Tobacco Mosaic Virus (TMV) [6], ribonucleic acid (RNA), and deoxyribonucleic acid (DNA) exist as helical coils. The nature of these helices is such that for hydrodynamic purposes the molecules behave as rigid rods. The TMV, RNA, and DNA molecules tend to form the cholesteric mesophase as do other helical coil systems. Systems such as poly(1,4-phenylene terephthalamide) (PPT) or poly(1,4-benzamide) (PBA) in strong acid solvents resemble true rigid rods and as such tend to form the nematic mesophase [7]. In the case of both the nematic and cholesteric mesophases the variables affecting the onset of the anisotropic phase include the molecular weight of the polymer, polymer concentration, temperature, and solvent type.

Block copolymers tend to form the smectic mesophase and can in some ways resemble soap molecules [8]. In block copolymers of the A-B type the A and B blocks are often incompatable and thus segregate into well defined domains. Three basic domain structures exist: Lamellar, cylindrical, and spherical. The lamellar structure is the simplest and most

encountered domain structure and resembles very closely the behavior of soap molecules in solution. These systems may exist in pure compounds such as polymer melts, or in solution in which perhaps one of the blocks is incompatible with the solvent. The major variables affecting the onset of this mesophase are the molecular weight of the blocks, the temperature, and in the case of solutions, the solvent.

Up to this point, mention has been made of rigid rods, helical coils, and block-like molecules in solution. In the case of the smectic systems it was pointed out that undiluted block copolymer materials could exhibit a smectic mesophase. For the most part then, these are all lyotropic systems. The thermotropic systems are formed quite differently than the previouly mentioned examples. In most cases, these thermotropic systems consist of polymers made from monomers which themselves form liquid crystalline mesophases. Typical examples include the polymeric esters of alkoxybenzoic acids. These materials differ from the previously mentioned systems in that it is the interactions between side groups and not main chain segments which determine the liquid crystalline order. For this reason these systems have been termed comb-like. All three mesophases have been observed in these systems [9].

1.3 SIGNIFICANCE OF LIQUID CRYSTALS

The study of liquid crystals is important due to their presence in living systems and their use in industrial applications. According to

Mishra [10] many functions of the human body as well as of other natural systems depend on the formation of liquid crystalline mesophases. Altering the structures of these systems can be accomplished through the input of mass or momentum, or by the use of magnetic fields. Therefore, an understanding of the formation of liquid crystalline phases could be useful in explaning some of the functions of the human body [10].

Both the low molecular weight and polymeric liquid crystals have important industrial applications. The polymeric materials, however, possess certain processing characteristics which set them apart from both low molecular weight liquid crystals and isotropic materials. The low molecular weight liquid crystals are used in the production of electro-optical displays. Certain low molecular weight liquid crystals, especially those exhibiting the cholesteric mesophase, change color with temperature which has lead to their use in temperature display devices. The polymeric liquid crystals are used in the production of ultra-strength fibers. In processing these fibers, the lyotropic systems are solution spun [7], while the thermotropic systems are melt spun [11]. In both cases fibers with exceptional properties are achieved. Of interest here is the fact that in both processes the exceptional physical properties arise in the as-spun fibers. In the case of the thermotropic systems the fibers are heat treated but not drawn. This differs significantly from fiber spinning processes using flexible chain polymers in which high strength fibers are achieved only after significant drawing of the fiber has taken place. The liquid crystalline materials have another

advantage over isotropic materials in that the viscosities of liquid crystalline materials are considerably lower that those of isotropic systems. This reduced viscosity allows for lower operating pressures which reduces energy requirements [12].

1.4 THE COPOLYESTER OF PHB AND PET

Although much work has been done on the lyotropic polymer liquid crystals, it has been only recently that interest has been generated in the thermotropic systems. One question of interest here is why such interest was not developed earlier. Thermotropic systems offer several processing advantages over lyotropic materials. In addition to being fiber spun, these materials can be injection molded as any ordinary thermoplastic. At this point some of the work done on one specific thermotropic system will be reviewed briefly.

One thermotropic liquid crystalline polymer which has received much attention is the copolyester of p-hydroxybenzoic acid (PHB) and poly(ethylene terephthalate) (PET) produced by the Tennessee Eastman Company. A schematic drawing of the PHB/PET structure is given in Figure 1.2. This polymer was studied extensively by Jackson and Kuhfuss [13] who investigated the physical properties of injection molded plaques made from copolymers in which the PHB content was varied. They found that the plaques processed from copolymers containing between 60 and 80 mole percent PHB possesed the highest values of flexural and tensile

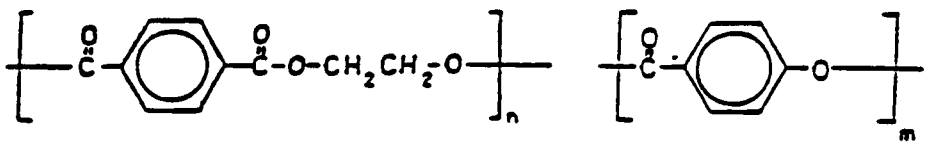

COPOLYESTER GEN. STRUCTURE

60 MOLE% PHB/PET n= .4 m= .6
80 MOLE% PHB/PET n= .2 m= .8

Figure 1.2 Molecular structure of the PHB/PET copolymer

moduli. In the case of the 60 mole% PHB/PET coplyester, Jackson and Kuhfuss measured the flexural modulus of the injection molded plaques along two directions; along the flow direction, and transverse to the flow direction into the mold. In addition, plaques were made at different mold thicknesses. The results of their investigation are summarized in Figure 1.3 in which a plot of flexural modulus versus mold thickness is shown. Both the flexural moduli measured along and transverse to the flow direction are plotted in the figure. Several interesting features of this graph are worth mentioning. It can be seen in the figure that the flexural modulus measured along the flow direction increases exponentially with decreasing mold thickness, reaching a maximum of approximately 1.8×10^{10} Pa (2.6×10^{6} PSI) at a mold thickness of 0.1 inches. This value is almost one fourth the flexural modulus of aluminum and exists in the as processed plaque. No post processing was used to achieve the exceptional physical properties. It can be seen in the figure that the modulus measured transverse to the flow direction does not change with mold thickness. This modulus is also an order of magnitude less than the modulus measured along the flow direction.

In addition to exhibiting anisotropic physical properites and a flexural modulus which depends on mold thickness, these injection molded plaques also exhibited a skin/core phenomenon [14]. The skin of such injection molded plaques was found to be highly oriented compared to the core of the plaque which was found to be less oriented. Of importance here is how the skin and core layers affect the physical properties of

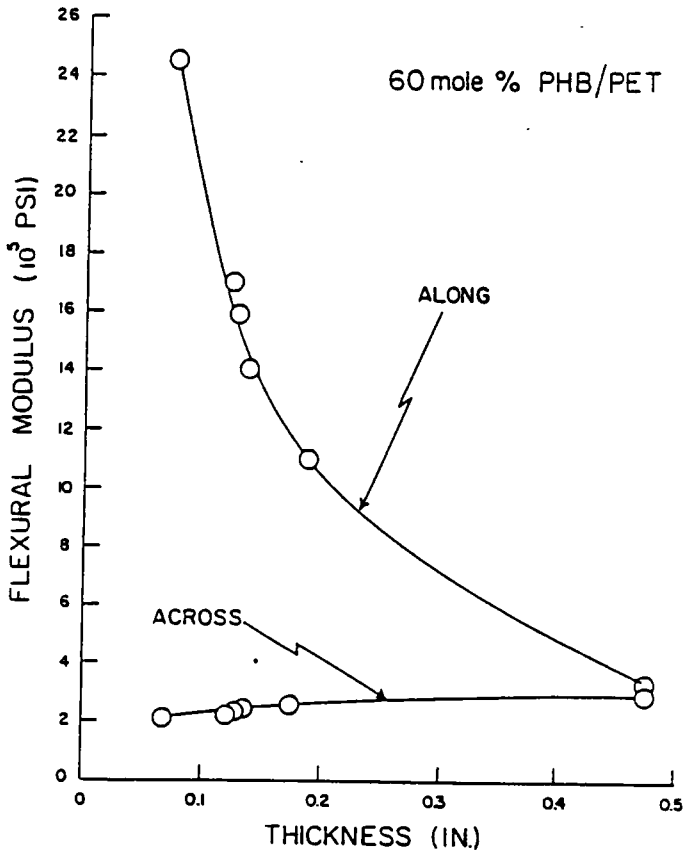

Figure 1.3 Flexural modulus versus mold thickness for injection molded plaques of the 60 mole% PHB/PET system. Melt temperature=275°C.

effect of elongational and shear flow on the orientation of a thermotropic liquid crystalline copolyester. His results indicate that in fiber spinning processes shear flow has little or no orienting capability. However, elongational flow was found to have a marked effect on orientation and also improved the physical properties of the spun fibers. Ide concluded that the skin/core morphologies present in injection molded plaques could be due to the fountain flow effect, and the elongational flow present at the advancing front. The fact that the oriented fibers possessed superior physical properties to the unoriented fibers would also suggest that the skin layer of injection molded parts is responsible for most of the physical strength of such parts.

As has been shown, the copolyester of PHB and PET can be processed to form injection molded plaques with interesting morphological and physical properties. Usually, in predicting the mold filling behavior of polymers, some knowledge of the rheological properties of the material is desirable. In order to try and understand the behavior of the system of PHB and PET some rheological studies have been done. In particular, Wissbrun [23] has noted some interesting phenomena concerning this material. These phenomena include negative normal stresses, an apparent yield stress, unusual temperature dependence of viscosity, and unusual overshoot behavior on inception of shear. In addition, the material is known to have a long relaxation time.

The interesting rheological and physical properties exhibited by the

copolymer of PHB and PET raise questions as to whether such behavior can be predicted. In order to predict the orientation of the molecules as a function of flow history as well as predict the rheological behavior of this system, some type of constitutive equation is needed. Specifically, a constitutive equation is needed that explicitly takes the orientation of the molecules into account. A number of attempts have been made to formulate continuum theories for liquid crystals. The earliest such attempt was that of Oseen [19] which was later revised by Frank [20]. Most recently, Ericksen [21], and Leslie [22], have proposed continuum theories for liquids whose molecules resemble rigid rods. Of the two, Ericksen's theory seems less complicated. In his theory, Ericksen assumes that the molecules all lie essentially parallel to a common axis denoted by a vector called the director, $\underline{n}$. The director is a unit vector for rigid rod-like molecules, and the direction in space to which $\underline{n}$ points can be affected by external forces such as electric or magnetic fields. For example, in a uniaxially oriented sample, $\underline{n}$ would lie along the axis of orientation. Suppose that this oriented fluid was sheared in a direction perpendicular to the axis of initial orientation. Ericksen's theory would predict that the director would rotate into a position in line with the shear direction thus having a final orientation perpendicular to its initial position. In addition, Ericksen's theory would predict the non-steady state behavior of the director. In other words, his theory would predict the time needed for the director to assume its new position. Therefore, Ericksen's theory predicts the orientation of the director as a function of time and the particular flow field.

Due to the anisotropic nature of an oriented fluid such as a liquid crystal, Ericksen's theory seems reasonable. Unfortunately, in its non-linear form Ericksen's theory requires the determination of five material parameters, all of which are a function of temperature, deformation rate, and the director $\underline{n}$. The state of the director must also be determined which involves determining its three principle components. Thus, eight parameters must be evaluated. In order to evaluate these parameters one needs to measure the shear and normal stresses as a function of shear rate as well as the direction of the director. To date, no material parameters have been reported for the copolyester of PHB and PET.

1.5 RESEARCH OBJECTIVES

The investigation into the processing behavior of the PHB/PET system conducted by Jackson and Kuhfuss raises some important questions concerning the flow behavior of liquid crystalline systems. Their results showed that injection molded plaques of the 60 mole% PHB/PET coplyester exhibited anisotropic physical properties which depended on mold thickness. Other investigators [14,18] have shown that such injection molded plaques possess a skin/core morphology which may be related to the fountain flow effect of mold filling. In order to more fully understand the behavior of this liquid crystalline system several important questions must be addressed. Although Ide [18] investigated the separate effects of shear and extensional flow on the development of molecular orientation in the PHB/PET system, his study overlooks several important factors.

Firstly, he did not quantify the shear rates and extensional rates necessary to produce a minimum amount of molecular orientation. Secondly, he did not investigate the morphological textures produced in either flow situation. If it is to be proven that the skin/core morphology present in injection molded plaques is a result of the fountain flow effect, then the types of textures produced in shear and extensional flow must be determined. Ide's study also did not address the effect of annealing on the degree of molecular orientation present in sheared and extended samples. It is possible that molecular orientation is produced by shear flow in the center of injection molded plaques. This orientation could relax, however, due to the longer cooling times in the core. One objective of this study will be to investigate the important areas just mentioned concerning the development of molecular orientation and texture in the PHB/PET copolyester under different flow situations.

Besides investigating the degree of molecular orientation and types of textures which develop in the PHB/PET system, other studies are needed to quantify its flow behavior. Most importantly, a knowledge of the rheological behavior of this system would be very useful. It was mentioned that Wissbrun [23] has noted some interesting rheological behavior for the 60 mole% PHB/PET copolyester system. His study lacks in several areas, however. His study does not address the choice of a possible constitutive equation for the PHB/PET system. He also did not indicate whether the behavior exhibited by the PHB/PET system is typical of other liquid crystalline systems. The flow properties of a liquid

crystalline system could differ from those of an isotropic material due to the amount of molecular orientation present. Although isotropic materials, such as polystyrene, do show flow anisotropy as evidenced by flow birefringence, the degree of anisotropy is not as high as in a liquid crystalline fluid. The highly anisotropic nature of a liquid crystalline fluid suggests that a special form of constitutive equation is needed, specifically, one which takes molecular orientation into account. Ericksen's continuum theory has already been presented as one possible approach. His theory describes anisotropic fluid behavior by giving the fluid a preferred molecular orientation denoted by a director, $\underline{n}$. Other theories have been proposed to describe anisotropic fluids. These include the theories of Leslie [22], Hand [24], and Duffy [25]. In Chapter Two the major features of each of these theories is reviewed. It will be shown that Ericksen's theory is perhaps the most suitable for investigation.

It has already been mentioned that in order to fully specify the quantities in Ericksen's theory, eight material parameters would have to be measured. It is not probable that an experimental method could be devised which could accurately measure all eight of these parameters. It should be possible, however, to qualitatively test the major assumptions and predictions of the theory. This would be accomplished by comparing the measured rheological properites to those predictied by the theory. Measurements of molecular orientation through the use of wide angle x-ray techniques will give information regarding the validity of the pred-

ictions of the state of the director in Ericksen's theory.

The purpose of part of this study, therefore, will be to address several areas of flow behavior of liquid crystalline fluids. One objective will be to define more clearly the types of textures and degree of molecular orientation which develop in different flow fields. This will be accomplished by preparing samples of the PHB/PET copolyester under known conditions of flow and temperature history. The 60 and 80 mole% PHB/PET copolyesters will be used as they exhibited the highest physical properties of all the PHB/PET compositions studied by Jackson and Kuhfuss. Wide angle x-ray scattering (WAXS) techniques will be used to qualitatively determine the degree of molecular orientation produced in each flow situation. The morphological textures produced in each flow situation will be investigated using scanning electron microscopy techniques.

In order to further understand the flow behavior of the PHB/PET system, a study of the rheological properties of this material will be performed. This study will include investigation of the steady state and transient behavior of the copolyester system. An indepth discussion of the measurement techniques employed to gather this information is given in the experimental section (Chapter 3). Besides studying the PHB/PET system, another liquid crystalline system will be studied. This is necessary to determine whether the rheological properties exhibited by the PHB/PET system are unique or characteristic of liquid crystalline polym-

er behavior. The other system studied will consist of a lyotropic solution of poly-p-phenyleneterephthalamide (PPT) in 100% pure sulfuric acid. This system is readily available, and is known to exhibit a nematic mesophase.

Finally, the results of the previous investigations will be compared to the predictions of Ericksen's theory. Although the comparison may only be on a qualitative basis it will be possible to test the major predictions of the theory. For instance, the results of the WAXS studies will determine if Ericksen's theory can predict the correct degree of molecular orientation present in a sample subjected to shear or extensional flow. Comparison of the prediction of rheological properties, such as stress growth upon inception of shear, with actual experimental results will indicate again whether the theory is valid. It is possible that Ericksen's theory is not applicable to to liquid crystalline polymers.

The purpose of this chapter has been to introduce the basic concepts of liquid crystallinity of polymeric substances and to outline the basic research objectives of this work. In the following chapter a detailed review of the literature associated with the rheology, orientation, and continuum theories of polymeric liquid crylstalline substances will be given.

CHAPTER TWO: LITERATURE REVIEW

In Chapter One, the basic definitions of liquid crystallinity were outlined. The three mesophase types were discussed and correlated to the various molecular conformations which exhibit liquid crystalline order. The significance of liquid crystalline polymers was reviewed and it was emphasized that in order to predict the flow behavior and structural development in these systems, a special form of constitutive equation may be necessary. Possible choices of a continuum theory for these materials were mentioned. The Chapter concluded with a brief account of the research objectives of this work.

In this Chapter, the ideas presented in Chapter One will be reviewed in more detail. It was mentioned in the prededing chapter that the rheological properties of liquid crystalline materials may be related to the development of molecular orientation during flow. In section 2.1, the rheological behavior of liquid crystalline materials will be reviewed in detail. A point will be made to highlight the major features of liquid crystalline polymer rheology which sets these materials apart from isotropic systems. The review will also serve to define the type of behavior a constitutive equation such as Ericksen's will have to be able to predict. The following section will describe in more detail the development of molecular orientation in liquid crystalline polymers. The difference in molecular orientation produced in shear and extensional flow will be compared, as will be morphological textures associated with such

orientation. The affects of orientation on physical properties will be discussed. In section 2.3, the possible choices of constitutive theories for use with anisotropic fluids will be examined. The theories are not rigorously derived, but some of the main features of each theory are described with comparisons being made between the various models. Ericksen's transversely isotropic fluid theory is discussed at length, and the equations for simple shear flow are analyzed.

The final section of this chapter is a summary of what is known at the present time concerning the rheology, orientation development, and constitutive theories of liquid crystalline materials. With this in mind, the research objectives of this work are described in detail. In Chapter Three, the experimental details of the methods used to achieve the research objectives are described.

2.1 THE RHEOLOGY OF LIQUID CRYSTALLINE POLYMERS

In this section, the rheological behavior of liquid crystalline polymers is reviewed. The point of this review will be to highlight the important features of liquid crystalline polymer rheology which sets these materials apart from isotropic materials. The review will also serve to point out the types of behavior that a constitutive equation such as Ericksen's will have to be able to predict. The rheological behavior of low molecular weight materials is not discussed. For an account of the rheology of these systems, one should see the review arti-

cle of Porter and Johnson [3]. For more material regarding the rheological behavior of liquid crystalline polymers, one should see the review articles of Baird [26], Wissbrun [27], and Benicewicz [28].

2.1.1 SCOPE

In Chapter One, it was shown that three specific molecular conformations could lead to liquid crystalline behavior. These conformations include helical, rod-like, and block-like molecules. It was stated that for hydrodynamic purposes, the helical and rod-like conformations could be considered to be quite similar. In this study, the rheological behavior of the PHB/PET and PPT/H_2SO_4 systems will be investigated. These systems owe their liquid crystalline character to molecules of the rod-like conformation. For this reason, the review of liquid crystalline rheology is restricted to the behavior exhibited by materials which possess molecules of the rod-like conformation. This includes both lyotropic and thermotropic systems, and materials of the helical molecular conformation. The rheological behavior of the helical systems is based on studies performed on lyotropic solutions of poly-α-benzyl-l-glutamate (PBLG), and poly-ε-carbobenzoxy-l-lysine (PCBZL). The rheological behavior of the purely rod-like systems is based on studies involving lyotropic solutions of poly-p-benzamide (PBA) in dimethyl acetamide (DMA), the PPT/H SO system, and the thermotropic PHB/PET copolymer system. The review is structured in the following manner. The viscosity behavior of liquid crystalline polymers is reviewed first. A point is

made to compare the behavior of isotropic and anisotropic materials. Comments are made regarding the onset of shear-thinning behavior, and the presence of yield stresses. The normal stress behavior exhibited by liquid crystalline systems is then discussed. A comparison of steady shear to dynamic mechanical properties is then presented. Finally, the shear and temperature history effects exhibted by certain thermotropic systems is reviewed.

2.1.2 VISCOSITY BEHAVIOR OF POLYMERIC LIQUID CRYSTALS

The viscosity behavior of liquid crystalline materials has been studied most extensively. Both lyotropic and theormotropic systems have been investigated. Onogi and Asada [55] have proposed that all liquid crystalline materials should exhibit a three region viscosity curve of the type depicted in Figure 2.1. Region I is a shear-thinning region indicating the presence of a yield stress at shear rates approaching zero. Region II is a "Newtonian" plateau region, and Region III is another shear-thinning region. Onogi and Asada attribute the existence of these three regions to the presence of a polydomain structure within the fluid. The three viscosity regions arise due to different stages of destruction of this polydomain structure during flow. As a test of the validity of such a three region flow curve, Figure 2.2 is presented in which the viscosity behavior of a number of polymeric liquid crystalline materials is shown. The viscosity behavior of both lyotropic and thermotropic systems is presented. Curves 1, 3, and 5 clearly show three

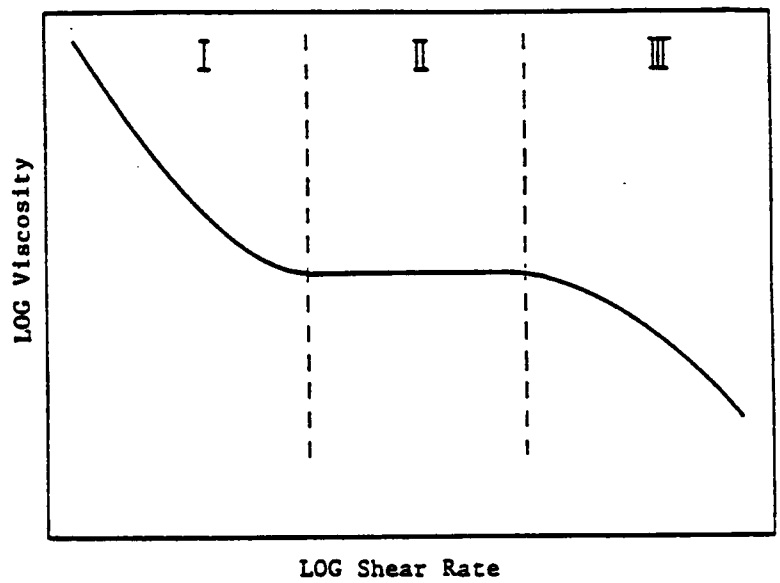

Figure 2.1 Three region flow curve proposed by Onogi and Asada for viscosity versus shear rate dependence of liquid crystalline materials 55.

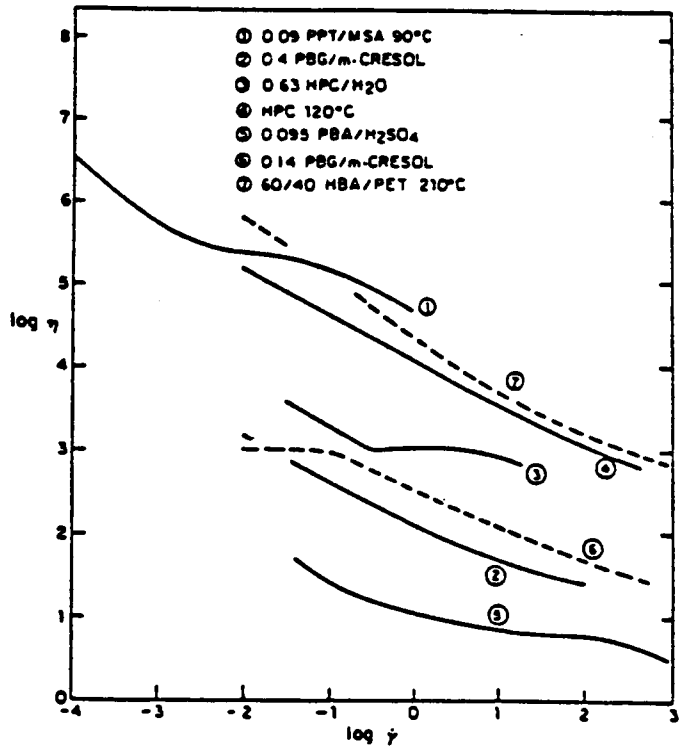

Figure 2.2 Viscosity versus shear rate for various liquid crystalline polymers [27].
curve 1 Wong and Berry [54]
curve 2 Asada and co-workers [124]
curve 3 Onogi and Asada [55]
curve 4 Shimamura and co-workers [125]
curve 5 Papkov [48]
curve 6 Kiss and Porter [31]
curve 7 Wissbrun [23]

regions of flow behavior. In the other curves, however, not all three regions are present and in three of them (2,4,7) only a shear-thinning region can be seen. In these curves it is difficult to tell whether the shear-thinning region is of the Region I (yield stress) or Region III (no yield stress) type. There is other evidence, however, such as the presence of a yield stress, and history dependent rheology, which would indicate that these shear-thinning regions are of the Region I type [27].

2.1.2.1 YIELD STRESSES

If the three region flow curve of Onogi and Asada is correct, then all liquid crystalline materials should exhibit yield stress values as indicated by the Region I shear-thinning region. The existence of yield stresses has been reported by several investigators for systems thought to exhibit liquid crystallinity. Collagen is a molecule of helical structure composed of three polypeptide strands which is thought to be a rigid rod in dilute HCl solutions [51]. Fukada and Date [44] measured the dynamic mechanical properties of the collagen system and reported that the viscosity exhibited a strong concentration dependence and a yield stress. The authors concluded that the gel-like nature of this material could have been due to a network-like structure composed of bundles of molecules which served as crosslinks. The molecular bundles were thought to possess liquid crystalline order.

Marchessault and co-workers [45] reported a gel-like structure for

aqueous solutions of chitin. Such solutions are thought to be liquid crystalline. Hermans [29] reported unusual yield stress behavior for aqueous solutions of wood and cotton cellulose also thought to be liquid crystalline. Hermans reported that the viscosity showed a marked shear history dependence. For the cotton cellulose solution two yield stress values were observed, one being much larger than the other. The larger value of yield stress was observed after the material had been sheared for a period of time. Such behavior was attributed to the formation of liquid crystalline regions due to the action of shear.

In the case of the PPT and PBA systems Aoki [33], and Papkov [48] report the presence of yield stress values. Baird has shown for the PPT system, however, that the yield stress could be removed by preheating of the material, and careful exclusion of moisture [49]. For the case of the PHB/PET system, Wissbrun [27] reports measuring yield stress values at temperatures of 240 and 250°C. These results are genuine, but it does not appear that the yield stress is a liquid crystalline phenomenon. At the temperatures used by Wissbrun it is possible that complete melting of the copolymer had not taken place, thus giving rise to a yield stress.

2.1.2.2 ONSET OF SHEAR-THINNING

One important aspect of the viscosity behavior of polymeric materials is their shear-thinning behavior. Specifically, one is usually interested in the point at which such materials begin to shear-thin. Such

information is useful in determining the relaxation time of the material [120]. By comparing the viscosity behavior of polymers in their anisotropic liquid crystalline state, to the same polymers in their isotropic state, differences in relaxation times may be determined. It is seen, however, that no general conclusions can be made regarding the onset of shear-thinning in liquid crystalline systems [27].

Perhaps the most useful data for comparison of isotropic to anisotropic viscosity behavior exists for lyotropic solutions of PBLG. Such a comparison is facilitated for the lyotropic systems in that the zero shear viscosity for the isotropic phase, and the region II plateau viscosity for the anisotropic phase can be made to be similar in magnitude [27]. Table 2.1 shows the results of several investigators working with the PBLG system. The Table summarizes the shear rate at which the viscosity has reached half of its zero shear, or plateau region value for isotropic and anisotropic solutions. It is seen in the Table that no general conclusion can be made regarding the onset of shear-thinning behavior for the PBLG system. Kiss and Porter [32] found that the isotropic solution began to shear-thin at a lower shear rate value than the anisotropic solution. Aoki and co-workers [33] found no difference in the value of the shear rate at which shear-thinning began for the two solutions. Iizuka [34] found the opposite of Kiss and Porter in that his studies indicate that shear-thinning occured at lower shear rate values for the anisotropic phase than for the isotropic phase. In other studies utilizing the PBLG and PCBZL systems, Miller and co-workers [30] found

Table 2.1

Onset of Shear Rate Dependence of Viscosity of PBLG

Solvent	Form[a]	Concentration (wt %)	Viscosity (poise)	$\dot{\gamma}_{1/2}$ (s^{-1})	Ref.
m-Cresol	I	6	25	100	32
	C	16	20	1000	
m-Cresol	I	6	4	>500	
	C	10	25	>500	33
	C	16	15	>500	
Dioxane	I	4	25	>200	34
	I	7	150	100	
	C	13	30	100	
CH_2Br_2	I	7	16	>200	
	N + I	10	5	150	
	N	13	6	150	

[a] I — isotropic, C — cholesteric, N — nematic, N + I — biphasic.

that the viscosity of the anisotropic phase was smaller in magnitude than that of the isotropic phase, and the anisotropic phase began to shear-thin at lower values of shear rate than the isotropic phase, in agreement with Iizuka [34].

Other studies comparing the isotropic to anisotropic solution viscosities were performed by Yang [35,36] for solutions of PBLG in m-cresol, and in dichloracetic acid (DCA). In m-cresol the PBLG molecule exists as a helix, while in DCA the PBLG molecular exists as a random coil. Yang found that while the solution viscosity was lower for the DCA solutions than for the m-cresol solutions, the DCA solutions exhibited almost total Newtonian behavior over the range of shear rates tested. The m-cresol solutions began to shear-thin at a shear rate of approximately 150 $secs^{-1}$ in general agreement with Miller [30], and Iizuka [34].

Comparison of isotropic and anisotropic viscosity behavior has also been performed for the PBA and PPT solutions. In this case, it also appears that no general conclusion exists as to the onset of shear-thinning in the anisotropic versus the isotropic phase. Baird [50] found that for isotropic and anisotopic solutions of PPT in 100% H SO with the same zero shear viscosity, the anisotropic solution began to shear-thin at lower values of shear rate than the isotropic solution. Aoki and co-workers [33] have also investigated the behavior of the PPT system. Although their data does not cover the same shear rate range as Baird's, for a comparable solution with a viscosity an order of magnitude

higher, there does not seem to be any appreciable shear-thinning [27]. Wong and Berry [54], working with the PPT system, also found that the anisotropic solution began to shear-thin at lower shear rate values than the isotropic solution. For solutions of PBA, Papkov [48] found that the anisotropic solutions began to shear-thin at lower shear rate values than the isotropic ones. According to Wissbrun [27], however, the results of Wong [54], and Papkov [48] are suspect because of Region I shear-thinning partially overlapping the Region II plateau.

As for thermotropic systems, the most extensive work has been done with the PHB/PET coplymer system. Jerman and Baird [51], Wissbrun and Griffin [52], and Jackson and Khufuss [13] all found that the PHB/PET copolymers exhibited lower values of viscosity than the PET homopolymer. In addition, the viscosity of the PHB/PET copolymers were seen to be much more shear-thinning than that of the PET homopolymer. Wissbrun [27] and Jackson [53] have determined values of relaxation times for the PHB/PET and other aromatic copolyester systems. They both found that with increased amounts of PHB the relaxation time of the material increased. This indicates in effect, that shear-thinning occurs at decreasing values of shear rate with increased PHB content. From Wissbrun's data [27] it is possible to calculate that the relaxation time of the 60 mole% PHB/PET copolymer system is 1000 times greater than that of the PET homopolymer. It should be noted, however, that the comparison of the viscosity behavior of the PHB/PET and the pure PET systems is not the same as the previous comparisons. It would be necessary to compare the viscosity

behavior of an isotropic PHB/PET melt to that of the anisotropic melt. This has not been done at the present time due to the fact that the PHB/PET system tends to degrade before undergoing the transition to an isotropic phase.

In summary, it seen that the viscosity behavior of liquid crystalline materials has been extensively investigated. The three region flow curve of Onogi and Asada is useful, but does not seem to be exhibited by all liquid crystalline systems. Many systems thought to exhibit liquid crystalline behavior have been shown to possess yield stresses. The work of Baird [49] suggests, however, that such yield stresses may not necessarily be a liquid crystalline phenomenon. There does not seem to be any clear conclusions as to the onset of shear-thinning in the anisotropic versus the isotropic phase. However, some investigators [27,70] have shown that in the case of the PHB/PET copolymer system, the liquid crystalline material possess a very long relaxation time that increases with the rigidity of the polymer molecules.

2.1.3 NORMAL FORCE BEHAVIOR

Many of the investigators cited above have also investigated the primary normal stress difference (N1) behavior of liquid crystalline polymers. For the case of the PBLG and PPT systems these investigators have found the same concentration dependence of N1 as exhibited by the shear viscosity. Specifically, N1 was seen to exhibit a maximum when plotted

against concentration [31,32,33,50]. For the PPT system, the results of Baird [50] indicate that solutions with the same viscosity exhibit the same values of N1 regardless of whether they are anisotropic or not. However, Aoki and co-workers [33] found that the value of N1 measured in the anisotropic phase was much larger than that measured in the isotropic phase. The differences between the results of these two investigators may be attributable to the fact that different shear rate ranges were investigated in each study.

For the PBLG system, Kiss and Porter [31,32] found that negative values of N1 were possible. Steady state negative values of N1 were exhibited over well defined shear rate ranges. No detailed explanation was given for the occurence of such behavior, however, the authors convincingly discounted the possibility of secondary flow effects. It is interesting to note that negative N1 values have been reported for other systems thought to exhibit liquid crystalline order. Iizuka [34] makes brief mention of negative N1 values for the PBLG system at low shear rates. Duke and Chapoy [37] report a transient negative N1 value for lechitin in dodecane, as do Hutton [38] for lubgrease, Wissbrun [23], Gotsis [123], and Baird and co-workers [39] for the PHB/PET copolymer system, and Huang [40] for a block copolymer. Gotsis [123] also reports measuring steady state negative N1 values over defined shear rate and temperature ranges for the 80 mole% PHB/PET copolymer system.

It is worth mentioning that there appears to be some theoretical evi-

dence for the existence of negative N1 values. Ogagawa, Cox, and Mason [41] have shown that dilute suspensions of spheroids could exhibit negative primary normal stress values. It has also been shown by Currie [42] that the theories of Leslie and Ericksen can predict negative values of N1.

2.1.4 COMPARISON OF STEADY SHEAR AND DYNAMIC MECHANICAL PROPERTIES

The comparison of steady shear to dynamic mechanical properties is useful for several reasons. Dynamic measurements are useful in that higher deformation rates are usually achievable than in steady shear experiments. Comparison of the steady shear and dynamic mechanical properties can give insight into structural changes which take place within the fluid for each type of flow [27]. Such a comparison can also be used to test constituitve equations, as Baird [50] has done.

Several investiagtors have examined the dynamic mechanical properties of the PBLG, PPT, and PHB/PET systems. A summary of the findings of these investigators for the comparison of dynamic and steady shear data appears in Table 2.2. In general it seen that η and η^* are usually comparible. For isotropic solutions of PPT, Baird [50] found good agreement between the steady shear and dynamic properties at all shear rates:

$$\eta(\dot{\gamma}) \approx \eta^*(\omega) \quad \dot{\gamma}=\omega$$

$$N1 \approx 2G'$$

For the anisotropic solutions both Baird and Aoki found reasonable agree-

Table 2.2

Comparison of steady and dynamic properties [27].

				Ref.
PPT (60°C)		$\eta(\dot{\gamma}) \approx \eta^*(\omega)$	$N_1(\dot{\gamma}) \approx 2G'(\omega)$	50
		$\eta \approx \eta^*$	$N_1 \gg 2G'$	
(25°C)		$\eta^* \gg \eta$	$N_1 \approx 2G'$	33
PBLG		$\eta \approx \eta^*$	$N_1 > 2G'$	32
Thermotropic Polyesters	High temp.	$\eta \approx \eta^*$	$N_1 > 2G'$	27
	Low temp.	$\eta^* > \eta$	$N_1 > 2G'$	

ment between η and η^*. Baird found, however, that at 60°C $N_1 \simeq 2G'$, while Aoki reported measuring N_1 values which were up to two orders of magnitude larger than $2G'$ at the same temperature. It was only at 25°C that Aoki reported seeing agreement between N_1 and $2G'$.

Kiss and Porter have reported on the comparison of steady shear to dynamic properties for the PBLG system. They found that at low shear rate values the steady shear and dynamic viscosities were equal ($\eta \simeq \eta^*$), while for all values of shear rate, N_1 was usually much larger than $2G'$.

For the PHB/PET system Wissbrun [27] found that η and η^* were comparable at high temperatures, but deviated from each other at low temperatures. At all temperatures and shear rates tested, N_1 was anywhere from 5 to 100 times greater than $2G'$. The above results are interesting as they indicate a deviation of the behavior of liquid crystalline systems from that of flexible chain istropic systems. For these systems, N_1 and $2G'$ are usually equivalent.

2.1.5 HISTORY DEPENDENCE AND OTHER RHEOLOGICAL MEASUREMENTS

For the case of thermotropic systems, several investigators have reported seeing history dependence of rheological properities. No such reports have been made for any other liquid crystalline systems. The reason for this may be that the shear history dependent effects are most evident in stress growth experiments. Such experiments have not been

reported in the literature for any of the lyotropic systems.

Wissbrun [27], Baird and co-workers [39], and Gotsis [123] have reported on the transient rheological behavior of the PHB/PET system. Upon inception of shear, a stress overshoot peak was exhibited by the shear stresses. Preshearing of the material was seen to completely destroy the overshoot peak. Both the 80 and 60 mole% PHB/PET copolymer systems exhibited this behavior.

Other shear and temperature history effects have been observed by Wissbrun and Griffin [52] for a thermotropic copolyester. Lower values of the dynamic viscosity and storage modulus (η^*,G') were found after preshearing of the material had taken place as compared to the values measured for an unsheared sample. The shear induced effects could be erased by raising the material above its transition temperature from the nematic to the isotropic liquid phase and then repeating the experiment at the lower temperature. A hysterisis effect was observed concerning the manner in which the dynamic data were collected. If η^* and G' were measured as the frequency increased, their values were higher than if measured as the frequency decreased during the experiment. Wissbrun attributed these phenomena to shear induced orientation of the liquid crystalline domains.

Other than the measurements of viscosity, dynamic mechanical properties, and transient behavior, the only other rheological properties

reported for the rodlike systems concerns the die swell and entrance pressure loss behavior as reported by Jerman and Baird [51] for the PHB/PET copolymer. In their study, Jerman and Baird investigated the temperature and shear dependence of viscosity, entrance pressure loss (ΔPent), wall shear stress (τw), and die swell ratio (D/Do) for the 60 and 80 mole% PHB systems. The viscosity data has already been mentioned. The die swell measurements indicated that the melt contracted at the lower end of the processing range, but expanded slightly at higher temperatures. This would tend to indicate that the PHB/PET has negligible elasticity. The measurements of ΔPent and τw indicate the opposite however. The ratio of ΔPent/τw can be used as a measure of fluid elasticity. According to experimental measurements the PHB/PET copolymer has values of ΔPent/τw which are almost almost an order of magnitude larger than those of the PET homopolymer, indicating that the PHB/PET polymer is quite elastic. One possible explanation for this contradiction involves the concept of negative values of the primary normal stress difference, N1. If negative N1 values were possible then it is possible that negligible values, or values of less than one, could be observed for the die swell ratio. The material would still exhibit considerable elasticity, however. This seems to be the case for the 80 mole% PHB copolymer. Baird and co-workers [39] report negative values of N1 for both transient and steady state experiments. It may be that in the case of the 80 mole% PHB copolymer the negative N1 values arise from crystallization of the PHB segments. This would probably cause an increase in density which would give rise to a negative N1 value. The

only other possible explanation for die swell values of one would be that plug flow existed in the capillary, thus, no velocity rearrangement would take place at the capillary exit. If this were the case the viscosity would exhibit a shear thinning region with a slope of negative one on a log-log plot of viscosity versus shear rate. The viscosity curves reported by Jerman and Baird do not exhibit such behavior, and thus the existence of plug flow in the capillary is not a valid explanation of the negligible die swell values.

2.1.6 SUMMARY

It is seen that the rheological behavior of liquid crystalline systems has been extensively investigated. The viscosity behavior seems to be well described in terms of a three region flow curve. There appears to be no general conclusion as to the onset of shear-thinning in the isotropic versus the anisotropic phase. Different investigators working with the same systems report different results. Several investigators have been able to determine, however, that the relaxation time of liquid crystalline materials can be orders of magnitude larger than those of isotropic materials. The presence of yields stresses as a liquid crystalline phenomenon does not seem to be a valid conclusion. Baird has shown for the PPT system, at least, that yield stresses could be removed with heat and exclusion of moisture.

Investigations of the normal stress behvaior of liquid crystalline

polymers indicates that these systems can exhibit negative normal stress values, and a concentration dependence of the value of N1. Comparison of dynamic to steady shear properties reveals that η and η^* are comparable, however, N1 is usually orders of magnitude larger than $2G'$. This result marks a difference between liquid crystalline fluids and isotropic materials for which N1 and $2G'$ are usually equivalent.

Other investigations of the transient behavior of thermotropic systems reveals shear history effects. Temperature history effects have also been noted. Measurements of die swell indicate that the PHB/PET systems may not possess a high degree of elasticity. However, qualitative measurements of elasticity such as the ratio of ΔP_{ent} to τ_w reveal that the PHB/PET possesses considerable elasticity.

2.2 ORIENTATION DEVELOPMENT IN LIQUID CRYSTALS

In the previous section, the rheological behavior of liquid crystalline polymers was reviewed. It was stated that these materials exhibit many unique phenomena. It is possible that these phenomena are related to the development of molecular orientation during flow. In this section a more indepth discussion of the manner in which liquid crystalline materials orient will be given. The low molecular weight materials are discussed briefly, followed by a summary of the mold filling process and its relationship to orientation development in injection molded parts. The final section discusses the effect of shear and elongational flow on molecular orientation in liquid crystalline materials. The relation between this orientation and morphological textures and physical properties is also discussed.

2.2.1 LOW MOLECULAR WEIGHT MATERIALS

In this section the early experiments concerned with molecular orientation in liquid crystals will be reviewed. These studies deal mainly with the effect of electric and magnetic fields on the nematic liquid crystalline materials of p-azoxyanisol (PAA) and anizaldizine. As with the studies presented here, most of the studies concerned with molecular orientation in liquid crystals deal with materials which form the nematic phase. This is due to the fact that the nematic phases orient most readily in flow and magnetic fields as opposed to materials which form the

cholesteric or smectic phase. The importance of these early studies lies in the fact that they give clues as to how the many material parameters in a theory such as Ericksen's or Leslie's may be evaluated. It is for this reason that they are being presented.

Perhaps the first experiment designed to test the effect of an electric field on a liquid crystalline material was performed by M. Neufield [56]. He placed materials such as PAA in a small diameter glass capillary, and then placed the capillary in the center of a solenoid. Neufield then measured the viscosity of the material with and without an electric current applied to the solenoid. Although his results were only qualitative he was able to show that a great difference in viscosity was achieved as a result of applying the electric field. Neufield concluded that the electric field created by the solenoid caused the liquid crystalline materials to orient parallel to the field, and thus cause a difference in viscosity from the case in which no field was present. Later, Miesowicz [4,57] performed similar experiments which resulted in the now famous Miesowicz Viscosities. In his experiments, Meisowicz suspended a glass plate from one arm of a balance. This glass plate hung between two metal plates which were connected to an electrical power source. The three plates themselves were housed in an insulated vessel. In order to determine the viscosity, the glass plate was oscillated at various frequencies, and the force necessary to oscillate the plate was measured. Miesowicz could adjust the electric potential to the plates such that three molecular alignments were possible : 1] Parallel to the flow

direction; 2] Parallel to the velocity gradient; and 3] Perpendicular to both the velocity gradient and the flow direction. These measurements lead to the determination of the three Miesowicz Viscosities, η_1, η_2, and η_3. corresponding to the three molecular alignments. Miesowicz found that the three viscosities were ordered in magnitude as:

$$\eta_1 < \eta_3 < \eta_2$$

which was later confirmed by Porter and Johnson [58] for the same materials. Both Miesowicz and Porter and Johnson concluded from measurements of the viscosity of PAA in the absence of electric fields that the η_1 viscosity corresponded to the viscosity normally measured for liquid crystalline materials in the absence of electric fields. This they stated was due to flow induced orientation of the molecules parallel to the flow direction.

In addition to low molecular weight materials, recent investigators have been interested in the effect of electric fields on thermotropic liquid crystalline polymers [59,60]. Finkelman [59] performed a qualitative study aimed at determining if thermotropic liquid crystalline materials were susceptible to electric fields. He conducted his experiments by placing his samples in the hot stage of a polarizing microscope. The glass slides he used were modified so that an electric field could be applied to the space in which the sample was placed. The effect of the electric field was determined by measuring the scattered light intensity of the polarized light. In general, Finkelman found that the thermotropic copolyesters he was working with were susceptible to elec-

tric fields. The stronger the applied voltage the more quickly orientation was achieved. Finkelman found that upon termination of the electric field, the orientation relaxed within 5 secs. He further stated that his results were only qualitative because no boundary conditions were prescribed. The prescription of boundary conditions would decrease the relaxation time of the orientation produced by the electric field. It should also be noted that Finkelman did not measure rheological properties under the presence of the magnetic field.

While also not measuring rheological properties, Maret [60] determined the effect of electric fields on molecular orientation in thermotropic copolyesters. Maret's study is interesting in that in addition to forming nematic mesophases, some of his compounds formed cholesteric mesophases. Maret found that the cholesteric materials barely oriented at values of the applied electric field at which the nematic mesophases were completely oriented. Maret explained this by stating that before the cholesteric mesophases could orient, the helix must first untwist. According to Kelker [64] the electric field strength required to untwist low molecular weight cholesteric compounds is approximately 30 Telsa. Maret concluded that this value would be comparible for the thermotropic polyesters, and since he used a maximum field strength of 20 Telsa no orientation would be expected for his materials. In general, Maret concluded that orientation of the nematic materials is quite straightforward. First the material is raised above its thermal transition temperature from the solid to the liquid crystalline state. The temper-

ature should not, however exceed the temperature at which the material becomes isotropic. Doing so tends to decrease the orientation produced. Once the sample has melted, the field is applied. Maret found no correlation between the applied field strength or the cooling rate of the material on orientation development. In all cases a high degree of molecular orientation was achieved. Similar results have been reported by other investigators working with other systems [61,62,63].

The few results of the investigators just described are important from a theoretical standpoint. DeGennes [65] has shown that the theories of Ericksen [21] and Leslie [22] can predict different values of η based on the direction of molecular orientation with respect to the flow direction. The linear theory of Ericksen predicts that these viscosities are constant, while the non-linear form of the theory predicts that they will be a function of shear rate. In the experiments of Miesowicz, it was not possible to determine the shear rate dependence of viscosity. This is because employing large strains could possibly destroy the orientation produced by the electric field. Besides, for the low molecular weight materials, the viscosity is not a strong function of shear rate. For the polymeric materials, however, knowledge of the three Miesowicz viscosities and their shear rate dependence could help in determining the material parameters in the non-linear theory of Ericksen. Since Finkelman and Maret have shown that thermotropic liquid crystalline materials seem to be susceptible to electric fields, it should be possible to perform the same experiments as Miesowicz for these compounds. There is

even a report of a parallel plate rheometer designed to measure viscosity in the presence of electric fields [66]. Yet, there are no reports of such viscosity measurements for thermotropic or lyotropic liquid crystalline polymers in the literature. The only explanation may be that in order to make measurements of the three Miesowicz viscositites it must be certain that the molecules are in fact oriented in the proper direction. It is difficult to determine the exact orientation of the polymeric liquid crystalline molecules. Also, the time necessary to orient polymeric liquid crystalline materials can be expected to be an order of magnitude larger than the time necessary to orient the low molecular weight materials due the difference in size of the molecules. Thus, such measurements are not very straightforward.

2.2.2 ORIENTATION DEVELOPMENT DURING PROCESSING

While it is apparent from the previous discussion that electric fields can greatly influence the molecular orientation development in liquid crystalline materials, the fact that these materials can also orient under flow conditions is also of importance. The ease with which molecular orientation can be produced in the low molecular wieght materials has lead to their use in optical display devices [67]. For the polymeric substances, however, it appears that flow induced orientation is much more important. There have been very few studies of the orientation produced during flow for the lyotropic and thermotropic polymeric systems. Those which have been done have dealt mostly with fiber spin-

ning operations and the injection molding behavior of such materials. In this section these operations will be separately investigated, and the effect of shear and elongational flow on molecular orientation in polymeric liquid crystalline materials will be discussed.

2.2.2.1 FIBER SPINNING

The only area in which polymeric liquid crystalline materials have gained any industrial importance has been in the area of fiber spinning. In processing these materials the lyotropic materials are solution spun [7] while the thermotropic systems are melt spun [11]. In this section, the processing conditions used to produce these fibers will be reviewed and related to the degree of molecular orientation produced in each processing operation. In processing the lyotropic systems, two processes are available: wet spinning and dry-jet wet spinning. The only difference between these two processes is that in the case of wet spinning, the spinnerette is submerged in the coagulation bath. It seems, however, that the dry-jet wet spinning process results in fibers with a higher modulus than the wet spinning prosess. The reason for this increase is not clear, but may be due to the possibility of additional stretching of the filament between the spinnerette and the bath. To understand how orientation develops in the fiber spinning process of lyotropic materials, some of the specific processing conditions reported by Blades [68] for solutions of PPT in 100% H_2SO_4 are listed below:

Dope: 20% PPT in 100% H_2SO_4

Spinnerette: 50 holes/ 0.002" dia. / .01" long

Spin Stretch Factor: $Vf/\langle v \rangle = 6.9$

Extrusion conditions: $\langle v \rangle = 240$ ft/min

$T = 100^{\circ}C$

where $\langle v \rangle$ is the velocity of the fluid at the die exit, and Vf is the velocity of the take up rolls. Two important points can be derived from the above list. The extrusion rates used are very high leading to shear rates in the spinnerette of the order of 10^5 sec^{-1}. Also the spin stretch factor is not very high, indicating that the as-spun fiber is not stretched very much.

The process by which thermotropic copolyesters are spun differs slightly from that just mentioned for the lyotropic systems. In general, a much higher spin stretch factor is used, sometimes approaching 400 [69]. Also, the fibers are usually heat treated after being spun to enhance the physical properties.

In looking at the processing conditions for both the lyotropic and thermotropic systems, several similarities occur. Very small hole diameters are used, as are low length to diameter ratios. Therefore, the predominant flow regime is at the entrance region of the spinnerette hole which is mostly an extensional flow. In the case of the thermotropic systems, much larger spin stretch factors are used than with the lyotropic systems. Also, the thermotropic systems usually need to be heat treated to obtain maximum physical properties. In both cases, however,

the bulk of the physical strength is obtained in the as-spun fiber. Therefore, it appears that most of the molecular orientation generated in such fibers comes from the melt or solution state when the fluid passes through the spinnerette holes. Since this flow is an extensional flow, it appears that extensional flow has a great effect on molecular orientation.

2.2.2.2 INJECTION MOLDING

In order to understand the orientation produced in injection molding operations using thermotropic copolyesters a brief description of the injection molding process is given here. Many studies of the mold filling process have been performed which have aimed at being able to predict pressure distributions and velocity gradients within the mold cavity. It is from these sorts of experiments that the concept of the fountain flow effect [15] came about. In this case, the polymer fills the mold as an advancing front. At the front itself, polymer from the core region flows outward like a fountain towards the mold walls where it solidifies. As the polymer approaches the advancing front, it decelerates in the axial direction, and then accelerates in the radial direction towards the mold walls. Therefore, at the front the polymer experiences an extensional flow, while in the center of the mold the fluid experiences a shear flow. The effect of these two flow regimes causes a difference in molecular orientation as a function of distance from the mold walls [17,70]

The existence of two regimes of flow in mold filling is evident in the degree of molecular orientation measured as a function of distance from the mold wall. The orientation exhibits a maximum near the mold walls and decreases as the distance from the mold wall increases and approaches a minimum at the center of the mold [17]. Menges [70] determined the molecular orientation as a function of distance from the mold wall for polystyrene plaques as measured by shrinkage analysis. His results showed that a minimum in orientation existed at the center of the plaque, and that two maxima existed. One at the plaque surface, and another just in from the plaque surface. Menges stated that the second maximum was due to the formation of a thin solidified layer of polymer along the mold wall, which moved the maximum in shear stress from the mold wall to the solidified layer. Studies by Nguyen [71] have shown that the 60 mole% PHB/PET and 80 mole% PHB/PET copolyesters exhibit similar results as those of Menges for polystyrene. Nguyen was able to show by using a tracer technique that both thermotropic copolyesters filled a mold according to the fountain flow effect. There was a slight deviation, however, in that it seemed that the polymer would flow outward to the mold walls before reaching the advancing front.

Further studies [14,72] have shown that the difference in molecular orientation between the skin and core region is very pronounced for the 60 and 80 mole% PHB/PET copolymer systems. Wide angle x-ray scattering and chemical etching in conjunction with scanning electron microscopy studies by Joseph [72] have shown that at the skin layer, a high degree

of molecular orientation and a fibrous texture exists. At the core of the plaque, however, a low degree of molecular orientation is exhibited, and an unoriented sponge-like texture exists.

In summary, it is seen that in fiber spinning and injection molding processes utilizing liquid crystalline materials, a high degree of molecular orientation arises in the as-processed article. From the nature of the flow schemes in these processes, it appears that elongational flow is much more effective than shear flow in producing molecular orientation. In the case of injection molding, orientation may develop in the core region. However, this orientaion may relax due to the longer cooling times in the core.

2.2.3 SHEAR VERSUS ELONGATIONAL FLOW

As was just stated, it appears that elongational flow is mostly responsible for the molecular orientation which develops during the processing of liquid crystalline materials. Several investigators [18,73] have performed studies aimed at understanding further the differences in molecular orientation, morphology, and physical properties which arise as a function of the types of deformation for liquid crystalline materials. In each of these studies samples were prepared under controlled conditions of temperature and flow history. It is interesting to note that both investigators worked with thermotropic copolyesters and concluded that elongational flow was indeed much more effective than shear

flow in producing molecular orientation in the systems studied. At this point a more indepth discussion of these studies is given.

Ide and Ophir [18] investigated the effect of shear and elongational flow on molecular orientation and physical strength of extruded fibers. In their study, these researchers used an Instron capillary rheometer to extrude fibers of a thermotropic copolyester. Different shear rates were investigated as were different capillary lengths to determine the effect of shear strain. The extruded fibers were examined using WAXS, and the tensile modulus of the fibers was measured. For the extruded fibers not subjected to any elongational flow history, the WAXS patterns revealed a total absence of molecular orientation. The tensile modulus of these fibers was very low, and was not seen to be a function of shear rate or shear strain.

In order to impart some extensional flow history to the fibers, a second test was performed in which the extrudate was taken up at various speeds upon exiting the capillary. Ide found that these fibers possessed much higher values of tensile modulus than those fibers subjected only to shear flow. In addition, the modulus of these fibers was seen to be a linearly increasing function of strain rate. WAXS patterns of the extruded fibers showed that the fibers possessed a high degree of orientation which increased with increasing extension rate. Ide concluded that elongational flow was much more effective than shear flow in producing molecular orientation in liquid crystalline materials. He went on to

say that in injection molding processes, it is the fountain flow effect with its two regimes of flow which is responsible for the skin/core morphologies of injection molded plaques. The fact that the fibers subjected to extensional flow outside the capillary possessed higher physical properties than those subjected to only shear flow also suggests that most of the physical properties of injection molded plaques is probably due to the skin layer.

Zachariades [73] also investigated the effect of shear and elongational flow on orientation and morphology of thermotropic liquid crystalline systems. Zachariades examined the 80 mole% PHB/PET copolymer. He prepared samples subjected to only shear flow by shearing the material between flat plates. As the material was being sheared, the temperature was allowed to drop until the material solidified. In this way it is believed that any orientation produced would not relax. Samples subjected to extensional flow consisted of melt spun fibers. Zachariades investigated the effect of flow history and temperature on physical properties and morphological texture. He found that the sheared disks prepared in the method just described did in fact possess a small degree of molecular orientation. In all samples exhibiting a high degree of molecular orientation, a fibrillar texture was seen which seemed to lie perpendicluar to the flow direction. In measuring the physical properties of the sheared disks and extended samples it was found that the extended samples possessed the highest values of tensile and flexural modulus. Zachariades concluded that the temperature at which the sample

is sheared greatly affects the molecular orientation produced, as well as the physical properties.

In conclusion, there is much evidence to support the claim that elongational flow is much more effective than shear flow in producing molecular orientation in liquid crystalline polymers. An explanation of why shear flow is not so effective in producing molecular orientation may be derived from studies involving lyotropic systems. These materials are easier to investigate in that some of them are transparent which allows the use of rheo-optical methods. It is generally accepted that when a lyotropic or thermotropic system enters the liquid crystalline mesophase the molecules spontaneously orient and form domains in which all the molecules are oriented along a given direction. This superstructure has been termed a polydomain structure [76,77]. Horio [75] has observed that for lyotropic liquid crystalline systems, when shearing is applied to the polydomain structure, the domains are broken up into smaller domains that rotate as they flow. In this case, no flow birefringence is observed indicating that no molecular orientation is present. Asada [76] and Onogi [77] have also shown that shearing can break up the polydomain structure. In elongational flow, however, a number of investigators have reported that strong birefringence is observed indicating the presence of a high degree of molecular orientation [76,77,78]. Unfortunately, most thermotropic liquid crtystalline systems are opaque which does not allow for the use of rheo-optic methods. However, since it is believed that both the thermotropic and lyotropic systems form the same polydo-

main structure it may be possible to extend the results of the lyotropic systems to the thermotropic systems.

2.2.4 SUMMARY

In the previous discussion it has been shown that molecular orientation in liquid crystalline materials can be achieved through the use of electric fields, or through the use of extensional flow. In the case of polymeric liquid crystalline materials, flow induced orientation seems to be much more important.

Although the studies mentioned give valuable information regarding the behavior of liquid crystalline materials in different flow schemes, some important questions remain. None of the studies mentioned determined whether or not a minumum deformation rate exists for the development of molecular orientation in shear or extensional flow. No annealing experiments were done to determine how long any orientation produced in shear or extensional flow would remain in the melt state. Also, none of the studies examined the morphological textures produced in each flow situation to determine whether a specific texture is associated with molecular orientation. These experiments would be quite useful in defining more clearly what occurs to the structure of a liquid crystalline fluid during mold filling or fiber spinning operations. Such studies would also help in understanding the transient rheological behavior of such fluids.

Some of the results of studies aimed at determining the effect of shear and elongational flow on molecular orientation have direct bearing on the evaluation of a continuum theory for these materials. For instance, if Ericksen's theory is used in its non-linear form, it is possible to predict that in shear flow molecular orientation will be a function of shear rate. There is experimental evidence, however, which would indicate that the orientation produced in shear flow is not a function of shear rate. Thus, the linear theory should be applicable at least in the cases mentioned so far.

In the next section some possible choices for constitutive equations for liquid crystalline fluids will be investigated. The predictions of these theories will be discussed in light of the previous data concerning the rheological and orientaion behavior of liquid crystalline fluids.

2.3 CONTINUUM THEORIES FOR ANISOTROPIC FLUIDS

In the previous sections, the rheological behavior of liquid crystalline polymers and the nature in which these fluids can orient in the presence of electric fields or in shear and extensional flows was discussed. Some of the rheological behavior exhibited by these materials appears to be related to the development of molecular orientation during flow. For instance, certain thermotropic systems were shown to exhibite shear history dependent rheological properties. Such behavior was attributed to shear induced orientation effects.

Many attempts have been made at forming continuum theories for liquid crystalline materials. Perhaps the first theories were those of Anzelius [79] and Oseen [19]), which was later revised by Frank [20]. These theories dealt with the liquid crystalline material in its static or equlibrium state and sought to predict the effect of magnetic fields on molecular orientation. More recently, Ericksen [21,80-89] and Leslie [26,90-93] developed a set of continuum relationships for both nematic and cholesteric liquid crystalline fluids. Many other alternative representations for nematic liquid crystalline materials have appeared including those of Davison [94,95], Davison and Amos [96], Martin and co-workers [97], Aero and Bulygin [98], Helfrich [99-102], Lee and Lee and Eringen [103-106], and Jahnig and Schmidt [107] According to Shainpoor [108], many of the above theories are very similar to those of Ericksen and Leslie.

Besides the theories just mentioned which were derived specifically for nematic liquid crystalline fluids, other attempts have been made at formulating constitutive relationships for anisotropic fluids. These include the theories of Hand [24], and Duffy [25,110-113] Hand's theory contains the Ericksen theory as a special case, and is particularly suitable for use with suspensions of spheroidal particles. Duffy has attempted to model fluid anisotropy by using a fourth rank viscosity tensor.

The purpose of this section will be to review several recently proposed constitutive equations designed for anisotropic fluids. Specifically, this discussion will include the theories of Hand, Duffy, and Leslie and Ericksen which were mentioned in the introduction. In each case, the major assumptions involved in the derivation of each theory will be presented. The predictions of each theory for simple shear flow behavior will be discussed. The drawbacks of each theory will be pointed out, and the section will end with recommendations for the choice of one theory for investigation.

2.3.1 THE THEORY OF ERICKSEN

Both Ericksen and Leslie have derived constitutive equations for use with anisotropic fluids. The theories of both investigators are the same except for extra terms in the theory of Leslie which account for the effects of external forces such as electric or magnetic fields. The pur-

pose of this section will be to discuss the derivation and predictions of Ericksen's anisotropic fluid theory. Basically, Ericksen has derived a set of equations which describe the extra or Ericksen stresses which arise due to moleclular orientation effects. Ericksen specifies a vector, $\underline{n}$, called the director, to account for fluid anisotropy. The director always points along the direction of preferred orientation of the fluid particles which are assumed to be rigid rods.

In deriving his theory, Ericksen has assumed that the stress tensor, $\underline{\underline{T}}$, is an isotropic function of the velocity gradients, and the state of the director, $\underline{n}$. The molecules are specified to be rigid rods, therefore:

(1) $\sum_i n_i\, n_i = 1$

The rate-of-deformation and vorticity tensors are defined as:

(2) $d_{ij} = 1/2(V_{i,j}+V_{j,i})$

(3) $\omega_{ij} = 1/2(V_{i,j}-V_{j,i})$

where: $V_{i,j} = \partial V_i / \partial X_j$

The stresses and the state of the director are taken to be functions of the director itself, and the velocity gradients as follows:

(4) $\tau_{ij} = \tau_{ji} = -P\delta_{ij} + f_{ij}(n_k, V_{m,n})$

(5) $\dot{n}_i = g_i(n_k, V_{m,n})$

where: τ_{ij} = The ij^{th} component of the Stress Tensor

P = Isotropic Pressure

δ_{ij} = Unit Matrix

$\dot{n}_i$ = Material Derivative of n_i.

Ericksen stipulates that the functions f_{ij} and g_i must be of the same form in all arbitrarily moving right or left handed coordinate systems. Noll [116] has found the correct form the functions f and g must take in order to be invariant under all time-dependent orthogonal transformations. He found that the velocity gradients must be replaced by the rate-of-deformation tensor, and that the material derivative of $\underline{n}$ must be replaced by the Jauman derivative defined as:

(6) $$\hat{n}_i = \dot{n}_i - \omega_{ij} n_j = g_i(n_k, d_{mn})$$

The function f_{ij} can be expressed in terms of two isotropic tensors, $\underline{d}$ and $\underline{N}=\underline{nn}$. Rivlin [115] has written the most general form of a symmetric tensorial function of two other symmetric tensors. Therefore, $\underline{f}$ may be written as:

(7) $$\underline{f}=\alpha_1\underline{N}+\alpha_2\underline{d}+\alpha_3\underline{d}^2+\alpha_4(\underline{Nd}+\underline{dN})+\alpha_5(\underline{Nd}^2+\underline{d}^2\underline{N})$$

in which the fluid has been assumed to incompressible, and the α's are functions of the invariants:

(8) $$\Sigma V_{i,i} = 0$$

$$\mathrm{tr}\underline{N} = n_i n_i$$

$$\mathrm{tr}\underline{Nd} = d_{ij} n_i n_j$$

(9) $$\mathrm{tr}\underline{Nd}^2 = d_{ik} d_{kj} n_i n_j$$

$$\mathrm{tr}\underline{d}^2 = d_{ij} d_{ij}$$

$$\mathrm{tr}\underline{d}^3 = d_{ij} d_{jk} d_{ki}$$

(tr=the trace of the tensor)

Similarly, $\underline{\hat{n}}$ is an isotropic function of $\underline{d}$ and $\underline{n}$. Using the facts noted

above, and the Cayley-Hamilton theorem for $\underline{\underline{d}}$ allows replacement of higher order terms in $\underline{\underline{d}}$ by $\underline{\underline{d}}$ and $\underline{\underline{d}}^2$:

(10) $$g_i = \beta_1 n_i + \beta_2 d_{ij} n_j + \beta_3 d_{ik} d_{kj} n_j$$

where the β's are functions of the above invariants. Imposing the rigid rod constraint on $\underline{n}$ gives:

(11) $$n_i \dot{n}_i = n_i \hat{n}_i = n_i g_i = 0$$

which leads to the following form for the director equation:

(12) $$g_i(n_k, d_{mn}) = \beta_2 (d_{ij} n_j - d_{km} n_k n_m n_i) + \beta_3 (d_{ik} d_{kj} n_j - d_{km} d_{mp} n_k n_p n_i)$$

At this point, Ericksen linearizes both equations for f_{ij} and g_i by dropping out all terms involving $\underline{\underline{d}}^2$ and higher. Thus, the stress and director equations become:

(13) $$\tau_{ij} = \tau_{ji} = -P\delta_{ij} + 2\mu d_{ij} + (\mu_1 + \mu_2 d_{km} n_k n_m) n_i n_j + 2\mu_3 (d_{jk} n_k n_i + d_{ik} n_k n_j)$$

(14) $$\hat{n}_i = n_i - \omega_{ij} n_j = \lambda (d_{ij} n_j - d_{km} n_k n_m n_i)$$

where the μ's and λ are constants. The major equations of Ericksen's linear anisotropic fluid theory are now complete. At this point, the major predictions of the linear form of the theory will be analyzed. It will then be obvious that the non-linear theory is perhaps more valid for the description of liquid crystalline fluid behavior.

2.3.1.1 PREDICTIONS OF ERICKSEN'S LINEAR THEORY

In this section, the predictions of the linear form of the Ericksen-Leslie anisotropic fluid theory for simple shear flow will be analyzed. The shear and normal stresses will be a function of the state of the director. It is more convenient, therefore, to begin with a description of the predictions of the director equations.

Steady shear flow is defined in the following manner:

(15) $V_1 = \dot{\gamma} X_2 \quad V_2 = V_3 = 0$

where $\dot{\gamma}$ is the shear rate (a constant). The rate-of-deformation and vorticity tensors have the following forms:

(16) $$\underline{\underline{d}} = \dot{\gamma}/2 \begin{bmatrix} 0 & 1 & 0 \\ 1 & 0 & 0 \\ 0 & 0 & 0 \end{bmatrix} \qquad \underline{\underline{\omega}} = \dot{\gamma}/2 \begin{bmatrix} 0 & 1 & 0 \\ -1 & 0 & 0 \\ 0 & 0 & 0 \end{bmatrix}$$

Use of equation [14] gives three coupled differential equations for the three components of the director:

(17) $\dot{n}_1 = 1/2\dot{\gamma} n_2 (\lambda + 1 - 2\lambda n_1^2)$

(18) $\dot{n}_2 = 1/2\dot{\gamma} n_1 (\lambda - 1 - 2\lambda n_2^2)$

(19) $\dot{n}_3 = -\lambda \dot{\gamma} n_1 n_2 n_3$

Two facts are apparent concerning the above equations. In order to solve them an initial condition is needed, and the value of λ must be specified. At steady state, $\dot{n}_1 = 0$ and so it is possible to arrive at the steady state position of the director. Ericksen has found that the

steady state direction of the director depends on λ in the following way:

$$(20) \qquad n_2/n_1=\tan\theta = \left[\frac{\lambda-1}{\lambda+1}\right]^{1/2}$$

in which θ defines the angle between the director and the direction of flow (X_1). Three different conditions exist depending on the value of λ chosen. If $|\lambda|>1$, then $0<\theta\leq 45$ as defined by equation [20]. If $|\lambda|=1$, then $\theta=0$ and the director aligns perfectly along the shear direction. If $0<|\lambda|<1$, then the solution is unstable, and the director tumbles in space. These results are summarized below:

$$(21) \qquad \begin{array}{llll} 1<\lambda & 0<\theta\leq 45 & n_1\neq n_2\,, & n_3=0 \\ \lambda=1 & \theta=0 & n_1=1, & n_2=n_3=0 \\ 0<\lambda<1 & \text{unstable} & n_1\neq n_2\neq n_3 & \end{array}$$

The above results indicate that certain combinations of λ and initial conditions will affect the predictions of the theory. For instance, if $\lambda=1$, and the initial condition is $n_1=1$, then all three director equations will be equal to zero. The initial condition is equivalent to the steady state solution. If an initial condition of $n_3=1$ were specified, then again all three differential equations for $\dot{n}_1$, $\dot{n}_2$, and $\dot{n}_3$ will be equal to zero (see equations [17]-[19]), thus, specifying steady state conditions. An initial condition of $n_3=1$ specifies that the fluid particles are lying perfectly within a plane of shear. Due to the kinematics of simple shear flow, there would be no driving force to align the fluid particle and so the predictions of Ericksen's theory are qualitatively correct.

The predictions of Ericksen's theory for the shear and normal stesses are calulated through substitution of equation [16] into equation [13] which yields:

(22) $$\tau_{12} = \mu_1 n_1 n_2 + [\mu + \mu_2 n_1^2 n_2^2 + \mu_3 (n_1^2 + n_2^2)]\dot{\gamma}$$

(23) $$\tau_{11} - \tau_{22} = \mu_1 (n_1^2 - n_2^2) + (n_1^2 - n_2^2)\mu_2 n_1 n_2 \dot{\gamma}$$

(24) $$\tau_{22} - \tau_{33} = \mu_1 (n_2^2 - n_3^2) + (n_2^2 - n_3^2)\mu_2 n_1 n_2 \dot{\gamma} + 2\mu_3 n_1 n_2 \dot{\gamma}$$

It can be seen that both the shear and normal stresses are linear in shear rate ($\dot{\gamma}$). Thus, the apparent viscosity, $\eta = \tau_{12}/\dot{\gamma}$, will be a constant independant of shear rate (the μ's are constants). It was shown in section 2.1 that most liquid crystalline polymers exhibit a region of shear rate dependent viscosity. Therefore, the linear form of Ericksen's anisotropic fluid theory does not seem to be adequate for the description of liquid crystalline fluid behavior. In the case of $\mu_1 \neq 0$, the theory predicts the existence of a yield stress in both the shear and normal stresses. Although some liquid crystalline polymers seem to exhibit yield stresses, it is not certain whether these yield stresses are due to the liquid crystalline nature of the material. Besides the inconsistences just mentioned, there remains the problem of specifying the initial conditions for the director, the value of λ, and the four μ values. In all, there are five independent variables to be specified ($\lambda, \mu - \mu_3$). In section 2.2 it was shown that liquid crystalline fluids do not appear to orient well in shear flow. Therefore, it is not certain what value of λ to choose. The difficulty of specification of all the necessary material parameters along with the inability of the linear theory to predict a shear rate dependent viscosity makes the linear theory unsuitable for

investigation. It is apparent that the non-linear form of the theory may be more appropriate as it at least allows for shear rate dependant material parameters.

2.3.1.2 PREDICTIONS OF ERICKSEN'S NON-LINEAR THEORY

In the previous section, it was shown that the linear form of the Ericksen anisotropic fluid theory is inadequate for describing the viscosity behavior of liquid crystalline polymers. In this section, the predictions of the non-linear form of Ericksen's equations will be examined. The non-linear form of the theory allows for the specificaion of shear rate dependent material parameters. Therefore, it should be possible to predict a shear rate dependent viscosity function.

Although the non-linear form of the stress equation will be used, it is more convenient to use the linearized form of the director equations. This is equivalent to setting $\beta_3=0$, and $\beta_2=\lambda$ in equation [12]. This is being done because the non-linear form of the director equations would predict that the final state of the director would depend on shear rate. It was shown in section 2.2, however, that Ide [18] did not see a shear rate dependence in the amount of molecular orientation produced in a thermotropic copolyester subjected to shear flow. For the purposes of this investigation, therefore, the linear forms of the director equations will be used. It is possible, however, that actual experimental evidence, in the form of WAXS measurements, will indicate a shear

rate dependence of molecular orientation. In this case, the non-linear forms of the director equations would have to be used. The predictions of the linear director equations have already been discussed. If equation [16] is substituted into equation [7], the following equations for the non-linear shear and normal stresses result:

(25) $$\tau_{12} = \alpha_1 n_1 n_2 + \alpha_2 \dot{\gamma}/2 + \alpha_4 \dot{\gamma}(n_1^2+n_2^2)/2 + 1/2(\alpha_5 \dot{\gamma}^2 n_1 n_2)$$

(26) $$\tau_{11} - \tau_{22} = \alpha_1 (n_1^2 - n_2^2) + \alpha_5 \dot{\gamma}^2 (n_1^2 - n_2^2)/2$$

(27) $$\tau_{22} - \tau_{33} = \alpha_1 (n_2^2 - n_3^2) + \alpha_3 \dot{\gamma}^2 + \alpha_4 n_1 n_2 \dot{\gamma} + \alpha_5 n_2^2 \dot{\gamma}^2/2$$

The α's in the above equations are functions of the invariants defined in equation [9]. Therefore, a shear rate dependent viscosity function is predicted ($\eta = \tau_{12}/\dot{\gamma}$). It can be seen that if $\alpha_1 \neq 0$, a yield stress will be predicted for both the shear and normal stresses just as in the linear form of the theory.

Although the non-linear form of Ericksen's theory may be more realistic for use with liquid crystalline polymers than the linear form in that it allows for a shear rate dependent viscosity, the non-linear theory is more difficult to evaluate. In the linear theory there are five independent variables to specify ($\lambda, \mu - \mu_3$). In the non-linear form of the theory there are six independent variables which must be specified ($\lambda, \alpha_1 - \alpha_5$) which are now functions of shear rate. Even given that α_1 is equal to zero due to the absence of a yield stress, there are still too many material parameters to be specified. In simple shear flow, only three material parameters are measureable, the viscosity (η) and the normal stress

differences (N1,N2). Therefore, only three of the six material parameters in Ericksen's theory could be specified.

It is apparent that while the Ericksen theory offers a very simplified approach to the specification of a constitutive equation for use with anisotropic fluids, there are a number of difficulties associated with using the theory. The linear form of the theory does not adequately describe the viscosity behavior of liquid crystalline polymers. While the non-linear version of the theory seems to be more realistic, there are too many material parameters in the theory which need to be specified. So far, only the steady shear flow predictions of the theory have been investigated. It would be instructive to determine the predictions of the theory for transient tests, such as stress growth, to determine whether stress overshoot can be predicted. This brings up another problem with the Ericksen theory, that of specifying an initial condition for the position of the director. It was shown that certain combinations of λ and initial conditions would lead to different results. The effect of initial conditions on the prediction of stress growth behavior is unknown. Finally, it is not known what the theory would predict for the behavior of the fluid under conditions of extensional flow. In section 2.2 it was shown that liquid crystalline fluids appear to orient more in extensional flow than in shear flow. It is not known whether the Ericksen theory would predict such behavior.

Clearly, a quantitative investigation of Ericksen's theory is not

possible due to the difficulty in evaluating the many material parameters needed. It may be possible, however, to conduct a qualitative study of the predictions of the theory for other flow situations. It may also be possible that a more suitable theory exists for investigation. In the next section, the approach of G. L. Hand for the specification of a constitutive equation for anisotropic fluids will be discussed.

2.3.2 THE THEORY OF HAND

In the previous section, the constitutive theories of Ericksen and Leslie were discussed. It was shown that these theories model fluid anisotropy by incorporating a vector, called the director, into the stress equations. Thus, the stresses were written as a function of the rate-of-deformation tensor, $\underline{\underline{d}}$, and the orientation of the fluid particles as expressed by the director, $\underline{n}$. The fluid particles were assumed to be rigid rods. In this section, the ideas of G. L. Hand (1962) will be discussed.

Hand has chosen to model fluid anisotropy through the use of a general tensor of his own invention called the structure tensor, $\underline{\underline{A}}$. The structure tensor is a symmetric tensor which describes the microstructure of the fluid. Hand has derived the equations describing the components of $\underline{\underline{A}}$ in such a way that the fluid particles are assumed to be spherical at rest. At low shear rates the fluid particles remain spherical, but at higher shear rates the particles become ellipsoidal with the

major axis of the ellipsoid oriented along the flow direction. In order to understand in more detail the predictions of Hand's theory, a brief description of his derivation is given here.

In keeping with the ideas set forth by Ericksen, Hand assumed that the stress tensor, $\underline{\tau}$, could be written as a function of two symmetric tensors, the rate-of-deformation tensor, $\underline{d}$, and his symmetric structure tensor, $\underline{A}$. Therefore:

(28) $$\tau_{ij} = f_{ij}(d_{km}, A_{op})$$

The deformation and vorticity tensors are defined as in equations [15] and [16]. The incompressibility condition of equation [8] is stipulated, and Hand used the the results of Rivlin [115] to write the most general form of $\underline{f}(\underline{d},\underline{A})$ as:

(29) $$\underline{\tau} = \underline{f}(\underline{d},\underline{A}) = \alpha_0\underline{\delta}+\alpha_1\underline{A}+\alpha_2\underline{d}+\alpha_3\underline{A}^2+\alpha_4\underline{d}^2+\alpha_5(\underline{Ad}+\underline{dA})$$
$$+\alpha_6(\underline{A}^2\underline{d}+\underline{dA}^2)+\alpha_7(\underline{Ad}^2+\underline{d}^2\underline{A})+\alpha_8(\underline{A}^2\underline{d}^2+\underline{d}^2\underline{A}^2)$$

The α's are functions of the invariants listed in equation [9]. In order to simplify his equations, Hand linearized equation [29] in a manner similar to that of Ericksen by dropping out all terms in $\underline{d}^2$ and higher. This gives:

(30) $$\underline{\tau} = (\mu_0+\mu_1 tr\underline{A}+\mu_2 tr\underline{Ad})\underline{\delta}+\mu_3\underline{A}+(\mu_4+\mu_5 tr\underline{A})\underline{d}+\mu_6(\underline{Ad}+\underline{dA})$$

in which the μ's are considered to be constants.

In order to be able to specify all the unknowns in his theory, Hand then wrote down the equations needed to specify the form of the structure tensor. In keeping with the work of Ericksen, Hand assumed that a const-

itutive equation of the following form would be needed to determine the components of the structure tensor:

(31) $\dot{A}_{ij}=g_{ij}(A_{kl},V_{m,n})$

Noll [116] has found the correct form equation [31] must take in order to be invariant under time-dependent orthogonal transformations. He found that the velocity gradients must be replaced by the rate-of-deformation tensor, and the material derivative of $\underline{\underline{A}}$ must be placed by the Jauman derivative defined as:

(32) $\hat{A}_{ij} = \dot{A}_{ij} - \omega_{ik}A_{kj} + A_{ik}\omega_{kj}$

where the vorticity tensor, $\underline{\underline{\omega}}$, has already been defined in equation [16]. This operation is exactly the same as that used by Ericksen to insure invariance of his equations. Using the results of Rivlin [115], Hand specified the most general form for $\underline{\underline{A}}$:

(33) $$\hat{\underline{\underline{A}}}=\underline{\underline{\omega A}}-\underline{\underline{A\omega}}+\beta_0\,\underline{\underline{\delta}}+\beta_1\,\underline{\underline{A}}+\beta_2\,\underline{\underline{d}}+\beta_3\,\underline{\underline{A}}^2+\beta_4\,\underline{\underline{d}}^2+\beta_5(\underline{\underline{Ad}}+\underline{\underline{dA}})$$
$$+\beta_6(\underline{\underline{A}}^2\underline{\underline{d}}+\underline{\underline{dA}}^2)+\beta_7(\underline{\underline{Ad}}^2+\underline{\underline{d}}^2\underline{\underline{A}})+\beta_8(\underline{\underline{A}}^2\underline{\underline{d}}^2+\underline{\underline{d}}^2\underline{\underline{A}}^2)$$

where the β's are functions of invariants similar to those listed listed in equation [9]. In order to make theory more tractable, Hand linearized equation [33] with respect to the rate-of-deformation tensor to yield:

(34) $$\dot{A}_{ij}=\omega_{ik}A_{kj}-A_{ik}\omega_{kj}+\delta_{ij}(\lambda_0+\lambda_1\,trA+\lambda_2\,trAd)+A_{ij}\lambda_3$$
$$+d_{ij}(\lambda_4+\lambda_5\,trA)+(A_{ik}d_{kj}+d_{ik}A_{kj})\lambda_6$$

where now the λ's are constants as in Ericksen's theory. At this point, the derivation of Hand's theory is complete. In the next section, the predictions of his theory for simple shear flow will be investigated.

2.3.2.1 PREDICTIONS OF HAND'S ANISOTROPIC FLUID THEORY

In the previous section, it was shown that the derivation of Hand's anisotropic fluid theory is similar to the derivation of the theory of Ericksen. The final equations of Hand differ, however, in that he retains more terms in his stress and structure tensor equations. In this section, the predictions of his equations for steady simple shear flow will be analyzed.

Steady simple shear flow has already been defined in equations [15] and [16]. In order to calculate the predictions of Hand's anisotropic fluid theory, equation [16] must be substituted into equations [30] and [34]. There are six independent components of the structure tensor. Therefore, there are six coupled differential equations, defined by equation [34], which must be solved in order to calculate the stresses. The six components of equation [34] are in detail:

$$
\begin{aligned}
\dot{A}_{11} &= \lambda_0+(\lambda_1+\lambda_3)A_{11}+\lambda_1 A_{22}+\lambda_1 A_{33}+\dot{\gamma}(\lambda_6+\lambda_2+1)A_{12} \\
\dot{A}_{22} &= \lambda_0+(\lambda_1+\lambda_3)A_{22}+\lambda_1 A_{11}+\lambda_1 A_{33}+\dot{\gamma}(\lambda_6+\lambda_2-1)A_{12} \\
\dot{A}_{33} &= \lambda_0+(\lambda_1+\lambda_3)A_{33}+\lambda_1 A_{11}+\lambda_1 A_{22}+\dot{\gamma}\lambda_2 A_{12} \\
\dot{A}_{12} &= 1/2\dot{\gamma}[\lambda_4+(\lambda_6+\lambda_5-1)A_{11}+(\lambda_6+\lambda_5+1)A_{22}+\lambda_5 A_{33}+\lambda_3 A_{12}] \\
\dot{A}_{13} &= 1/2\dot{\gamma}(\lambda_6+1)A_{23}+\lambda_3 A_{13} \\
\dot{A}_{23} &= 1/2\dot{\gamma}(\lambda_6-1)A_{13}+\lambda_3 A_{23}
\end{aligned}
\tag{35}
$$

From the last two expressions of equation [35], Hand notes that in order to obtain a steady state solution, the shear rate ($\dot{\gamma}$) must satisfy the following condition:

$$
\dot{\gamma} < -2\lambda_3/(\lambda_6^2-1)^{1/2} \tag{36}
$$

The above relationship is equivalent to specifying $\lambda_3 < 0$, and $|\lambda_6| > 1$. Hand also notes that if λ_0 and λ_4 are zero, then the particles remain spherical for large times until a critical shear rate is reached. At this point, the spheres would begin to deform into ellipsoidal particles.

In order to solve for the steady state stresses, Hand first determined the steady state values of the components of the structure tensor by setting the right hand side of equation [35] to zero. In order to determine the orientation of the ellipsoid with respect to the shear direction, Hand found the eignevectors of $\underline{A}$. These three eigenvectors are unit vectors which point along the major axes of the ellipsoid. Hand's theory predicts that at rest, the particles are spherical. At low shear rates the sphere elongates into an ellipsoid. The larger of the two principle axes of the ellipsoid in the (X1,X2) shear plane will lie at an angle of approximately 45 degrees from the X1 axis. (This is equivalent to the condition in Ericksen's theory in which λ is larger than 1.) As the shear rate is increased, the angle made between the principle axis of the ellipsoid and the X1 axis decreases. For very high shear rates, the ellipsoid aligns itself perfectly along the flow direction, X1. Thus, Hand's theory can predict a shear rate dependence of the degree of molecular orientataion.

At this point, it is possible to analyze the predictions for the steady state shear and normal forces. In terms of the various components of the structure tensor, the equations for the stresses are:

(37) $$\tau_{12} = \mu_3 A_{12} + \dot{\gamma}(\mu_4 + \mu_5 \mathrm{tr}A)/2 + \dot{\gamma}\mu_6 (A_{11}+A_{22})/2$$

(38) $$\tau_{11} - \tau_{22} = \mu_3 (A_{11} - A_{22})$$

(39) $$\tau_{22} - \tau_{33} = \mu_3 (A_{22} - A_{33}) + \mu_6 A_{12}\dot{\gamma}$$

In order to calculate the actual values of the steady state stresses, the components of the structure tensor must be substituted into the above equations. After performing the necessary substitutions and much simplification, the following final equations for the apparent viscosity and primary normal stress differences are achieved:

(40) $$\eta = \tau_{12}/\dot{\gamma} = (m+n\dot{\gamma}^2)/(p+q\dot{\gamma}^2)$$

(41) $$\tau_{11} - \tau_{22} = \dot{\gamma}^2/(p+q\dot{\gamma}^2)$$

in which m,n,p, and q are constants. It can be seen that as $\dot{\gamma}$ approaches zero, the primary normal stress difference tends to $\dot{\gamma}^2/p$, and as $\dot{\gamma}$ approaches infinity, the primary normal stress difference tends to 1/q. The viscosity approaches m/p as $\dot{\gamma}$ goes to zero, and n/q as $\dot{\gamma}$ goes to infinity. Thus, it can be seen that Hand's theory predicts a shear dependent viscosity with zero and infinite shear values. In addition, the constants m,n,p and q are easily calculated from steady shear data. Baird [50] has used Hand's theory to correlate the behavior of anisotropic solutions of PPT in 100% H_2SO_4 with good success. These results would tend to suggest that the liquid crystalline domain structure may behave as ellipsoids in solution. If Hand's theory is correct, there should be a critical shear rate at which the domains change from being spherical and become ellipsoidal.

It has been shown that Hand's anisotropic fluid theory is extermely

similar to that of Ericksen. Hand chooses to express the stresses a function of a structure tensor, whereas Ericksen expresses the stresses in terms of the director. A more indepth study shows other differences. Hand's linear theory predicts a shear dependent viscosity function. His theory can be simplified to the point where only four material parameters are needed to predict the steady state rheological properties. His linear theory also predicts that the direction of preferred orientation of the particles will be a function of shear rate. In effect, the linearized version of Hand's theory is capable of predicting the same behavior as the non-linear theory of Ericksen, offering a more simplified approach. There are, however, several aspects of Hand's theory which make it much more difficult to use than Ericksen's. Most important of these is the complexity of the structure tensor. A higher number of differential equations must be solved in Hand's theory in order to determine the state of orientaion of the fluid particles. In addition, these differential equations contain many more constants than those of Ericksen. One consequence of the added complexity of the structure tensor is that it makes calculation of the transient stress growth predictions very difficult. Also, there is no physical significance to the structure tensor. Thus, it is not obvious how the structure tensor should be formed for different anisotropic fluid behavior. It is also not known how the components of the structure tensor could be determined experimentally.

The theories discussed so far have attempted to model fluid anisotropy by expressing the stress tensor as a function of two symmetric

tensors; the rate-of-deformation tensor and a tensor related to fluid structure. In both cases, the fluid was assumed to be isotropic at rest and was predicted to become anisotropic during flow. In the next section, a more classical approach to the formulation of a constitutive equation for anisotropic fluids will be discussed.

2.3.3 THE THEORY OF DUFFY

Duffy (1978) has derived his constitutive model based on well known continuum mechanics principles. Assuming that the strain energy function, U, can be expanded in a power series in the rate-of-deformation tensor, the following relationship holds:

(42) $U=\alpha+\beta_{ij}\,d_{ij} + \Gamma_{ijkl}\,d_{ij}\,d_{kl}+\ldots..$

where:

U = strain energy

$\alpha,\underline{\beta},\underline{\Gamma}$ are constants

Normally, the strain energy can be referenced to any zero point. Therefore, α can be taken to be zero. Since the reference point should be one in which the stresses go to zero, β is also taken to be zero. Finally, since a linear expression is preferable, all higher order terms are neglected, therefore:

(43) $U = \Gamma_{ijkl}\,d_{ij}\,d_{kl}$

In order to calculate stress from the strain energy function, the partial of the strain energy function with respect to the rate-of-deformation tensor is taken:

(44) $\tau_{ij} = \partial U/\partial d_{ij}$

which yields:

(45) $\tau_{ij} = \Gamma_{ijkl}\,d_{kl}$

where it should be mentioned that $\underline{\Gamma}$ is in fact a fourth rank tensor. If at this point symmetry arguments are introduced, it is possible to show

for an isotropic, homogeneous, Newtonian fluid:

(46) $\tau_{ij} = \eta d_{ij}$

where η is a constant called the viscosity and is a result of performing the symmetry operations on $\underline{\Gamma}$. Equation [46] is known as Newton's law of viscosity. In deriving his theory, Duffy took equation [45] as his starting point. He decided to leave $\underline{\Gamma}$ as a fourth rank tensor and introduce fluid anisotropy through manipulation of the various components of $\underline{\Gamma}$. In defining his treatment, Duffy first writes his equations in terms of a co-ordinate system, ξ, which is convected with the fluid according to Oldroyd [114]. The equations are then transformed to a co-ordinate system X, which is fixed in space. Duffy breaks the stress into two components:

(47) $T(\xi,t) = T'(\xi,t) - P(\xi,t)\delta$

where: T = Total stress

T' = Extra stress due to deformation of fluid

P = Isotropic pressure

δ = Unit tensor

t = Time

To complete the specification of his model, the extra stress is related to the kinematic variables by:

(48) $T'_{ijkl} = 2\eta_{ijkl} d_{kl}$

with:

(49) $\eta_{ijkl} = 1/2\eta_o (\delta_{ik}\delta_{jl} + \delta_{il}\delta_{jk}) + 1/2\Lambda_{ijkl}$

where:

$\underline{\eta}$ = Anisotropic viscosity tensor

$\underline{d}$ = Rate-of-deformation tensor (equation [16])

$\underline{\delta}$ = Kronecker delta (unit tensor)

$\underline{\underline{\Lambda}}$ = Fourth rank stress tensor

Duffy assumes that there are no finite body couples per unit mass in the fluid and so the stress tensor is symmetric with:

(50) $\Lambda_{ijkl} = \Lambda_{jikl}$

which leaves thirty-six independent components of $\underline{\underline{\Lambda}}$. In general, the components of $\underline{\underline{\Lambda}}$ will be a function of time and position as the orientation of the fluid molecules will change during flow. However, if at time t=0 all the fluid particles are uniformly oriented, and if a Cartesian co-ordinate system is chosen, the components of $\underline{\underline{\Lambda}}$ are known constants for the whole material. Duffy then specifies that at t=0 a Cartesian co-ordinate system exists in which at every point in the fluid, the molecules are aligned along the 3-direction. Thus, for the fluid to be transversely isotropic with respect to the 3-direction, the stress tensor has at most six independent components:

(51) $\Lambda_{3333} = C \quad \Lambda_{1313} = \Lambda_{2323} = E \quad \Lambda_{1122} = \Lambda_{2211} = G \quad \Lambda_{1212} = H$

$\Lambda_{3311} = -D \quad \Lambda_{1133} = \Lambda_{2233} = -F \quad \Lambda_{1111} = \Lambda_{2222} = G+2H$

where all other components not related to those above by symmetry are zero, and C, D, E, F, G, H, are constants.

At this point Duffy transforms his equation to the fixed Cartesian co-ordinate system with:

(52) $\tau_{ij} = \tau'_{ij} - P\underline{\delta}$

where now τ_{ij} is the total stress and τ'_{ij} is the extra stress which is giv-

en by:

(53) $\tau'_{ij} = 2\eta_o d_{ij} + \Lambda_{ijkl} d_{kl}$

The anisotropic stress tensor in the convected coordinate frame, Λ, is transformed to an anisotropic stress tensor, B, in the fixed coordinate frame:

(54) $$B_{ijkl} = \frac{\partial \xi_m}{\partial X_i}\frac{\partial \xi_n}{\partial X_j}\frac{\partial X_k}{\partial \xi_o}\frac{\partial X_l}{\partial \xi_p}\ \Lambda_{mnop}$$

The components of B_{ijkl} can be shown to vary with position and time such that the fluid does not remain transversely isotropic. This differs greatly from the theories of Leslie and Ericksen in which it is assumed that the fluid is always transversely isotropic with respect to the director.

2.3.3.1 PREDICTIONS OF DUFFY'S ANISOTROPIC FLUID THEORY

In this section, the predictions of Duffy's anisotropic fluid theory will be discussed. Simple constant shear flow was defined in equations [15] and [16]. In order to understand the predictions of Duffy's theory, however, a more general definition will be needed. In the previous section, it was stated that Duffy chose to model a fluid which at time t=0 was transversely isotropic with respect to the 3-direction. This is equivalent to saying that the fluid is everywhere oriented along the 3-direction. He then specifed how the components of Λ, the fourth rank stress tensor in the convected coordinate system, would have to be specifed in order to retain tranverse isotropy. Three different conditions exist with respect to shearing of a fluid which is oriented along the

3-direction depending on the direction of shear. For this purpose, (i,j) shearing is defined as:

(55) $V_i = X_j \dot{\gamma}$ for $i \neq j$

(56) $V_i = 0$ for $i=j$

From the above definition, there are three possible types of shear with respect to the 3-direction. These are defined below:

(3,1) shearing $V_3 = X_1 \dot{\gamma}$, $V_1 = V_2 = 0$

(1,3) shearing $V_1 = X_3 \dot{\gamma}$, $V_2 = V_3 = 0$

(2,1) shearing $V_2 = X_1 \dot{\gamma}$, $V_1 = V_3 = 0$

In the case of (3,1) shearing, the flow direction is along the 3-direction with the shear planes lying in the (X3,X2) plane. In effect, the molecules are perfectly aligned with the flow direction. Duffy finds that in order for the fluid particles to remain aligned along the 3-direction, the following condition must hold:

C,D,E,G,H=0, F=unrestricted

Consider now the case of (1,3) shearing. In this case, the shearing is such that the fluid particles are lying perpendicular to the planes of shear. Duffy now finds that a different condition must exist for the fluid to retain its initial transverse isotropy:

C,E,F,G=0, D=unrestricted

Finally, consider the case of (2,1) shearing of a fluid initially oriented along the 3-direction. In this case, the fluid particles are lying within a plane of shear. This condition is similar to the case in

Ericksen's theory in which an intial condition of n =1 would be specified. Ericksen's theory would predict that no transient behavior would be observed. This is because the initial condition is one solution of the differential equations needed to be solved for the final state of the director. Duffy specifies that in order for the fluid to retain its initial transverse isotropy in (2,1) shearing, the following condition would have to be true:

D,F,G=0, C,E=unrestricted

Duffy states that the above conditions define two types of fluids which are transversely isotropic with respect to the 3-direction in which the components of Λ are given by:

Liquid D: $\Lambda_{3311} = \Lambda_{3322} = -D \neq 0$, other $\Lambda_{ijkl} = 0$

Liquid F: $\Lambda_{1133} = \Lambda_{2233} = -F \neq 0$, other $\Lambda_{ijkl} = 0$

The behavior of these two fluids in shear flow is quite different and depends on the initial orientation of the fluid particles. For an F type fluid initially oriented in the 2-direction under conditions of (3,1) shearing, the model predicts that the transverse isotropy is lost upon start up of flow. However, the stress pattern is Newtonian and no normal forces are predicted. For the D fluid under the same conditions, a Newtonian stress field is predicted. In this case, however, a normal force of the following form is predicted:

(55) $N1 = -D\dot{\gamma}\dot{\gamma}$

Notice that the normal force is linearly related to the strain and thus increases indefinitely with time.

For an F type fluid originally oriented in the 1-direction and subjected to (3,1) shearing the viscosity is no longer Newtonian but depends on the strain and the shear rate, as does the normal force. Thus, both the viscosity and normal force increase linearly with time indefinitely. The apparent vicosity is given by:

(56) $$\eta = \tau_{12}^{\prime} / \dot{\gamma} = \eta_o + F\dot{\gamma}^2$$

In general, it is seen that although Duffy's approach is based on classical continuum mechanics, in practice it is very difficult to apply. It is not obvious if the F and D fluids are the only ones which give rise to transverse isotropy. Indeed, Duffy states that in all cases, once shearing starts the transverse isotropy is lost giving way to some more complicated form of anisotropy. However, his theory can not predict the form of this more complicated anisotropy. The general predictions of his theory are also not in line with the rheological behavior which was presented for liquid crystalline materials. It was shown in 2.1 that the viscosity does exhibit a Newtonian region, but for all the liquid crystalline materials a region of shear-thinning was also observed. The viscosity certainly was not seen to increase linearly with time. The normal force predictions are also inconsistent as the experimental data do not support a linear increase of N1 with time. Perhaps the most difficult aspect of Duffy's approach is that there seems to be no obvious way of determing C,D,E,F,G, and H. It would seem that with so many material parameters a more definite experimental procedure is needed to be able to specify the type of anisotropy that exists.

2.3.4 SUMMARY

The purpose of this section has been to examine three constitutive theories which have been especially derived for use with anisotropic fluids. Three different approaches to the specification of fluid anisotropy have been discussed. In the theory of Ericksen, a vector called the director is used to model fluid anisotropy. The director always points along the direction of preferred particle alignment. In Hand's theory, a general structure tensor is defined. The purpose of the structure tensor is to define the microstructure of the fluid. In the last theory presented, Duffy has specified a general fourth viscosity tensor to arrive at a model for anisotropic fluids. In the theories of Ericksen and Hand, fluid anisotropy is predicted to develop during flow. In the theory of Duffy, however, the fluid is assumed to be anisotropic at rest and is predicted to lose this anisotropy during flow. At this point, the good and bad features of each model will summarized resulting in the choice of one of them for study.

Of the three theories presented, the theory of Duffy is perhaps the most difficult to apply, and the most inconsistent with experimental data. The predictions of viscosity and normal forces which increase with time do not seem to be in agreement with experimentally observed behavior. In addition, it is not clear if the D and F type fluids are the only ones which give rise to fluid anisotropy. This fact makes it difficult to decide how the material parameters should be measured, or, if they can be measured at all.

Hand's anisotropic fluid theory was shown to be similar to that of Ericksen. The predictions of Hand's linearized theory agree with those of Ericksen's non-linear theory. Hand's linearized theory can predict shear rate dependent viscosity, and a shear rate dependence of molecular orientation, as can the non-linear version of Ericksen's theory. Also, the idea of spherical particles which can deform and orient in flow is an interesting one. The fact that Hand's theory has been used to model anisotropic fluid behavior is also promising. There are, however, several problems associated with using Hand's equations. He has specifed how the structure tensor should be formed for one type of fluid behavior. It is not certain, though, how one would specify the components of the structure tensor in order to predict other types of fluid behavior. Additionally, there are a great number of material parameters which must be determined. There is no apparent physical significance to the structure tensor. Therefore, it is not obvious how one would go about measuring these material parameters. The tranient stress growth and stress relaxation predictions of such a model would be of interest. In order to calculate such predictions, some knowledge of the values of the material parameters is needed. Also, there are six coupled differential equations which must be solved, and each equation will need an initial condition. It would be difficult to specify realistic initial conditions for the structure tensor without knowing something about the values of the material parameters. In conclusion, although the predictions of Hand's theory look promising, there appeárs no way to apply the theory experimentally.

Of the three theories presented, it would seem that the non-linear theory of Ericksen is the most suitable for study. Because the material parameters in the non-linear theory are functions of shear rate, the predictions of the non-linear theory appear to be more realistic. There are only three coupled differential equations which must be solved inorder to solve for the state of the director. These equations are not complicated in that the linear director equations contain only one parameter, λ. There remain a number of questions concerning the predictions of a theory such as Ericksen's. Only the steady shear flow predictions were presented. It was shown that different combinations of λ and initial conditions would give rise to different behavior. It is not known what the theory would predict for transient stress growth and stress relaxation. It would be of interest to determine whether the initial conditions and the value of λ affected such transient predictions. In section 2.2 it was shown that extensional flow appears to more effective than shear flow in producing molecular orientaion. At this point, it is not known whether Ericksen's theory could predict such behavior.

It may not be possible to quantitatively test the predictions of Ericksen's theory. This is because it would be quite difficult to measure all of the necessary material parameters. It should be possible, however, to qualitatively test the predictions of the theory. The transient stress growth and extensional flow predictions would be of great interest.

2.4 FUTURE WORK

Three areas of research concerned with liquid crystalline polymer behavior have been analyzed in this literature review. The rheological properties of liquid crystalline polymers have been discussed. The manner in which molecular orientation develops in these systems was reviewed. Several possible choices for a constitutive equation for use with anisotropic fluids were also analyzed. An attempt was made to show the relationship between these three areas for liquid crystalline polymers.

Many different liquid crystalline polymer systems were referred to in the literature review. The copolyester of PHB and PET warrants further investigation, however, due to the unique processing behavior it exhibits. Injection molded plaques of the 60 mole% PHB/PET copolymer were shown to possess highly anisotropic physical properties which depend on mold thickness. The flexural moduli of the as-prossessed plaques are exceptionally high. In addition, these plaques exhibit a skin/core morphology which has been partially attributed to the fountain flow effect of mold filling. Preliminary studies using the 80 mole% PHB/PET copolymer and another thermotropic copolyester have shown that extensional flow is more effective than shear flow in producing molecular orientation. In addition, initial studies of the rheological properties of the 60 mole% PHB/PET copolymer indicate that this material exhibits some interesting phenomena. These phenomena include unusual shear and temperature history dependence of rheological properties, unique transient stress

response, and negative transient normal stresses.

The rheological and processing characteristics exhibited by the 60 mole% PHB/PET copolyester are not very well understood. It seems reasonable that much of the behavior exhibited by this material is related to the development of structure and molecular orientation during flow. No previous investigators, however, have attempted to correlate the processing and rheological characteristics of this material to structural development during flow. Also, no work has been done to determine whether a constitutive equation which includes molecular orientation effects is needed, or is sufficient, to descirbe the flow properties of such a material.

In order to gain a better understanding of the flow properties of the 60 mole% PHB/PET copolyester, a number of studies will be performed. A more indepth study of the rheological properites of this material will be done. More information is required regarding the transient response of this material and the effect of shear history on flow behavior. A comparison between the flow properties of the 60 mole% PHB/PET system and other liquid crystalline materials is warranted. It would be instructive to know if the properties of the PHB/PET system are unique, or characteristic of liquid crystalline polymers in general. Also, in order to test the predictions of Ericksen's theory, a complete knowledge of the rheological behavior of this system will be useful.

A qualitative test of Ericksen's anisotropic fluid theory will be conducted. Several predictions of the theory must be analyzed. It is necessary to know if the theory can predict stress overshoot behavior, and what types of initial conditions effect these predictions. It would be instructive to test the predictions of the theory for extensional flow behavior. Specifically, it is desired to know if the theory predicts different molecular orientation behavior in extensional flow than in shear flow. Finally, the predictions of the theory should be compared with experimental evidence to test the validity of the theory. Comparison of actual tranient stress growth measurements with theoretical predictions is one way to test the theory. Also, the predictions of molecular alignment by the theory can be compared to actual WAXS measurments of molecular orientation in sheared and extended samples.

It is important to know the separate effects of shear and extensional flow on the development of molecular orientation and structure in the PHB/PET system. Such information would indicate if the fountain flow effect was indeed responsible for the skin/core morphologies present in injection molded plaques. It is also possible that such structure formation is responsible for the unique rheological properties exhibited by this material. Therefore, samples of the 60 and 80 Mole% PHB/PET copolyester will be prepared under controlled conditions of temperature and flow history. These samples will be analyzed for molecular orientation using WAXS techniques. A qualitative measure of the effect of shear and extensional flow on the development of molecular orientation in the

PHB/PET system will result. Joseph (1983) has shown that etching of the PHB/PET system with n-propylamine causes an enhancement of the liqud crystalline texture in solidified samples. The etching technique combined with scanning electron microscopy will be used to determine the types of textures which develop under different flow conditions. A range of shear rates will be used to determine if a minimum deformation rate exists for the production of a high degree of molecular orientation. Also, annealing experiments will be done to determine how long orientation remains in the melt state. Such information is vital to understand the processing behavior of the PHB/PET system.

The literature review has served to summarize the work of previous investigators. There appear to be a number of areas in which further work is warranted concerning the flow behavior of liquid crystalline polymers. A brief discussion of such work has just been presented. In the following chapter, a detailed plan of investigation will be given. There will also be given an indepth discussion of the experimental procedures which will be used to fulfill the experimental objectives.

CHAPTER THREE: EXPERIMENTAL AND NUMERICAL METHODS

A number of research objectives associated with understanding the flow behavior of liquid crystalline fluids were proposed in the last chapter. In this chapter, a detailed description of the experimental methods used to fulfill those objectives is given. The plan of investigation is presented along with brief discussions of the analytical and experimental techniques used to complete this work. The rheological measurements are discussed first, followed by a presentation of the analytical methods used to explore the development of texture and molecular orientation in specially prepared samples. Finally, the computer techniques used to solve Ericksen's equations are presented.

3.1 PLAN OF INVESTIGATION

A study of the rheological properties of the 60 mole% PHB/PET copolyester has been carried out. A Rheometrics mechanical spectrometer (model RMS 605) was used to perform these measurements. The steady shear viscosity and normal forces were examined as were the dynamic mechanical properties, G', G'', and η^*. These measurements were performed using both plate/plate and cone/plate geometries in which the fixture diameters were 5 cm. The gap used for the cone/plate geometry was fixed at 0.05cm, while different gap values were used for the plate/plate geometry. Cone angles of 0.1 and 0.04 radians were used. The shear rates used ranged from 10^{-1} to 10^{3} $secs^{-1}$. A series of transient tests

was also performed. These tests included the investigation of stress growth and relaxation behavior. Some unique transient tests, including reversal of shear direction and interrupted shear, were used to better qualify the behavior of the PHB/PET system. Similar tests were performed using an anisotropic solution of 12 wt% PPT in 100% H_2SO_4. A jump strain experiment was used to qualitatively determine the effect of deformation on disruption of texture in both the PHB/PET and PPT/H_2SO_4 systems. In the transient tests, only the cone/plate geometry was used. This was done to insure that all of the sample within the gap was subjected to the same amount of strain. In a plate/plate geometry this would not have been possible. In all tests, temperatures ranging from 250 to 275°C were used for the 60 mole% PHB/PET system, while the PPT/H_2SO_4 solution was examined at a temperature of 60°C.

In order to determine the effect of shear and extensional flow on the development of structure in the PHB/PET system, specially prepared samples were made. Sheared disks were prepared using the plate/plate geometry of the RMS. Pellets of the 60 mole% PHB/PET copolymer were placed in the plate/plate fixture and brought to the desired temperature (275°C). The gap was then set and the sample sheared by rotation of the top plate. The shearing was then stopped and the sample quenched with cool air. Extended ribbons were prepared through use of a slit die attached to an Instron capillary rheometer. At a distance of approximately 5 cms below the die exit a set of calender rolls took up the extrudate. The difference between the die exit velocity and roll speed

imparted an extensional deformation to the melt. Both the sheared disks and extended ribbons were prepared at temperatures of 250 and 275°C for the case of the 60 mole% PHB/PET system. In the case of the 80 mole% PHB/PET copolymer, a temperature of 320°C was used. Wide angle x-ray scattering (WAXS) was used to qualitatively determine the degree of molecular orientation present in the sheared and extended samples. In addition, the samples were etched in n-propylamine from 4 to 6 hours at room temperature in order to enhance the liquid crystalline textures present. The etched samples were then examined using scanning electron microscope techniques.

Ericksen's anisotropic fluid theory was analyzed. A method of qualitatively determining the material parameters was determined. Using the experimentally measured values of viscosity and normal force, approximate values of the material parameters in the non-linear theory were calculated. These material parameters were used to predict the stress growth and extensional flow behavior of the PHB/PET material. In order to solve the necessary differential equations in the theory, an IMSL routine employing the Adam's predictor-corrector method was used. Different initial conditions and λ value combinations were analyzed. The effect of the choice of λ on the extensional flow properties was determined.

3.2 SAMPLES USED AND SAMPLE PREPARATION

The polymer used in this study consists of a copolymer of p-hydroxybenzoic acid (PHB) and poly(ethylene terephthalate) (PET). The copolymer is made through the acidolysis reaction between the PET and PHB monomers. A detailed description of the preparation of this copolymer is given by McFairlane and co-workers [122]. Two copolymer compositions were used in this study. One of 60 mole% PHB/40 mole% PET and another with 80 mole% PHB/20 mole% PET. The properties of these systems are reported in detail by McFairlane [122]. The polymers were provided by the Tennessee Eastman Corporation.

The PHB/PET copolymer systems retain moisture. For this reason, all samples were dried before being used. The drying procedure consisted of placing the samples in a vacuum oven under -30 inches Hg at a temperature of 110°C. The samples were left in the oven for 72 hours. Upon being removed from the oven, the samples were sealed in glass bottles. The sample bottles were then placed in a desiccator under vacuum until the samples were needed. The samples were used within one day of their removal from the vacuum oven.

An anisotropic solution of poly(p-phenylene terephthalamide) (PPT) in 100% H_2SO_4 was also used in this study. 100% H_2SO_4 was prepared by mixing the correct amounts (on a molar basis) of reagent grade H_2SO_4 (98% H_2SO_4) with Oleum (30% free SO_3). The PPT polymer was supplied by the Monsanto Corporation in the form of Kevlar® fiber. The fiber was spe-

cially prepared through a series of steps. First, the fiber was chopped into pieces approximately 0.5 inches long. These fibers were then packed into a Soxlet extractor and extracted for 6 hours using acetone. When the extraction operation was completed, the fibers were dried in a vacuum oven at 60°C for 24 hours. The final step in preparation involved the mixing of the H_2SO_4 and PPT materials. A Helicone mixer with jacketed mixing bowl was used to mix the PPT solution. The PPT and H_2SO_4 components were mixed for a period of six hours. A temperature of 60 °C was maintained in the mixing bowl.

3.3 RHEOLOGICAL MEASUREMENTS

The rheological properties of the PHB/PET copolymers and PPT/H_2SO_4 solution were measured using a Rheometrics mechanical spectrometer (model RMS 605). A diagram of the RMS system is shown in Figure 3.1. Basically, the polymer sample of interest in placed in the gap between two plates, or the gap between a cone and plate. The top plate is connected to a motor which can rotate the plate in clockwise or counterclockwise directions. The motor can also be used to oscillate the top plate about some zero point at varying frequencies. The bottom plate is connected to a series of transducers which measure torque and normal forces. With fluid in the gap between the plates, rotation of the top plate causes a torque to be transmitted through the fluid to the bottom plate. Knowledge of the rotational speed of the top plate, the plate diameter, and the gap between the two plates allows calculation of an apparent shear

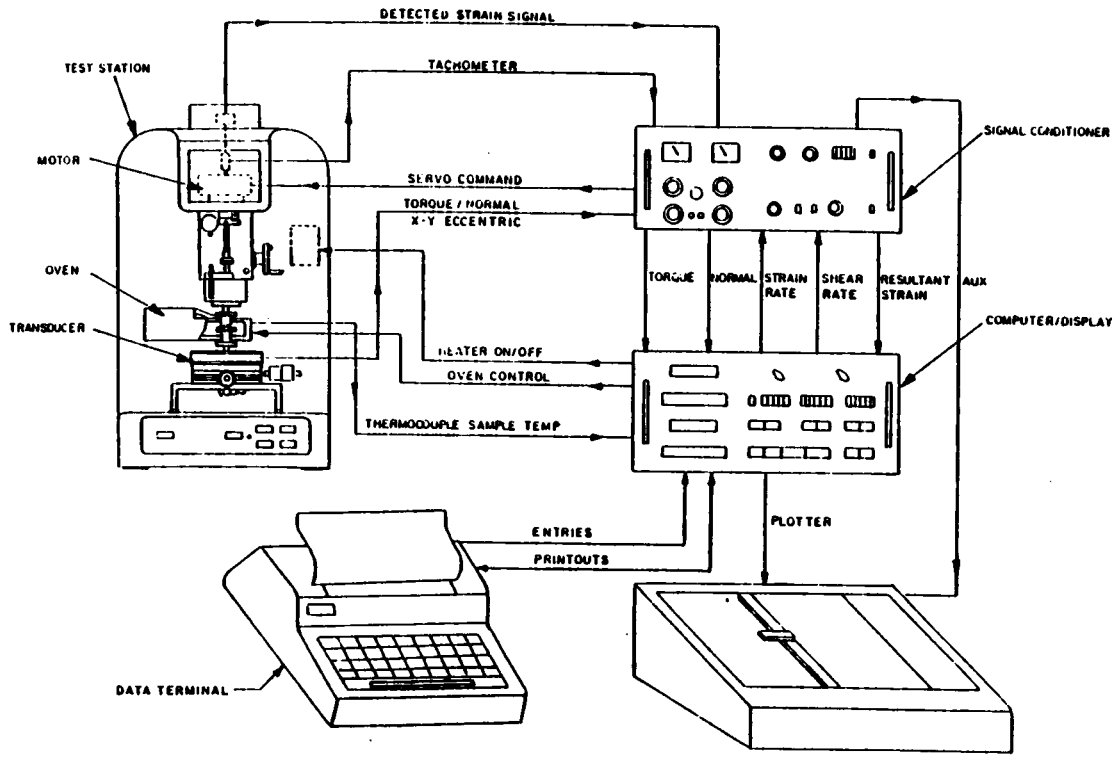

Figure 3.1 Schematic representation of the Rheometrics mechanical spectrometer. [146]

rate, $\dot{\gamma}$. This shear rate, combined with the torque measurement, gives the fluid viscosity. Polymeric materials exhibit considerable elasticity because of the nature of their molecular structure. This elasticity exhibits itself in shear flow experiments. In the case of a polymer flowing between parallel plates, there will be a force generated by the polymeric material pushing the plates apart. This force is called the normal force and arises from the fact that as the molecules are being stretched along the flow direction, they try to contract along this same direction.

During any flow experiment, the torque and normal forces measured by the transducers attached to the bottom plate are fed to a central processing unit (CPU). Before being analyzed by the CPU, the analog signals are electronically filtered so as to eliminate any errors due to noise. These analog signals are then converted into digital signals which the computer uses to calculate the viscosity and normal force values in a steady shear experiment. In other experiments, such as dynamic oscillatory testing, the same torque and normal forces are used to calculate the dynamic mechanical properties (G',G'',η^*). The properties calculated by the CPU are specified by the user. In the following sections a description of the sample loading techniques used are described. The major equations used by the CPU are described in detail elswhere [119,120], but a description of the measurement techniques used for transient and jump strain measurements is provided.

3.3.1 SAMPLE LOADING

In the case of both the PHB/PET samples and the Kevlar solution (PPT in H_2SO_4), special sample loading techniques were needed. As was shown in section 2.2, liquid crystalline materials exhibit very low viscosities. This fact makes it difficult to measure the rheological properties of these materials in a normal plate/plate or cone/plate fixture. This is because these materials tend to flow out of the gap between the plates. These polymers apparently do not possess sufficient surface tension to retain their shape within the gap. In order to combat this difficulty, a special plate designed for use with solutions was used for the two liquid crystalline systems studied in this work. This special bottom plate was fixed with a removable baffle. The purpose of the baffle was to hold a pool of liquid on the bottom plate. The top plate, therefore, rotated in a pool of liquid much like a couette device. Due to the low values of viscosity possessed by these polymers, it is not probable that edge effects affected the viscometric measurements. In the case of the Kevlar solution, an additional precaution was taken. The Kevlar solution is very sensitive to moisture. In order to lengthen the useful life of the Kevlar samples, a layer of mineral oil was placed over the Kevlar solution in the plates. The oil was held in place by the baffle fixed to the lower plate. Care was taken to insure that no oil penetrated between the sample and the plates.

3.3.2 TRANSIENT RHEOLOGICAL MEASUREMENTS

Transient rheological measurements include a number of tests in which the non-steady state response of the shear and normal stresses are investigated. Typically, these experiments consist of stress growth and stress relaxation tests. However, other transient tests are possible. In Figure 3.2 is shown a number of transient tests which are possible with the RMS. In a stress growth experiment, the fluid is assumed to be at rest for all times prior to time t=0. At time t=0 steady constant shear flow is initiated at some constant shear rate, $\dot{\gamma}$. For the case of a flow reversal experiment, the fluid is assumed to have achieved steady state conditions in steady shear for all times t<0. At time t=0, the shear direction is reversed and the stresses are monitored as they achieve steady state conditions again. An interrupted stress growth experiment is much like a stress growth experiment except that as the stresses are coming to steady state the shearing is stopped. After a certain rest period, t_r, the shearing is restarted. Finally, in a stress relaxation experiment, the fluid is assumed to have achieved steady state in shear flow for all times t<0. At time t=0 the shearing is stopped and the stresses are monitored as they relax to some constant value.

In performing the transient tests using the PHB/PET and Kevlar materials, certain precautions were taken. Only the cone and plate geometry was used. Clearly, the transient response of a fluid is related to the degree of disruption of texture which takes place in the melt. It is desirable that all of the sample within the gap be subjected to the same

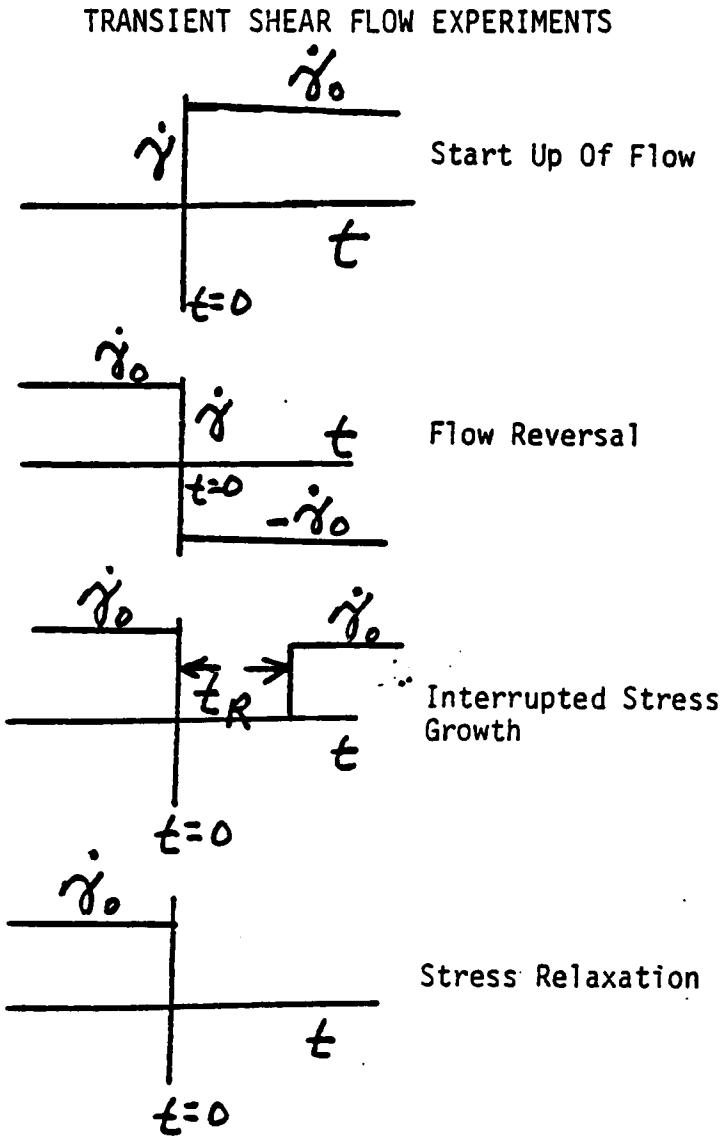

Figure 3.2 Schematic representation of the different types of tranient tests possible with the RMS.

amount of deformation. The strain rate in a cone and plate is independent of radius. Therefore, all of the material within the gap is subjected to the same amount of strain. For a cone and plate geometry the strain (γ) at any time, t, during a stress growth experiment is given as:

(59) $\gamma = t\omega/\beta$

where ω is the angular frequency of rotation of the top plate, and β is the cone angle. In addition to using only the cone and plate geometry, only one sample was used per transient test. This was to insure that shear history effects would not introduce errors.

For all transient tests the data can be represented in terms of four viscosity and normal stress functions which depend on time:

(60) $\eta+(t) = \tau(t)/\dot{\gamma}$

(61) $N1+(t) = \tau(t) - \tau(t)$

(62) $\eta-(t) = \tau(t)/\dot{\gamma}$

(63) $N1-(t) = \tau(t) - \tau(t)$

where by convention, the + sign signifies the stress growth behavior and the - sign signifies the stress relaxation behavior of the material.

Special data gathering techniques were used to insure that an accurate measure of the stress growth behavior was being measured. The RMS has been equipped with a Gould digital storage oscilliscope (model OS4100). The torque and normal forces measured by the transducers are sent directly to the storage oscilliscope. After being stored, the signals are played back to a Hewlett Packard strip chart recorder (model

7132A). The oscilliscope has an extremely small response time, therefore, the transient response is accurately measured.

3.3.3 JUMP STRAIN EXPERIMENTS

Another test which can yield information regarding the structure of a polymer in its melt state is the jump strain experiment. In this test, the sample is subjected to a finite strain at time t=0. The response of the stresses for all times t>0 is monitored. The cone and plate fixture is used for this experiment as it is important that all of the sample within the gap be subjected to the same amount of strain. For a cone/plate geometry, the strain is given as: on

(64) $\gamma = \theta/\beta$

where θ is the angle of rotation of the top plate, and β is the cone angle. The results of jump strain experiments are usually expressed in terms of a relaxation modulus (G(t)). This modulus is calculated by dividing the stress by the applied strain:

(65) $G(t) = \tau(t)/\gamma$

where $\tau(t)$ is the shear stress as measured as a function of time. The time taken for G(t) to reach zero is a measure of the relaxation time of the material. If G(t) approaches some constant value other than zero, the material possesses a yield stress.

The same data gathering techniques used for the stress growth experiments were used for the jump strain experiments. The transducer signals

were directly sent to the Gould digital storage oscilloscope, and played back to the Hewlett Packard strip chart recorder. Applied strains of between 0.1 and 20 strain units were investigated for both the PHB/PET and H SO systems.

3.4 PREPARATION OF SHEARED AND EXTENDED SAMPLES

In order to determine the separate effects of shear and extensional flow on the development of structure in the PHB/PET system, specially prepared samples were examined. These samples consisted of sheared disks and extended ribbons subjected to controlled conditions of temperature and deformation history. In this section, the preparation of these samples is discussed followed by a presentation of the analytical methods used to investigate their structure.

3.4.1 SHEARED DISKS

Sheared disks of the 60 and 80 mole% PHB/PET copolyester were prepared using the parallel plate geometry of the RMS. A mold release agent was sprayed on the plates to facilitate removal of the samples. The pellets were placed on the plates and the temperature brought to the desired temperature (275°C for the 60 mole% PHB/PET copolyester and 320 °C for the 80 mole% PHB/PET copolyester). Once the desired temperature was reached, the gap was set and the shearing started. The samples were sheared for a period of 30 seconds at constant temperature. At the end

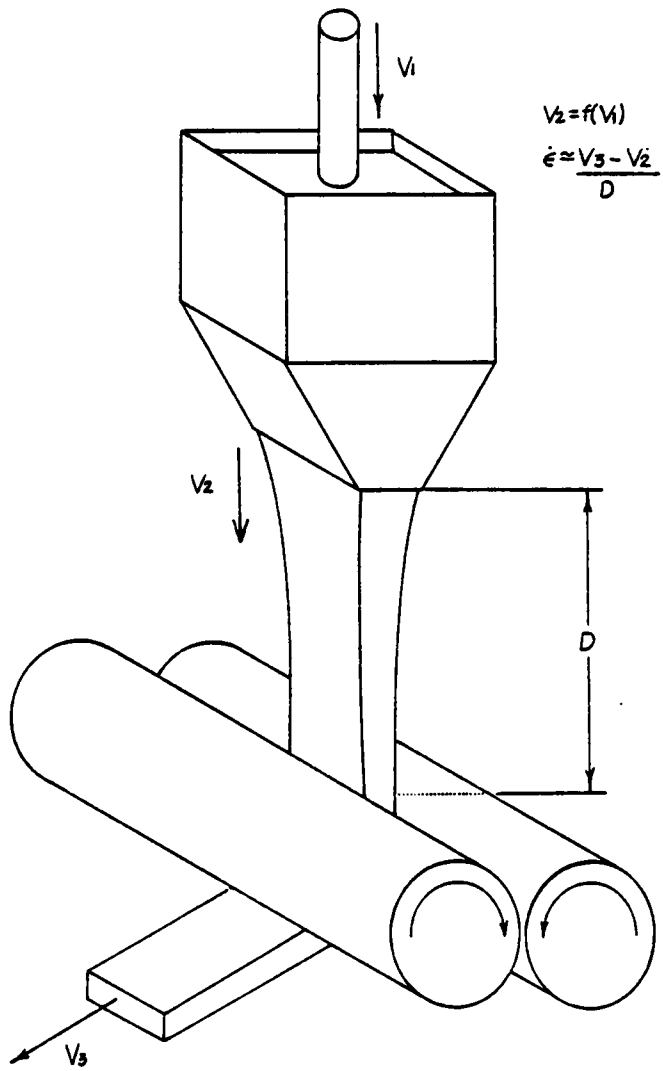

Figure 3.3 Schematic representation of the Instron, Die, and roller system used to make extended ribbons.

of 30 seconds the shearing was stopped and the samples cooled using cool air. The bottom plate was not attached to the transducer to avoid damage. Once the sample had solidified sufficiently, the plates and sample were quenched in ice water. At this point, the sample was removed from the fixture. Samples were prepared in this manner using shear rates ranging from 10 to 50 $secs^{-1}$.

3.4.2 EXTENDED RIBBONS

Extended ribbons were prepared using a slit die attached to an Instron capillary rheometer (model 3211). A schematic diagram of the equipment is given in Figure 3.3. At a distance of approximately 5 cms below the die exit, a set of calender rolls took up the extrudate. The plunger speed velocity used was 20 cm/minute. Knowledge of the barrel diameter (.9825 cms) and the cross sectional area of the die exit gives the velocity of the melt at the die exit. In terms of the appropriate variables this exit velocity is written as:

(66) $$V_2 = V_1 \pi R_b^2 / A_d$$

where V_2 = Velocity at die exit

V_1 = Plunger speed

R_b = Barrel radius

A_d = Cross sectional area of die exit

The velocity of the melt at the roller surface is given by the rotational speed of the rollers as:

(67) $$V_3 = 2\pi R_r \omega_r$$

where V_3 = Speed at roller surface

R_r = Roller diameter

ω_r = Rotational speed of rollers

An approximate average extensional rate is calculated by determining the difference between the die exit velocity and the velocity at the roller surface divided by the distance over which this change in velocity occurs:

(68) $\dot{\varepsilon} = (V_3 - V_2)/L$

where $\dot{\varepsilon}$ = Average extensional rate

L = Distance between die exit and center of rollers

Two rotational speeds of 60 and 120 rpm were used corresponding to average extension rates of 1.5 and 2.5 $secs^{-1}$. Temperatures of 275 and 250°C were used for the 60 mole% PHB/PET copolyester while a temperature of 320°C was used for the 80 mole% PHB/PET copolyester.

3.4.3 ANNEALING OF SAMPLES

Annealing of sheared disks and extended ribbons was used to determine the degree to which molecular orientation and texture remained in the melt. The heating oven of the RMS was used to anneal the samples. The use of this oven allowed precise control of the annealing time. The plate/plate geometry was used with a piece of Teflon placed on the bottom plate. The oven temperature was brought to the desired annealing temperature and the sample placed in the oven quickly so as not to allow a drop of temperature within the oven. After a specified period of time, the

sample was removed and quenched in ice water. Annealing temperatures of 250 and 275°C were used for the 60 mole% PHB/PET copolyester, while a temperature of 310°C was used for the 80 mole% PHB/PET copolyester. Annealing times ranging from 30 seconds to five minutes were investigated.

3.5 ANALYTICAL TECHNIQUES

Wide angle x-ray scattering (WAXS) and scanning electron microscopy (SEM) techniques were used to investigate the structures present in the sheared disks and extended ribbons. No attempt is made here to describe the theory behind x-ray scattering by polymeric materials. Only the techniques used to mount the samples and produce the x-ray scattering patterns is discussed. The Bragg scattering equation is presented only because it was used to determine the d-spacings in the x-ray patterns.

3.5.1 WIDE ANGLE X-RAY SCATTERING MEASUREMENTS

Wide angle x-ray scattering arises from fluctuations in electron density that occur over small distances of approximately 20A. Such x-ray scattering can be used to examine the degree of crystallinity in a crystalline or semi-crystalline solid [72].

WAXS may also by used to qualitatively determine the degree of molecular orientation in polymeric samples. To better illustrate the use of WAXS measurements, some example scattering patterns are presented. In Figure

3.4 is shown the diffuse scattering pattern exhibited by an amorphous polymer. In contrast, in Figure 3.5 is shown the scattering pattern exhibited by PET, a semi-crystalline polymer. The sharp rings occur due to scattering of the x-rays by equally spaced crystalline planes. The size of the rings is related to the d-spacing by Braggs Law. The sharpness of the rings is related to the perfectness of the crystalline structure. In a randomly oriented sample, the intensity of the x-ray scattering will be uniformly distributed about the ring. However, in a perfectly oriented sample, the x-ray scattering will be concentrated along the azimuthal axis.

In the case of a parallel plate geometry, the shear rate is a function of distance from the rim of the plate. Therefore, WAXS measurements were made only on samples taken from the edge of such disks where the shear rate is well known. Two views were used corresponding to different orientation of the samples with respect to the direction of the x-ray beam. In Figure 3.6 is shown a schematic of these different views. In the edge-edge view, the x-ray beam is passed along a direction perpendicular to the direction of shear within a shear plane, i.e. the direction of the x-ray beam coincides with the X3 axis. In the edge-top view, the x-ray is passed along a direction perpendicular to the shearing planes, i.e. the X1 axis. In the case of extended ribbons, the x-ray beam was passed along a direction perpendicular to the plane of the ribbon. In Figure 3.7 is shown the manner in which the sheared disk samples and extended ribbons samples were mounted with respect to the x-ray beam. The scat-

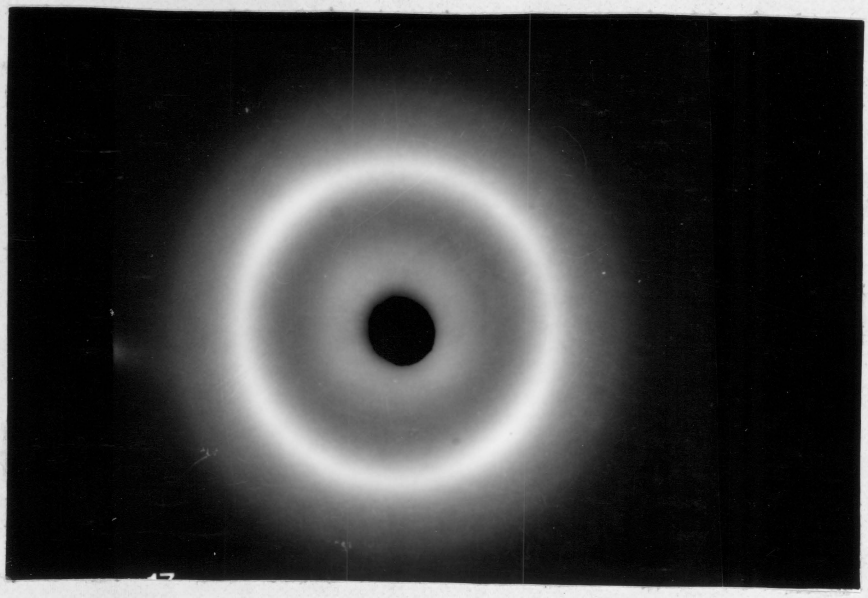

Figure 3.4 WAXS pattern of an amorphous material.
60 mole% PHB/PET

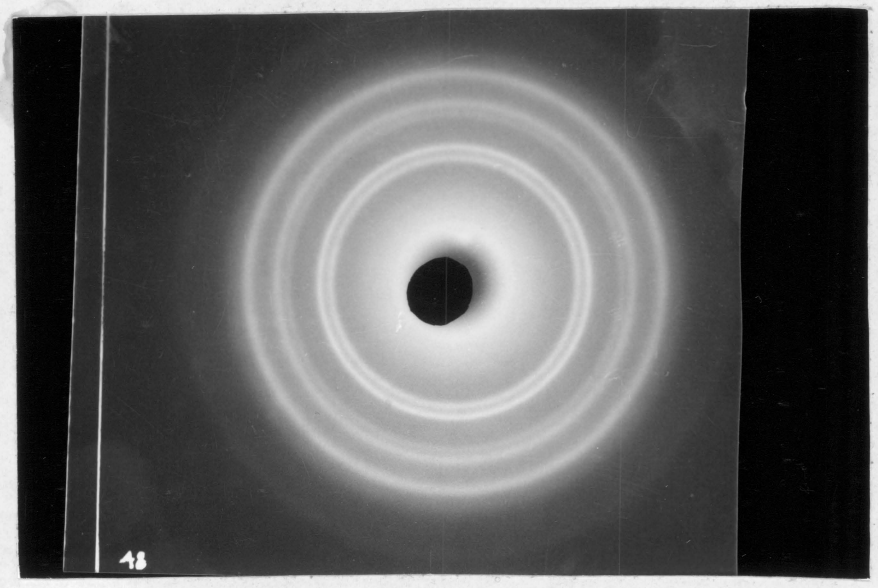

Figure 3.5 WAXS pattern of PET

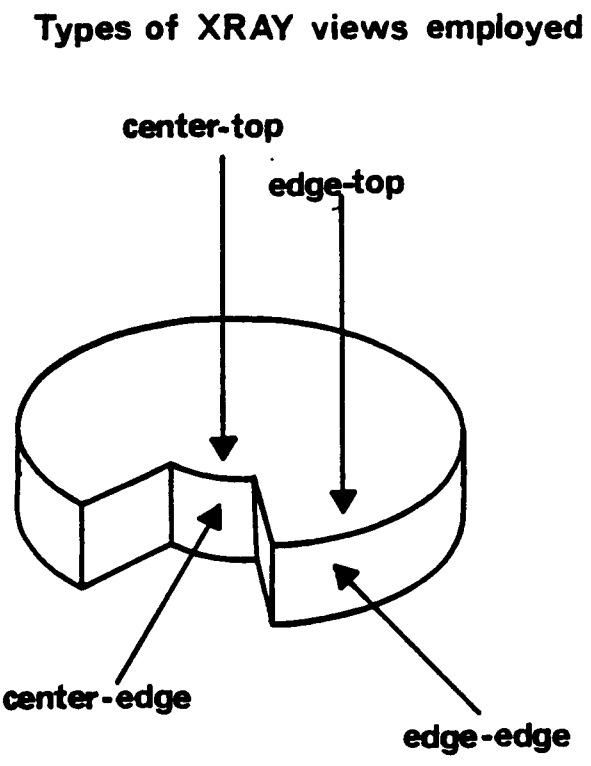

Figure 3.6 Schematic representation of the different X-ray views employed for sheared disks.

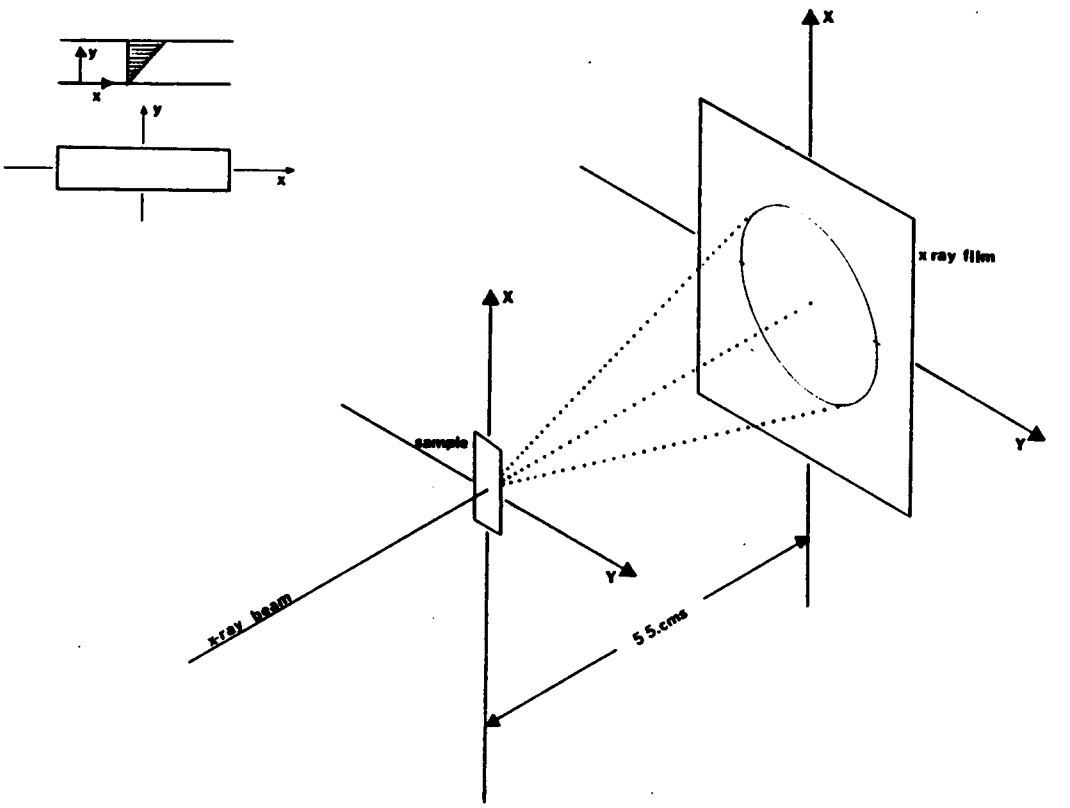

Figure 3.7 Schematic representation of the sample mounting position with respect to the x-ray beam.

tering patterns were recorded photographically with the flow direction always along the vertical. A Philips PW 1720 table top generating systems equipped with a Wahrus (Statton) camera was used to photographically record the scattering patterns. Sample to film distances of 5.5 cms were used for all samples and the film was exposed for 20 hours. Typicaly x-ray tube generator conditions consisted of an applied voltage of 40Kv at a current of 20 milliamps producing an x-ray beam with a wavelength of 1.541Å.

Braggs law was used to qualitatively determine the degree of PET or PHB crystallinity present in the sheared and extended samples. Braggs law relates the crystalline d-spacing to the wavelength of x-rays used, and the angle at which the x-rays are scattered. Braggs law can be written:

(69) $n\lambda = 2d\sin\theta$

where n = Any real integer

λ = Wavelength of x-rays

θ = Angle at which x-rays are being scattered

d = d-spacing of unit scattering the x-rays.

3.5.2 CHEMICAL ETCHING

Scanning electron microscopy in conjunction with chemical etching was used to qualitatively investigate the types of textures which develop in shear and extensional flow. The etching technique involves the use of

n-propylamine to etch the sheared disks and extended ribbons. The amine attacks the ester linkage in the PET molecule. In the case of the PHB/PET system, the etchant preferentially attacks amorphous regions of PET and unordered regions of PHB/PET molecules within the sample. The result is an enhancement of the liquid crystalline structure possessed by the sample.

In the etching procedure, samples were placed in a petri dish containing the etchant. These petri dishes were placed in a hood to avoid spreading of the harmful n-propylamine fumes. All samples were etched for a period of 4 to 6 hours at room temperature. At the end of this time, the samples were removed and rinsed with water.

3.5.3 SCANNING ELECTRON MICROSCOPY

Scanning electron microscopy is a desirable analytical tool due to its simplicity of sample preparation and the high resolution obtainable. Basically, the sample is placed in the path of a beam of electrons. This electron beam is produced by heating a tungsten filament. The stream of electrons produced by the tungsten filament is accelerated by means of an accelerating voltage usually on the order of 15Kv. The beam is then focussed through a series of aperatures. The final lens through which the beam passes contains a series of coils which cause the beam to trace out a rectangular raster on the sample of interest.

When the electron beam strikes the sample, several events occur. The event of interest is the emission of secondary electrons. This emission occurs when an electron penetrates the sample and ionizes atoms as it loses energy. Only the secondary atoms emitted near the surface (~100Å) possess enough energy to escape the sample. These electrons are accelerated towards the beam detector. The beam detector is synchronized with the beam raster. Therefore, it is possible to reproduce the image of the sample on a cathode ray tube. Images can be recorded photographcially by taking a picture of the image on the cathode ray tube.

The sample preparation procedure is straightforward and involves gluing of the sample of interest to an aluminum stud. To prevent charging of the sample, the aluminum stud and sample are grounded to each other through the use of silver paint. In order to enhance the amount of secondary electrons emitted by the sample, a layer of gold (~100-150Å) is usually coated onto the sample. This layer of gold also helps to reduce charging of the sample. In this study, an ISI Super III-A scanning electron microscope was used to analyze etched samples. An SPI sputter coater (model 13131) was used to coat the samples with a layer of gold.

3.6 NUMERICAL METHODS

An IMSL routine, DGEAR, was used to solve the differential equations predicted by Ericksen's theory. The DGEAR program uses the Adam's predictor-corrector method to calculate the solution to an initial value problem. Using the DGEAR program, the predictions of Ericksen's theory for stress growth and stress relaxation behavior were investigated. The effect of initial conditions and λ values on the steady shear and extensional flow predictions were also examined. In the following discussion, the ideas behind the numerical technique are presented along with a summary of the conditions under which Ericksen's equations were analyzed.

Many differential equations exist which do not possess analytical solutions. In these cases, numerical integration techniques offer the only route towards gaining a solution. In order to solve a differential equation numerically, the domain over which solution values are desired is discretized. Once the discretization has been accomplished, the solution is calculated over small regions. It becomes possible, therefore, to step through the whole domain and achieve a complete solution. The predictor-corrector method is a multistep method which uses information about the solution and its derivatives at more than one point in order to extrapolate to the next point [121]. Consider an ordinary differential equation of the form $y'=f(x,y)$. If this equation is integrated over the interval x_i to x_{i+1}, the following equation is obtained:

$$(70) \qquad \int_{x_i}^{x_{i+1}} y' \, dx = \int_{x_i}^{x_{i+1}} f(x,y(x))dx$$

or:

$$(71) \qquad y(x_{i+1}) = y(x_i) + \int_{x_i}^{x_{i+1}} f(x,y(x))dx$$

where y is the exact solution. One way to solve the above equation is to numerically integrate the integral term. Let u be the approximate solution which will be calculated by the numerical technique. Therefore, equation [71] becomes:

$$(72) \qquad u(x_{i+1}) = u(x_i) + \int_{x_i}^{x_{i+1}} f(x,y(x))dx$$

Notice that if $u(x_i)$ is known, it is possible to calculate $u(x_{i+1})$. Thus, in an initial value problem, $u(x_i)$ is known and the solution propagates from there.

The simplest method of solution of equation [72] involves replacement of the integral term with:

$$(73) \qquad \int_{x_i}^{x_{i+1}} f(x,y(x))dx = hf(x,y(x))$$

where h is the step size $(x_{i+1}-x_i)$. The above result is obtained by assuming f(x,y(x)) to be independent of x. Therefore, the iteration formula may written:

$$(74) \qquad u_{i+1} = u_i + hf(x,u(x))$$

which is known as the Euler formula. In order to gain a more accurate solution to the differential equation, however, a more complicated procedure is used. In this case, the integral term in equation [71] is approximated using the trapezoidal formula:

$$(75) \qquad \int_{x_i}^{x_{i+1}} f(x,y(x)) = h/2[f(x_i, u_i) + f(x_{i+1},u_{i+1})]$$

which gives for the iteration formula:

$$(76) \qquad u_{i+1} = u_i + h/2[f(x_i, u_i) + f(x_{i+1},u_{i+1})]$$

If $f(x_i, u_i)$ is non-linear, u_{i+1} cannot be solved for directly. In this case, the Euler formula may be used to predict a first approximation to u_{i+1}:

(77) $$u_{i+1}^{[0]} = u_i + hf_i$$

This approximation is then corrected using the trapezoidal formula:

(78) $$u_{i+1}^{[s+1]} = u_i + h/2[f + f(u_{i+1}^{[s]})] \qquad s=0,1....$$

Successive values of u_{i+1} are calculated using equation [94] until a tolerance condition is met. This tolerance condition is usually of the form:

(79) $$\left|u_{i+1}^{[s+1]} - u_{i+1}^{[s]}\right| < \text{tolerance}$$

For most problems, convergence is reached within the first or second iteration.

The iteration scheme just described is the basis behind the predictor-corrector method used by the DGEAR program. DGEAR was used to solve the three coupled director equations in Ericksen's theory. For simplicity, these equations are reproduced here for the case of simple constant shear flow. The three director equations are:

(17) $$\dot{n}_1 = 1/2\dot{\gamma} n_2 (\lambda + 1 - 2\lambda n_1^2)$$

(18) $$\dot{n}_2 = 1/2\dot{\gamma} n_1 (\lambda - 1 - 2\lambda n_2^2)$$

(19) $$\dot{n}_3 = -\lambda\dot{\gamma} n_1 n_2 n_3$$

The above equations comprise a set of three coupled differential equations. In order to solve them, a value of λ must be specified and an initial condition on the state of the director must be given. In this study, different λ values and initial conditions were investigated. A summary of these conditions is given below.

λ Value	Initial Conditions
1	$n_1=1,\ n_2=1,\ n_3=1$
5	$n_1=1,\ n_2=1,\ n_3=1$

For all cases, the transient behavior was calculated through substitution of the values for n_1, n_2, and, n_3 at each time increment into the equations for the stresses (equations [25]-[27]).

A listing of the source program is given in the appendix. In order to use the program, one needs only to specify the initial conditions, and supply a subroutine which evaluates the derivatives. More information on the use of DGEAR is available in the IMSL manual covering the DGEAR software.

CHAPTER FOUR: RESULTS

The results of the experimental plan of investigation given in Chapter Three are presented in this chapter. In section 4.1, the predictions of Ericksen's theory are discussed. A method of qualitatively evaluating the material parameters from steady shear data is presented. The steady shear viscosity and normal force values measured for the 60 mole% PHB/PET copolyester are analyzed. From these measurements, values of the material parameters in Ericksen's non-linear theory are calculated. The predictions of Ericksen's theory for stress growth and elongational flow behavior are then analyzed. In order to test the validity of the predictions of Ericksen's theory for stress growth behavior, a number of transient rheological measurements were performed using the PHB/PET copolymer system. A lyotropic solution of PPT in 100% pure H_2SO_4 was also investigated so that more general conclusions could be made regarding the behavior of liquid crystalline materials. The results of these rheological measurements are presented in section 4.2. WAXS and SEM analyses were performed on specially prepared samples to determine the effect of shear and elongational flow on the development of texture and molecular orientation. Such analyses also provides data for testing the predictions of Ericksen's theory for the state of the director under different flow conditions. The WAXS and SEM results are presented in section 4.3.

4.1 ERICKSEN'S THEORY

The forms of the equations for the stresses in steady simple shear flow predicted by Ericksen's non-linear theory were given in section 2.3. These equations are as follows:

(80) $\tau_{12} = \alpha_1 n_1 n_2 + \alpha_2 \dot{\gamma}/2 + \alpha_4 \dot{\gamma}(n_1^2+n_2^2)/2 + \alpha_5 \dot{\gamma}^2 n_1 n_2/2$

(81) $N1 = \tau_{11}-\tau_{22} = \alpha_1(n_1^2-n_2^2) + \alpha_5 \dot{\gamma}^2(n_1^2-n_2^2)/2$

(82) $N2 = \tau_{22}-\tau_{33} = \alpha_1(n_2^2-n_3^2) + \alpha_3 \dot{\gamma}^2/4 + \alpha_4 n_1 n_2 \dot{\gamma} + \alpha_5 n_2^2 \dot{\gamma}^2/2$

In order to evaluate the five material parameters in the above equations, a number of simplifying assumptions were made. It was assumed that the PHB/PET system does not possess a yield stress, therefore $\alpha_1=0$. (It was stated in the Literature Review that the values of yield stress measured by Wissbrun [27] for the 60 mole% PHB/PET system were suspect due to the temperatures used. In this study, it was found that in stress relaxation experiments, no yield stress value was exhibited. Thus, justifying the above assumption. The results of the transient tests are discussed in later sections.) It was also assumed that in simple shear flow the molecules align perfectly along the flow direction. Therefore, $\lambda=1$ and at steady state $n_1=1$, and $n_2=n_3=0$ Using the above assumptions, the steady state stress equations reduce to:

(83) $\eta = \tau/\dot{\gamma} = (\alpha_2+\alpha_4)/2$

(84) $N1 = \alpha_5 \dot{\gamma}^2/2$

(85) $N2 = \alpha_3 \dot{\gamma}^2/4$

Unfortunately, there are still four unknowns and only three equations. To determine all four material parameters, it was assumed that the extensional viscosity (η) could be expressed as three times the shear viscosity at low shear rates (i.e. $\eta_e = 3\eta$). In the case of uniaxial extension along the X1 axis, the deformation and vorticity tensors may be written:

$$(86) \qquad \underline{d} = \dot{\varepsilon}\begin{bmatrix} 2 & 0 & 0 \\ 0 & -1 & 0 \\ 0 & 0 & -1 \end{bmatrix} \qquad \underline{\omega} = \emptyset$$

where $\dot{\varepsilon}$ is the extensional rate in $secs^{-1}$. Substitution of the above form for d into Ericksen's non-linear stress equations yields for the extensional viscosity:

$$(87) \qquad \eta_e = (\tau_{11} - \tau_{22})/\dot{\varepsilon} = 3\alpha_2/2 + 3\dot{\varepsilon}\alpha_3/4 + \alpha_4(2n_1^2 + n_2^2) + \alpha_5\dot{\varepsilon}(2n_1^2 - n_2^2/2)$$

If n =1 at steady state, the above equation reduces to:

$$(88) \qquad 3\eta = \eta_e = 3\alpha_2/2 + 3\alpha_3\dot{\varepsilon}/4 + 2\alpha_4 + 2\alpha_5\dot{\varepsilon}$$

Therefore, measurement of the shear rate dependence of η, N1, and N2 combined with the assumptions made above allows for a qualitative evaluation of the five material paramters (α_1 to α_5).

4.1.1 EVALUATION OF MATERIAL PARAMETERS

The steady shear properties of the 60 and 80 mole% PHB/PET copolyester system have been discussed in detail by Gotsis [123]. For the purposes of this study, only the viscosity and normal force values for the 60 mole% PHB system were measured. In Figures 4.1 thru 4.7 are shown the

results of the viscosity measurements. These measurements were performed at 260 and 275°C using both cone and plate and parallel plate geometries. It was decided to fit the material parameters at 275°C. At this temperature the 60 mole% PHB/PET system is known to exhibit liquid crystalline behavior [13]. A number of different gap values were used in the parallel plate measurements to determine if any gap effects existed. It can be seen that the viscosity exhibits a shear-thinning region only, and the viscosity values are fairly independent of geometry.

The results of the normal force measurements are shown in Figures 4.8 thru 4.14. At 275°C, it can be seen that there is a slight descrepancy in the normal force values measured with different gap values at the lower shear rates. The values measured using a parallel plate geometry with a 1.0mm gap are consistent, however, with the cone and plate data both at 260 and 275°C.

All of the data plotted in Figures 4.1 thru 4.14 are tabulated in Tables B.1 thru B.14 in the appendix. The viscosity and normal force values measured at 275°C with the 1.0mm gap parallel plate and the cone and plate geometries were used to fit values of the viscosity, and the normal forces. Using least squares analysis, a simple power law model was fit to the data. Comparison of the N1 values measured with the cone and plate and parallel plate geometries was used to evaluate N2. The following forms for the material properties were found:

(89) $\eta(\dot{\gamma}) = 60\dot{\gamma}^{-0.46}$ Pa·S

(90) $N1(\dot{\gamma}) = 36.5\dot{\gamma}$ Pa

(91) $N2(\dot{\gamma}) \sim 0.0$

Using the above material properties, and solving the equations for η, η_e, N1 and N2 simultaneously results in the following forms for the material parameters in Ericksen's non-linear theory:

$$\alpha_1(\dot{\gamma}) = 0$$

$$\alpha_2(\dot{\gamma}) = 48\dot{\gamma}^{-0.46} + 117$$

$$\alpha_3(\dot{\gamma}) = 0$$

$$\alpha_4(\dot{\gamma}) = 72\dot{\gamma}^{-0.46} - 117$$

$$\alpha_5(\dot{\gamma}) = 73\dot{\gamma}^{-1}$$

for the 60 mole% PHB/PET copolymer system at 275°C.

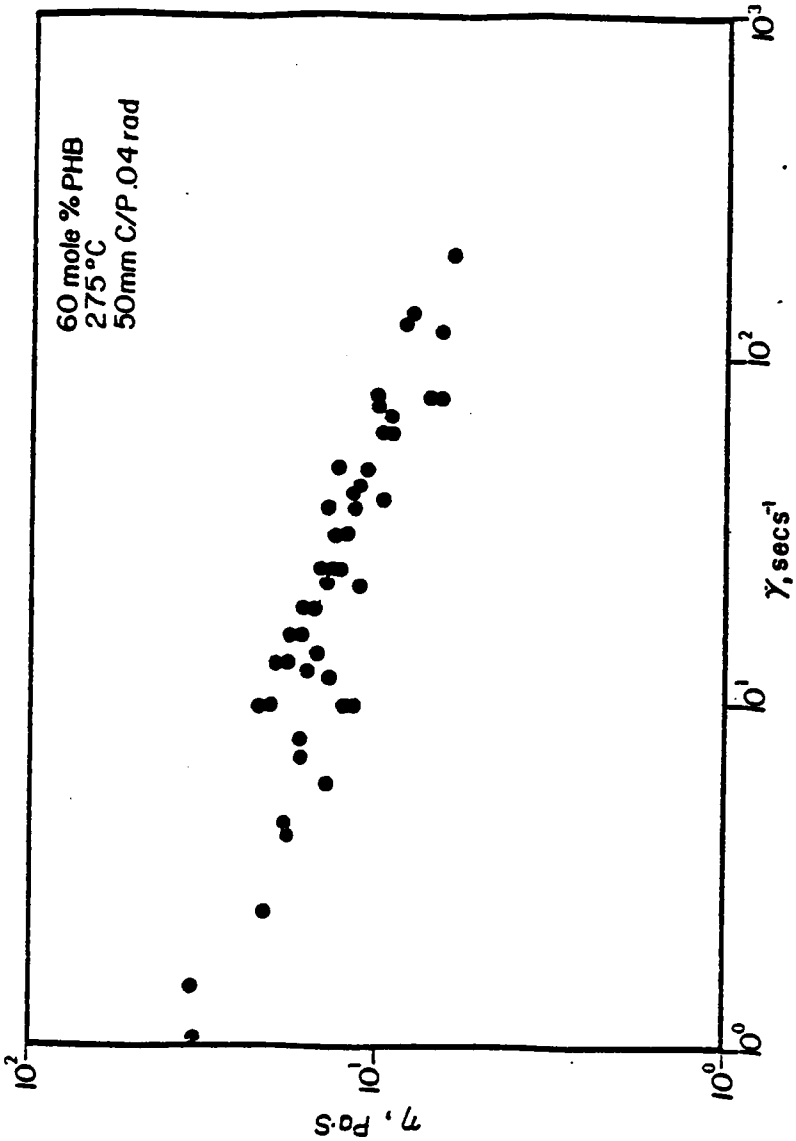

Figure 4.1 Steady Shear Data: η vs $\dot{\gamma}$ for 60 mole% PHB Copolymer 275°C, 50mm C/P 0.04 rad.

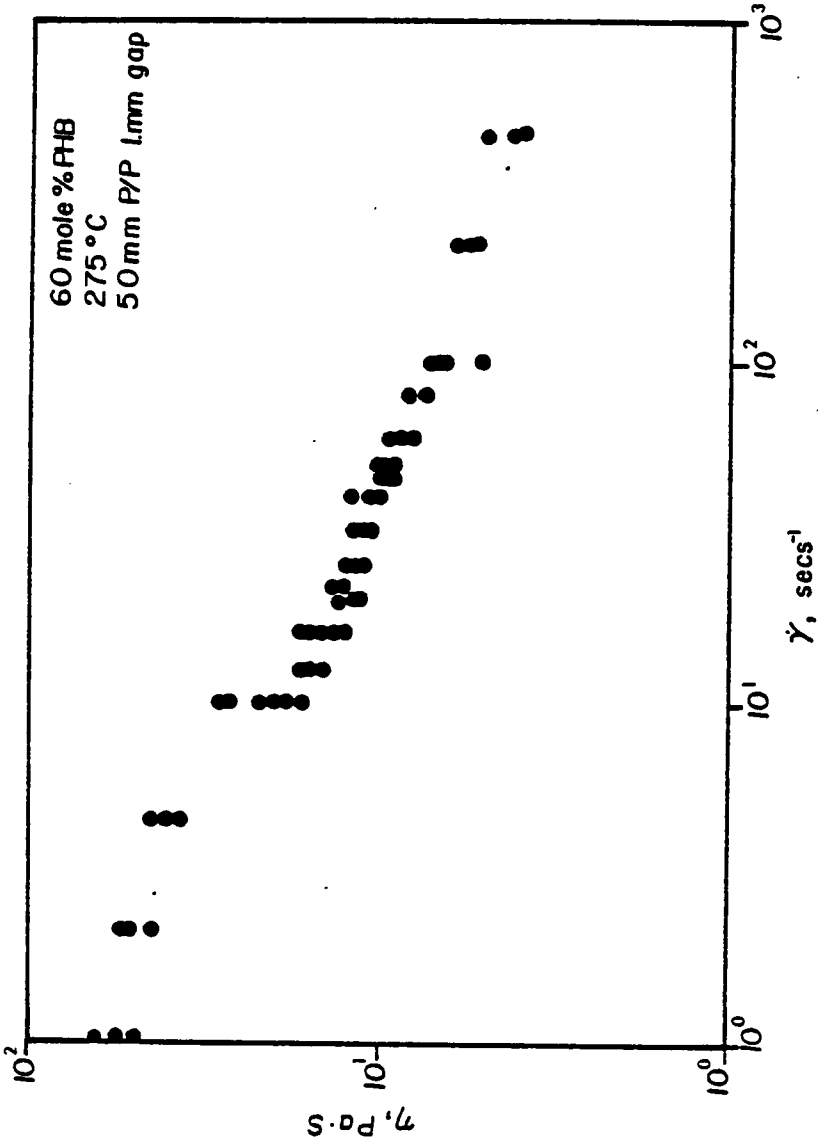

Figure 4.2 Steady Shear Data: η vs $\dot{\gamma}$ for 60 mole% PHB Copolymer 275°C, 50mm P/P 1.0mm gap.

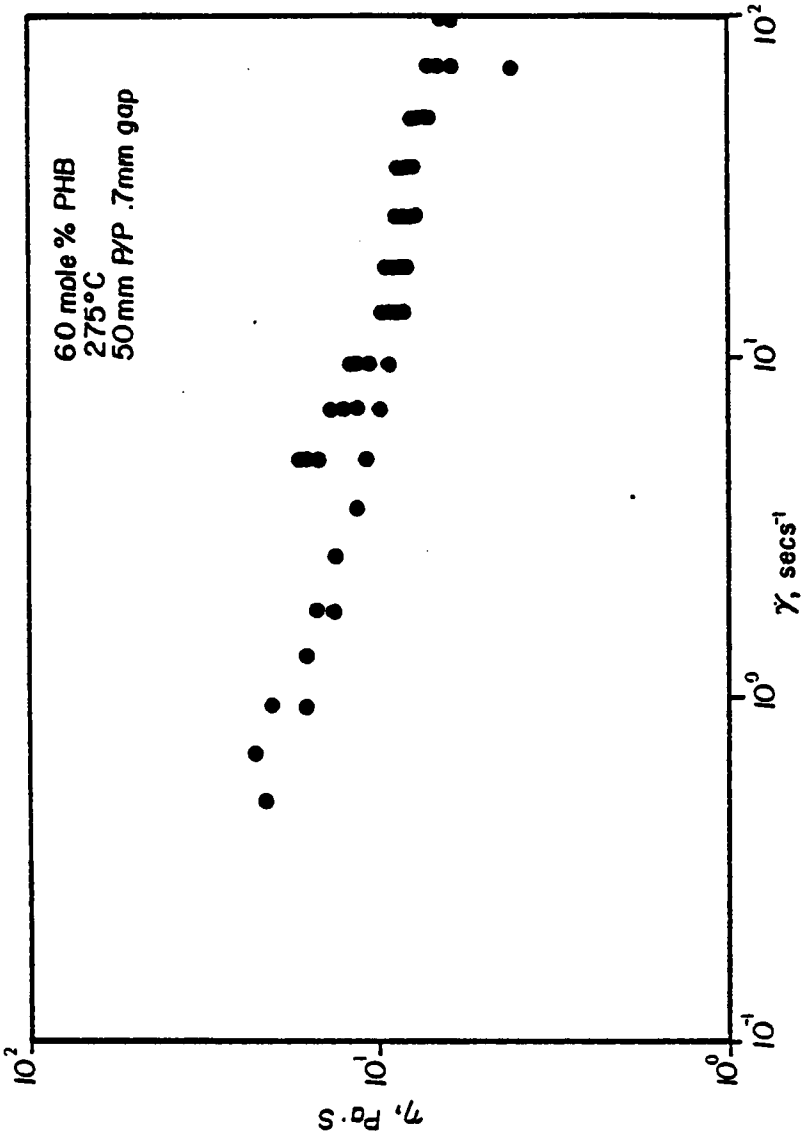

Figure 4.3 Steady Shear Data: η vs $\dot{\gamma}$ for 60 mole% PHB Copolymer 275°C, 50mm P/P 0.7mm gap.

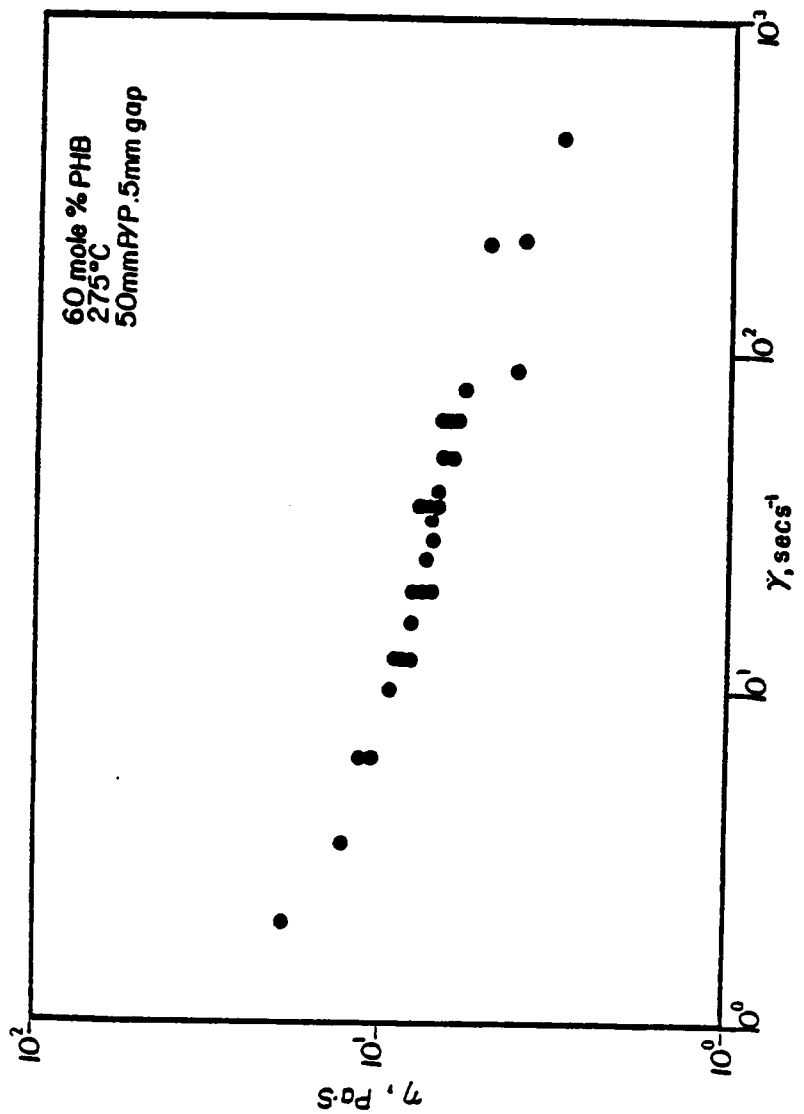

Figure 4.4 Steady Shear Data: η vs $\dot{\gamma}$ for 60 mole% PHB Copolymer 275°C, 50mm P/P 0.5mm gap.

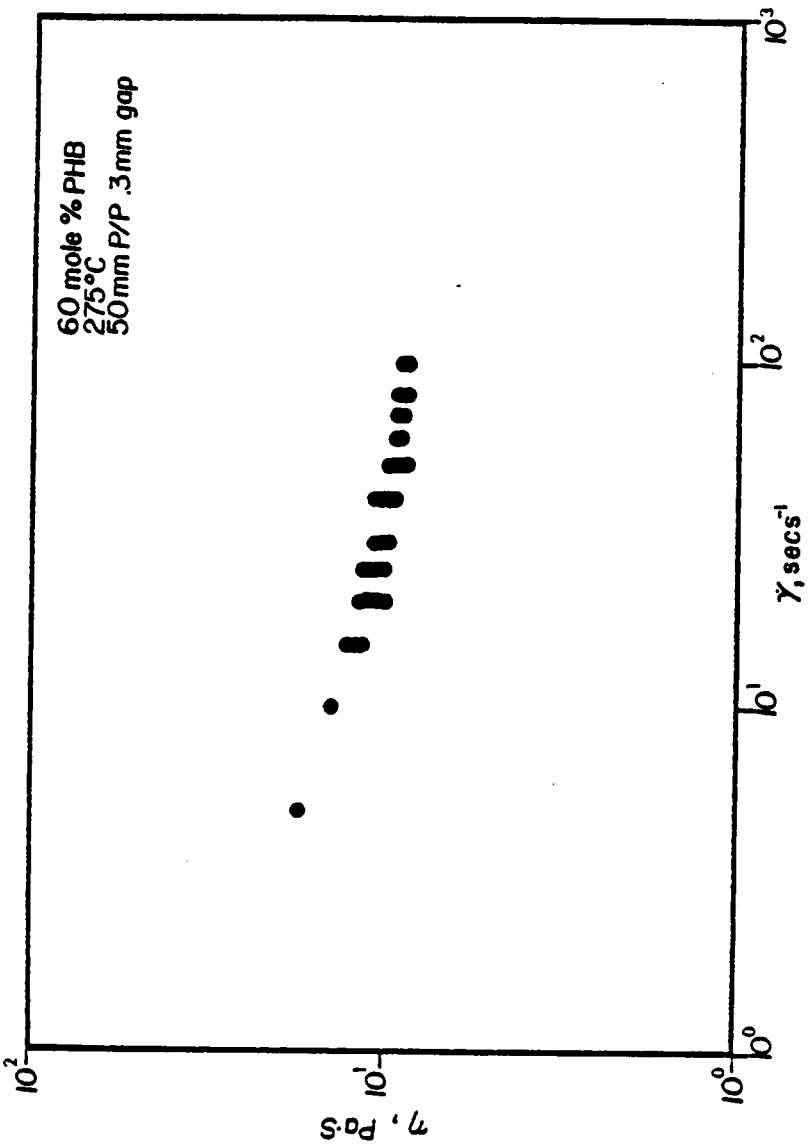

Figure 4.5 Steady Shear Data: η vs $\dot{\gamma}$ for 60 mole% PHB Copolymer 275°C, 50mm P/P 0.3mm gap.

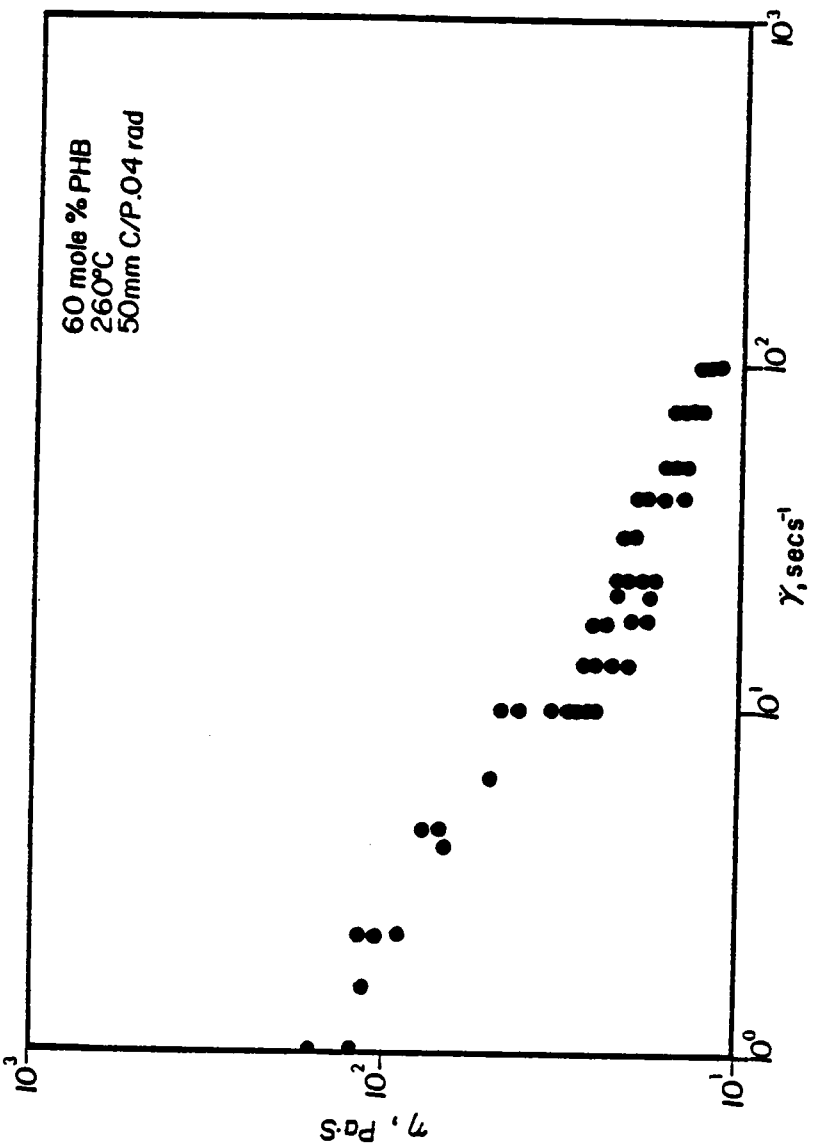

Figure 4.6 Steady Shear Data: η vs γ for 60 mole% PHB Copolymer 260°C, 50mm C/P 0.04 rad.

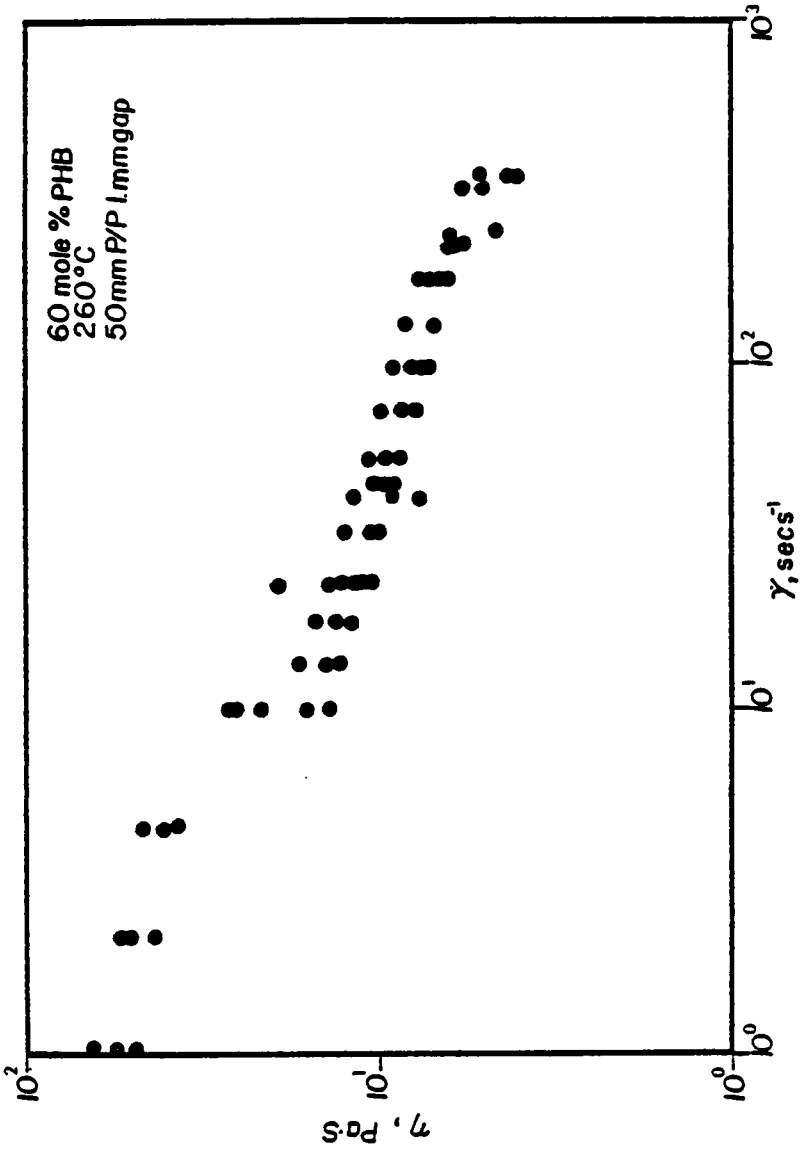

Figure 4.7 Steady Shear Data: η vs $\dot{\gamma}$ for 60 mole% PHB Copolymer 260°C, 50mm P/P 1.0mm gap.

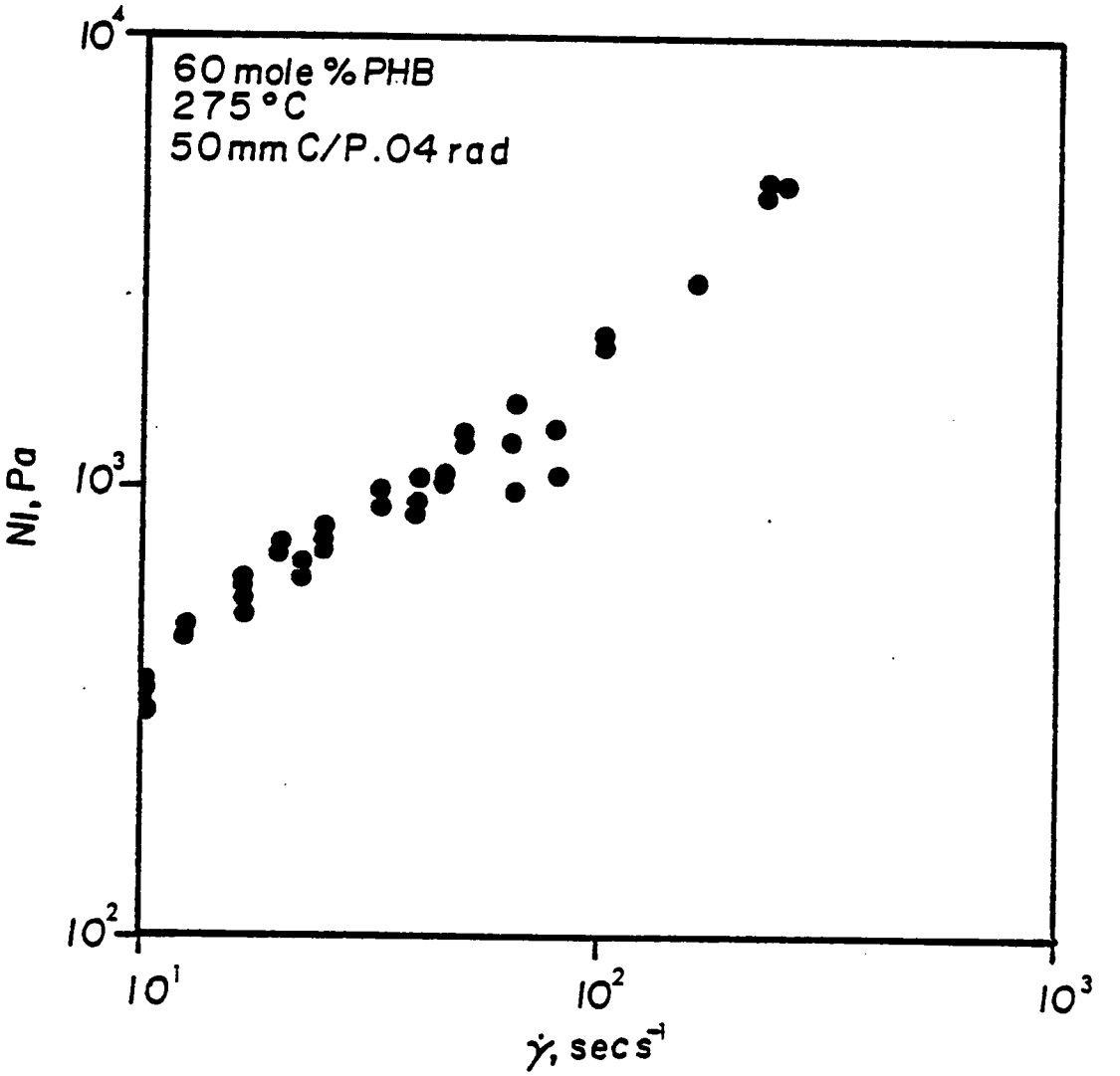

Figure 4.8 Steady Shear Data: N1 vs $\dot{\gamma}$ for 60 mole% PHB Copolymer 275°C, 50mm C/P 0.04 rad.

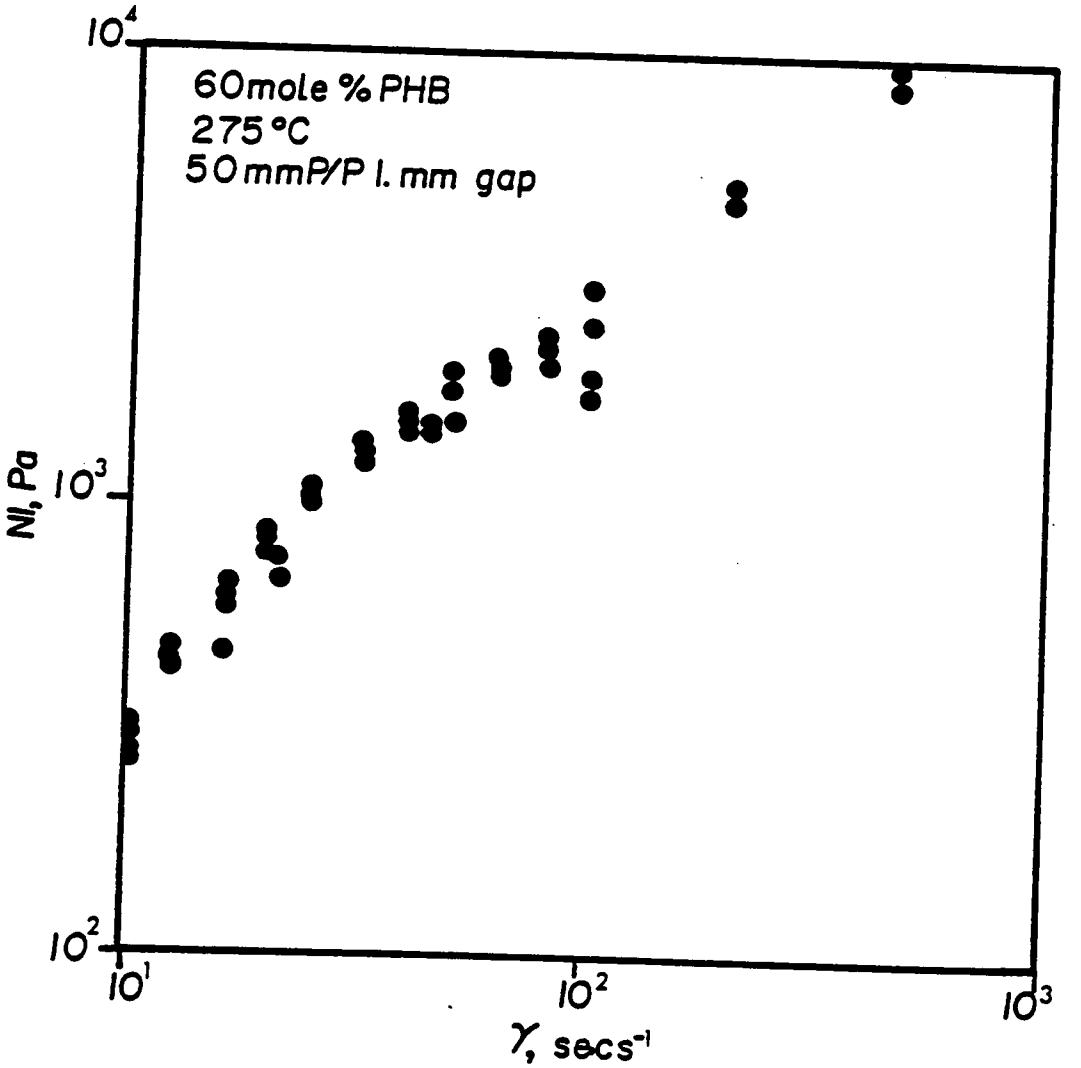

Figure 4.9 Steady Shear Data: N1 vs $\dot{\gamma}$ for 60 mole% PHB Copolymer 275°C, 50mm P/P 1.0mm gap.

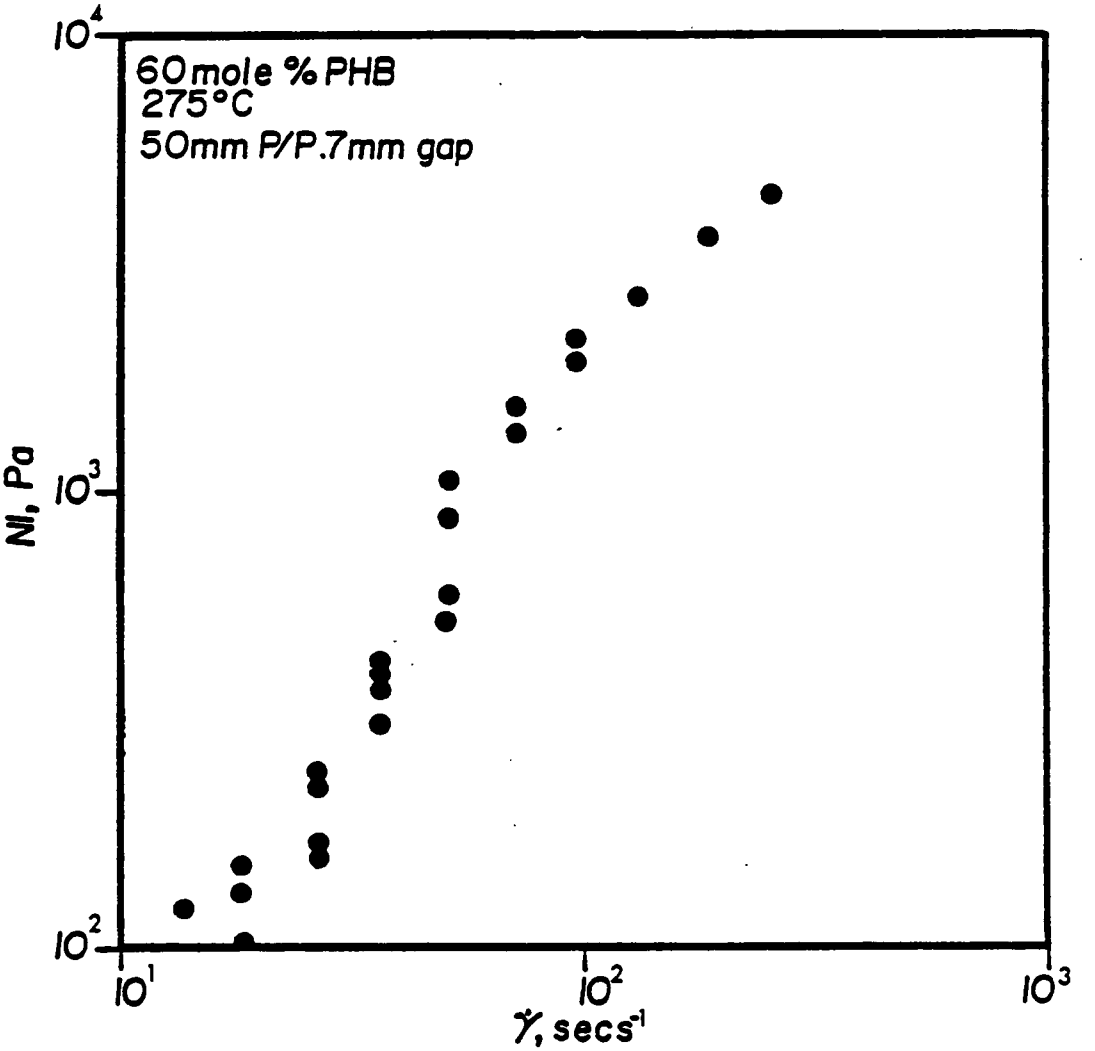

Figure 4.10 Steady Shear Data: N1 vs $\dot{\gamma}$ for 60 mole% PHB Copolymer 275°C, 50mm P/P 0.7mm gap.

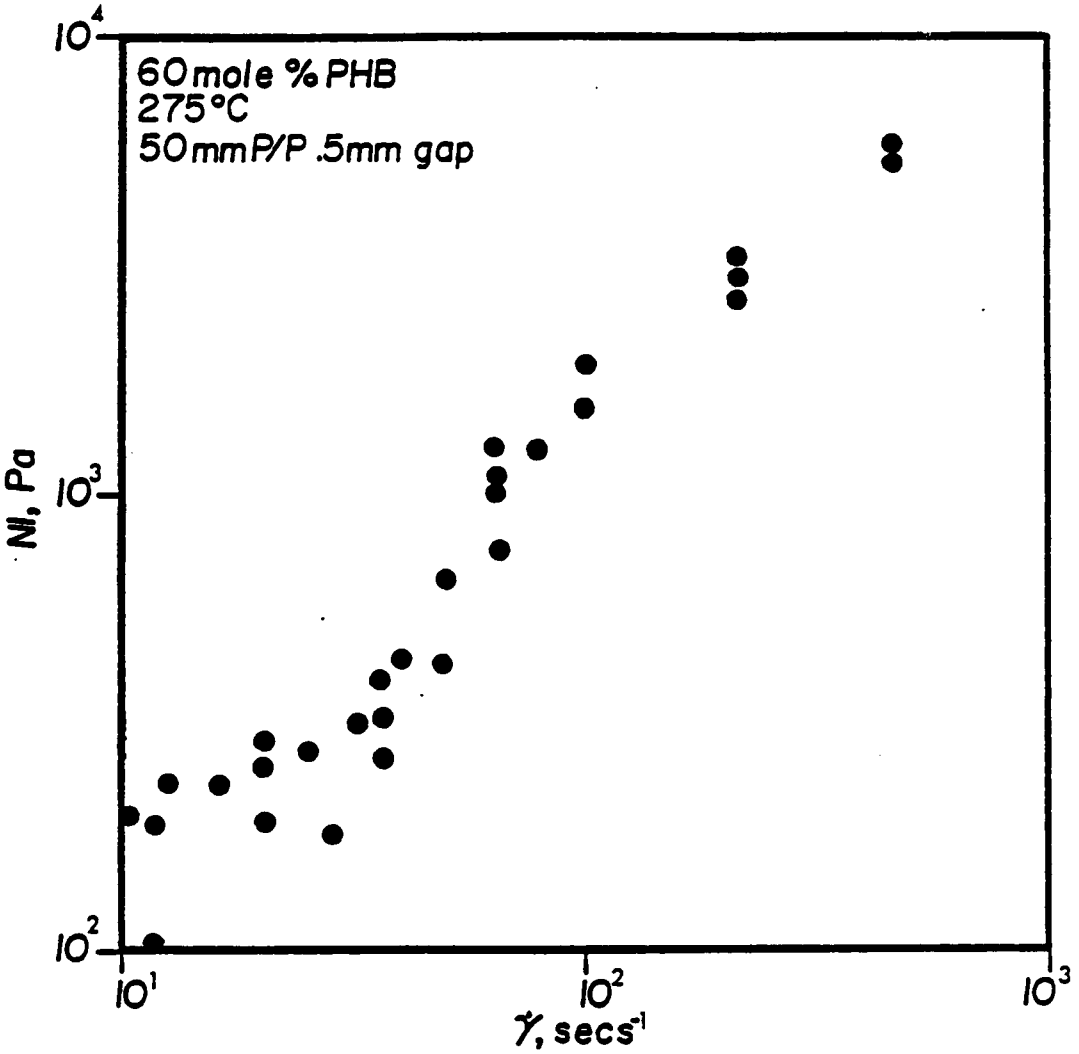

Figure 4.11 Steady Shear Data: N1 vs $\dot{\gamma}$ for 60 mole% PHB Copolymer 275°C, 50mm P/P 0.5mm gap.

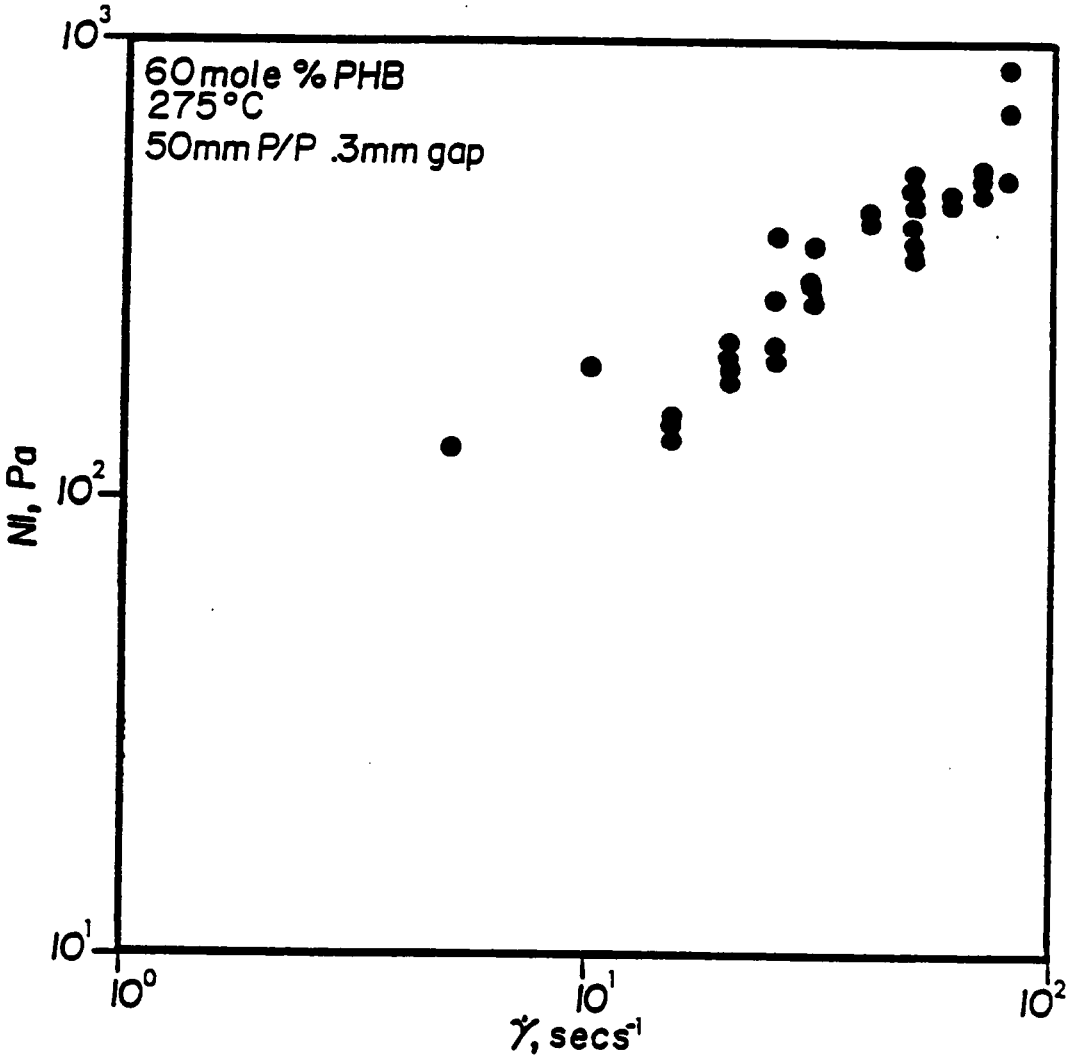

Figure 4.12 Steady Shear Data: N1 vs $\dot{\gamma}$ for 60 mole% PHB Copolymer 275°C, 50mm P/P 0.3mm gap.

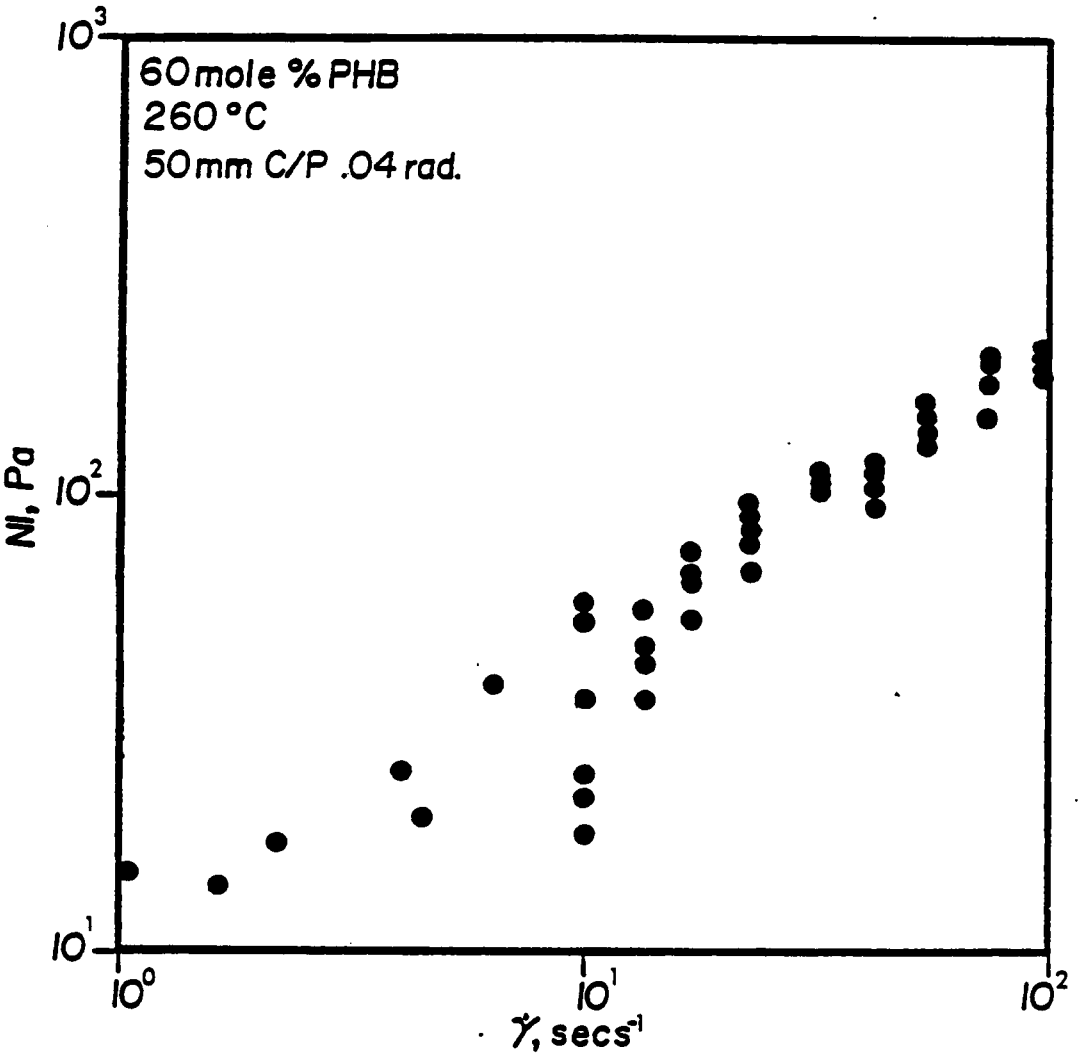

Figure 4.13 Steady Shear Data: N1 vs $\dot{\gamma}$ for 60 mole% PHB Copolymer 260°C, 50mm C/P 0.04 rad.

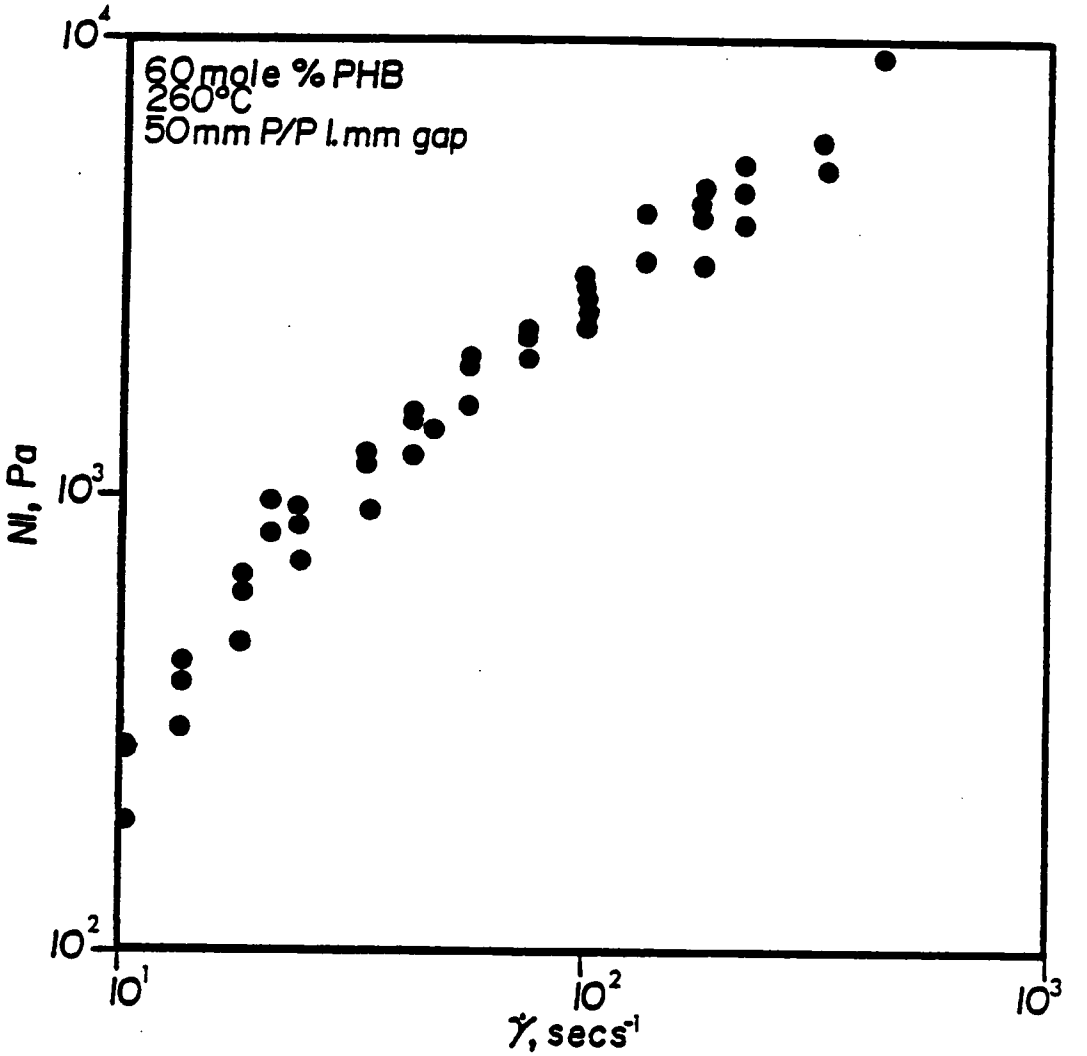

Figure 4.14 Steady Shear Data: N1 vs $\dot{\gamma}$ for 60 mole% PHB Copolymer 260°C, 50mm P/P 1.0mm gap.

4.1.2 PREDICTIONS OF ERICKSEN'S THEORY

Using the computer techniques outlined in section 3.6 and the experimentally determined forms for the material parameters, the predictions of Ericksen's non-linear theory for stress growth and extensional flow behavior were calculated. Three different initial conditions were examined using λ values of 1 and 5. These λ values were picked based on the predictions of equation [20] in Chapter Two. For a λ value of 1 the fluid particles align perfectly with the flow direction. For a λ value of 5 the director will come to rest at an angle to the flow direction determined by equation [20]. It was desired to know the different effects of these two steady state director positions on the transient behavior predicted by the theory.

In Figures 4.15 thru 4.18 are shown the predictions of the theory for the case in which an initial condition of $n_1=1$ is assumed. In general, the shear and normal stresses rapidly reach their steady state values without exhibiting any overshoot behavior. In the case of $\lambda=5$, however, the normal stresses overshoot their steady state value by 500%.

For the case of an initial condition of $n_2=1$, overshoot behavior is predicted in both the shear and normal stresses. These results are depicted in Figures 4.19 thru 4.24. For the case of $\lambda=1$ and $\dot{\gamma}=1$, the shear stresses overshoot their steady state value by 20%, while the normal forces undershoot and go negative before gradually reaching their

steady state value. Increasing the shear rate to $\dot{\gamma}$=10 secs^{-1} enlarges the magnitude of the overshoot and undershoot values and causes them to occur at shorter times. With λ=5, the shear stresses do not overshoot, but the normal stresses still go negative before reaching steady state.

In the case of an initial condition of n_3=1 and λ=1, it was shown that all three director equations would equal zero, specifying steady state. However, if n_3 is slightly perturbed, the director undergoes a slow rotation to end up aligned with the flow direction. The effect is that the shear and normal stresses take much longer to reach steady state than with the previous examples. This is shown in Figures 4.25 and 4.26. In the case of λ=5, the stresses do not take as much time time to reach steady state as for the case of λ=1. The shear stresses overshoot but the normal streses do not. These results are depicted in Figures 4.27 and 4.28.

The predictions of Ericksen's theory for extensional flow behavior are expressed in terms of the state of the director as a function of time. The effect of specifying different λ values on the transient behavior of the director was investigated. In uniaxial extension along the X1 direction, the X2 and X3 directions will be equivalent. Therefore, only one initial condition of n_2=1 was used. In Figures 4.29 and 4.30 are shown plots of n and n as a function of time. It can be seen that regardless of the λ value used, the director eventually ends up aligned with the principle stretch direction (n_1=1).

The previous results are important as they indicate a number of experiments which would be of interest. It is seen that Ericksen's theory predicts stress overshoot behavior in terms of changes in the state of the director (i.e. molecular orientation). This overshoot behavior is dependent on the initial conditions specified and the value of λ chosen. Ericksen's theory can predict negative values of the primary normal stress difference, N1. In the case of λ=1 with an initial condition of n_1=1, no overshoot occured. Therefore, once the fluid is oriented, no overshoot behavior is predicted by the theory. The stress relaxation behavior was not shown, but analysis of the stress equations [80-82] shows that if the shear rate goes to zero, the shear and normal stress will go to zero immediately. Finally, Ericksen's theory has been derived such that the +n and -n directions are equivalent. Thus, in a stress reversal experiment, Ericksen's theory predicts no overshoot behavior once the fluid is oriented. The predictions of Ericksen's theory have been investigated. The transient behavior of the PHB/PET and PPT/H_2SO_4 systems has been studied. The results of these investigations are presented in the next section.

The predictions of Ericksen's theory for extensional flow behavior indicate that molecular orientation occurs regardless the value of λ chosen. In shear flow, the degree of molecular orientation achieved depends on λ in a prescribed manner. These predictions are tested through the use of WAXS analysis to determine the degree of molecular orientation present in samples subjected to shear and extensional flow. The results

of the WAXS analysis appear in section 4.3

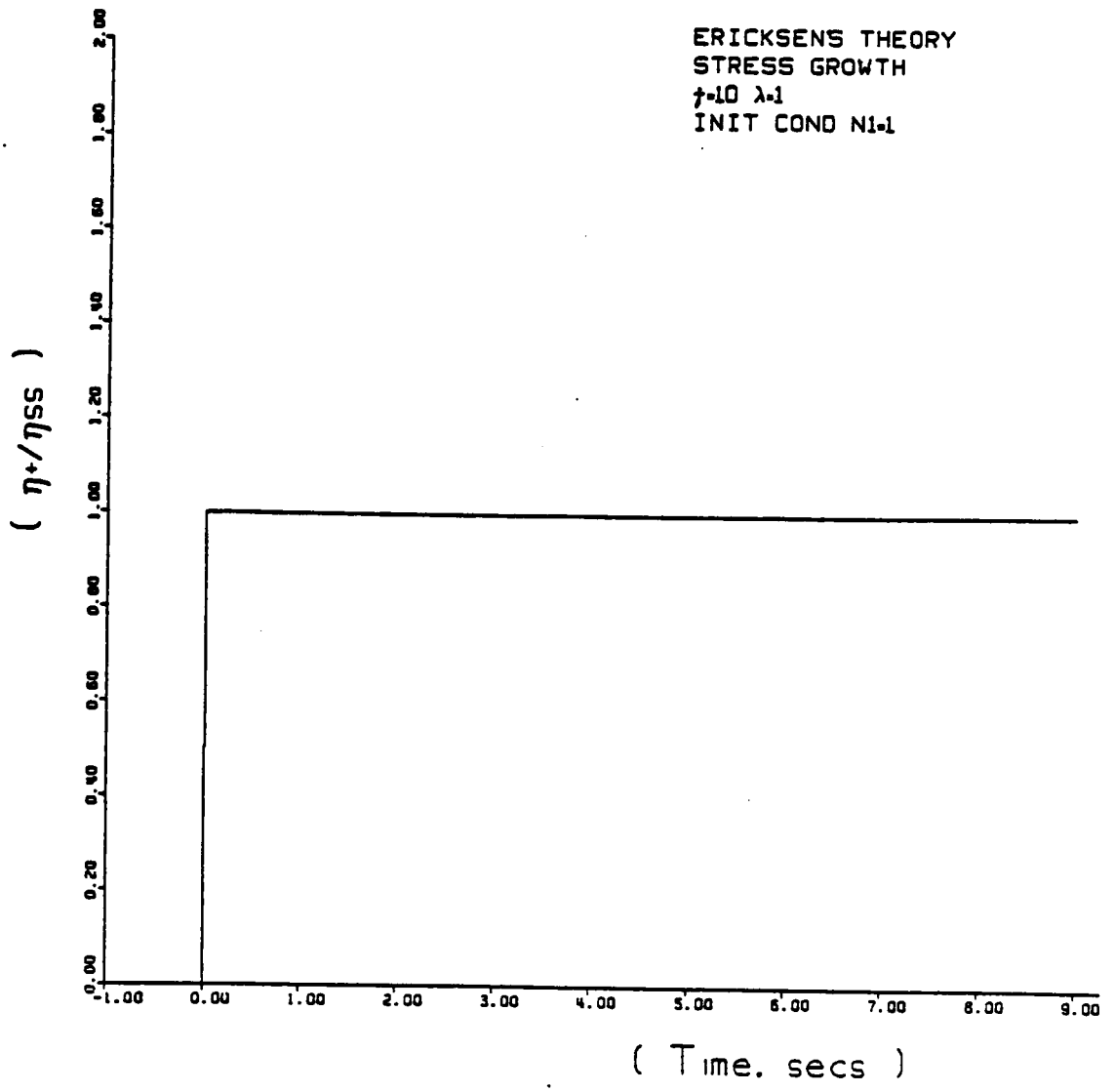

Figure 4.15 Predictions of Ericksen's Theory: Stress Growth η^+/η_{ss} vs t for Simple Shear Flow. $\dot{\gamma}=10$ secs^{-1}, $\lambda=1.0$, I.C.: n1=1.0

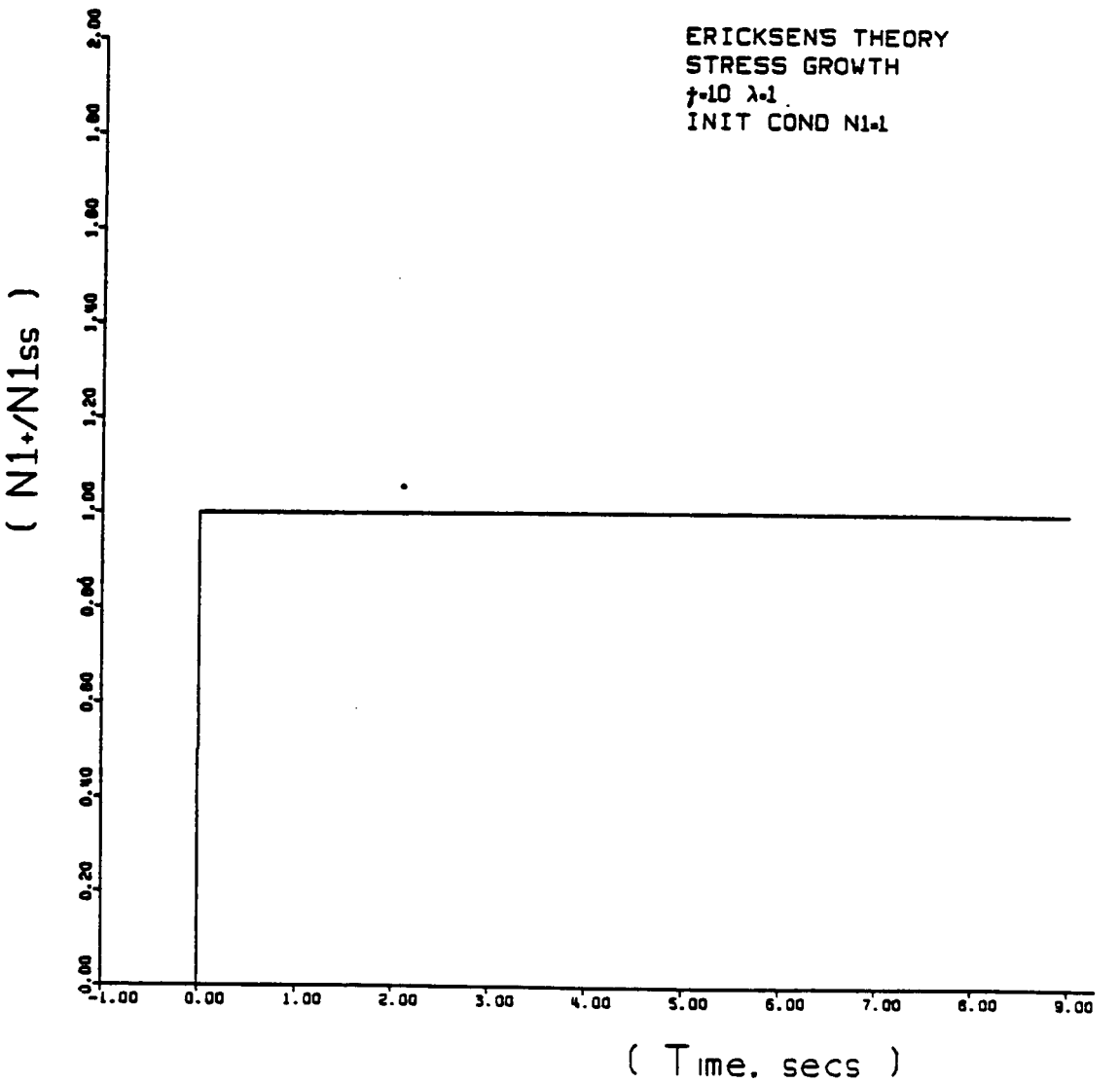

Figure 4.16 Predictions of Ericksen's Theory: Stress Growth N1+/N1ss vs t for Simple Shear Flow. $\dot{\gamma}$=10 secs^{-1}, λ=1.0, I.C.: n1=1.0

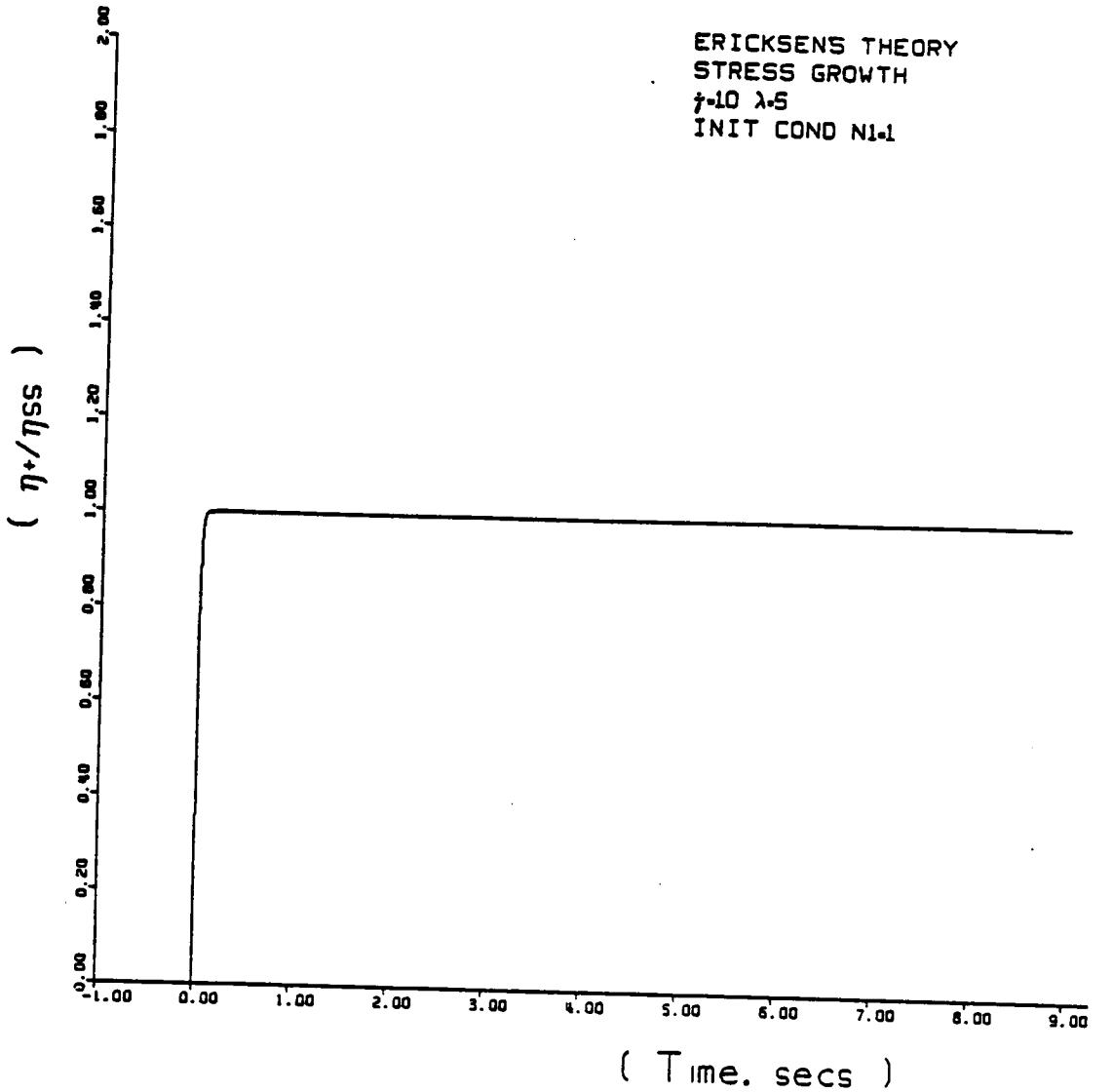

Figure 4.17 Predictions of Ericksen's Theory: Stress Growth η^+/η_{ss} vs t for Simple Shear Flow. $\dot{\gamma}$=10 secs^{-1}, λ=5.0, I.C.: n1=1.0

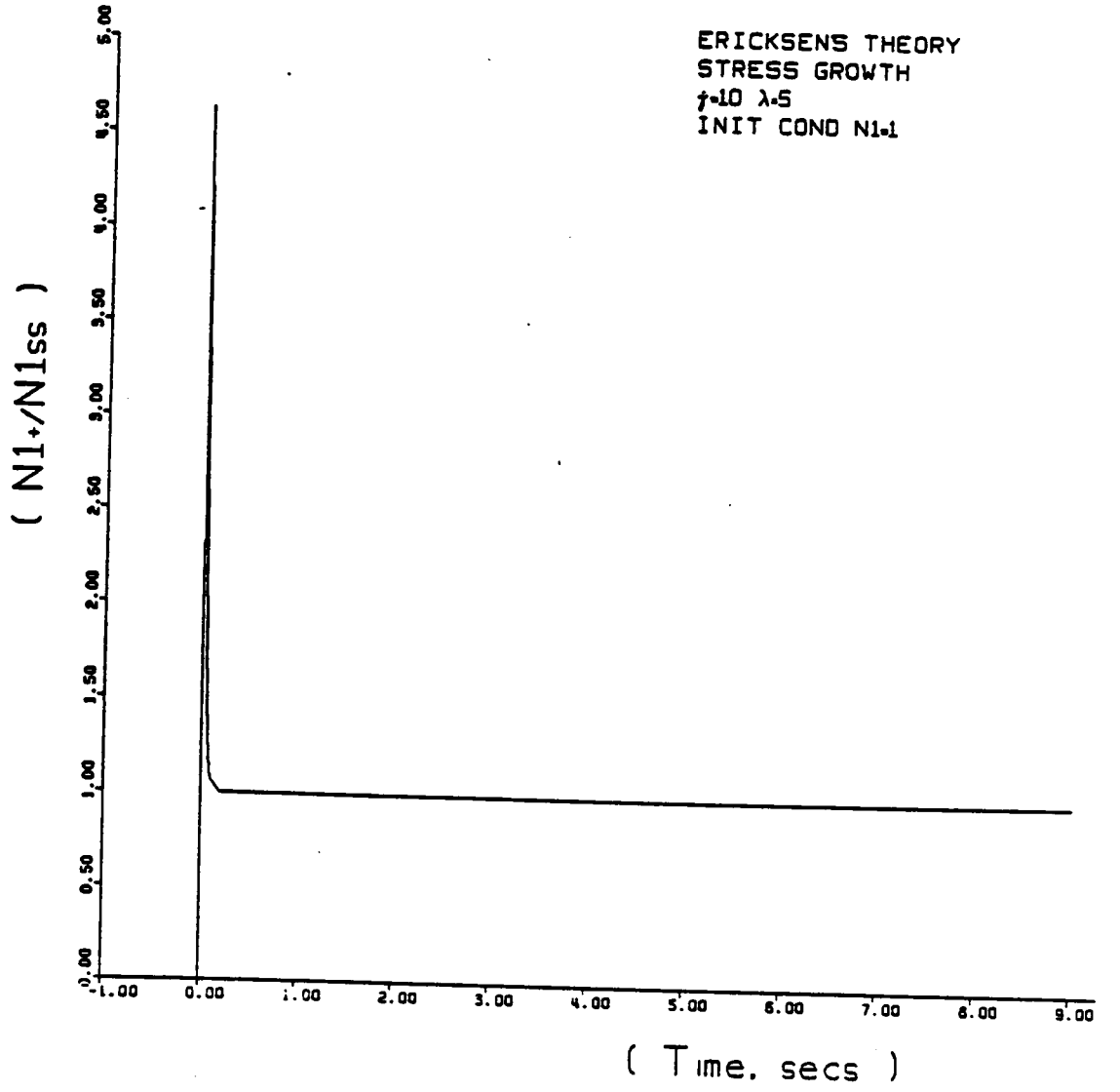

Figure 4.18 Predictions of Ericksen's Theory: Stress Growth N1+/N1ss vs t for Simple Shear Flow. $\dot{\gamma}$=10 secs^{-1}, λ=5.0, I.C.: n1=1.0

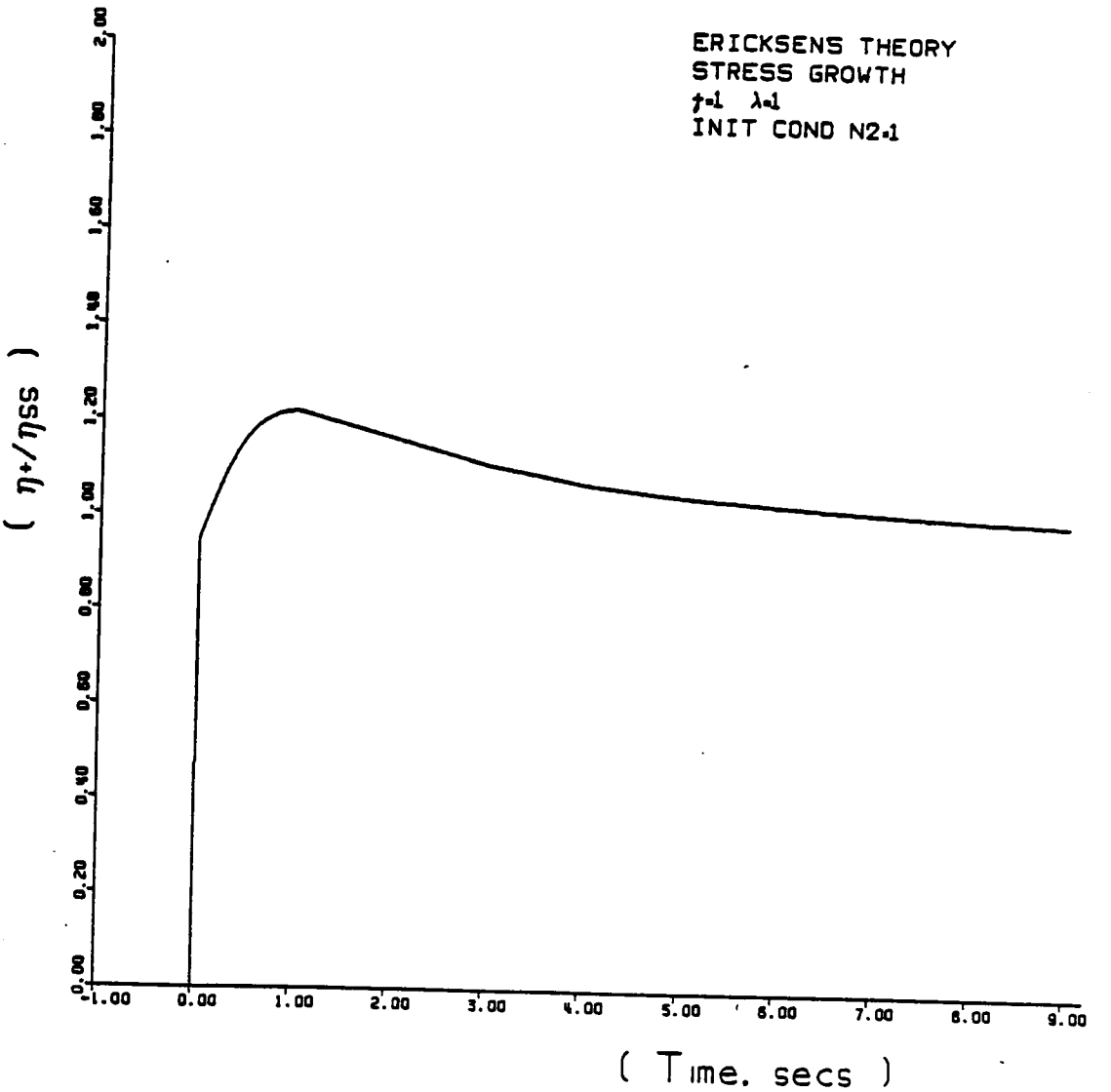

Figure 4.19 Predictions of Ericksen's Theory: Stress Growth η^+/η_{ss} vs t for Simple Shear Flow. $\dot{\gamma}=1$ secs^{-1}, $\lambda=1.0$, I.C.: n2=1.0

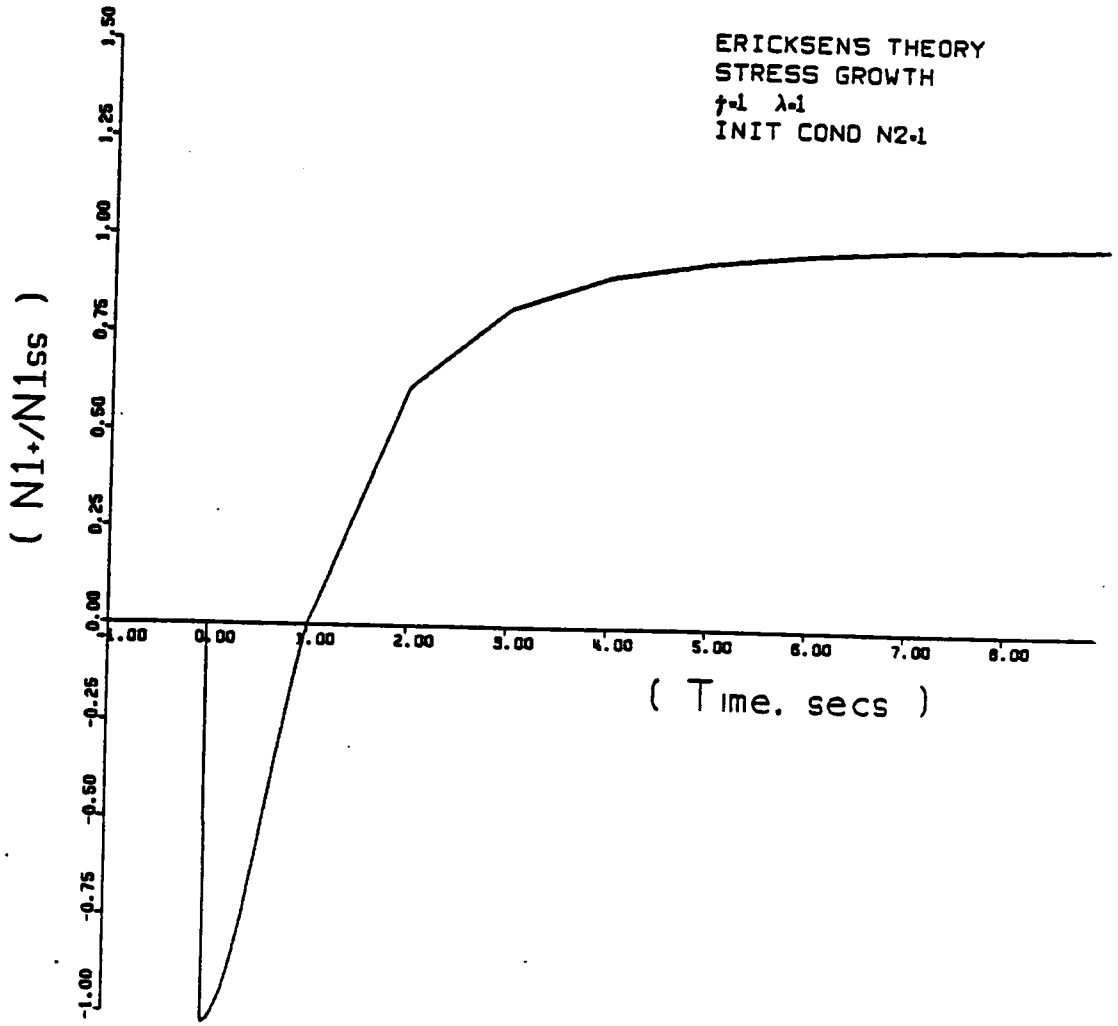

Figure 4.20 Predictions of Ericksen's Theory: Stress Growth $N1+/N1_{ss}$ vs t for Simple Shear Flow.
$\dot{\gamma}=1$ secs^{-1}, $\lambda=1.0$, I.C.: n2=1.0

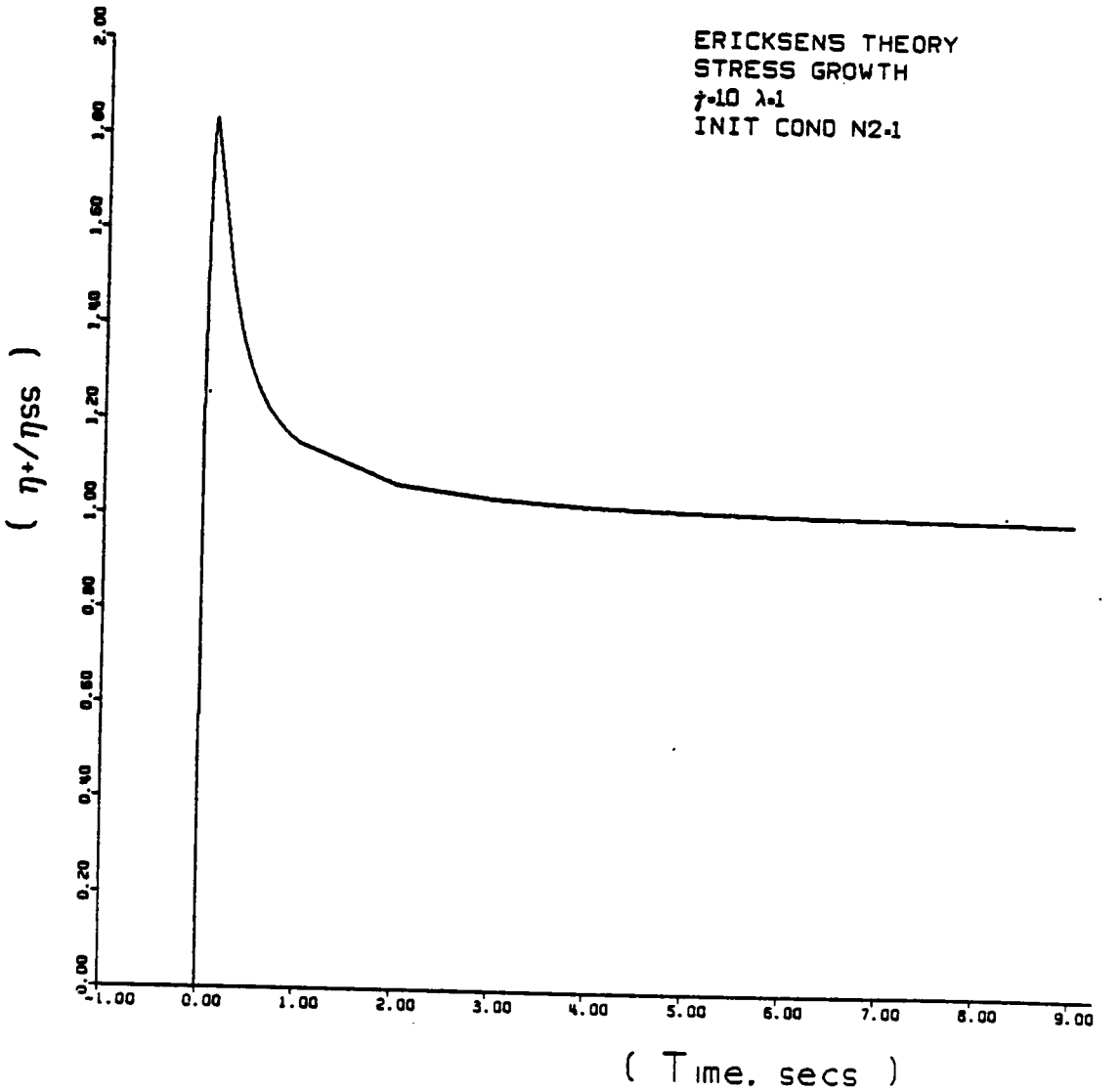

Figure 4.21 Predictions of Ericksen's Theory: Stress Growth η^+/η_{ss} vs t for Simple Shear Flow. $\dot{\gamma}$=10 secs^{-1}, λ=1.0, I.C.: n2=1.0

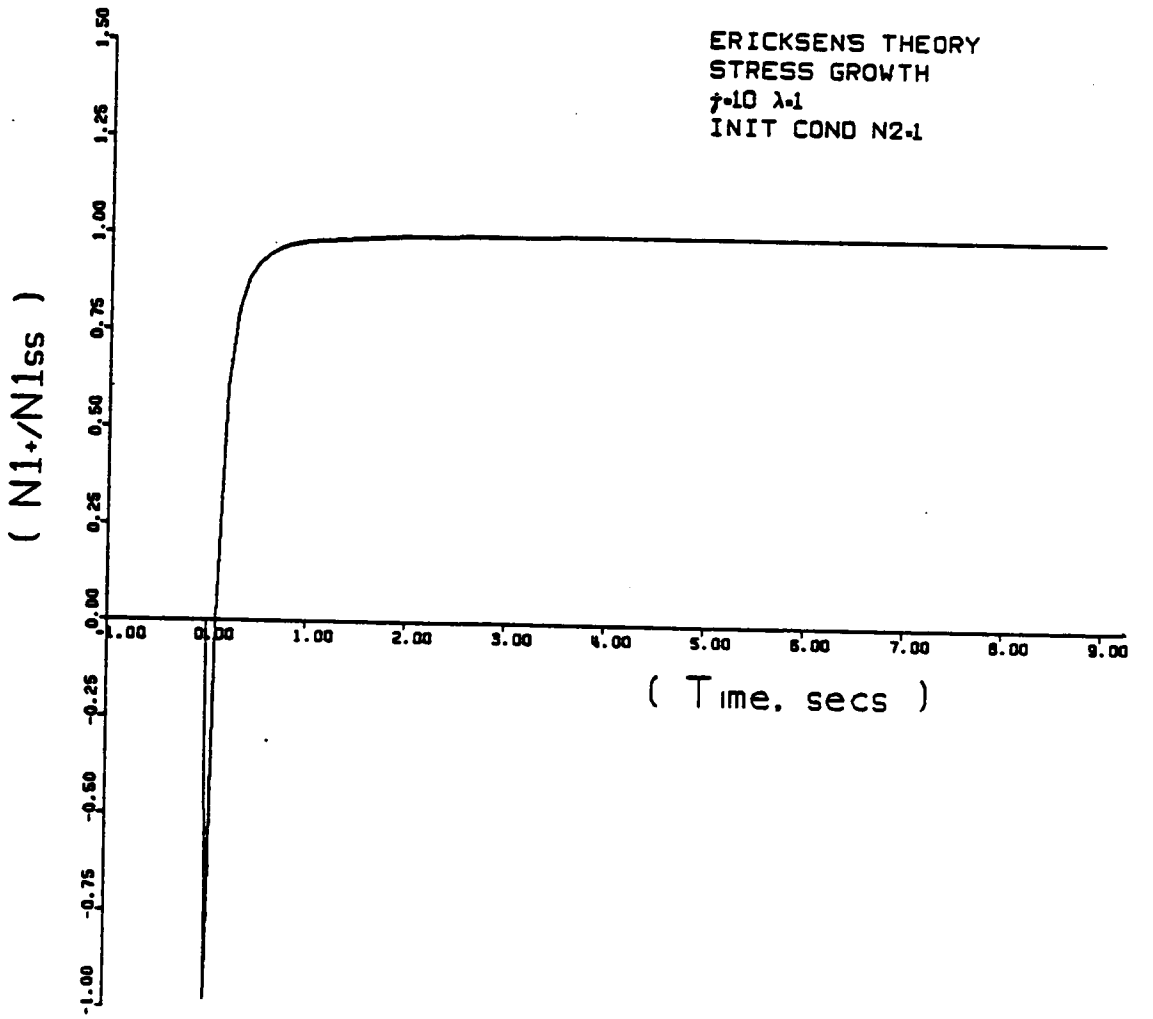

Figure 4.22 Predictions of Ericksen's Theory: Stress Growth N1+/N1ss vs t for Simple Shear Flow. $\dot{\gamma}$=10 secs^{-1}, λ=1.0, I.C.: n2=1.0

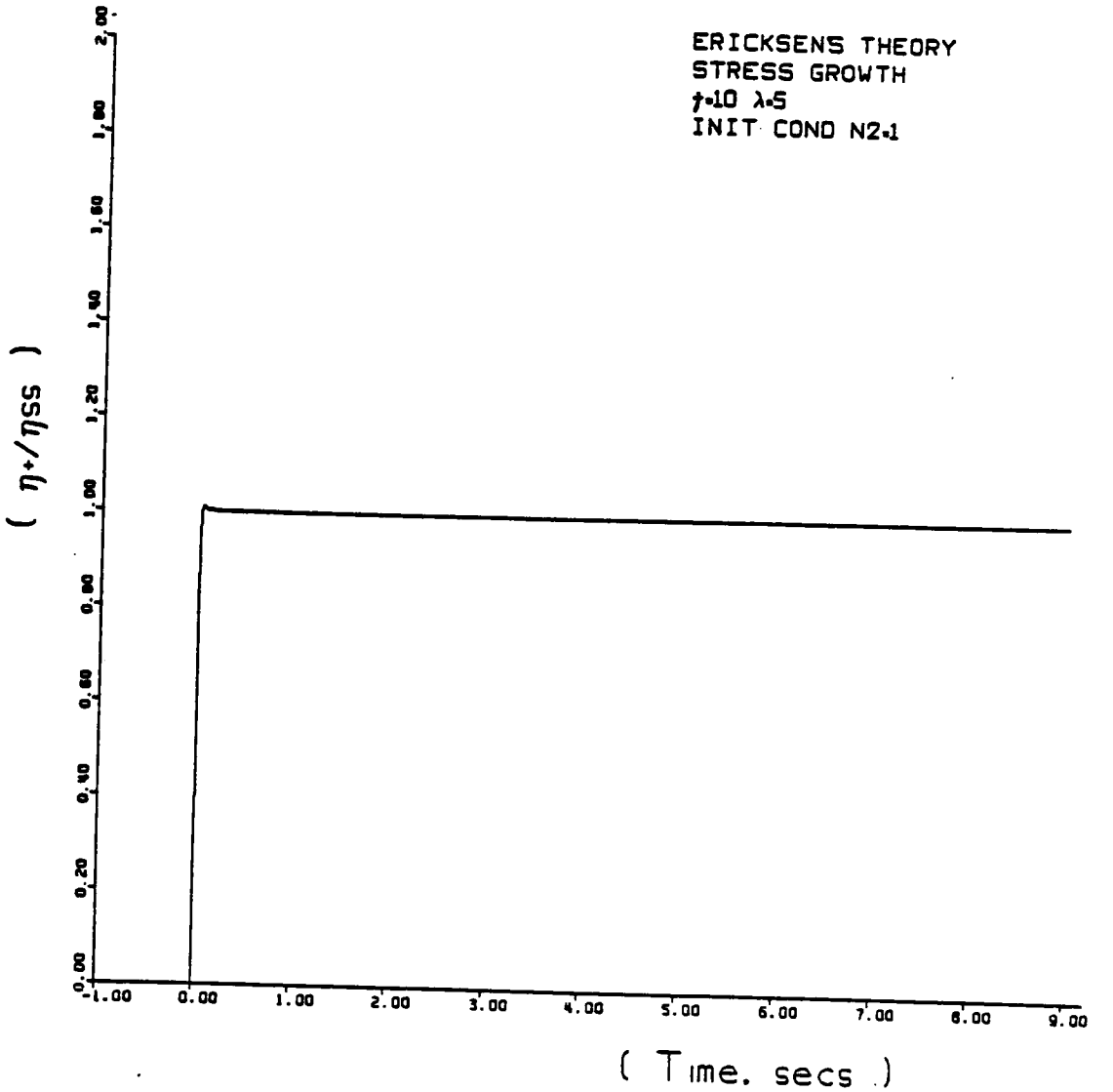

Figure 4.23 Predictions of Ericksen's Theory: Stress Growth η^+/η_{ss} vs t for Simple Shear Flow. $\dot{\gamma}$=10 secs^{-1}, λ=5.0, I.C.: n2=1.0

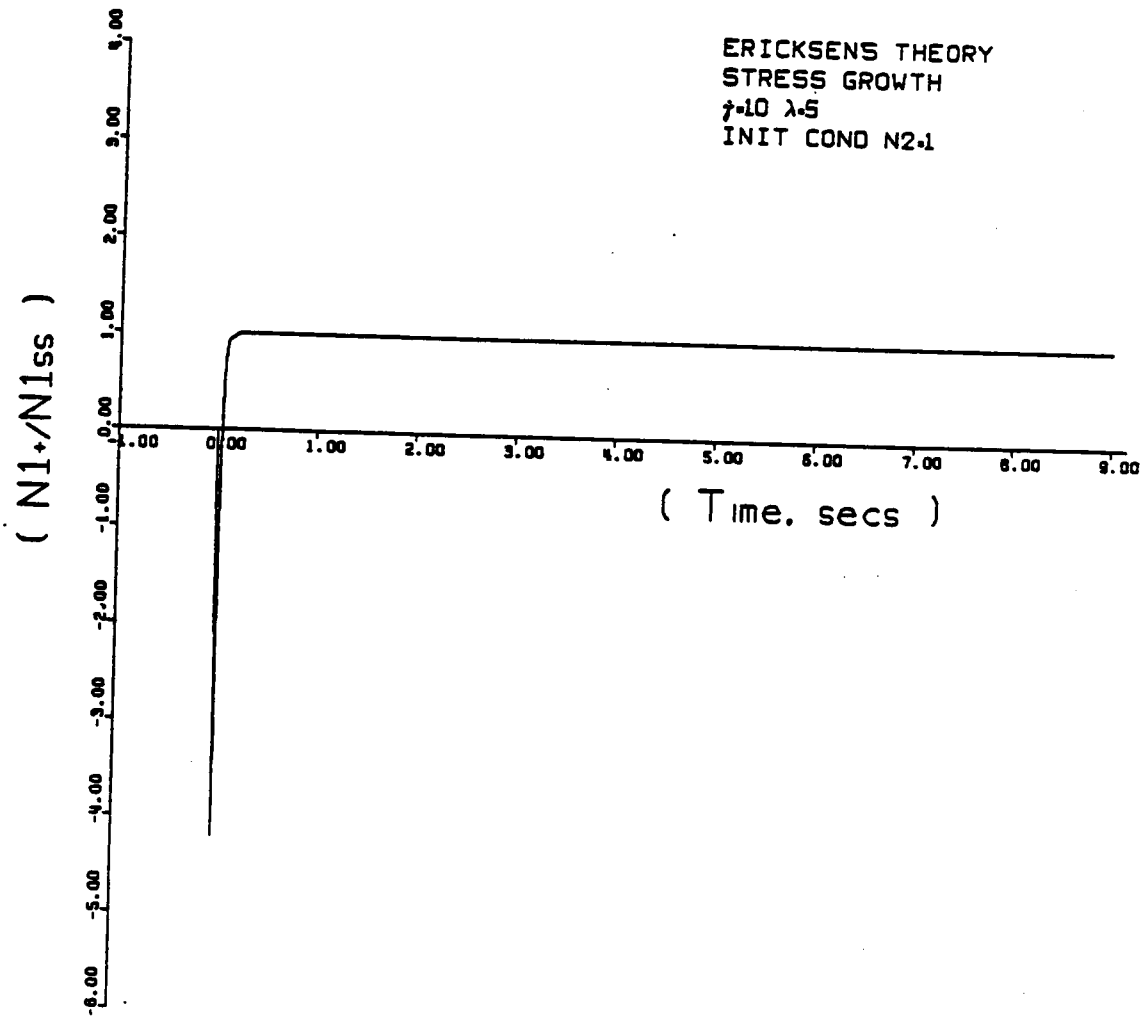

Figure 4.24 Predictions of Ericksen's Theory: Stress Growth $N1^+/N1_{ss}$ vs t for Simple Shear Flow. $\dot{\gamma}=10$ secs^{-1}, $\lambda=5.0$, I.C.: n2=1.0

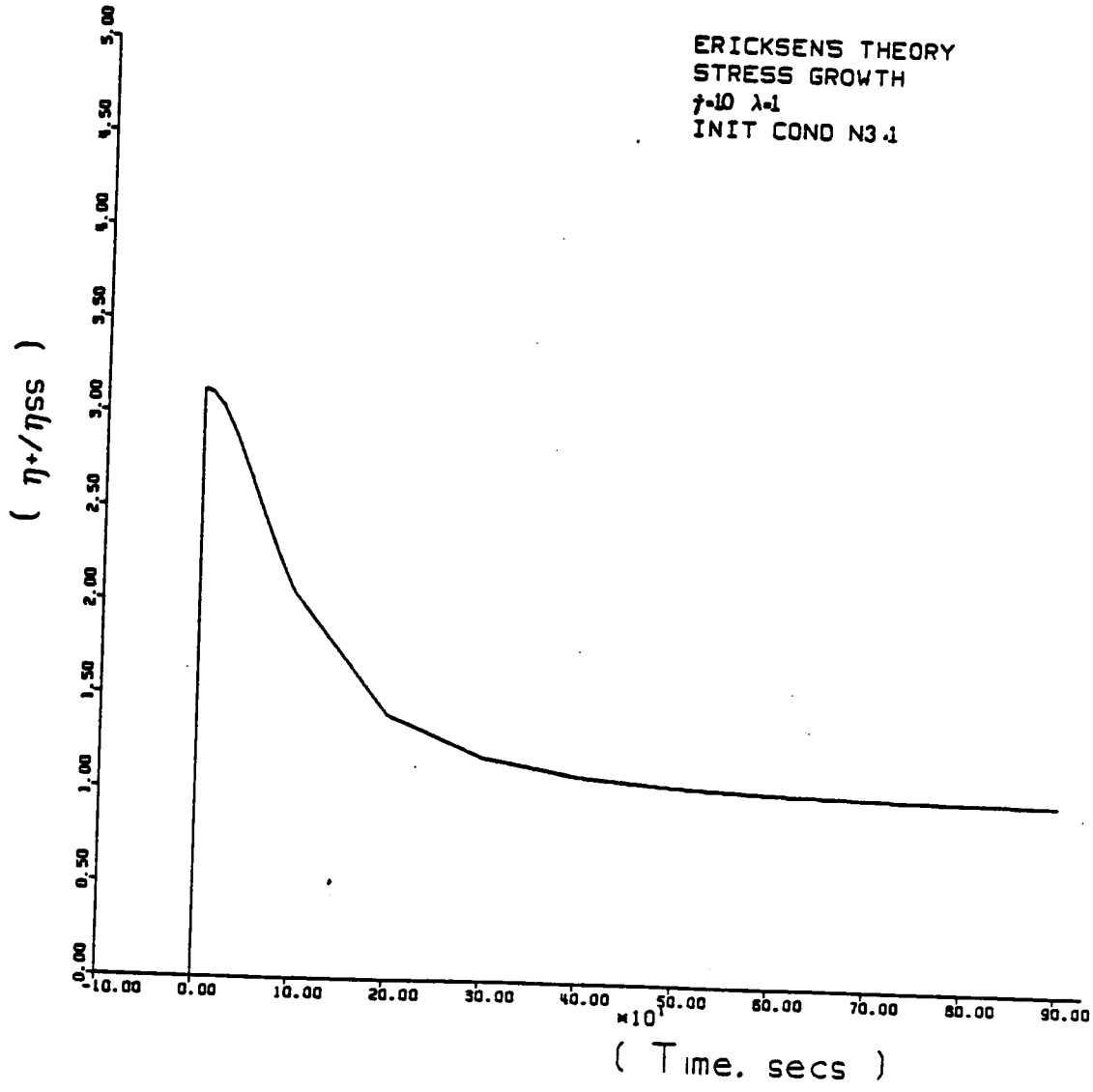

Figure 4.25 Predictions of Ericksen's Theory: Stress Growth $\eta+/\eta_{ss}$ vs t for Simple Shear Flow. $\dot{\gamma}$=10 secs^{-1}, λ=1.0, I.C.: n3=1.01

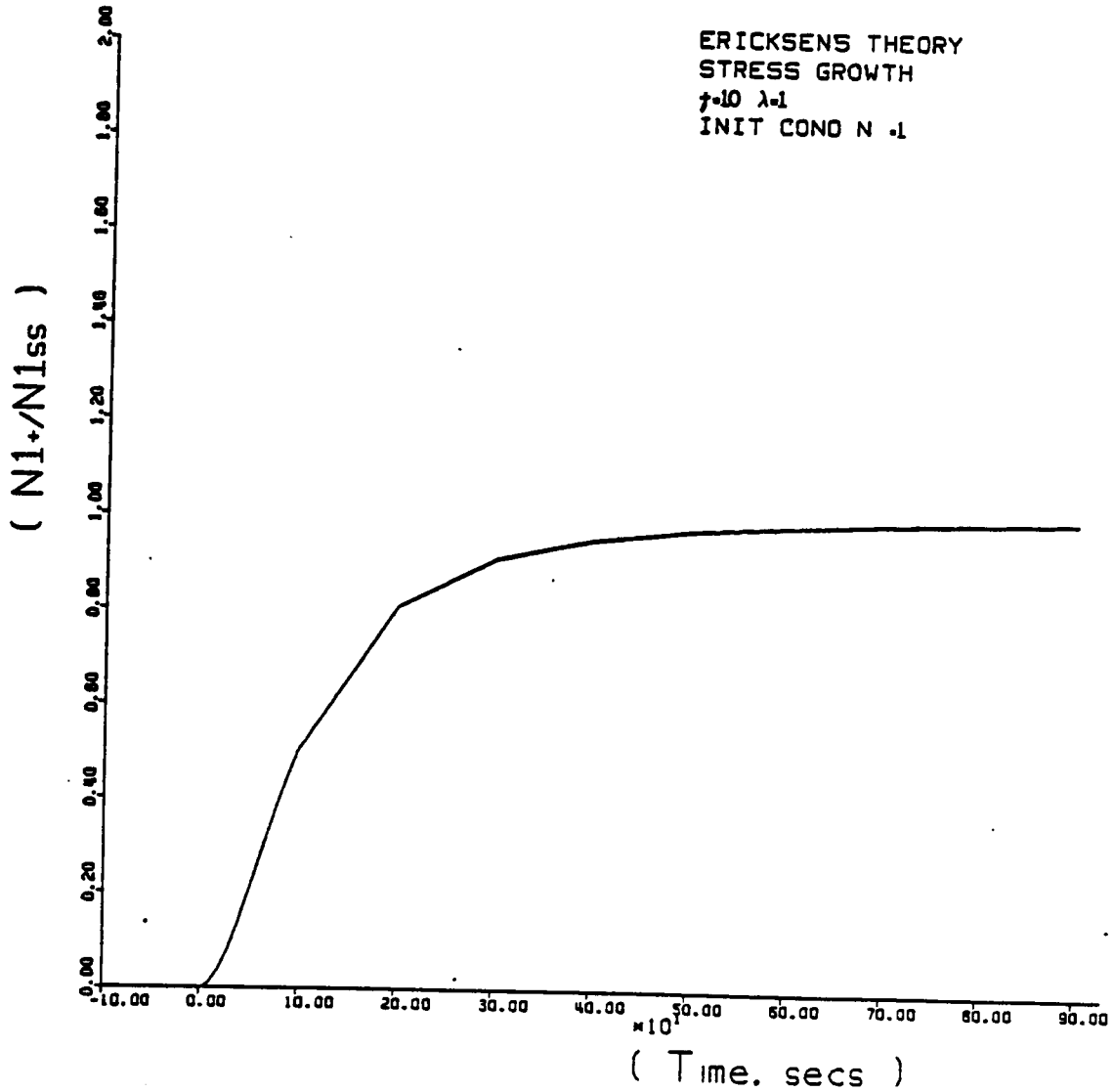

Figure 4.26 Predictions of Ericksen's Theory: Stress Growth N1+/N1ss vs t for Simple Shear Flow. $\dot{\gamma}$=10 secs^{-1}, λ=1.0, I.C.: n3=1.01

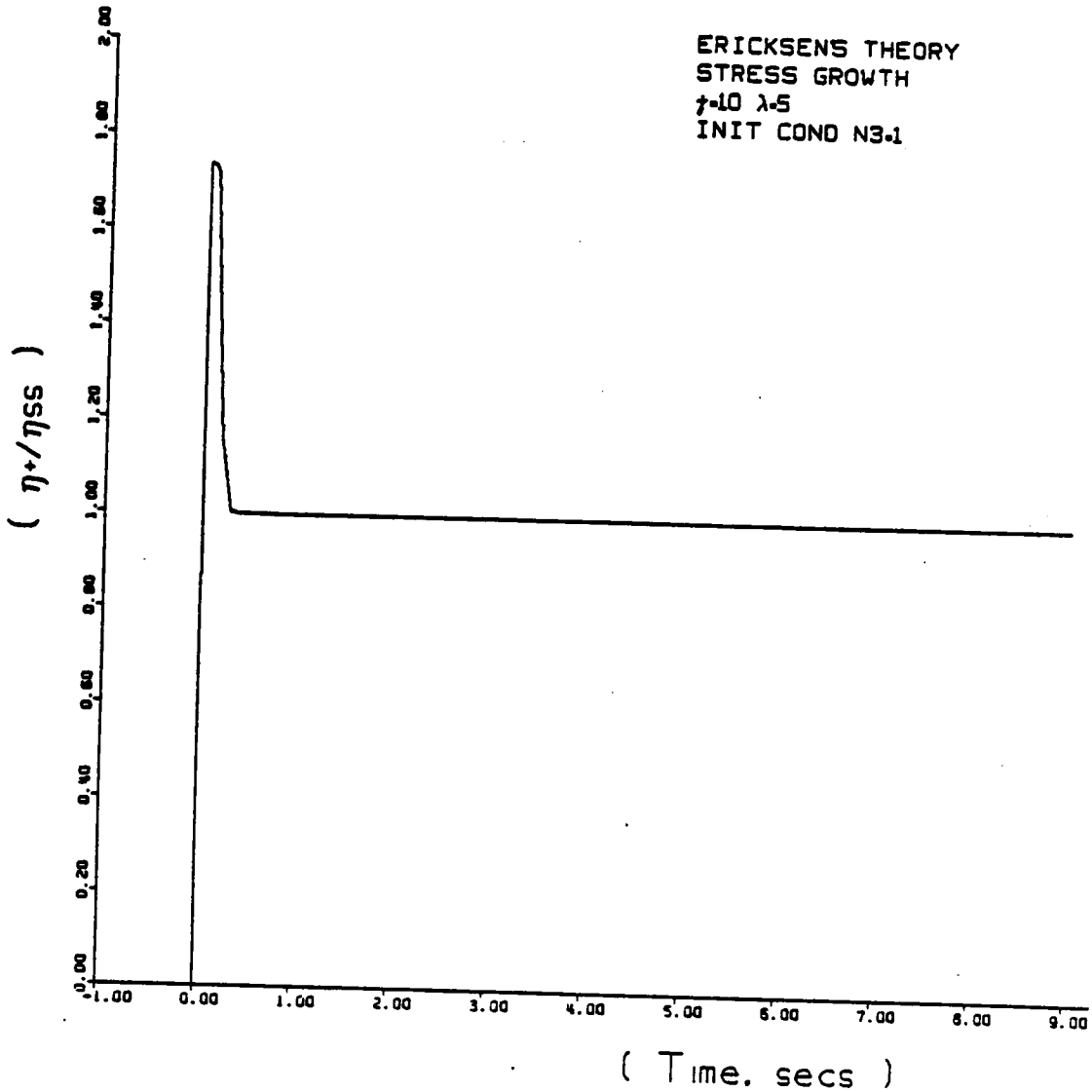

Figure 4.27 Predictions of Ericksen's Theory: Stress Growth η^+/η_{ss} vs t for Simple Shear Flow. $\dot{\gamma}=10$ secs^{-1}, $\lambda=5.0$, I.C.: n3=1.0

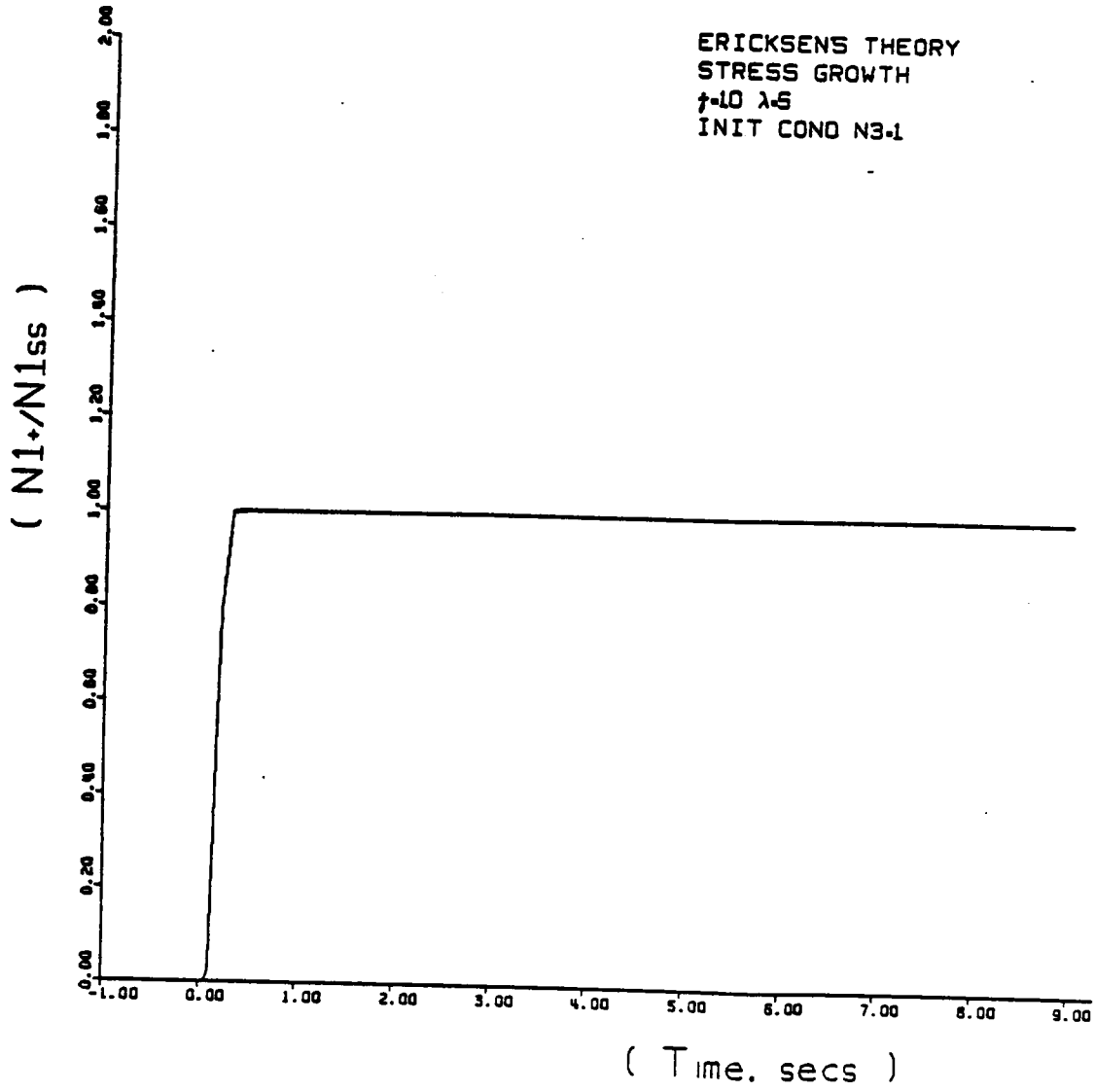

Figure 4.28 Predictions of Ericksen's Theory: Stress Growth N1+/N1ss vs t for Simple Shear Flow. $\dot{\gamma}$=10 secs^{-1}, λ=5.0, I.C.: n3=1.0

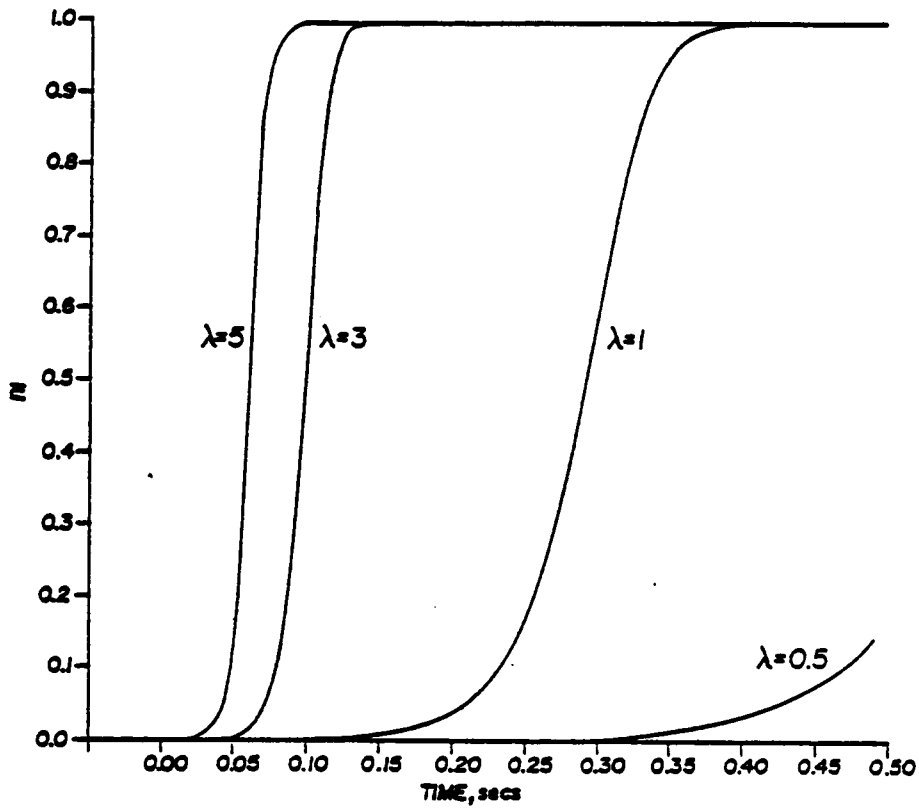

Figure 4.29 Predictions of Ericksen's Theory: Extensional Flow
n1 vs t for different λ values
$\dot{\epsilon}$=10 secs^{-1}, I.C.: n2=1.0

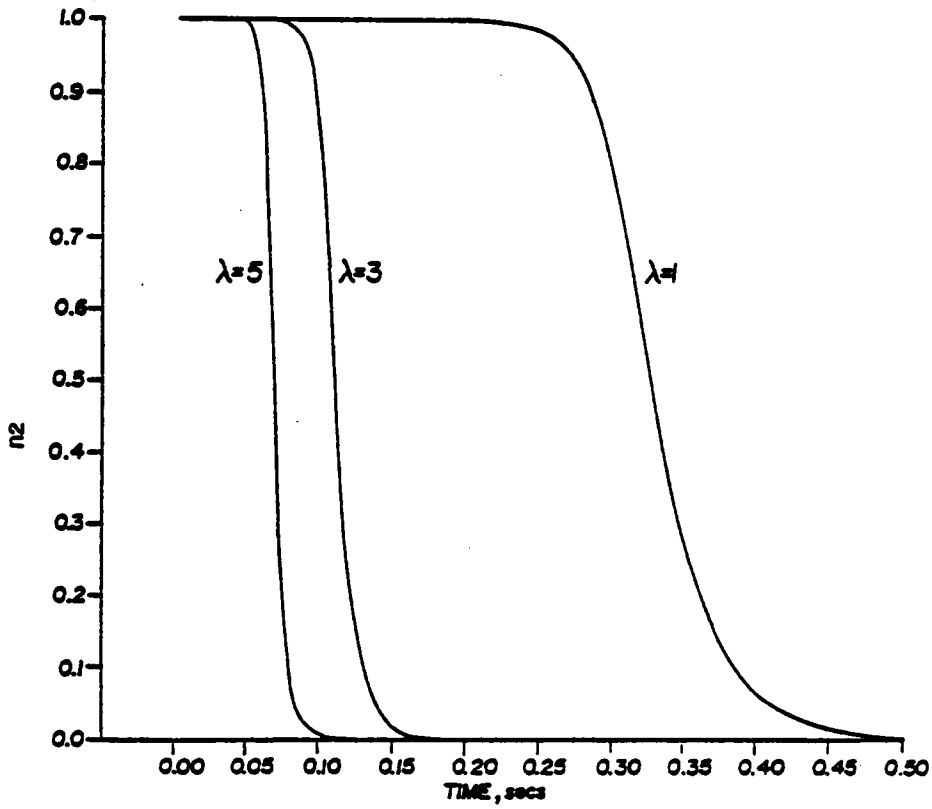

Figure 4.30 Predictions of Ericksen's Theory: Extensional Flow
n2 vs t for different λ values
$\dot{\epsilon}$=10 secs^{-1}, I.C.: n2=1.0

4.2 RHEOLOGICAL MEASUREMENTS

A number of rheological tests were performed in order to determine the validity of the predictions of Ericksen's theory. These tests were also performed to see if the behavior of liquid crystalline materials is any different from that of flexible chain polymers. Besides studying the PHB/PET systems, a lyotropic solution of 12 wt% PPT in 100% pure H_2SO_4 was tested in order to make the results more general.

4.2.1 STRESS GROWTH/RELAXATION BEHAVIOR

The transient behavior of the 60 mole% PHB/PET copolyester was studied at different temperatures and shear rates. The results of these measurements are summarized in Figures 4.31 thru 4.33. At all temperatures, the shear stresses are seen to overshoot their steady state values. This overshoot occurs at a strain value of approximately two strain units, and the magnitude of overshoot increases with shear rate. At all temperatures and shear rates, the stresses relax immediately to a zero value upon the cessation of shear. This indicates that the material does not possess a yield stress, and the stress relaxation time is small. Above 250°C, a second overshoot peak is exhibited at a strain value of approximately 50-60 strain units. Joseph [72] has shown that above 250°C, a two phase structure may exist in the 60 mole% PHB/PET system. This may account for the two overshoot peaks seen.

One of the predictions of Ericksen's theory indicated that once molecular orientation had been achieved, no stress overshoot behavior would occur. In order to test this prediction, interrupted stress growth experiments were performed. The shearing was stopped after the stresses reached their steady state values and was resumed after some rest period, t_r. The results of these measurements are depicted in Figures 4.34 thru 4.36. At all temperatures, the first overshoot peak is noticeably absent upon resumption of shear. In some cases, the shear direction was reversed after relaxation of the stresses had taken place. No difference in the response of the stresses is shown in the figures. In Figure 4.37 is shown the behavior of the 60 mole% PHB/PET copolyester at 275°C for a number of rest times ranging from 1 second to 3 minutes. Even after three minutes at the melt temperature, the first peak remains absent.

Another prediction of Ericksen's theory involved the concept of the +n and -n directions being equivalent. Thus, once the fluid is oriented no stress overshoot behavior is predicted by the theory for reversal of shear direction. In order to test this assumption, shear reversal experiments were conducted. The shear direction was reversed during shearing, or after stress relaxation had taken place. The results of these measurments are shown in Figures 4.38 thru 4.40. At all temperatures it is seen that the stresses do not exhibit the first overshoot peak upon reversal of shear direction. The behavior of the shear stresses is also seen to be the same, independent of whether reversal occurs during shear or after stress relaxation has taken place.

4.2.1.1 STRESS GROWTH BEHAVIOR OF OTHER SYSTEMS

All of the results discussed thus far have dealt exclusively with the behavior of the 60 mole% PHB/PET system. In order to determine if such behavior is common to all liquid crystalline systems, the behavior of other liquid crystalline systems has been investigated.

In Figure 4.41 is shown a typical stress growth curve exhibited by the 80 mole% PHB/PET system. It is seen that upon inception of shear, the shear stress overshoots it steady state value. Two overshoot peaks are present. The first overshoot peak occurs at a strain value of approximately two strain units, while the second occurs at a strain value of approximately of 30 strain units. Upon reversal of the shear direction, the shear stress immediately reaches its steady state value with no apparent overshoot. Upon cessation of shear, the shear stress assumes a zero value within several seconds. This behavior is exactly the same as that exhibited by the 60 mole% PHB/PET system.

The transient response of an anisotropic solution of 12 wt% PPT in 100% pure H_2SO_4 has also been investigated. In Figure 4.42 is shown a typical stress growth curve for this system. A large overshoot peak occurs at a strain value of at most 2 strain units. After three minutes relaxation, the shearing is resummed. Only a slight overshoot peak is seen. In Figure 4.43 is shown the behavior exhibited in a stress reversal experiment from steady state conditions. The magnitude of the overshoot peak is greatly reduced by preshearing. Finally, in Figure

4.44 is shown the stress behavior exhibited by reversing the shear direction during shear. The overshoot peak is still greatly reduced by preshearing. In all three figures concerned with the PPT/H_2SO_4 system, the stresses relax to a zero value immediately upon the cessation of shear. It should also be noted that no second overshoot peak is apparent in any of the figures indicating that such behavior may be unique to the PHB/PET system.

4.2.2 SUMMARY OF TRANSIENT EXPERIMENTS

The stress growth/relaxation behavior of three liquid crystalline systems has been investigated. In general, the behavior exhibited by these systems is in qualitative agreement with the predictions of Ericksen's theory. It is seen that preshearing of these materials affects the magnitude of the first overshoot peak. Once the first overshoot peak has been destroyed, it remains absent even after three minutes at the melt temperature. The stresses relax very quickly to a zero value indicating that these materials do not possess yield stresses. The fluids appear to be insensitive to the reversal of shear direction after the first overshoot peak has been erased. Ericksen's theory predicts that the previously observed behavior would be due to the development of molecular orientation within the melt. However, it is possible that some other phenomenon, such as rearrangement or destruction of texture, occurs within the melt.

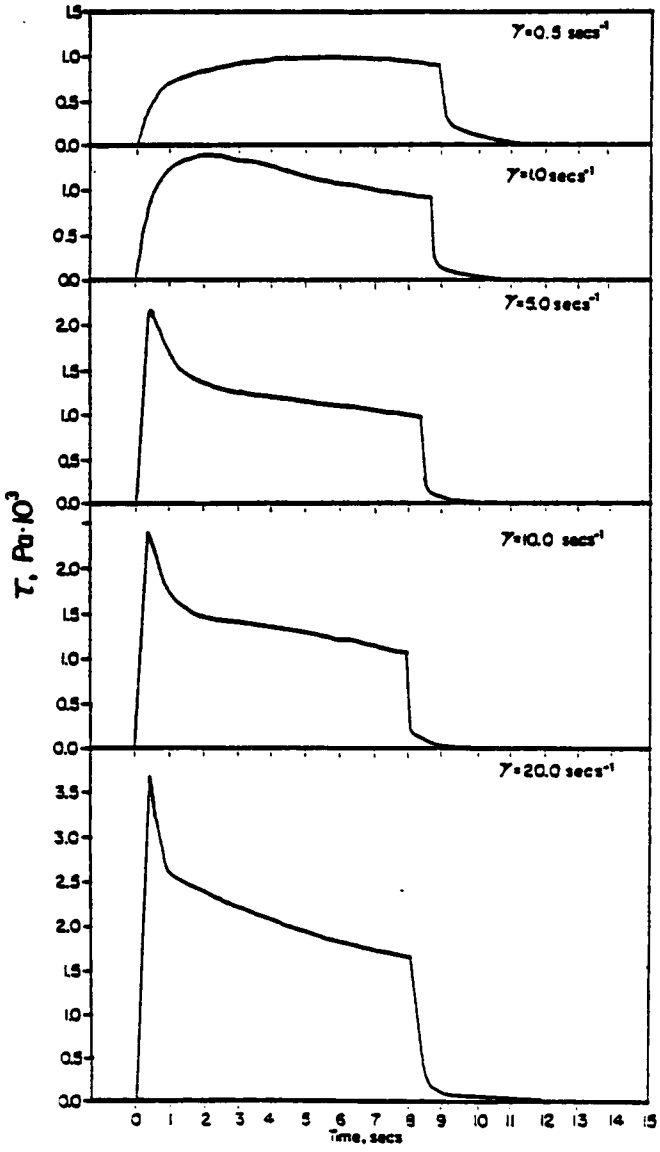

Figure 4.31 Transient Behavior: Stress Growth/Relaxation
τ₁₂ vs t for 60 mole% PHB Copolymer
250°C, 50mm C/P 0.04 rad, γ̇=0.5-20 secs⁻¹.

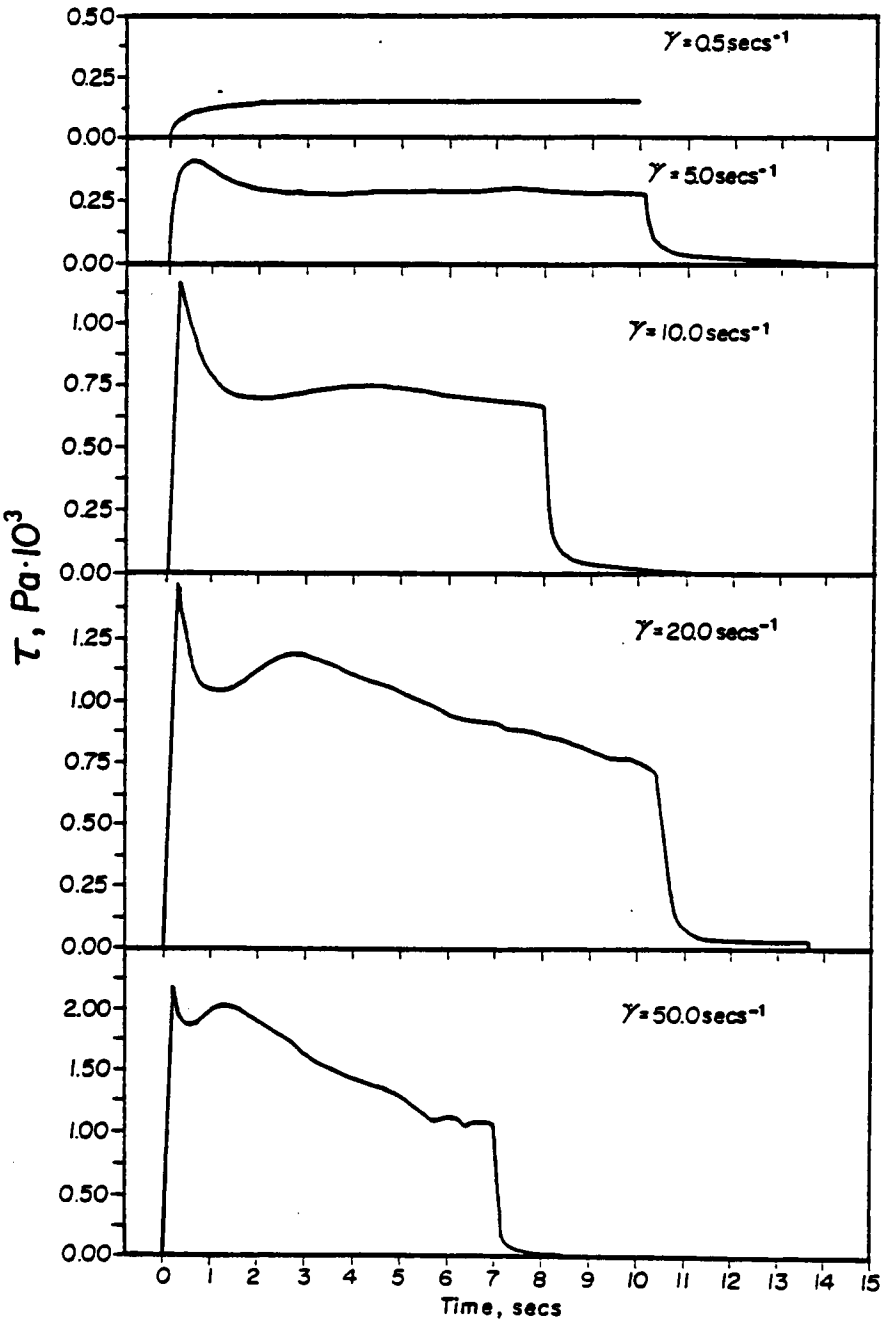

Figure 4.32 Transient Behavior: Stress Growth/Relaxation
τ_{12} vs t for 60 mole% PHB Copolymer
260°C, 50mm C/P 0.04 rad, $\dot{\gamma}$=0.5-50 $secs^{-1}$.

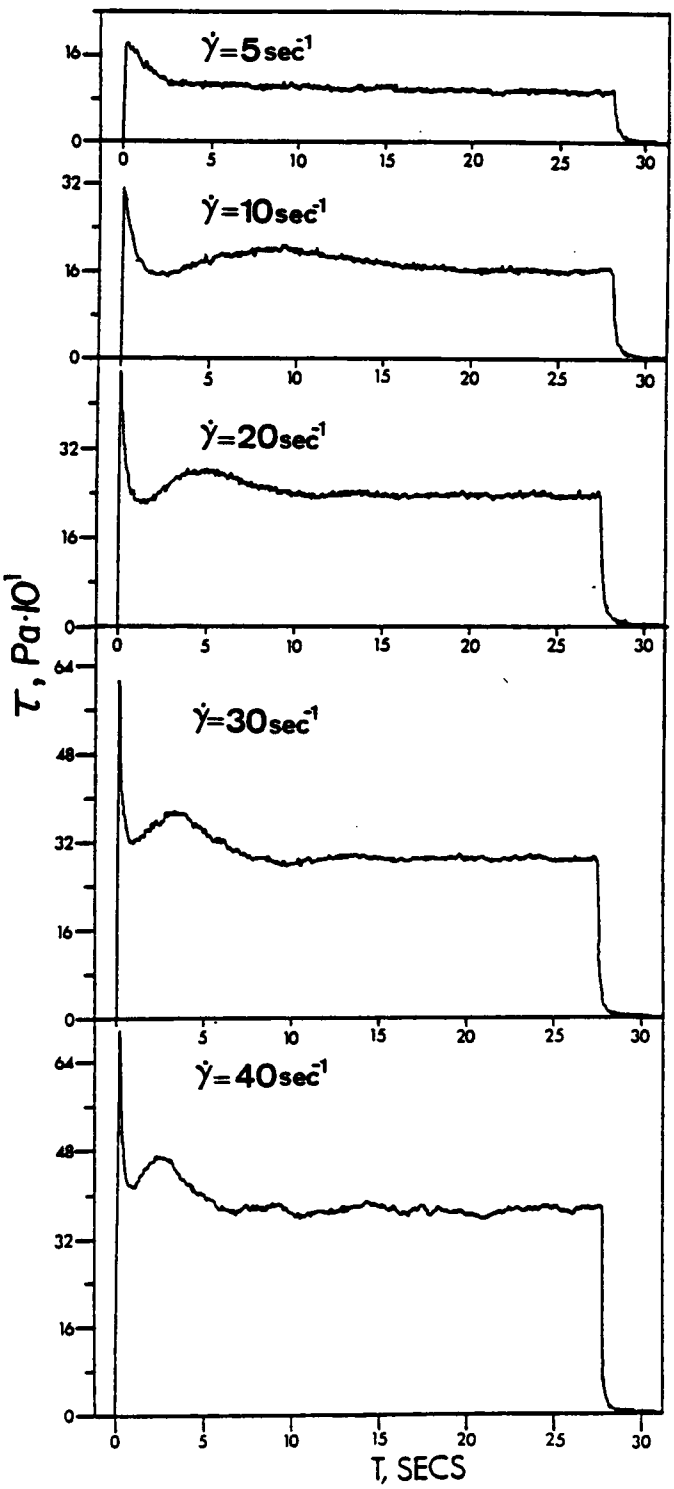

Figure 4.33 Transient Behavior: Stress Growth/Relaxation
τ_{12} vs t for 60 mole% PHB Copolymer
275°C, 50mm C/P 0.04 rad, $\dot{\gamma}$=5-40 secs^{-1}.

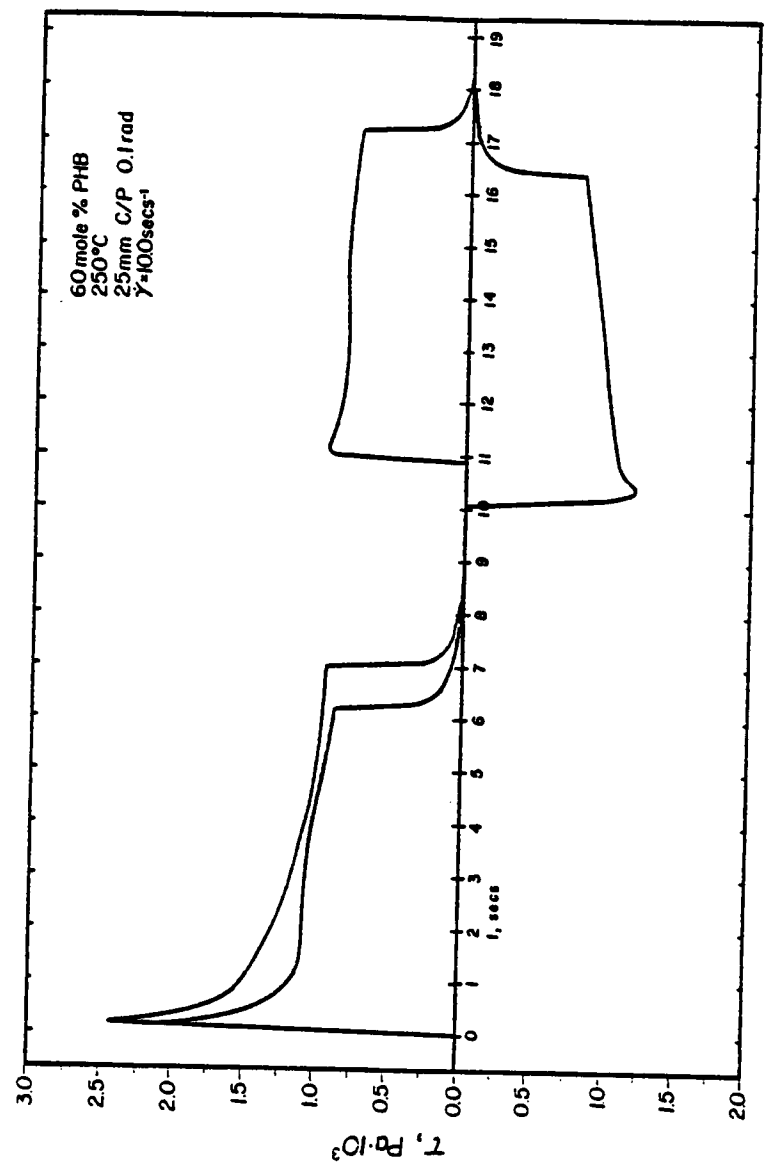

Figure 4.34 Transient Behavior: Interrupted Stress Growth
τ_{12} vs t for 60 mole% PHB Copolymer
250°C, 25mm C/P 0.1 rad, $\dot{\gamma}$=10 secs^{-1}.

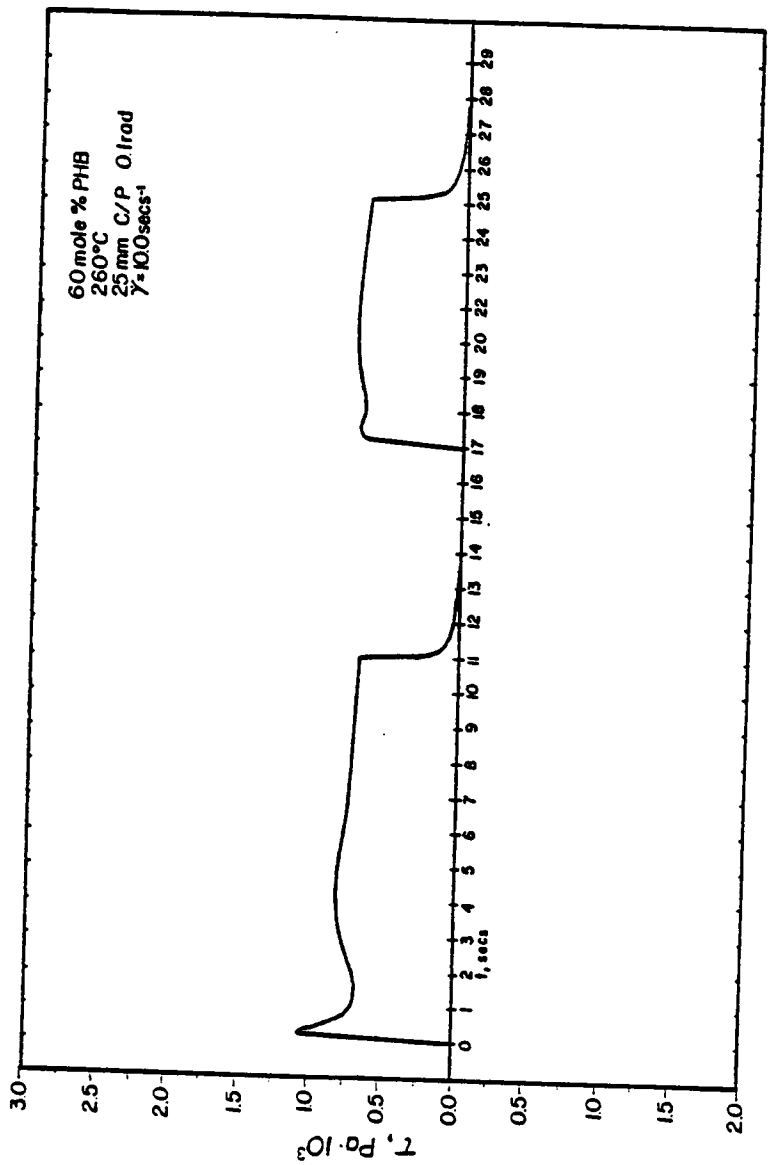

Figure 4.35 Transient Behavior: Interrupted Stress Growth
τ_{12} vs t for 60 mole% PHB Copolymer
260°C, 25mm C/P 0.1 rad, $\dot{\gamma}$=10 secs^{-1}.

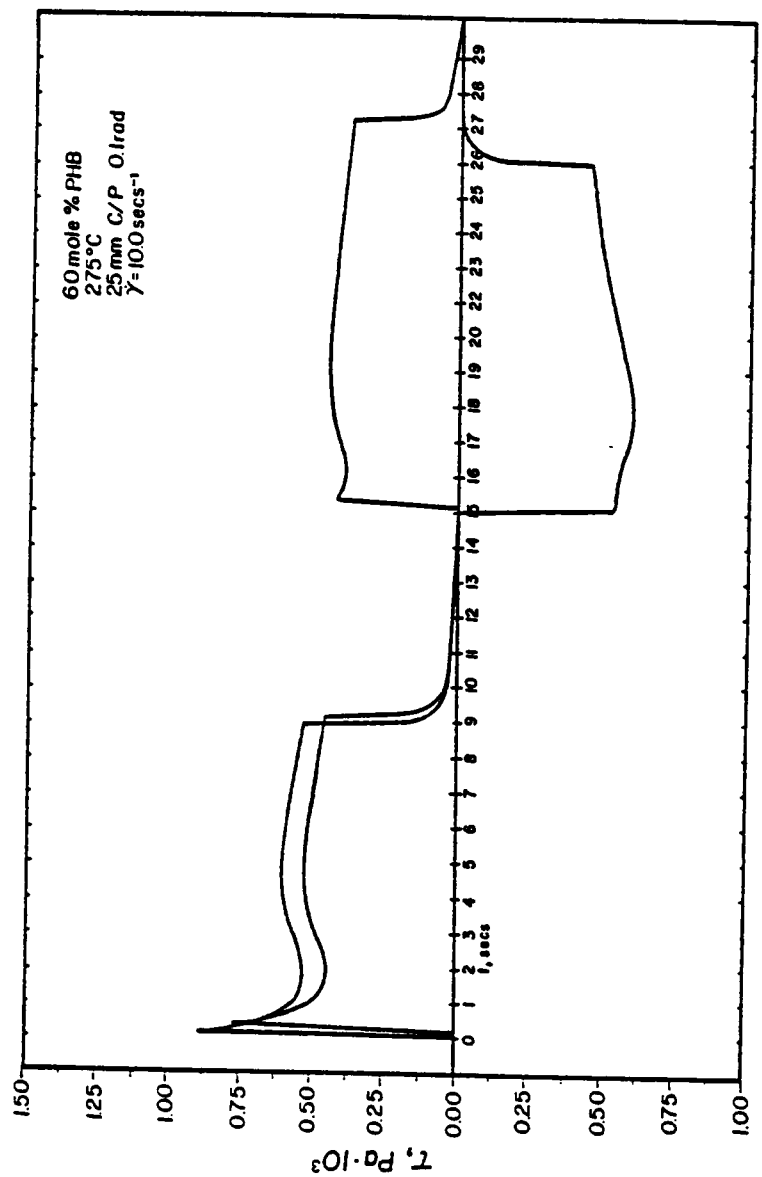

Figure 4.36 Transient Behavior: Interrupted Stress Growth
τ_{12} vs t for 60 mole% PHB Copolymer
275°C, 25mm C/P 0.1 rad, $\dot{\gamma}$=10 secs^{-1}.

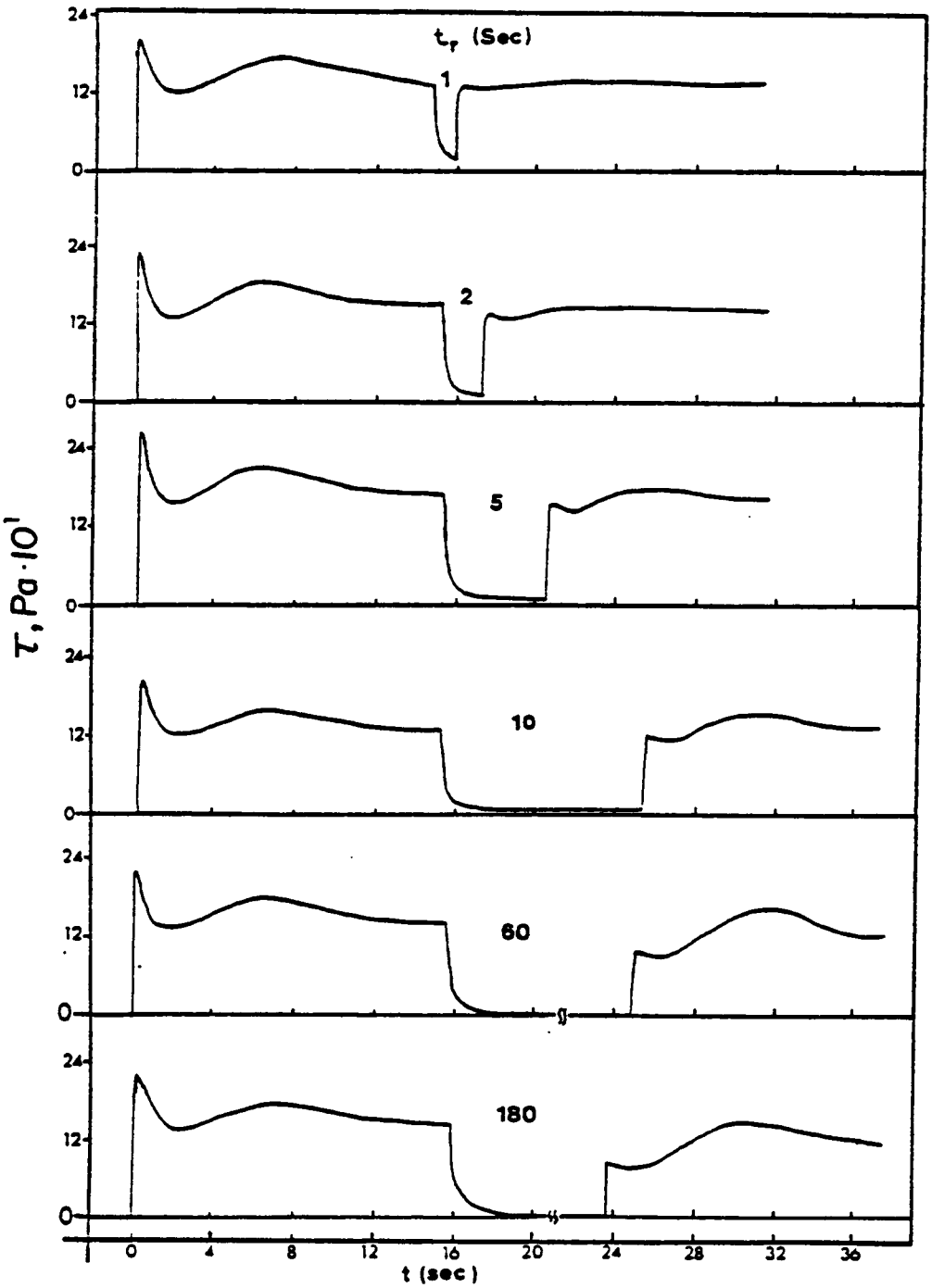

Figure 4.37 Transient Behavior: Interrupted Stress Growth
τ_{12} vs t for 60 mole% PHB Copolymer
275°C, 25mm C/P 0.1 rad, $\dot{\gamma}$=10 $secs^{-1}$.

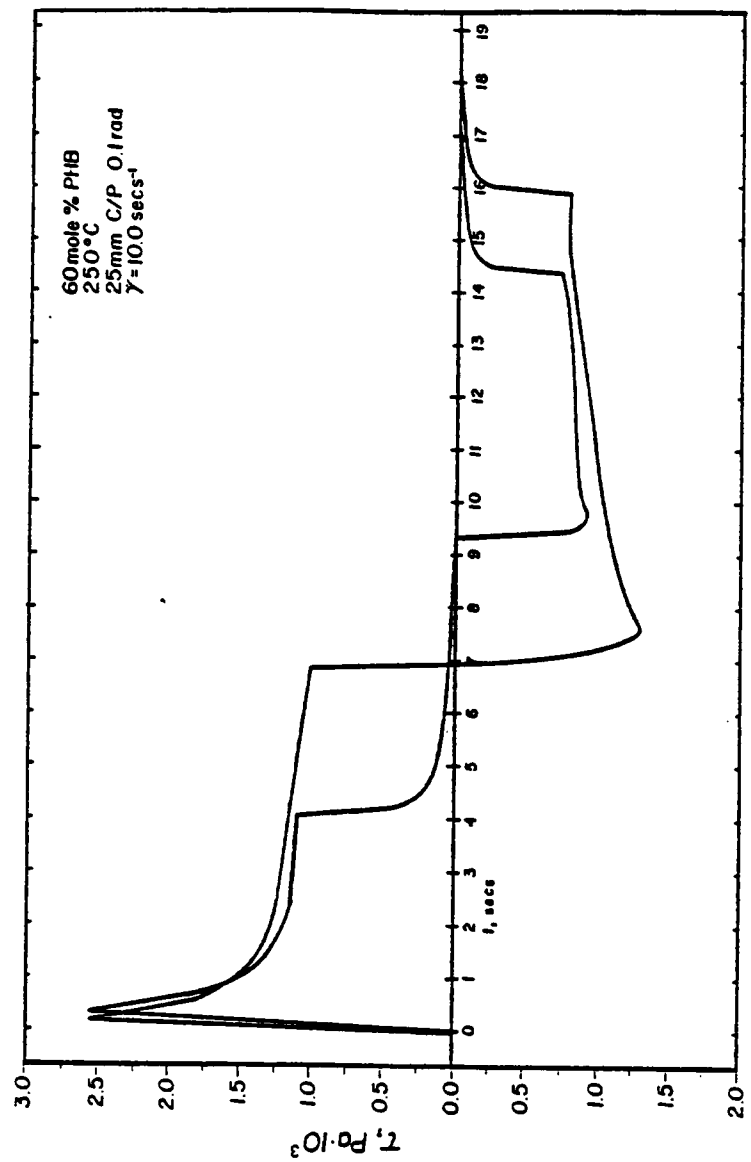

Figure 4.38 Transient Behavior: Reversal of Shear Direction
τ_{12} vs t for 60 mole% PtB Copolymer
250°C, 25mm C/P 0.1 rad, $\dot{\gamma}$=10 secs $^{-1}$.

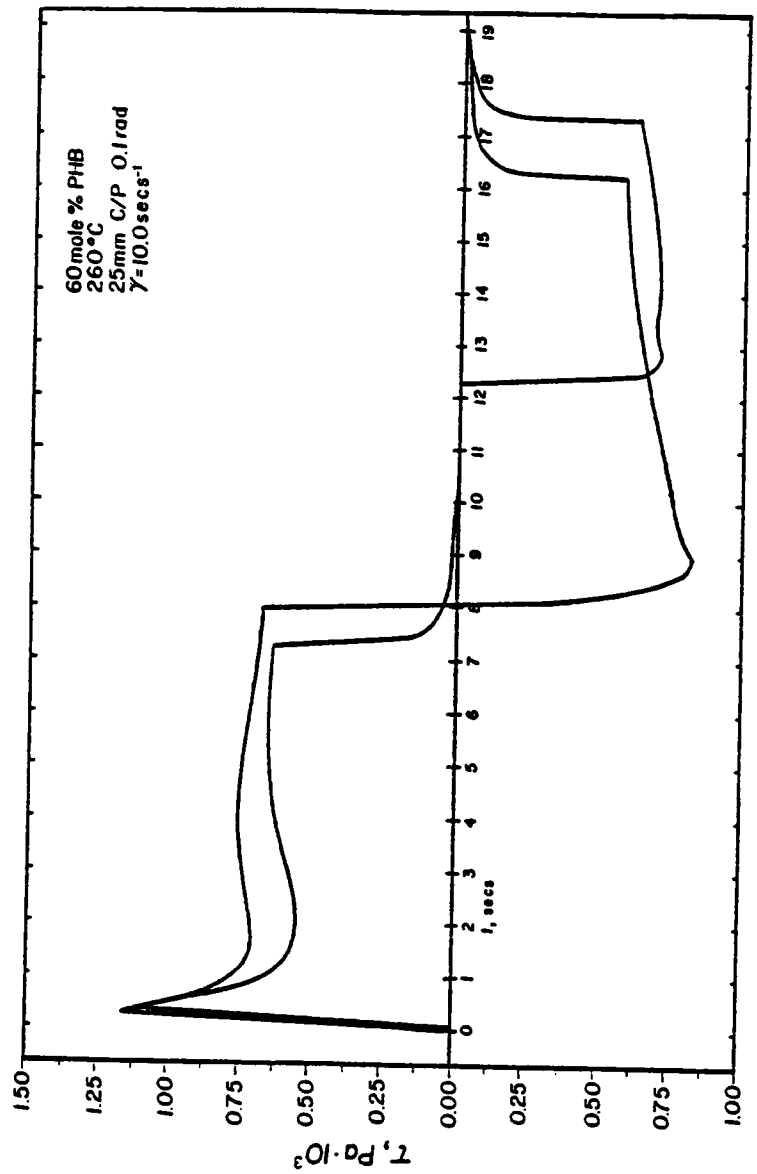

Figure 4.39 Transient Behavior: Reversal of Shear Direction
τ_{12} vs t for 60 mole% PHB Copolymer
260°C, 25mm C/P 0.1 rad, $\dot{\gamma}$=10 secs^{-1}.

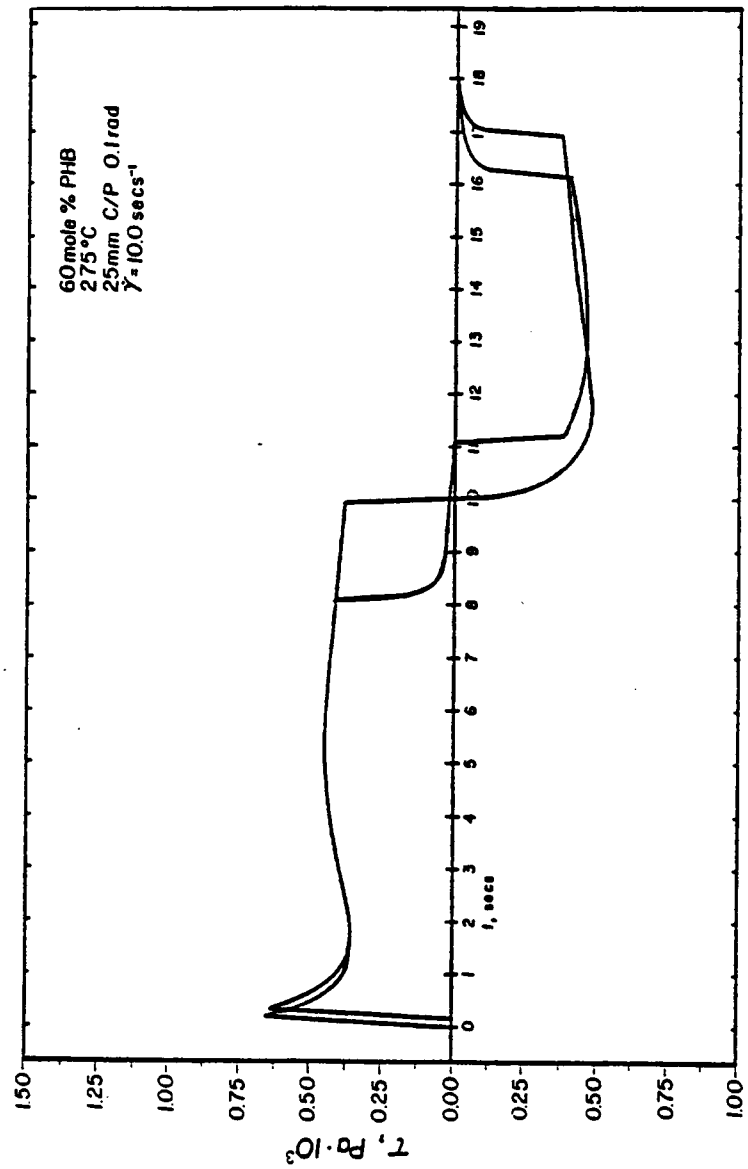

Figure 4.40 Transient Behavior: Reversal of Shear Direction
τ_{12} vs t for 60 mole% PHB Copolymer
275°C, 25mm C/P 0.1 rad, $\dot{\gamma}$=10 secs^{-1}.

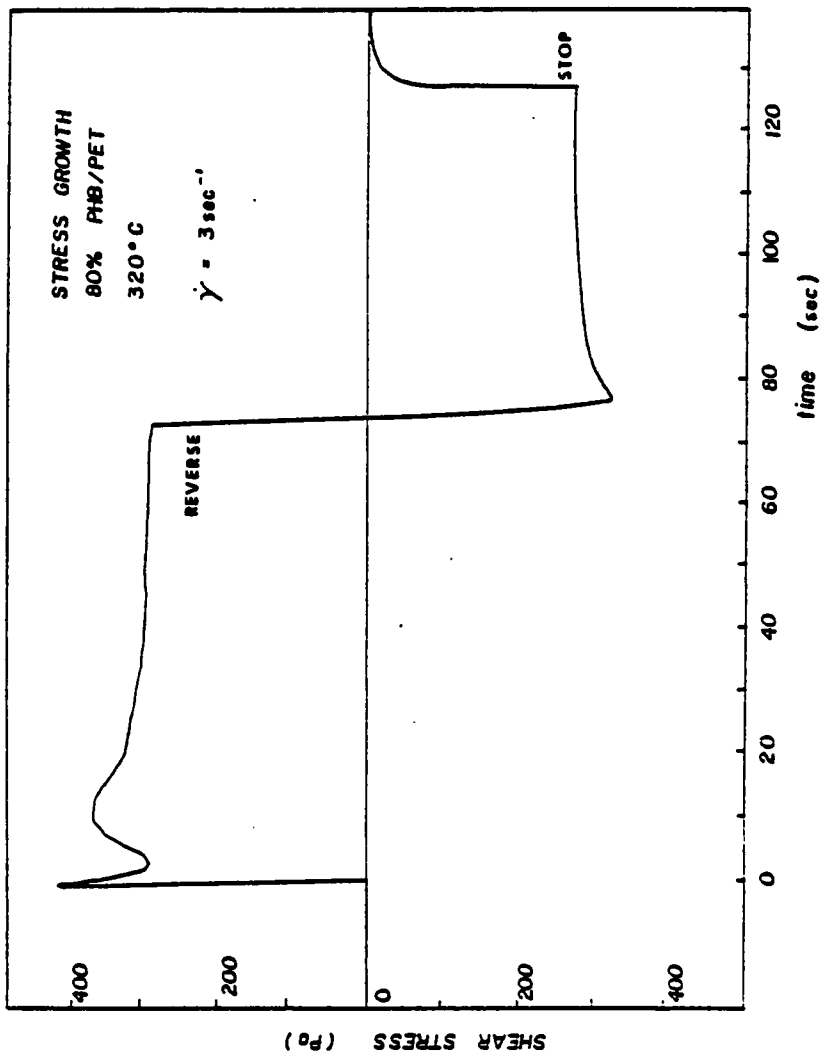

Figure 4.41 Transient Behavior: Reversal of Shear Direction
τ vs t for 80 mole% PHB copolymer
320°C, 25mm C/P 0.1 rad, $\dot{\gamma}$=3 secs^{-1}.

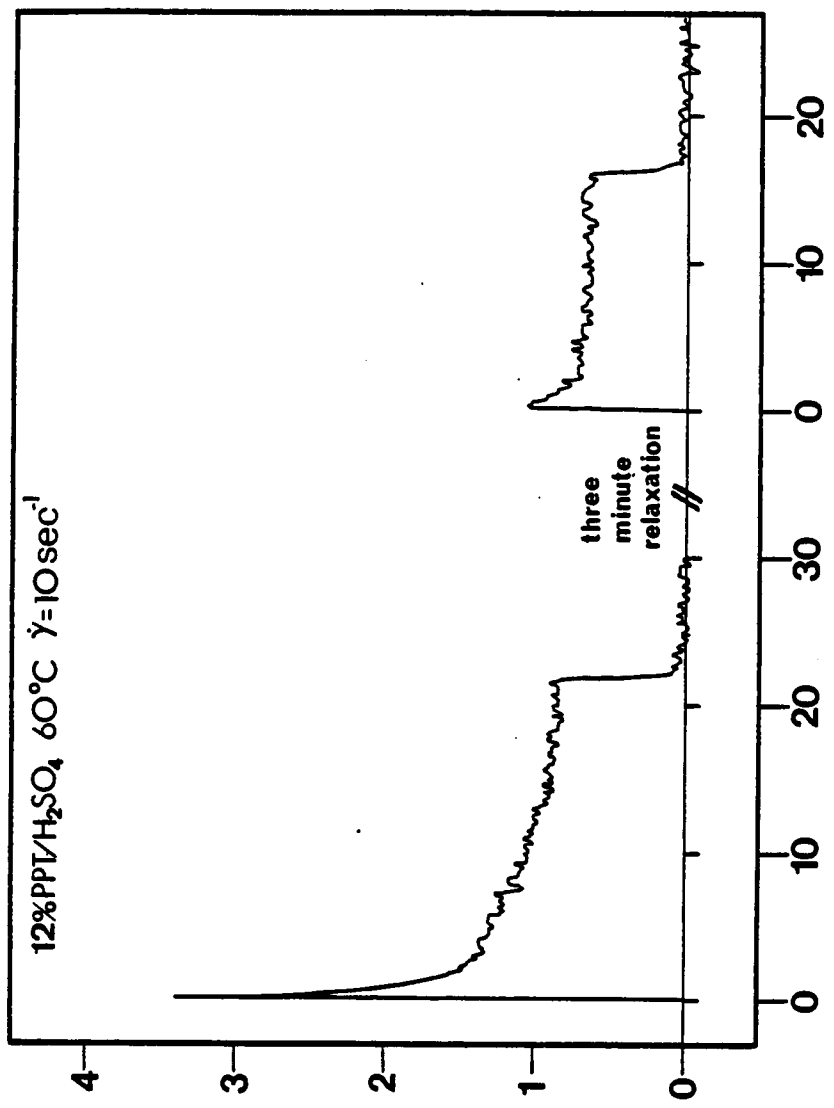

Figure 4.42 Transient Behavior: Interrupted Stress Growth
τ_{12} vs t for 12 wt% PPT/H SO Solution
60°C, 25mm C/P 1.0 rad, $\dot{\gamma}$=10 secs^{-1}.

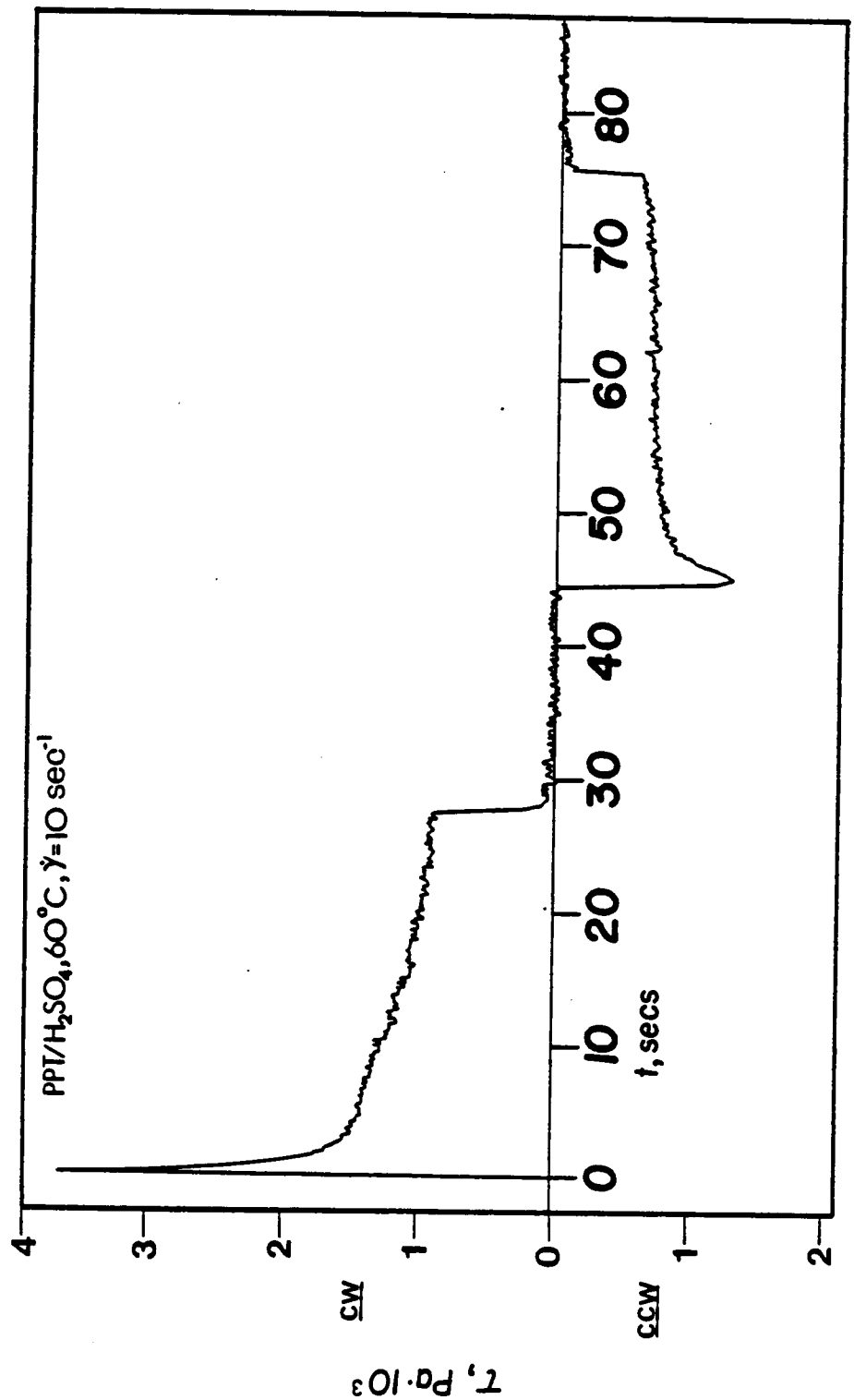

Figure 4.43 Transient Behavior: Interrupted Stress Growth
τ_{12} vs t for 12 wt% PPT/H_2SO_4 Solution
60°C, 25mm C/P 1.0 rad, $\dot{\gamma}$=10 $secs^{-1}$.

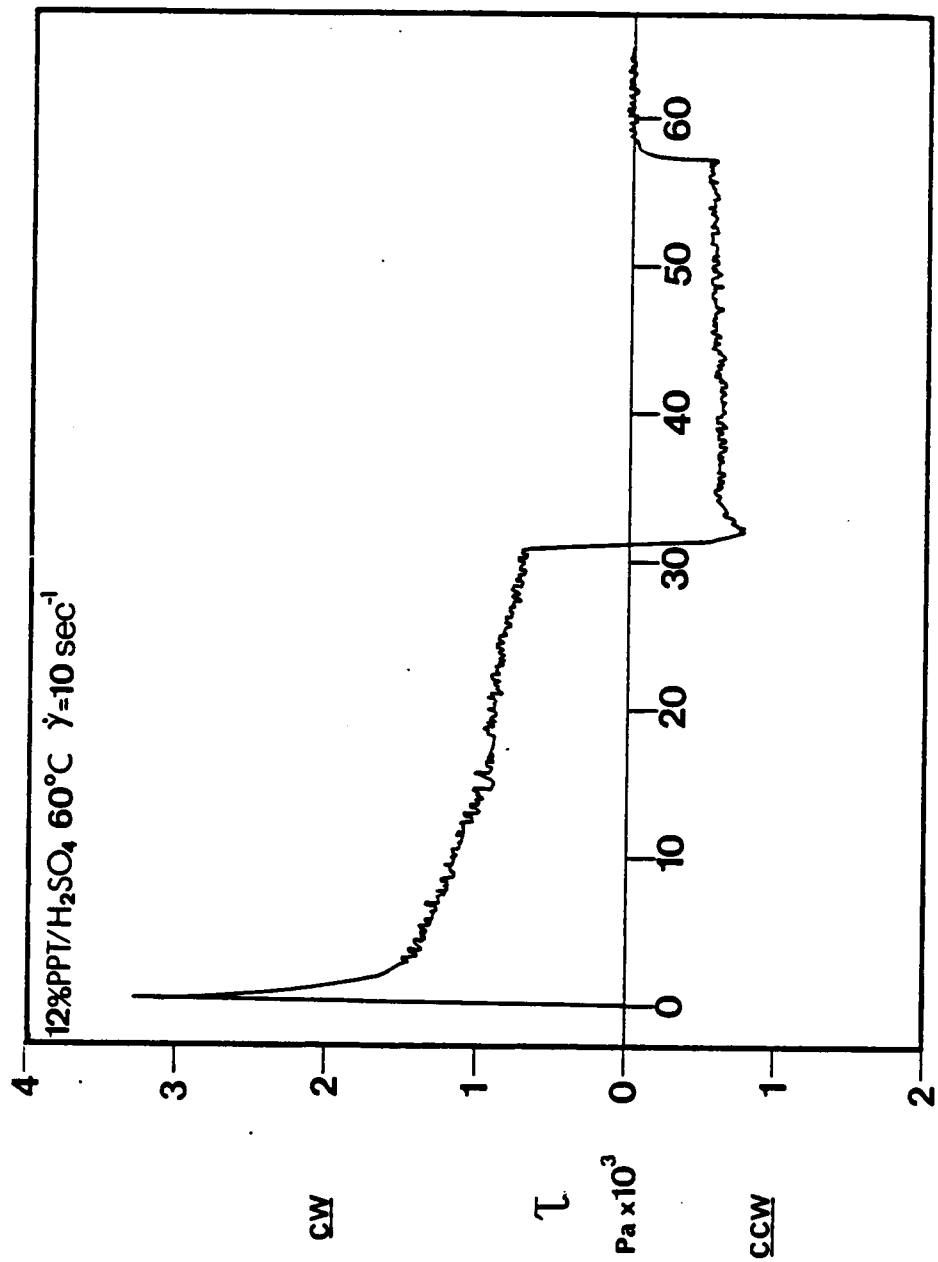

Figure 4.44 Transient Behavior: Reversal of Shear Direction
τ_{12} vs t for 12 wt% PPT/H_2SO_4 Solution
60°C, 25mm C/P 1.0 rad, $\dot{\gamma}$=10 $secs^{-1}$.

4.2.3 JUMP STRAIN MEASUREMENTS

It has just been shown that the stress growth curves exhibited by the 60 mole% PHB/PET system can be affected by preshearing. It is possible that such behavior is due to the development of molecular orientation, or to some other rearrangement of the melt structure during flow. In order to better understand the melt structure of the PHB/PET system the dynamic mechanical properties (η^*, G', and G'') were measured, and a series of jump strain experiments were performed. The results of the jump strain measurements are expressed in terms of a relaxation modulus, G(t), which is plotted as a function of time and applied strain at different temperatures. For a linear viscoelastic material, G(t) should be independent of the applied strain value. Also, a plot of G(t) versus t, and a plot of G' versus $1/\omega$ should coincide. Differences between G(t) and G', or a dependence of G(t) on strain value are usually an indication of some structure rearrangement taking place in the melt. In order to determine more accurately the linear viscoelastic range of the 60 mole% PHB/PET material, a strain sweep experiment has also been conducted. Finally, comparison between the steady shear properites, η and N1, and the dynamic mechanical properites, η^* and $2G'$, gives information regarding the possible differences in structure development in shearing and oscillatory flows.

The results of the strain sweep measurements are shown in Figures 4.45 and 4.46. The data plotted in these figures are tabulated in Tables

B.15 and B.16 in the appendix. The storage and loss moduli have been plotted as a function of strain at temperatures of 250, 260, and 275°C. It is seen that the moduli are fairly independent of strain up to strain values of 10 strain units. These results indicate that the 60 mole% PHB/PET copolymer should remain linearly viscoelastic to strains of at least 10 strain units.

The dynamic mechanical properties were measured at 250, 260, and 275°C. The results of these measurements are plotted in Figures 4.47 thru 4.49, and the data for these graphs is tabulated in Tables B.17 thru B.19. The dynamic viscosity appears to exhibit a zero shear viscosity, and is of approximately the same magnitude as the steady viscosity. The storage modulus is approximately two times greater than the primary normal stress difference, N1.

The results of the jump strain measurements are plotted in Figures 4.50 thru 4.52. The data plotted in these figures is tabulated in Tables B.20 thru B.21 in the appendix. In each figure, the relaxation modulus, G(t), is plotted as a function of time and strain for a number of applied strain values ranging from 0.1 to 10 strain units. For comparison, G' versus $1/\omega$ has also been plotted. It can be seen that at all temperatures, the relaxation modulus is a strong function of the applied strain. In some cases, the magnitude of G' is smaller than the magnitude of G(t) measured at the smaller strain values. These results do not agree with the strain sweep data which would indicate that G(t) should be

independent of strain up to an applied strain value of 10 strain units. It can also be seen that in all cases, the stresses relax very quickly, and there does not appear to be a yield stress. These results are in apparent agreement with the stress relaxation behavior discussed earlier.

In order to determine if the non-linearity exhibited by the 60 mole% PHB/PET systems is unique, the relaxation modulus of the 12 wt% PPT/H_2SO_4 system was also measured. In Figure 4.53 is shown the results of a strain sweep experiment conducted using the PPT/H_2SO_4 system. The data plotted in this figure is tabulated in Table B.23 in the appendix. It can be seen that the storage and loss moduli begin to decrease in magnitude at strain values as low as 0.6 strain units. The storage modulus has also been measured for comparison against G(t). The dynamic mechanical properties are shown in Figure 4.54 and tabulated in Table B.24 in the appendix. The results of the jump strain measurements are plotted in Figure 4.55, the data for which is tabulated in Table B.24 in the appendix. It can be seen that G' and G(t) coincide at low applied strain values. However, G(t) is a strong function of the applied strain, decreasing with increasing strain value. These results agree with the behavior exhibited by the 60 mole% PHB/PET system.

As a final test of the effect of applied strain on the melt structure of the 60 mole% PHB/PET system, a unique stress growth experiment was conducted. The purpose of this test was to determine if a step in strain

could acheive the same effect on the magnitude of the stress overshoot peak, as preshearing of the material. The experiment was also designed to determine if a quantitative measure of the strain necessary to destroy the stress overshoot peak could be found. In Figure 4.56 is shown a series of stress growth curves. In each case, the material has been subjected to a known amount of strain prior to the stress growth experiment. The strain has been applied through the use of a jump strain experiment. It can be seen that as the initial amount of input strain is increased from 0 to 50 strain units, a decrease in the magnitude of the first overshoot peak occurs. In Figure 4.57 is shown a plot of the ratio of the stress overshoot peak to the steady state stress value as a function of applied strain for two shear rates. It can be seen that with the application of 5 strain units the first peak is almost totally destroyed.

4.2.4 SUMMARY OF RHEOLOGICAL MEASUREMENTS

The transient rheological response exhibited by the liquid crystalline systems studied has been shown to be in qualitative agreement with the predictions of Ericksen's theory. The deformation history dependence of the stress overshoot peak appears to be a liquid crystalline phenomenon. According to the predictions of Ericksen's theory, the behavior of the stress overshoot peak is related to the development of molecular orientation within the fluid.

It is seen that the application of strain can affect the magnitude of

the first overshoot peak. Jump strain measurements indicate that the liquid crystalline systems are highly non-linear. This non-linearity is most probably due to some structure rearrangement within the melt. It is not certain, however, that this structure rearrangement is related to the development of molecular orientation. The strain sweep measurements are in conflict with the jump strain data. According to the strain sweep data, the 60 mole% PHB system should remain linearly viscoelastic at strain values approaching 10 strain units. The jump strain experiments do not support this. Finally, it is seen that the dynamic and steady shear properties are of similar magnitude. This result is not expected as it is thought that molecular orientation would not occur in an oscillatory flow. The similarity between the dynamic and steady shear properties indicates that orientation may not be occuring in shear flow.

In order to test more fully the predictions of Ericksen's theory, measurments of molecular orientation present in specially prepared samples of the 60 mole% copolymer have been made. Examinations of the morphological textures present in such samples has also been conducted through the use of SEM techniques. These analyses will yield information regarding the extent to which shear and extensional flows promote the development of molecular orientaion and structure in processed articles. Such analyses may also help explain why injection molded plaques of the 60 mole% PHB/PET copolyester exhibit exceptional physical properties which are extremely anisotropic.

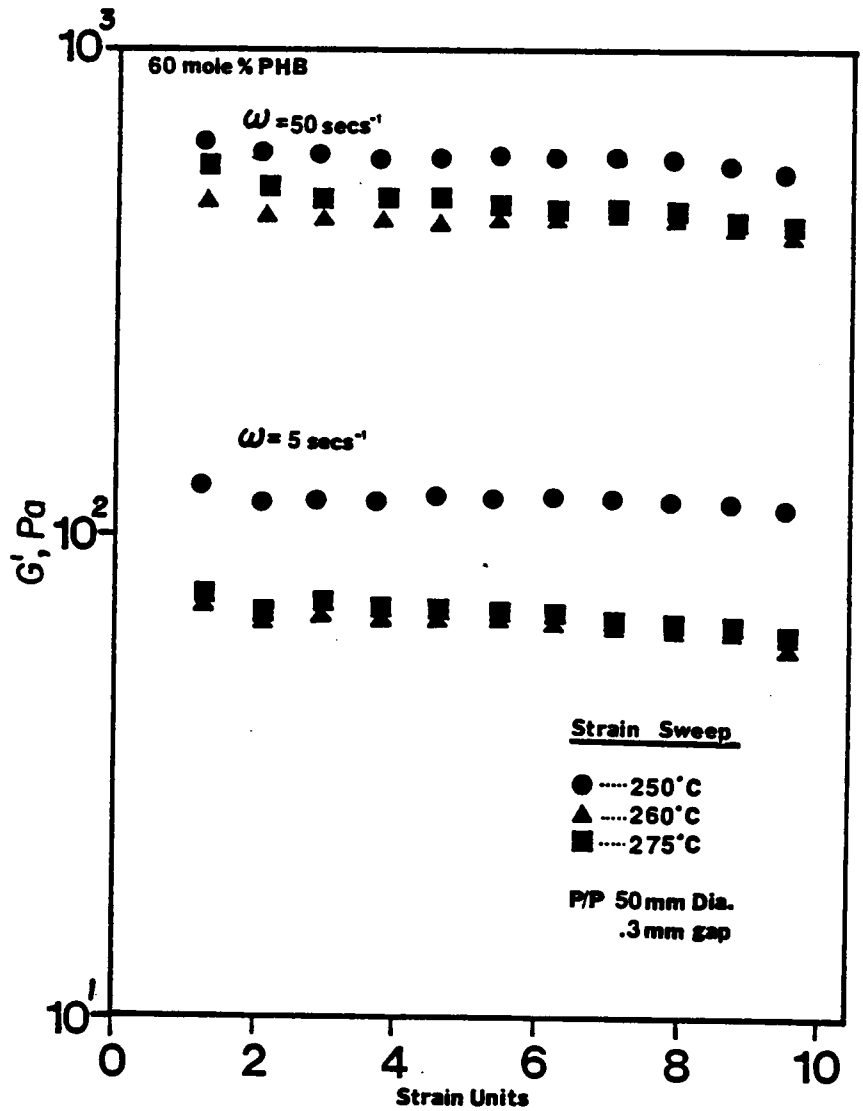

Figure 4.45 Dynamic Properties: G' vs ϒ for 60 mole% PHB Copolymer 250, 260, and, 275°C, 50mm P/P 0.3mm gap.

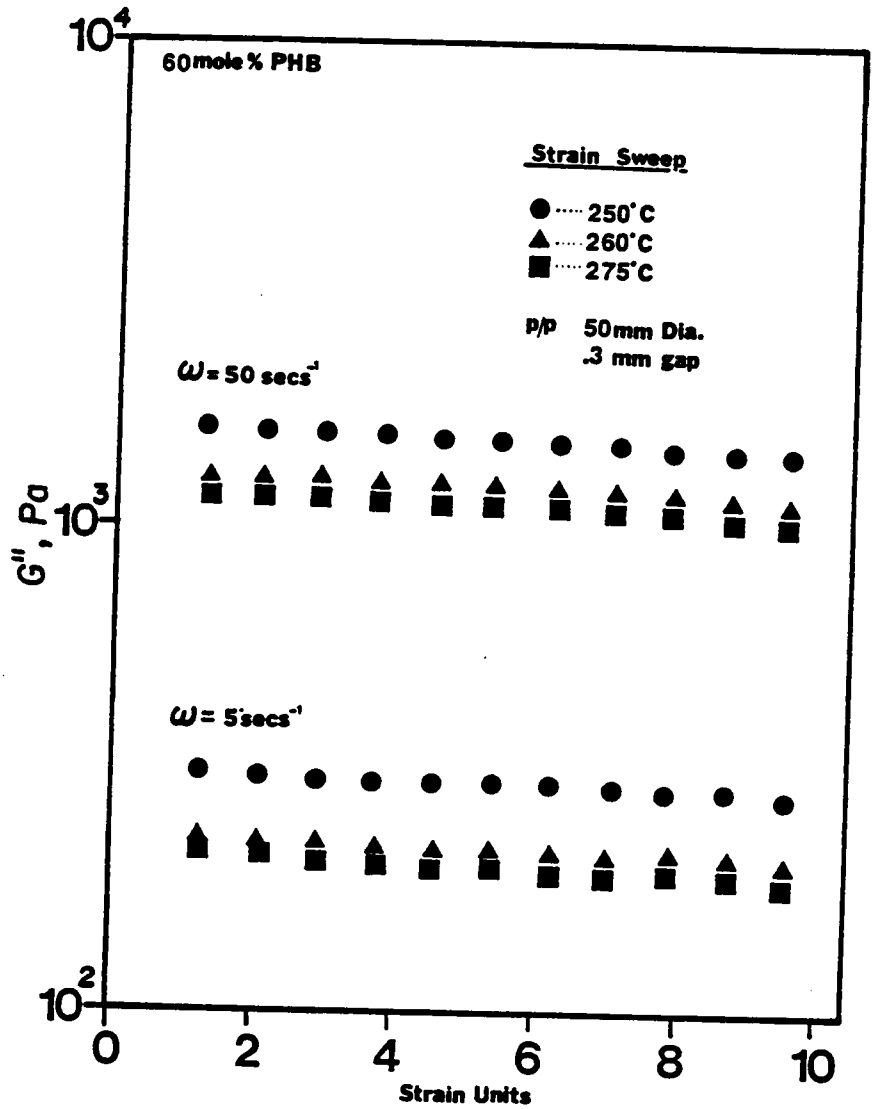

Figure 4.46 Dynamic Properties: G'' vs γ for 60 mole% PHB Copolymer 250, 260, and, 275°C, 50mm P/P 0.3mm gap.

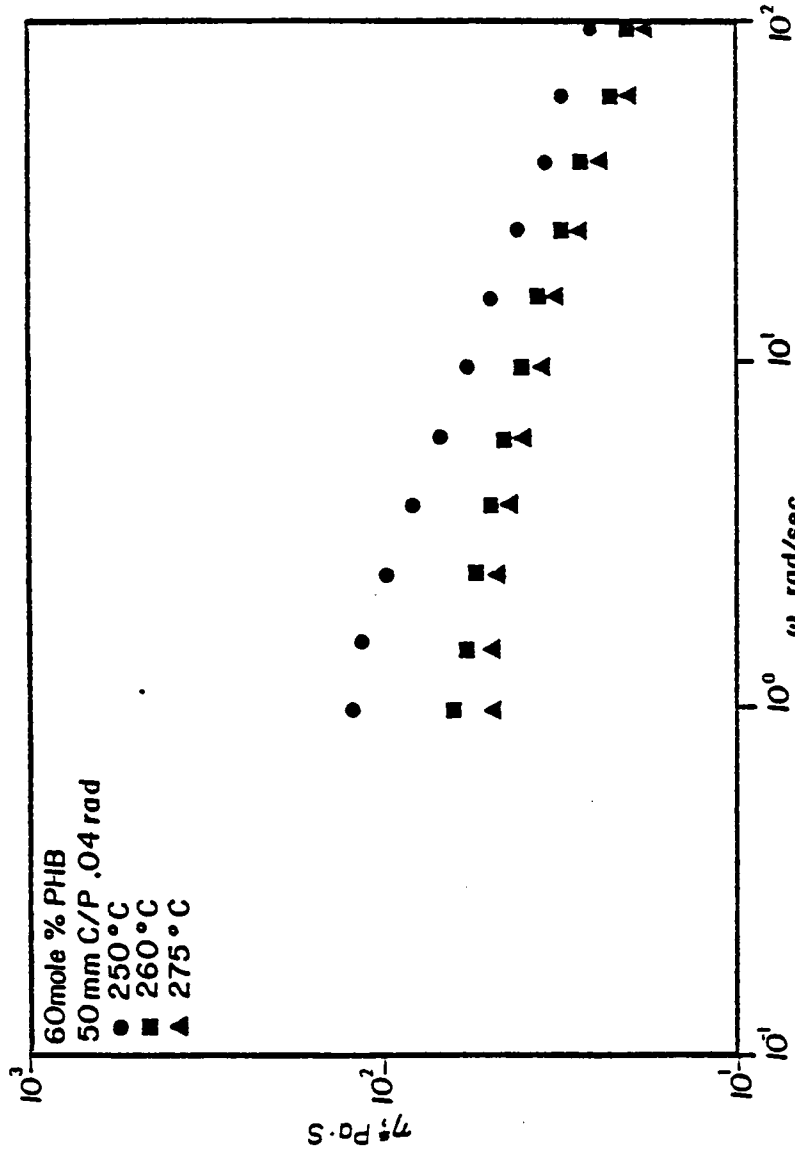

Figure 4.47 Dynamic Properties: η* vs ω for 60 mole% PHB Copolymer 250, 260, and, 275°C, 50mm C/P 0.04 rad.

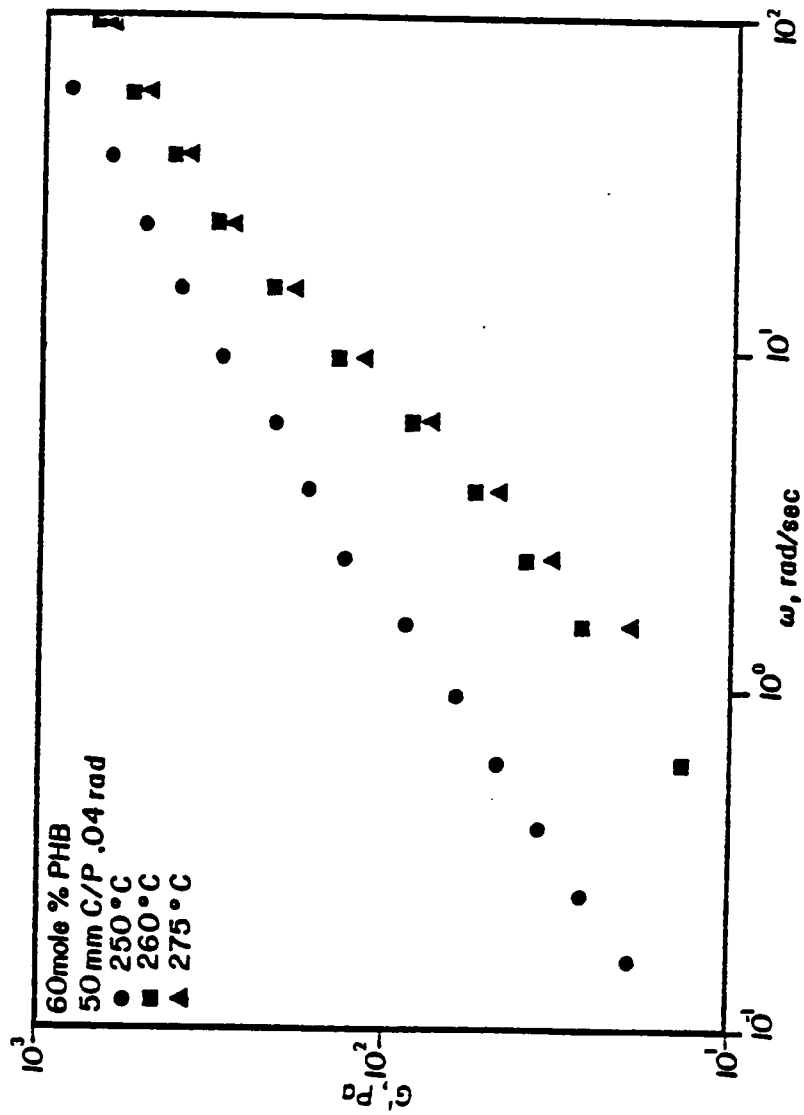

Figure 4.48 Dynamic Properties: G' vs ω for 60 mole% PHB Copolymer 250, 260, and, 275°C, 50mm C/P 0.04 rad.

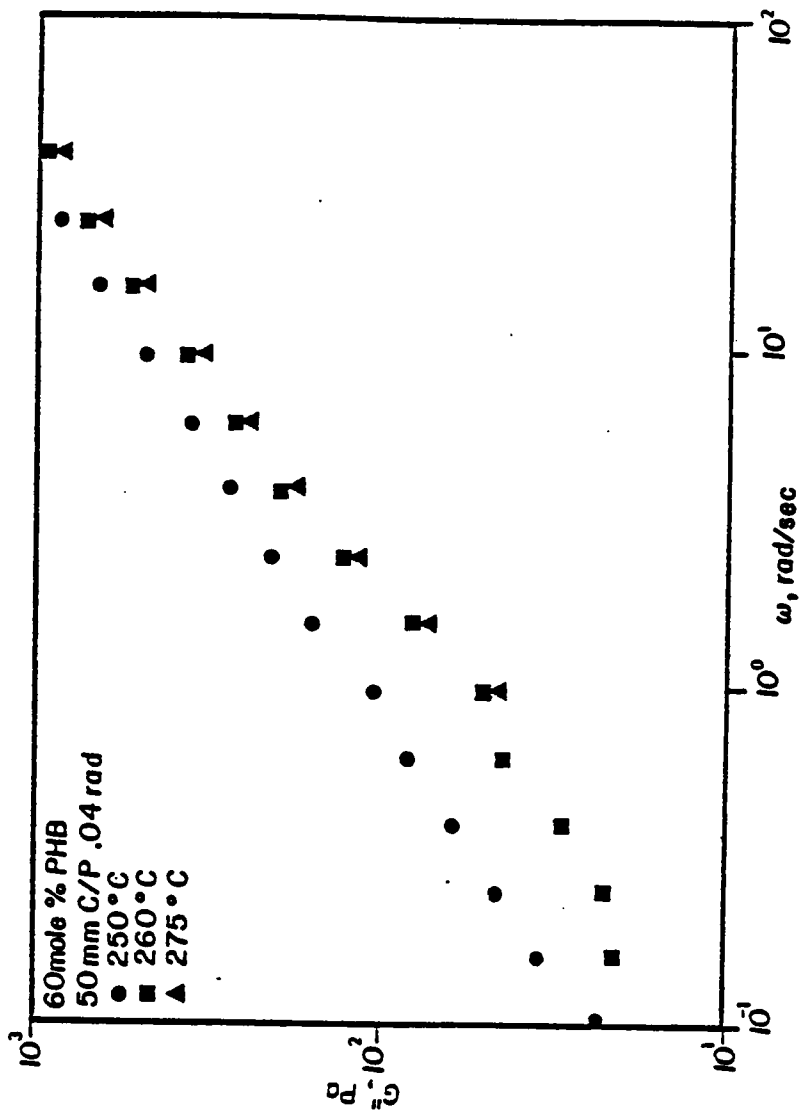

Figure 4.49 Dynamic Properties: G'' vs ω for 60 mole% PHB Copolymer 250, 260, and, 275°C, 50mm P/P 0.04 rad.

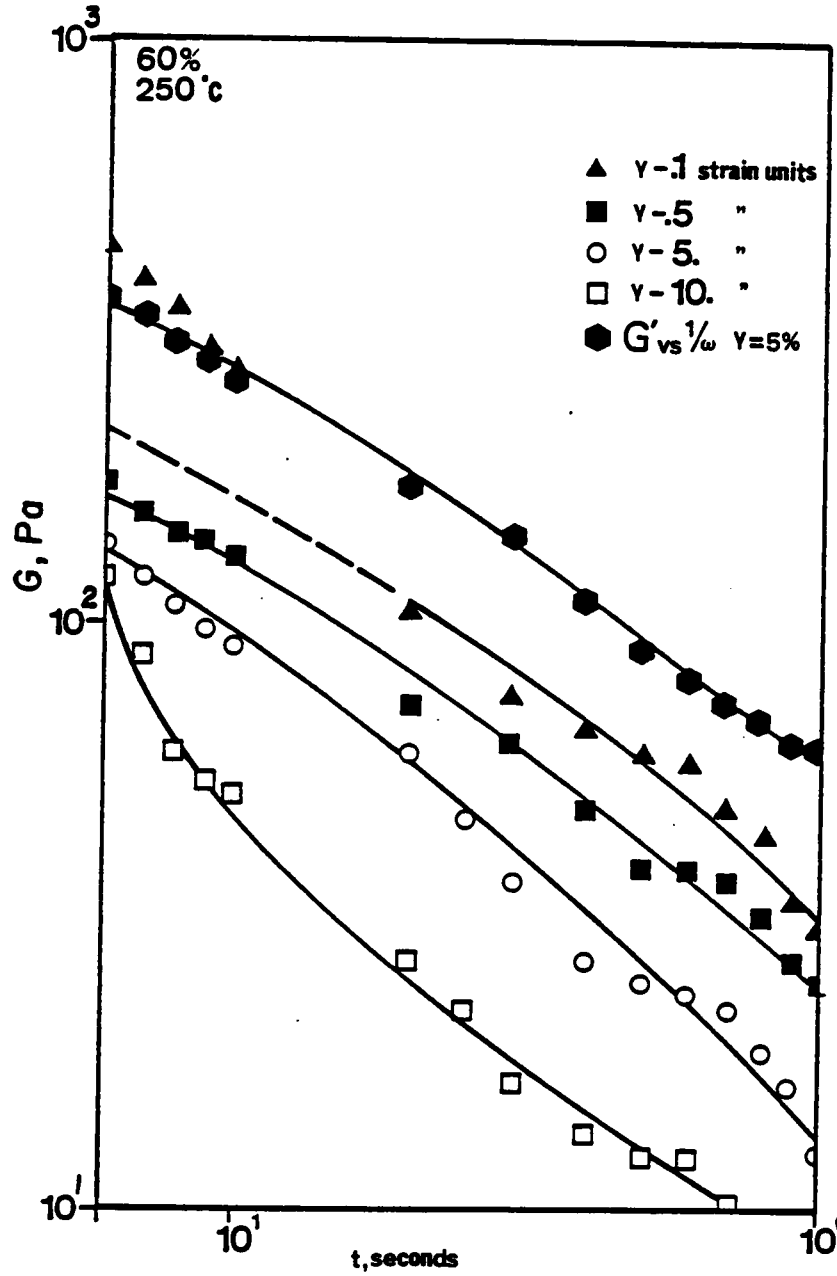

Figure 4.50 Jump Strain Data: G vs t for 60 mole% PHB Copolymer 250°C, 50mm C/P 0.04 rad.

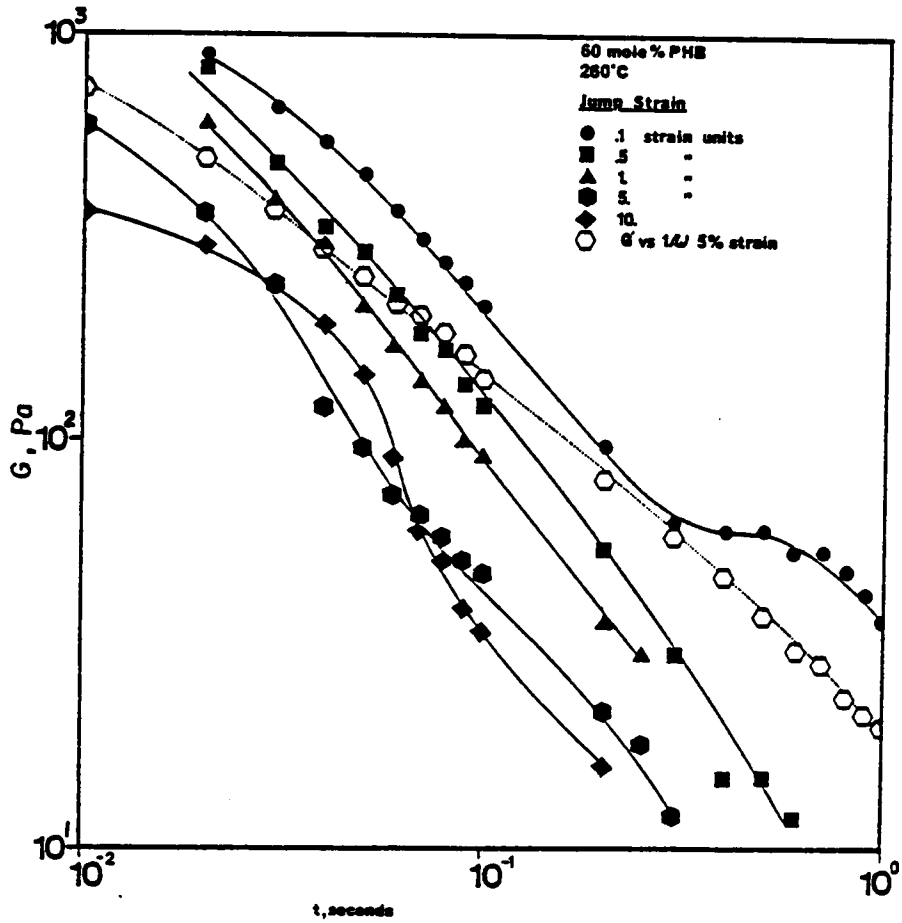

Figure 4.51 Jump Strain Data: G vs t for 60 mole% PHB Copolymer 260°C, 50mm C/P 0.04 rad.

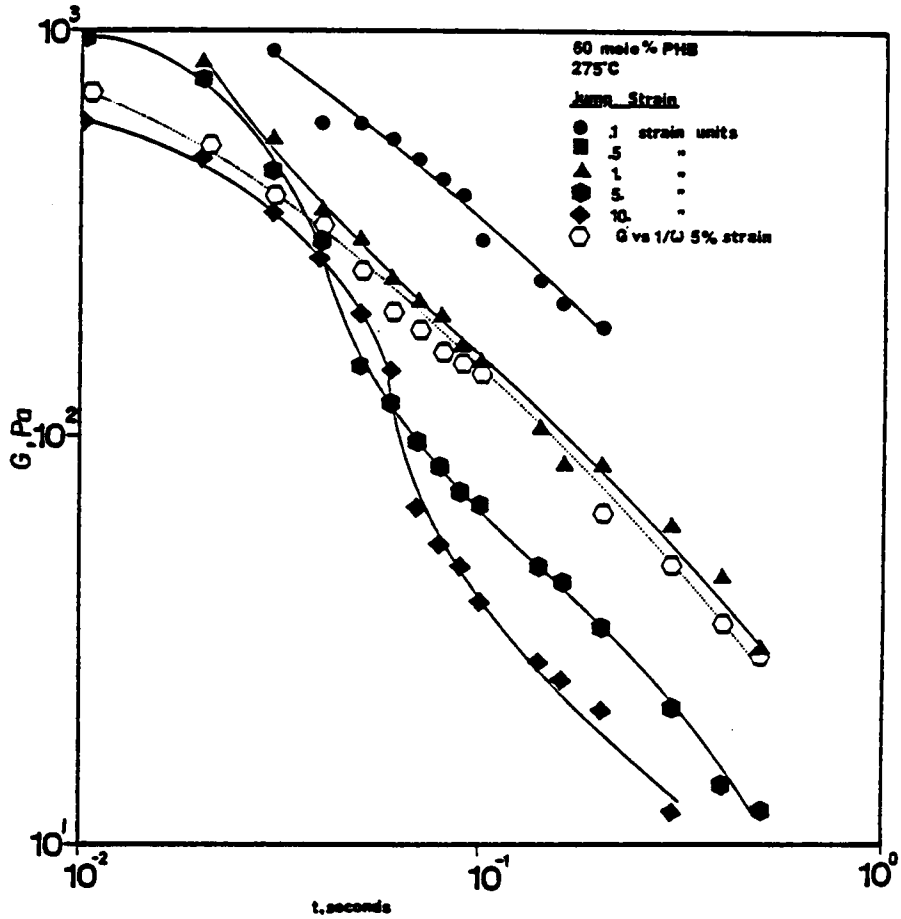

Figure 4.52 Jump Strain Data: G vs t for 60 mole% PHB Copolymer 275°C, 50mm C/P 0.04 rad.

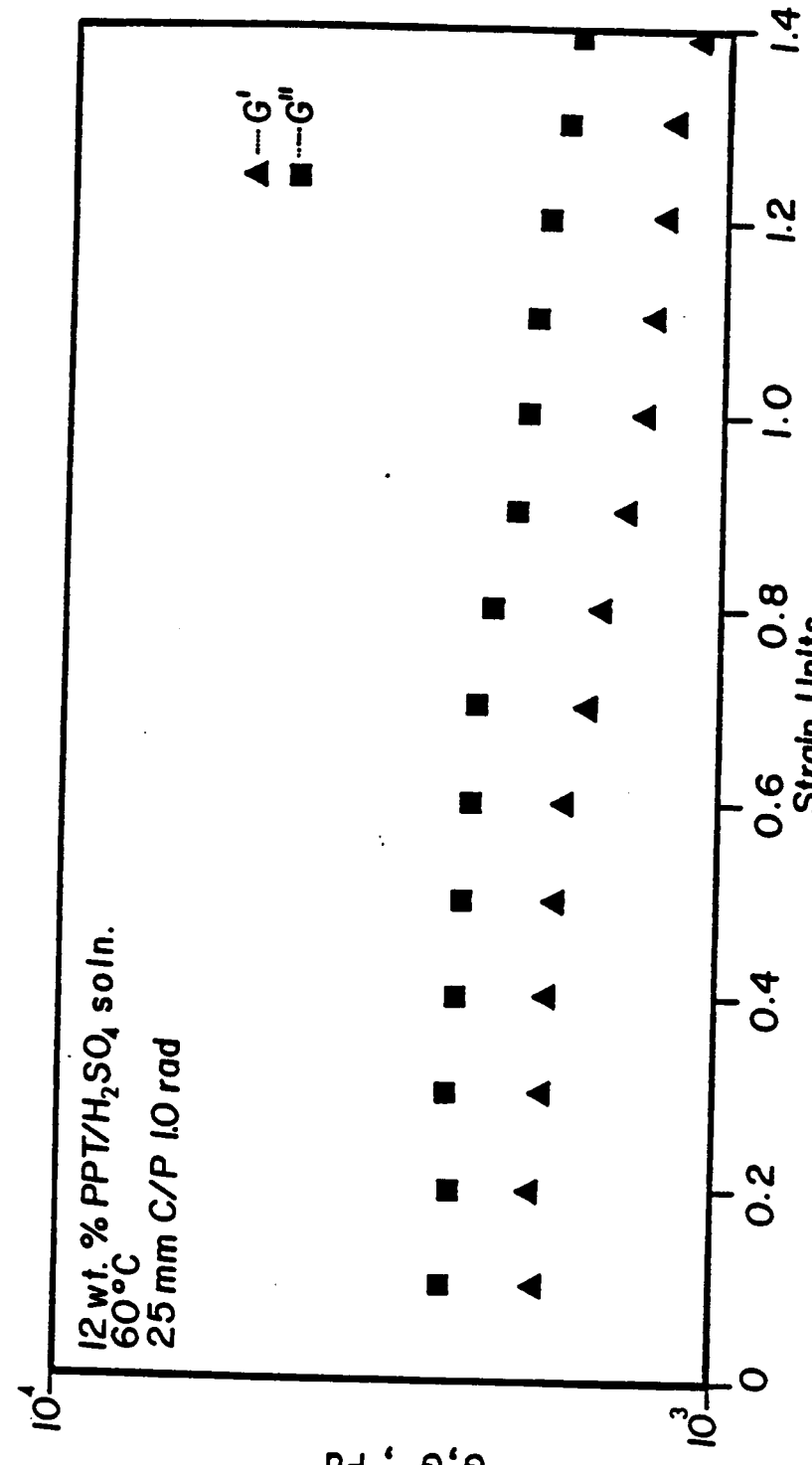

Figure 4.53 Dynamic Properties: G', G'' vs γ for 12 wt% PPT/H_2SO_4 Solution. 60°C, 25mm C/P 1.0 rad.

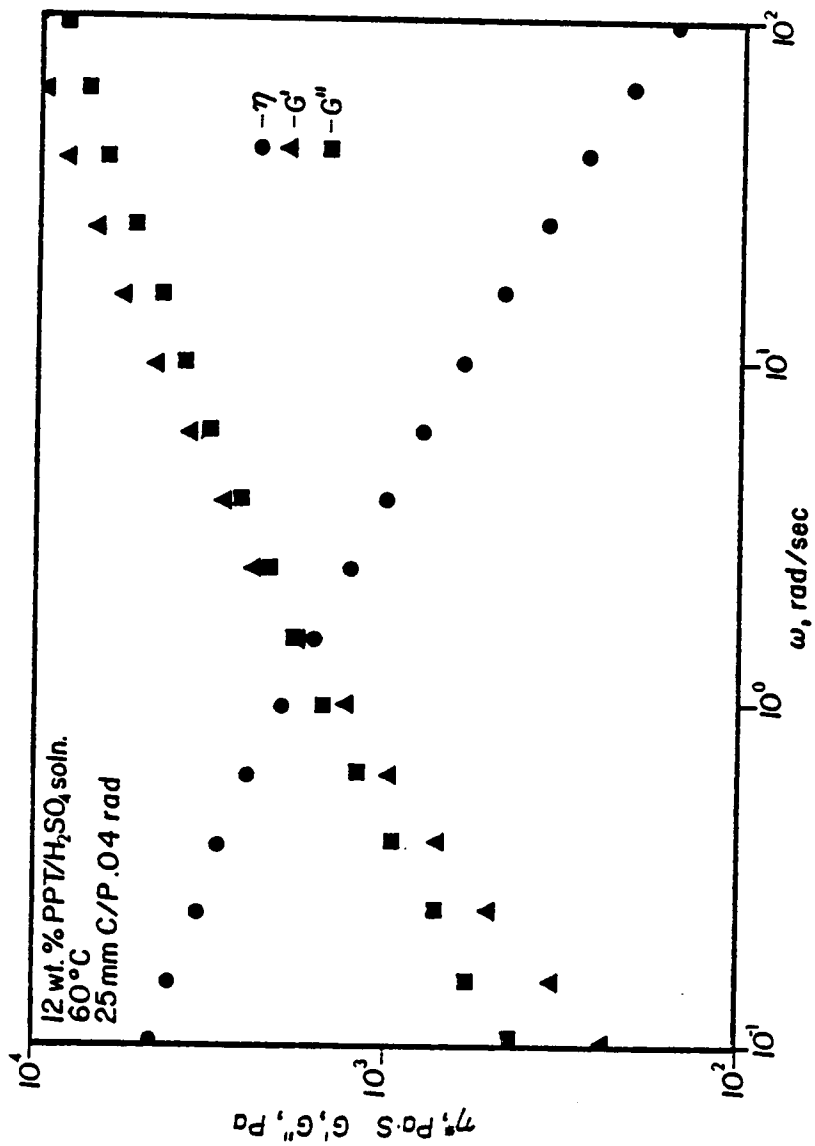

Figure 4.54 Dynamic Properties: η^*, G', and, G'' vs ω for 12 wt% PPT/H_2SO_4 Solution. 60°C, 25mm C/P 1.0 rad.

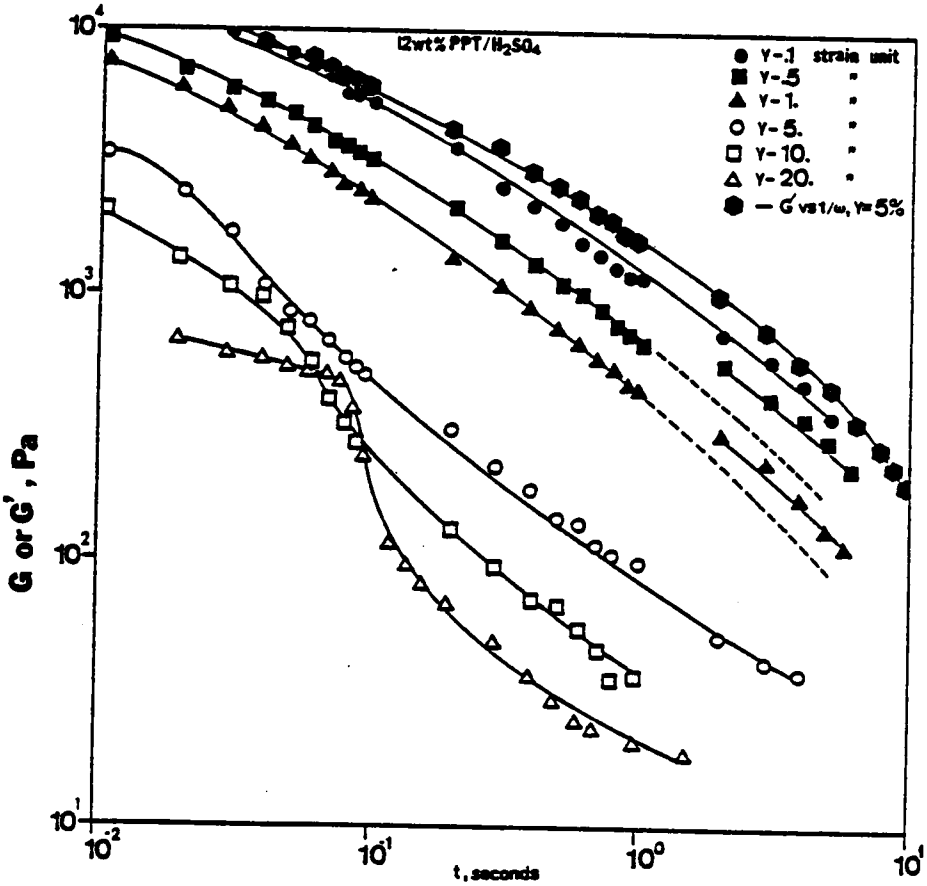

Figure 4.55 Jump Strain Data: G vs t for 12 wt% PPT/H_2SO_4 Solution. 60°C, 25mm C/P 1.0 rad.

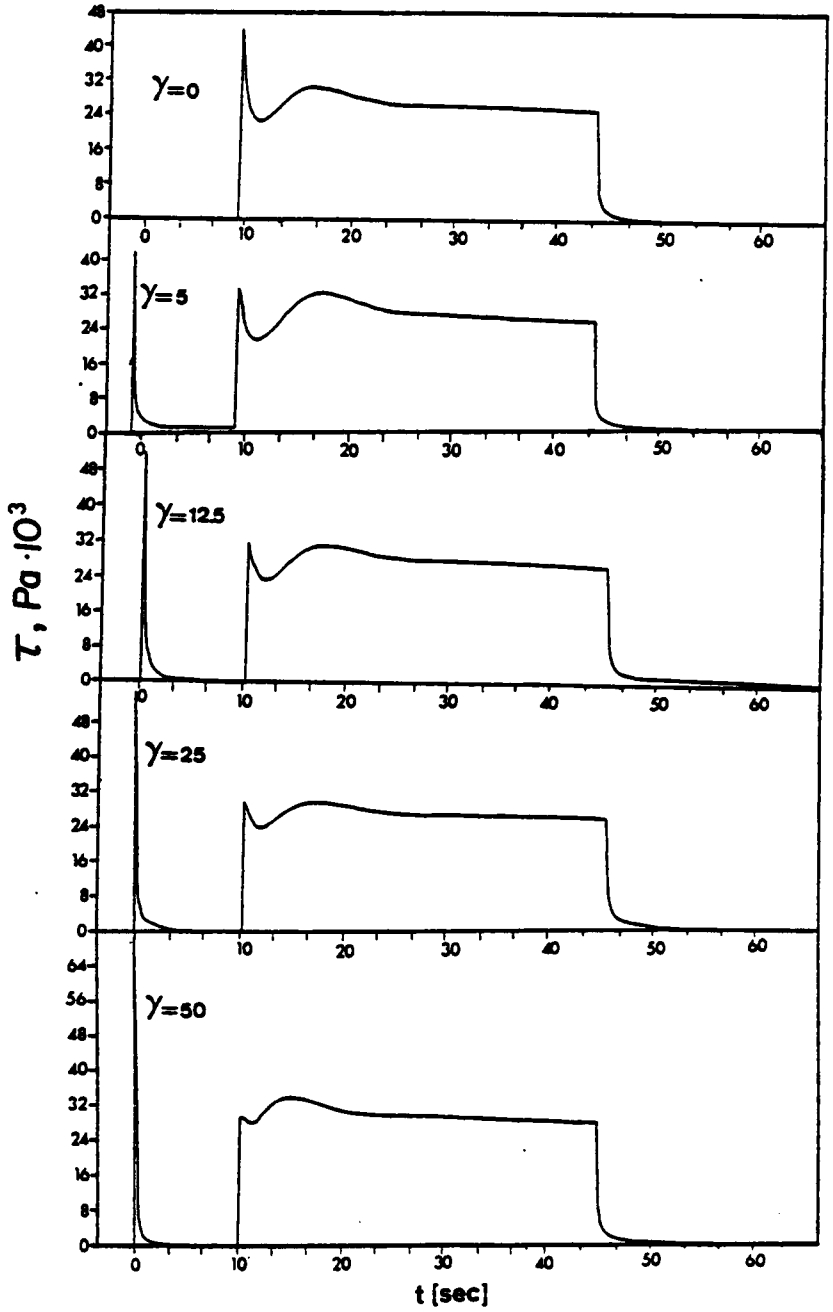

Figure 4.56 Transient Behavior: Jump Strain/Stress Growth
τ_{12} vs t for 60 mole% PHB Copolymer
275°C, 50mm C/P 0.04 rad, $\dot{\gamma}$=10 $secs^{-1}$.

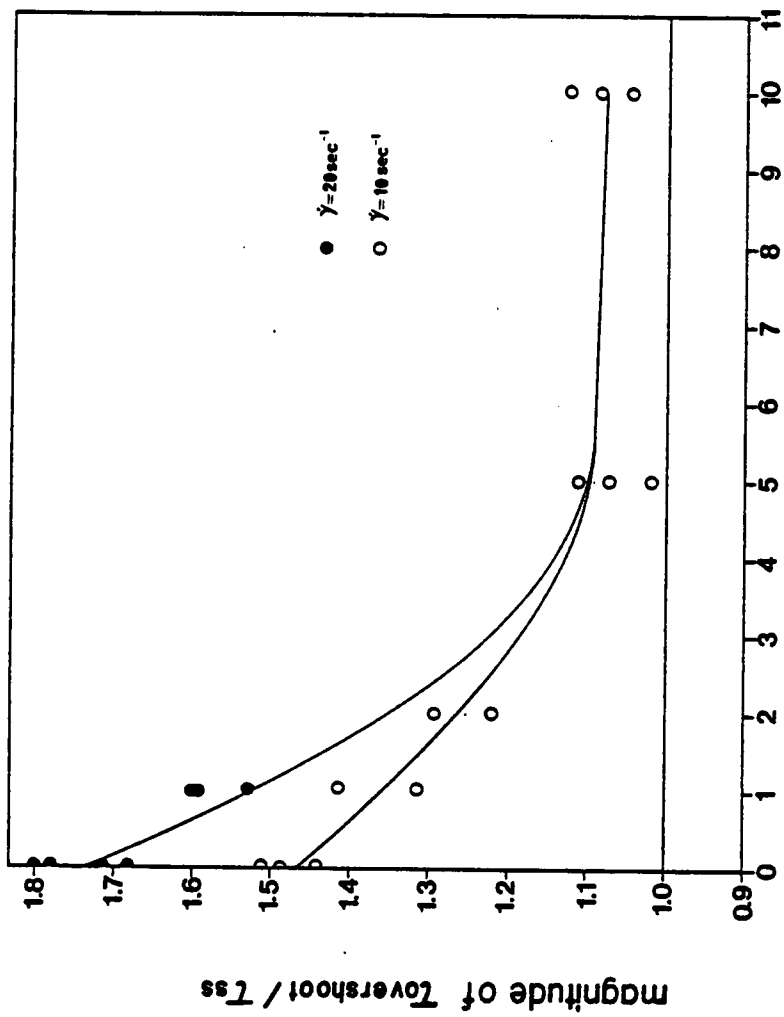

Figure 4.57 Transient Behavior: Jump Strain/Stress Growth
Peak Height vs Initial Jump Strain Value
275°C, 50mm C/P 0.04 rad, $\dot{\gamma}$=10,20 secs^{-1}.

4.3 WAXS AND SEM STUDIES

Wide angle x-ray scattering was used to qualitatively determine the degree of molecular orientation present in samples subjected to controlled conditions of deformation and temperature history. Chemical etching in conjunction with scanning electron microscope techniques was used to analyze the morphological textures present in these samples. In this section, the results of these investigations will be presented. The results pertaining to extended samples will be presented first, followed by the results for samples subjected to shear flow. The 60 mole% PHB system has been studied most extensively, but results are also available for the 80 mole% PHB system.

4.3.1 EXTENSIONAL FLOW

In Figure 4.58 is shown the WAXS pattern exhibited by a sample of 60 mole% PHB/PET copolymer subjected to extensional flow at 275°C. The extension rate used was 2.5 $secs^{-1}$, and in the figure the flow direction is along the vertical axis. The sample possesses a high degree of molecular orientaion as evidenced by the azimuthal dependence of scattering intensity. The small sharp rings present in the pattern correspond to d-spacings of 5.02 and 4.53 Å are are due to PET and PHB crystallinity respectively.

The morphological texture exhibited by this sample is shown in the

micrograph in Figure 4.59. Here, the flow direction is along the horizontal axis. It is seen that a fibrous texture oriented along the flow direction exists.

4.3.2 SHEAR FLOW

The WAXS patterns exhibited by a sample of the 60 mole% PHB system subjected to shear flow are shown in Figure 4.60. The sample was sheared at a rate of 10 $secs^{-1}$ at a temperature of 275°C. The flow direction is along the vertical axis in the figure. The top pattern corresponds to an edge edge view, while the bottom pattern corresponds to an edge top view. In both patterns it is seen that a low degree of azimuthal dependence of scattering intensity exists. This would indicate a low degree of molecular orientation on a qualitative basis. Notice also that no PHB or PET crystallinity is present as shown by the lack of any sharp scattering rings. The morphological texture exhibited by this sample is shown by the SEM micrograph is Figure 4.61. Here, the flow direction is along the vertical. It is seen that an unoriented, sponge-like texture exists.

In an attempt to generate a larger amount of molecular orientation in the sheared samples, higher values of shear rate were used. In Figure 4.62 is shown a series of WAXS patterns exhibited by three samples subjected to shear flow. The shear rates used ranged from 20 to 50 $secs^{-1}$. It is seen that as the shear rate is increased, the degree of azimuthal dependence of scattering intensity increases. This would tend to suggest

an increase in the amount of molecular orientation. It is also apparent that as the shear rate increases, the degree of PHB and PET crystallinity within the samples increases. This is shown by the small scattering rings in the patterns which become more visible with increasing shear rate.

The effect of increasing the shear rate on the morphological textures is shown in Figure 4.63. The top micrograph corresponds to the morphological texture exhibited by a sheared sample using a shear rate of 40 $secs^{-1}$. For the sample pictured at the bottom, the shear rate used was 100 $secs^{-1}$. The textures shown in these figures appear to be quite similar to that shown in Figure 4.61 for a shear rate of 10 $secs^{-1}$.

The results discussed so far indicate that on a qualitative basis, extensional flow has a much more pronounced affect on the development of molecular orientaiton and texture than shear flow. In extensional flow, a high degree of molecular orientation is achieved and a fibrous texture exists. In shear flow, a low degree of molecular orientation exists and an unoriented sponge-like texture is exhibited.

4.3.3 SHEARED WHILE COOLED SAMPLES

The previous results would tend to suggest that shear flow does not promote the development of molecular orientation. It was thought that the method of preparation of the sheared samples may have had an effect

on the results. In preparing the sheared samples, relaxation of molecular orientation may have occured due to the length of the cooling times involved. In order to combat this problem, a different method of sample preparation was examined. Samples were prepared by cooling the sample during shear. The results of this investigation are now presented.

In Figure 4.64 are shown the WAXS patterns exhibited by a sample of the 60 mole% PHB system prepared by shearing while cooling at 275°C. The top view corresponds to an edge edge view, while the bottom view corresponds to an edge top view. The sample possesses a high degree of molecular orientation as evidenced by the degree of azimuthal dependence of scattering intensity. The sharp rings in the pattern correspond to d-spacings of 5.02 and 4.53 Å and indicate the presence of PET and PHB crystallinity.

The morphological texture exhibited by this sample is shown in Figure 4.65. Two different magnifications are shown. The fibrous texture exhibited by this sample is very similar to that exhibited by the extended sample shown in Figure 4.59.

4.3.4 ANNEALING EXPERIMENTS

Annealing of samples was used to determine the extent to which molecular orientation remains in the melt state. Extended ribbons were used as they exhibited the highest degree of molecular orientation. In Figure

4.66 is shown the WAXS pattern exhibited by an extended ribbon annealed at 240°C for one minute. The ribbon was initially prepared at 275°C using an extension rate of 2.5 $secs^{-1}$. In comparison with Figure 4.58, it is seen that a broader dependence of scattering intensity is present. This would tend to suggest that a lower degree of molecular orientation exists within the sample.

If the sample is annealed at higher temperatures, it is possible to completely destroy all of the initial molecular orientation. In Figure 4.67 are shown the WAXS patterns of four samples originally subjected to extensional flow at 275°C. The samples have been annealed at 275°C for various times ranging from 30 seconds to five minutes. It is seen that within 30 seconds at 275°C the sample loses much of its original molecular orientation. This is evident through comparison of Figure 4.67a with Figure 4.58. Between 30 seconds and 2 minutes, not much change in molecular orientation occurs. By five minutes, however, most of the original molecular orientation has been lost. It should also be noticed that the annealed samples do not exhibit any PHB or PET crystallinity.

The morphological textures exhibited by the annealed samples are shown in Figure 4.68. It is seen that no difference exists between the texture possessed by all three samples. The texture seen is very similar to that seen in Figure 4.61 for a sheared sample.

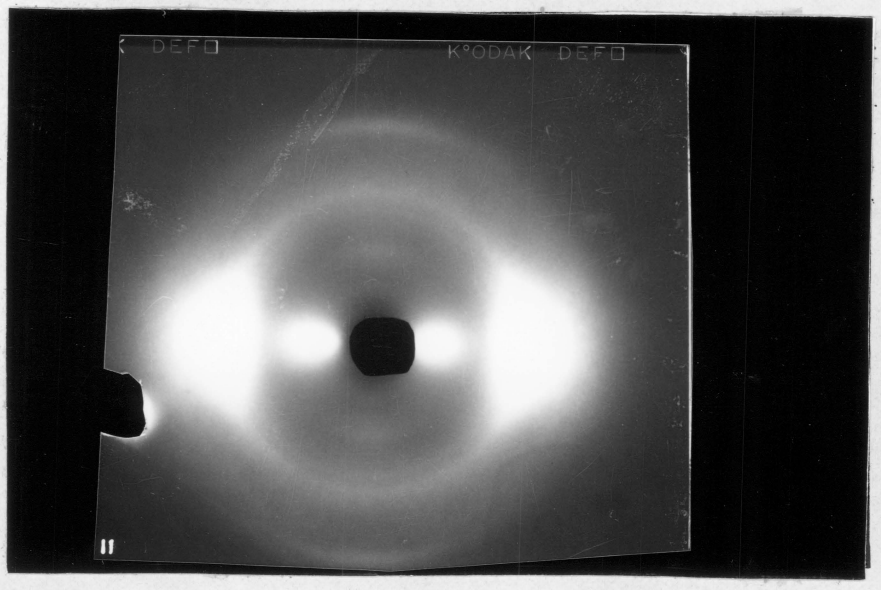

Figure 4.58 WAXS Pattern: 60 mole% PHB Copolymer
Extensional Flow, 275°C, $\dot{\varepsilon}$=2.5 secs^{-1}
Flow direction is vertical.

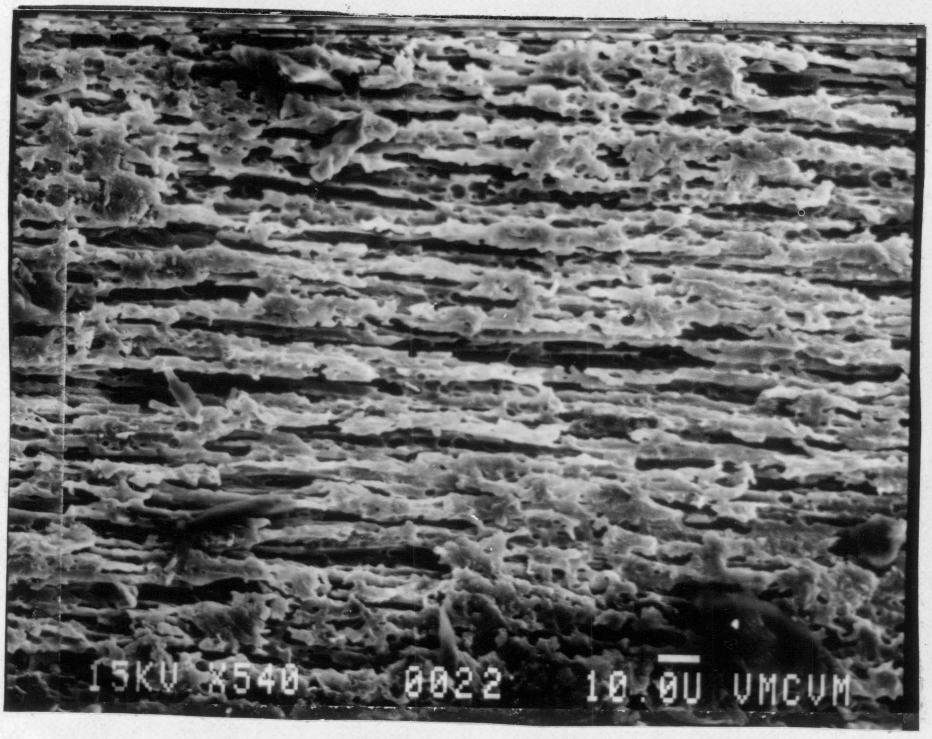

Figure 4.59 SEM Photograph: 60 mole% PHB Copolymer
Extensional Flow, 275°C, $\dot{\varepsilon}$=2.5 $secs^{-1}$
Magnification: 540X.

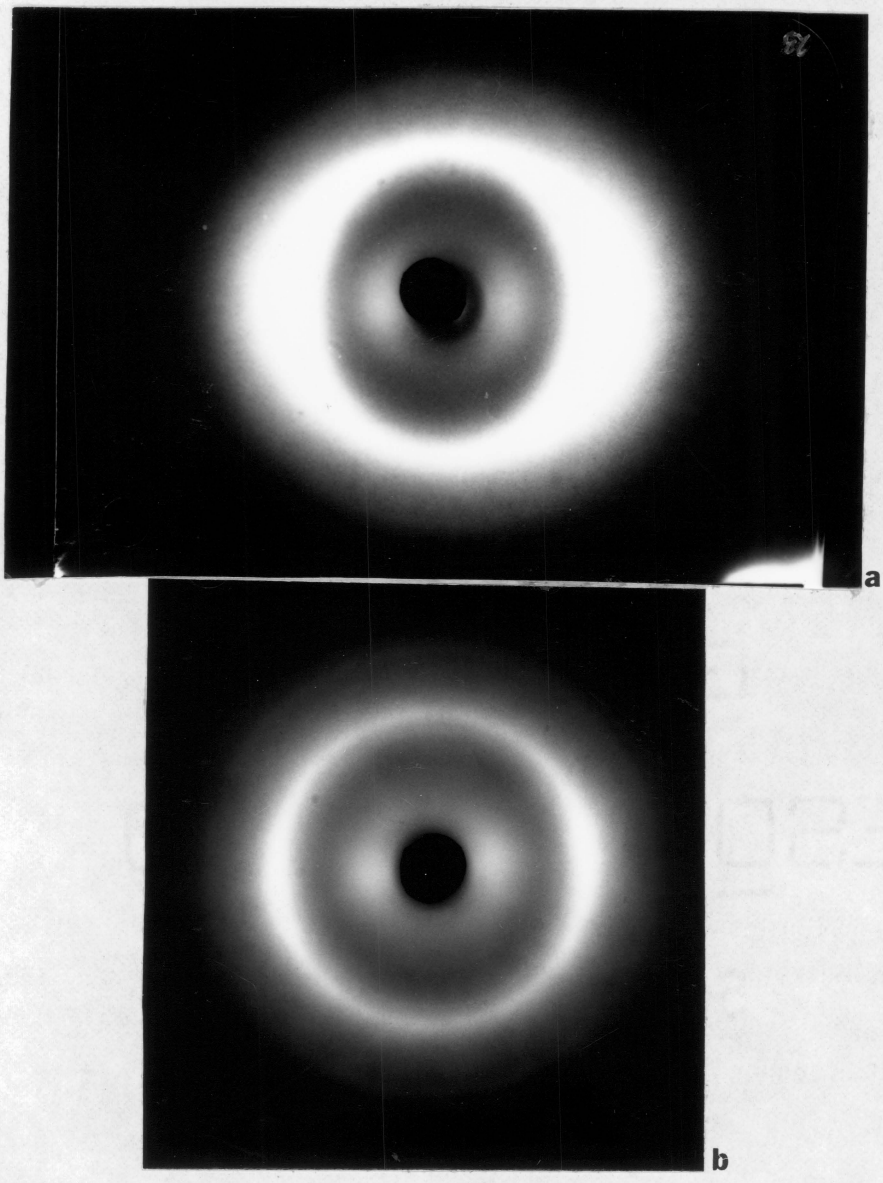

Figure 4.60 WAXS Patterns: 60 mole% PHB Copolymer Sheared Then Cooled, 275°C, $\dot{\gamma}$=10 $secs^{-1}$
a) Edge Edge View b) Edge Top View
Flow direction is vertical.

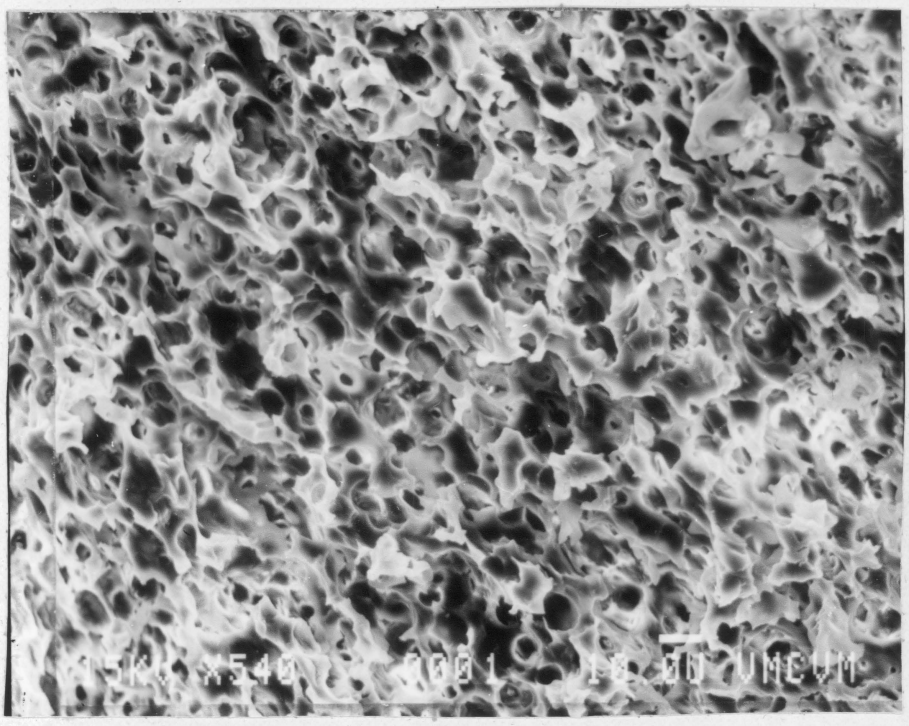

Figure 4.61 SEM Photogtaph: 60 mole% PHB Copolymer
Sheared Then Cooled, 275°C, $\dot{\gamma}$=10 $secs^{-1}$
Magnification: 540X.

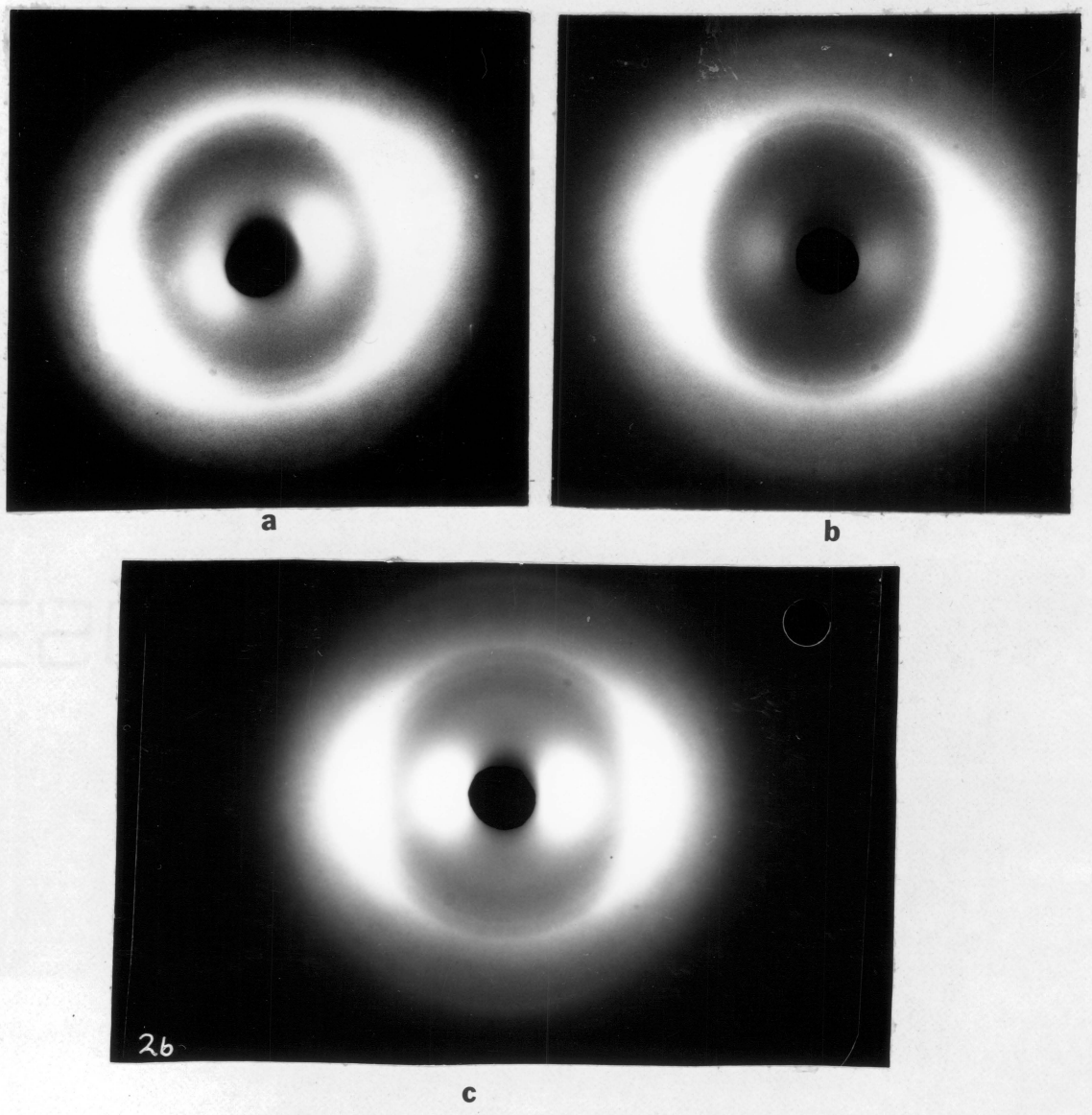

Figure 4.62 WAXS Patterns: 60 mole% PHB Copolymer
Sheared Then Cooled, 275°C, Edge Edge View
a) $\dot{\gamma}$=20 $secs^{-1}$ b) $\dot{\gamma}$=40 $secs^{-1}$ c) $\dot{\gamma}$=50 $secs^{-1}$
Flow direction is vertical.

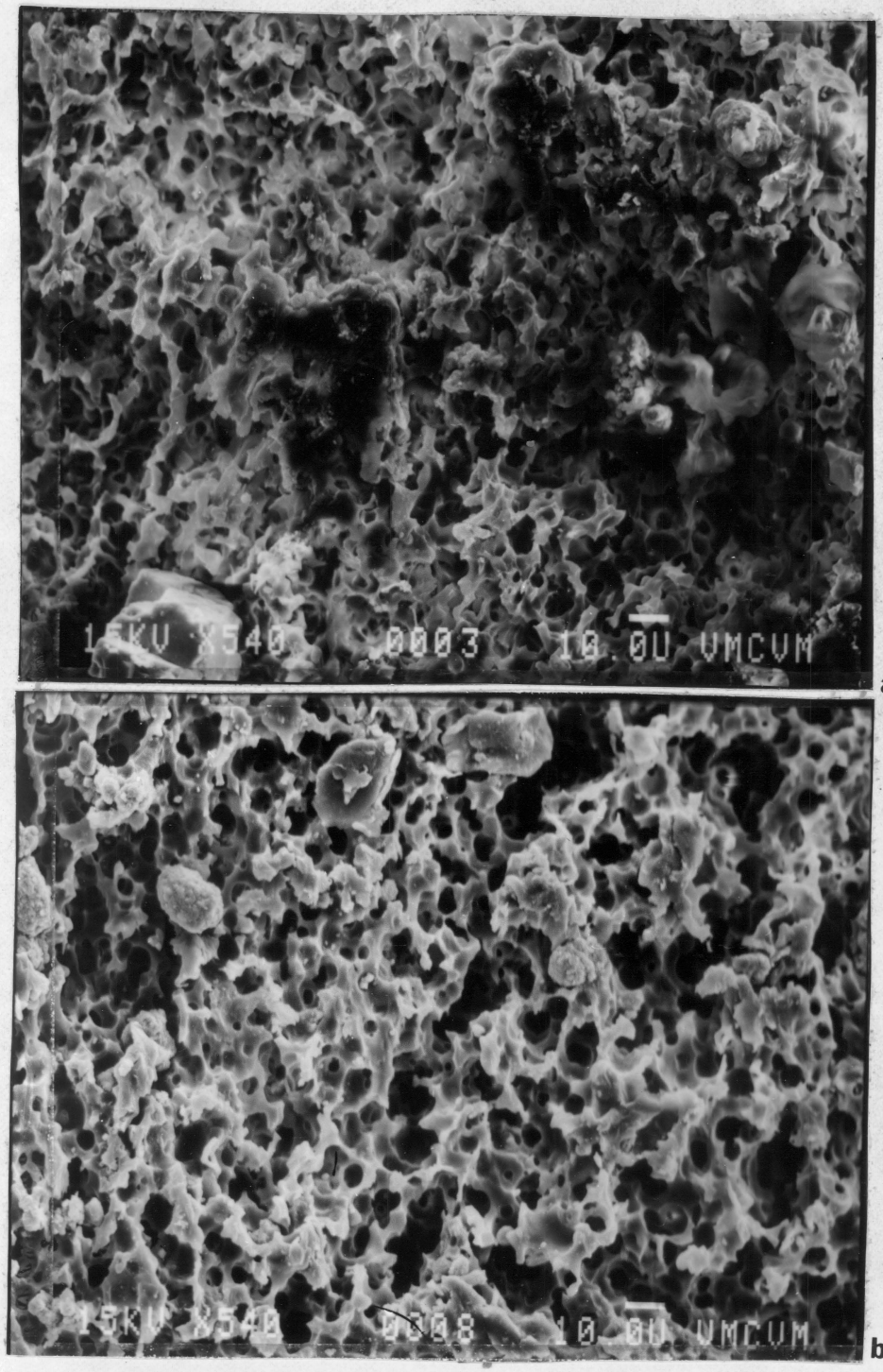

Figure 4.63 SEM Photogtaphs: 60 mole% PHB Copolymer
Sheared Then Cooled, 275°C
a) $\dot{\gamma}$=40 $secs^{-1}$ b) $\dot{\gamma}$=100 $secs^{-1}$
Magnification: 540X.

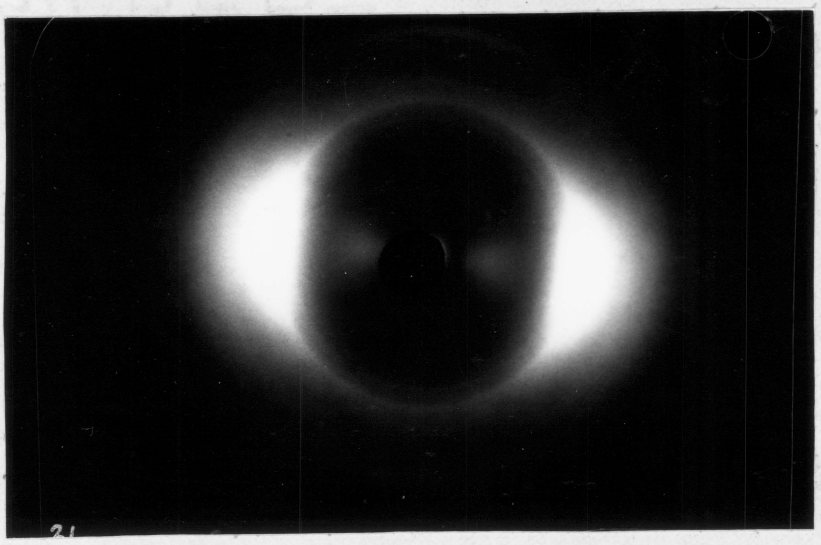

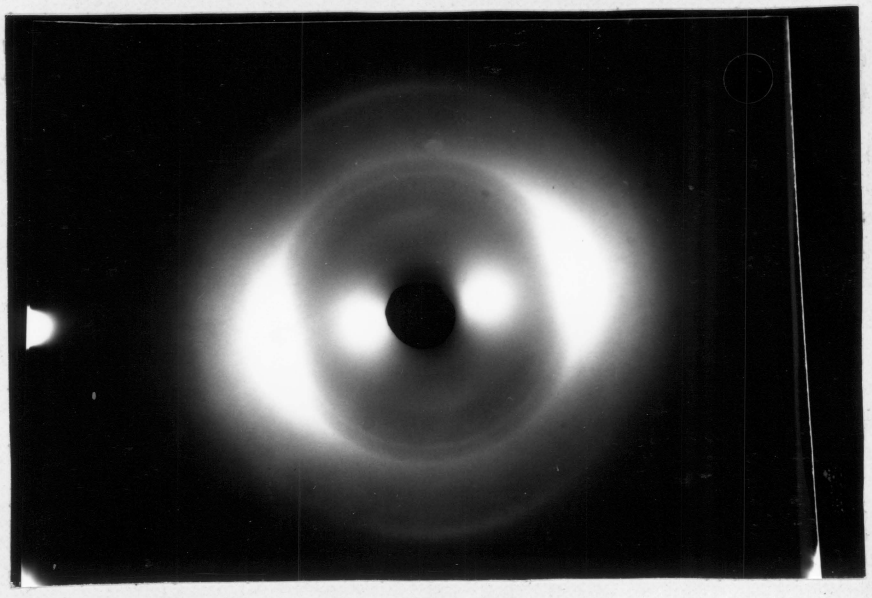

Figure 4.64 WAXS Patterns: 60 mole% PHB Copolymer
Sheared While Cooled, 275°C, $\dot{\gamma}$=10 $secs^{-1}$
a) Edge Edge View b) Edge Top View
Flow direction is vertical.

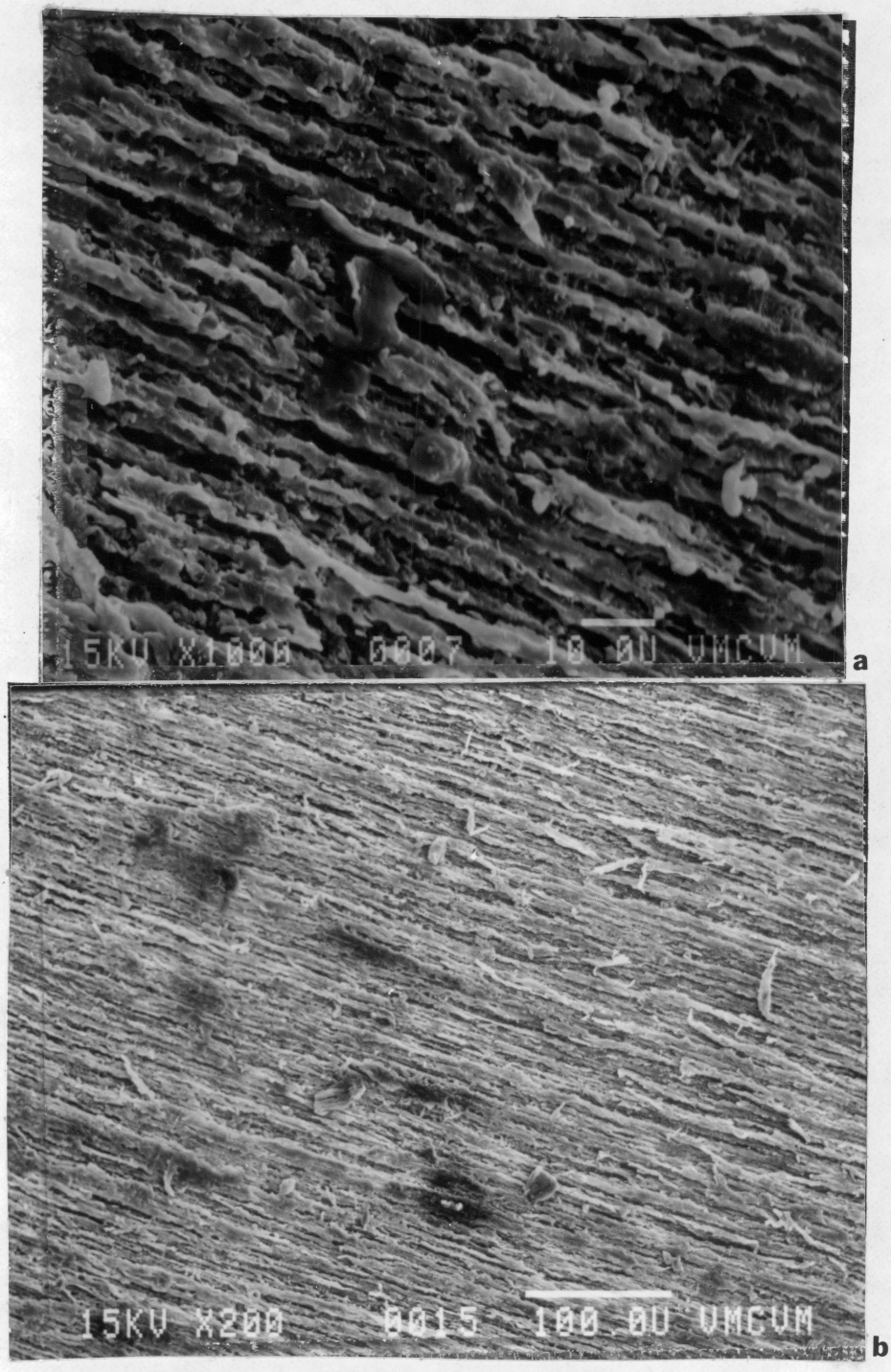

Figure 4.65 SEM Photographs: 60 mole% PHB Copolymer Sheared While Cooled, 275°C, $\dot{\gamma}$=10 secs^{-1} Magnification: a) 1000X b) 200X

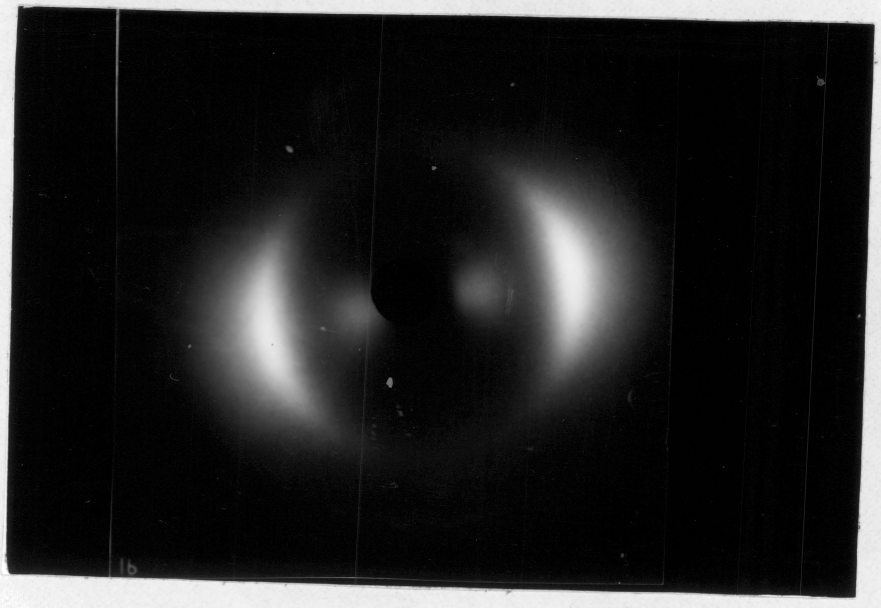

Figure 4.66 WAXS Pattern: 60 mole% PHB Copolymer
Extensional Flow, 275°C, $\dot{\varepsilon}$=2.5 $secs^{-1}$
Annealed: 1 minute 240°C
Flow direction is vertical.

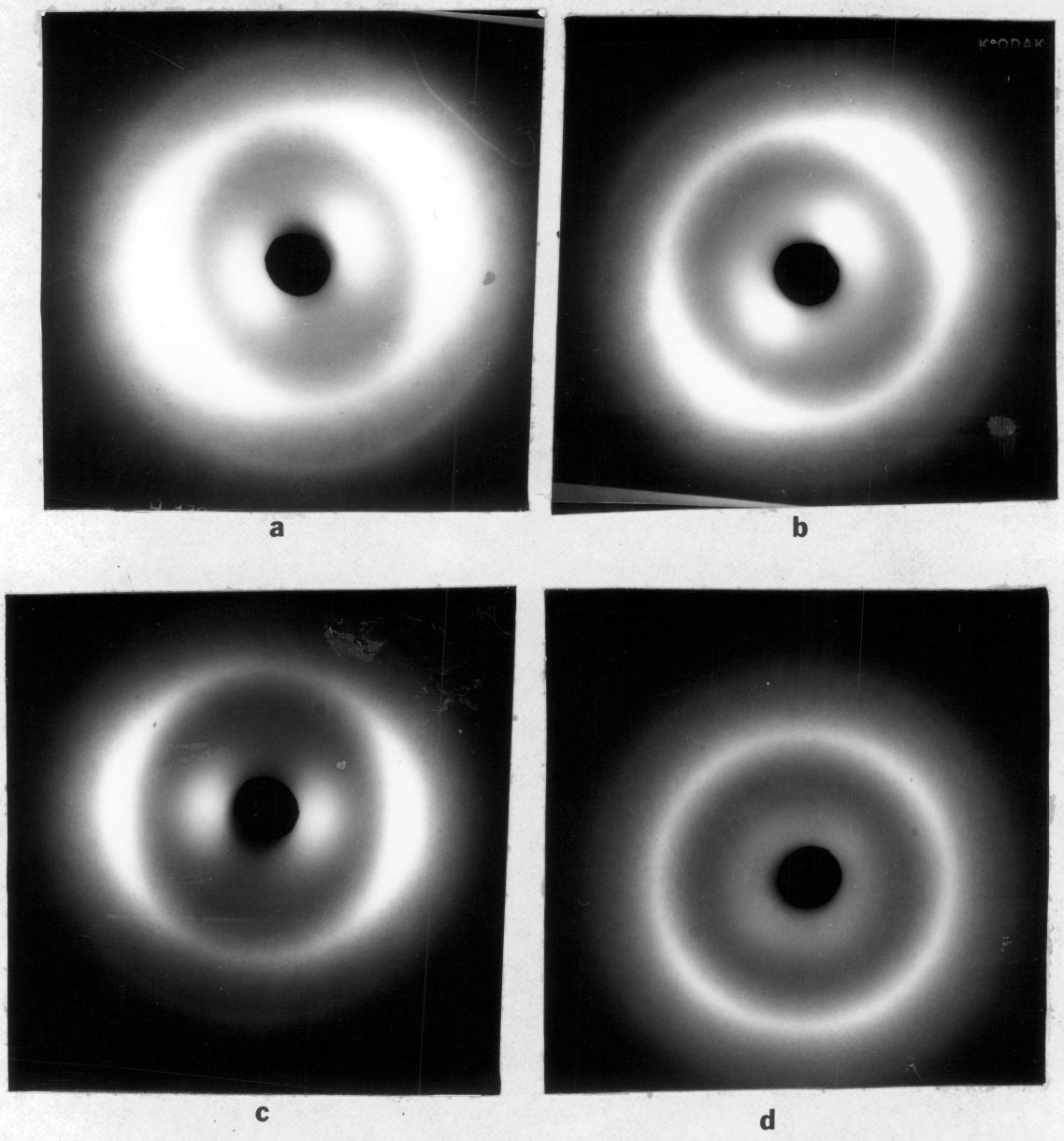

Figure 4.67 WAXS Patterns: 60 mole% PHB Copolymer
Extensional Flow, 275°C, ε=2.5 secs ^{1}
Annealed at 275°C: a) 30 secs b) 1 min.
c) 2 min. d) 5 min. Flow direction is vertical.

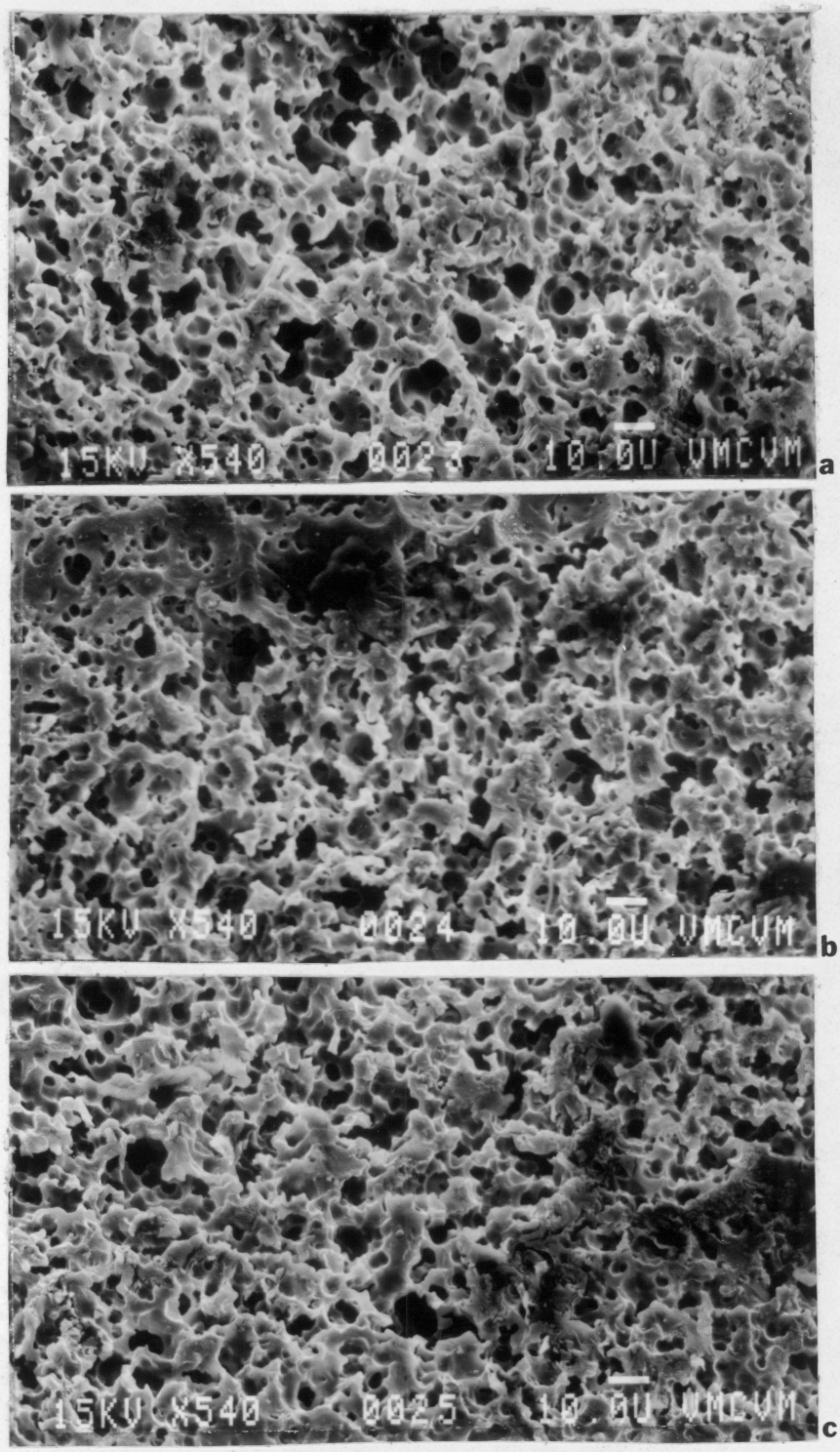

Figure 4.68 SEM Photographs: 60 mole% PHB Copolymer
Extensional Flow, 275°C, $\dot{\varepsilon}$=2.5 $secs^{-1}$
Annealed at 275°C: a) 30 secs b) 1 min.
c) 2 min.

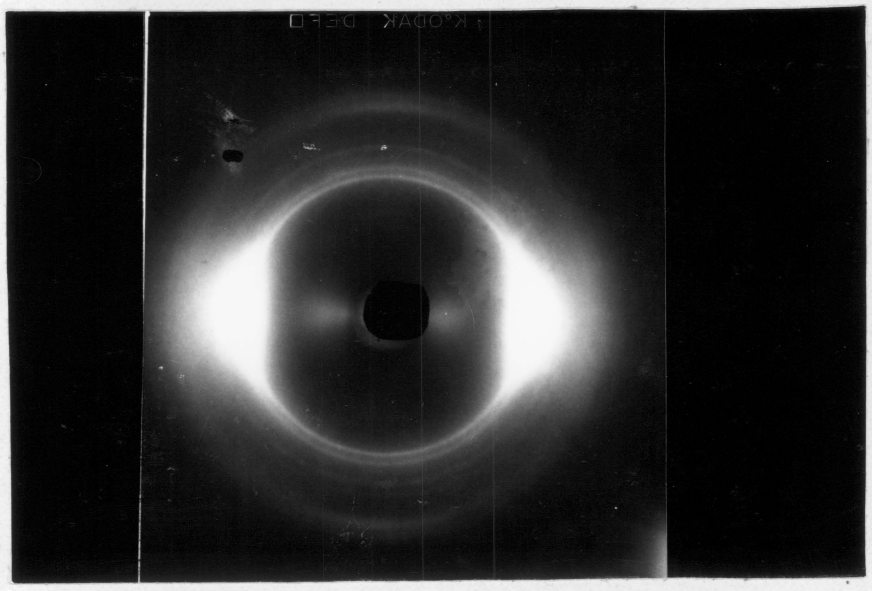

Figure 4.69 WAXS Pattern: 80 mole% PHB Copolymer
Extensional Flow, 320°C, $\dot{\varepsilon}$=2.5 secs^{-1}
Flow direction is vertical.

4.3.5 80 MOLE% PHB/PET STUDIES

Extended and sheared samples were prepared using the 80 mole% PHB system to determine whether the results found for the 60 mole% PHB copolymer could be generalized. The n-propylamine etchant does not produce much of an effect on the 80 mole% PHB system, therefore, only WAXS measurements were conducted.

In Figure 4.69 is shown the WAXS pattern generated by a sample of the 80 mole% PHB system subjected to extensional flow at a temperature of 320°C. The extension rate used was 2.5 $secs^{-1}$, and the flow direction is along the vertical axis in the figure. The high degree of azimuthal dependence of scattering intensity indicates that the sample possesses a high degree of molecular orientation. The sharps rings visible indicate the presence of crystallinity. Three of the rings are related to PHB crystallinity and have d-spacings of 3.12, 3.72, and 4.53 Å. The fourth visible ring corresponds to a d-spacing of 4.20Å and is related to PET crystallinity.

In shear flow, it does not appear as if much molecular orientation develops. This is shown by the WAXS patterns in Figure 4.70. The two patterns correspond to the edge edge and edge top views of a sheared disk of the 80 mole% PHB copolymer. The sample was prepared using a shear rate of 10 $secs^{-1}$ at a temperature of 320°C. In the edge top view, the sharp rings have d-spacings of 3.12, 3.72, 4.20, and 4.53 Å, and are

indicative of the presence of PHB and PET crystallinity.

Cooling of the 80 mole% PHB samples during shear does not seem to achieve the same effect seen with the 60 mole% PHB system. In Figure 4.71 is seen the WAXS pattern exhibited by a sample of 80 mole% PHB copolymer subjected to shearing at a rate of 10 $secs^{-1}$. The initial melt temperature was 320°C, and the sample was cooled during the shearing step. It is seen that not much molecular orientation or crystallinity is present in the sample.

As a final test, extended ribbons of the 80 mole% PHB system were annealed at the melt temperature. Annealing times of 30 seconds and one minute were investigated. The WAXS patterns exhibited by these samples are shown in Figure 4.72. In comparison to the pattern shown in Figure 4.69, it seen that a broadening of the azimuthal dependence of scattering intensity occurs upon annealing of the samples. This is indicative of some loss of molecular orientation. On a qualitative basis, however, the loss of orientation seen for the 80 mole% PHB sample does not appear to be as great as that observed for the 60 mole% PHB samples.

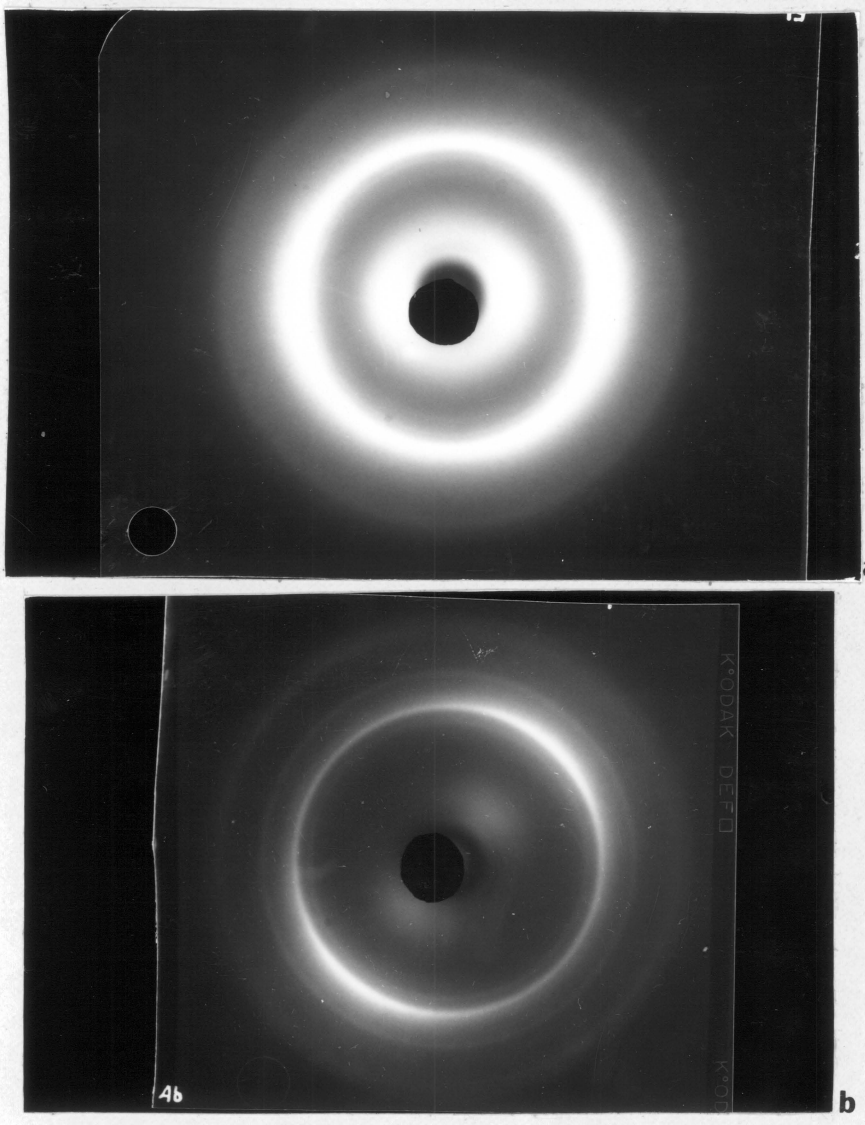

Figure 4.70 WAXS Patterns: 80 mole% PHB Copolymer Sheared Then Cooled, 320°C, $\dot{\gamma}$=10 secs^{-1}
a) Edge Edge View b) Edge Top View
Flow direction is vertical.

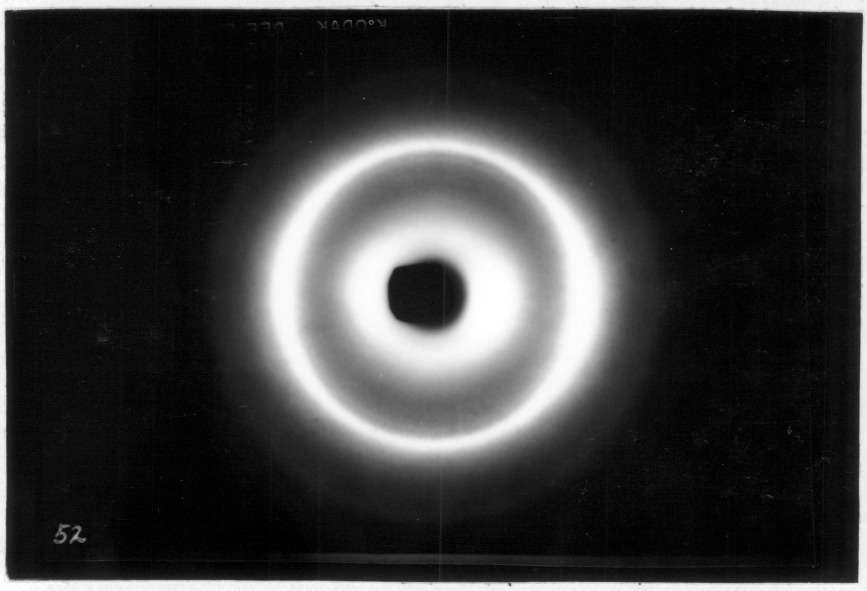

Figure 4.71 WAXS Pattern: 80 mole% PHB Copolymer
Sheared While Cooled, 320°C, $\dot{\gamma}$=10 $secs^{-1}$
Edge Edge View, flow direction is vertical.

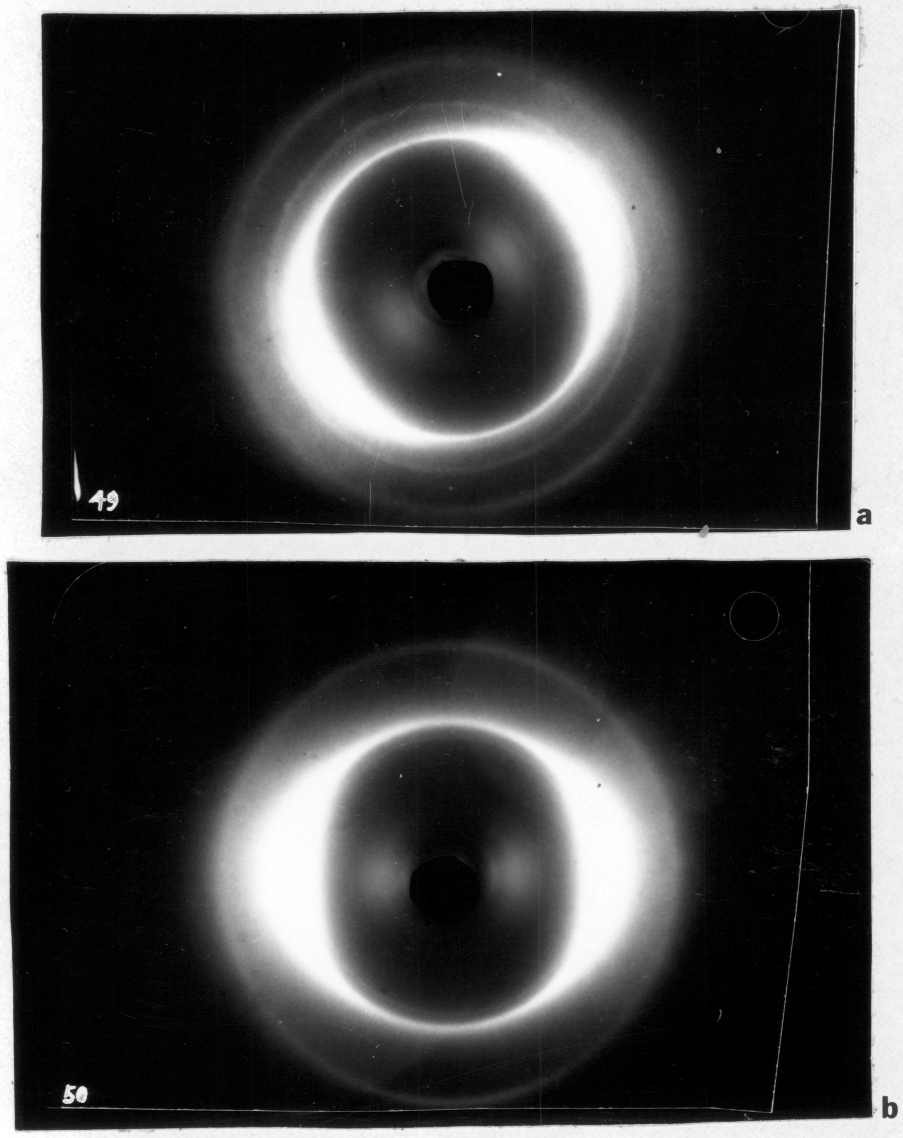

Figure 4.72 WAXS Patterns: 80 mole% PHB Copolymer
Extensional Flow, 320°C, $\dot{\varepsilon}$=2.5 $secs^{-1}$
Annealed at 320°C: a) 30 secs b) 1 min.
Flow direction is vertical.

4.3.6 SUMMARY OF WAXS AND SEM STUDIES

The results of the WAXS and SEM studies have shown that extensional flow has a greater effect on producing molecular orientation than shear flow. This result was seen for both the 60 and 80 mole% PHB samples. For the case of the 60 mole% PHB/PET copolymer, a fibrous texture was seen to exist in extensional flow, while an unoriented sponge-like morphology existed in shear flow. Increasing the shear rate had little effect on the morphology, but slightly increased the degree of molecular orientation and crystallinity exhibited. Samples prepared by cooling during shear exhibited the same degree of molecular orientation and fibrous texture seen with extended samples. Heat treatment of samples showed that within 30 seconds at the melt temperature, all of the structure produced during flow could be lost. This may explain the difference between the sheared and the cooled while sheared samples. PHB and PET crystallinity was seen to be present in the extended and the cooled while sheared samples. This crystallinity was most probably produced through strain induced crystalization. Annealing of the samples removed this crystallinity. The 80 mole% and the 60 mole% PHB/PET copolyester systems exhibited the same behavior in shear and extensional flow. However, no improvement in the degree of molecular orientation was seen in samples of 80 mole% PHB copolymer produced by cooling during shear. Also, annealing of the 80 mole% PHB system did not cause as great a loss in molecular orientation as seen for the 60 mole% PHB system. These differences may be due to a difference in relaxation times based on the amount of PHB in each

copolymer composition.

CHAPTER FIVE: DISCUSSION

An analysis of Ericksen's anisotropic fluid theory has been conducted. The predictions of this theory for steady shear and extensional flow have been investigated. Based on measurements of the rheological behavior of several liquid crystalline materials, the predictions of Ericksen's theory are qualitatively correct. However, measurements of molecular orientation in specially prepared samples yields results which conflict with some of the predictions of the theory. These results are now examined in more detail.

5.1 ERICKSEN'S THEORY VERSUS EXPERIMENTAL EVIDENCE

An investigation of the predictions of Ericksen's theory shows that certain transient behavior, such as stress overshoot upon inception of shear, can be accounted for. Such transient response is accounted for by the theory solely on the basis of the rearrangement of the position of the director during flow. To illustrate this more clearly, the steady shear director and stress equations are reproduced below:

(92) $\dot{n}_1 = 1/2\dot{\gamma}n_2(\lambda+1-2\lambda n_1^2)$

(93) $\dot{n}_2 = 1/2\dot{\gamma}n_1(\lambda-1-2\lambda n_2^2)$

(94) $\dot{n}_3 = -\lambda\dot{\gamma}n_1 n_2 n_3$

(95) $\tau_{12} = \alpha_1 n_1 n_2 + \alpha_2 \dot{\gamma}/2 + \alpha_4 \dot{\gamma}(n^2+n^2)/2 + 1/2(\alpha_5 \dot{\gamma}^2 n_1 n_2)$

(96) $\tau_{11}-\tau_{22} = \alpha_1 (n_1^2-n_2^2)+\alpha_5 \dot{\gamma}^2(n_1^2-n_2^2)/2$

It is seen that the time dependence of the shear and normal stresses

arises from the time dependence of the director components, n_1 and n_2. An example of the time dependence of the state of the director is shown in Figure 5.1. At time t=0, the director coincides with the n_2 axis. As t increases, however, the director rotates in order to align with the flow direction ($n_1 = 1$). Analysis of the shear stress equation shows that a maximum occurs when $n_1 = n_2 = \sqrt{2}/2$. Thus, as the director rotates through an angle of 45^0 a stress overshoot peak is predicted. Once the director becomes aligned, steady state conditions exist and no further change in the position of the director will occur. Examination of the director equations shows that setting the shear rate ($\dot{\gamma}$) equal to zero will cause the director to stay in its current position. This is because all three director equations will be equal to zero, specifying steady state.

The previous discussion provides insight as to how Ericksen's theory can predict stress overshoot behavior. It becomes clear that the choice of initial condition or λ value affects the path taken by the director in order to reach steady state. This explains why the predictions of the theory for stress growth behavior discussed in Chapter Four were seen to be a function of λ and initial condition. In addition, once the fluid is oriented, no overshoot behavior will be predicted by the theory. This is because steady state conditions will have been achieved.

Measurements of the transient response of several liquid crystalline fluids indicates that the predictions of Ericksen's theory are qualitatively correct. Upon inception of shear, an overshoot peak is exhibited

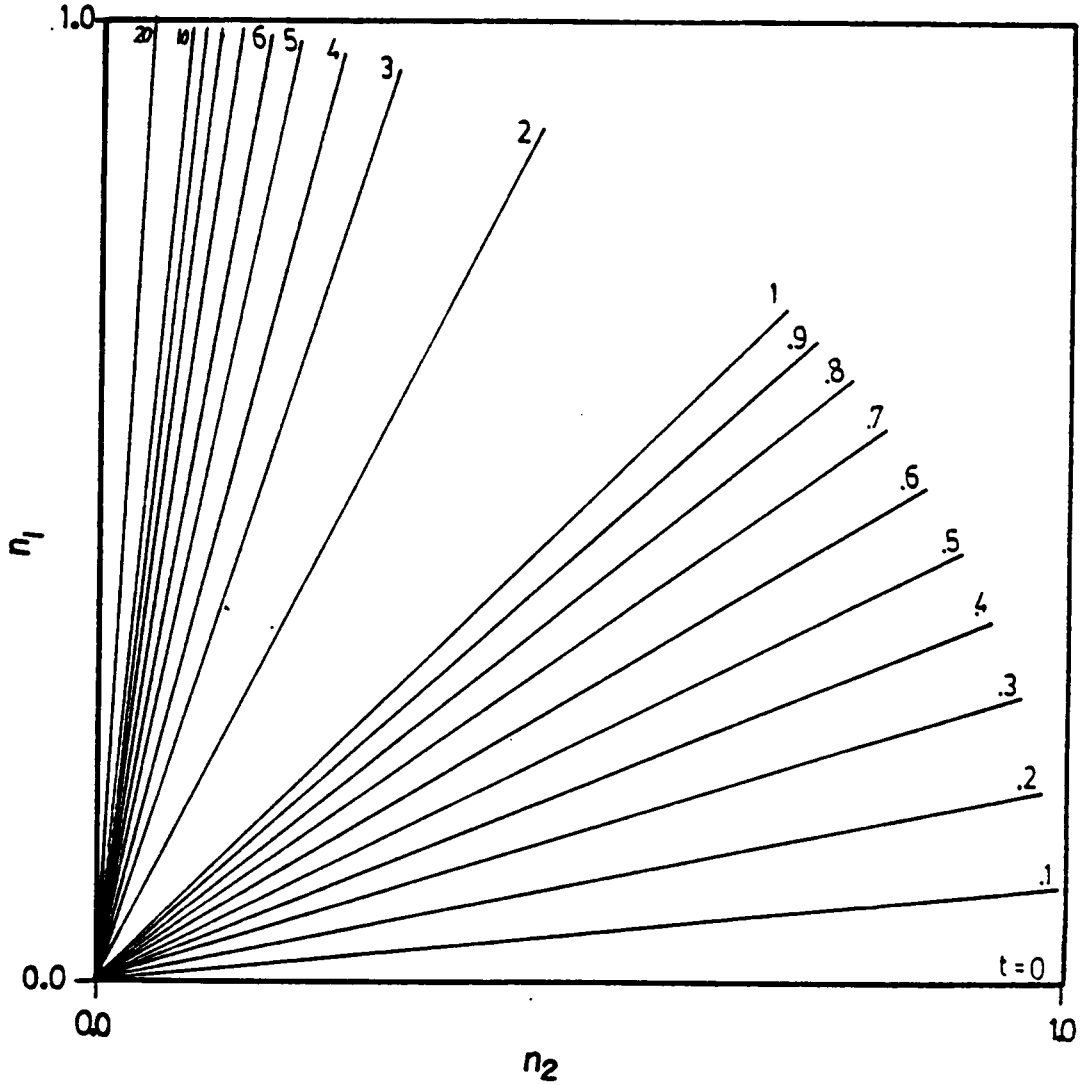

Figure 5.1 Schematic representation of the path of the Director $\lambda=1$, Initial condition: $n_2=1$, $\dot{\gamma}=10$ secs^{-1}.

in the shear stresses. This overshoot peak is shear history sensitive and can be made to disappear by preshearing of the fluid. Upon cessation of shear flow the stresses relax to zero immediately. Thus, the assumption that these fluids do not exhibit yield stresses is valid. In shear reversal experiments, no overshoot behavior is exhibited after preshearing of the fluid.

Further testing of the predictions of Ericksen's theory was conducted through the use of WAXS measurements. As shown in Chapter Four, these results indicated that a high degree of molecular orientation develops in extensional flow. This result is in agreement with theory. However, it should be stated that the results of the sheared while cooled samples indicates that extensional flow alone may not be responsible for the high degree of orientation exhibited by the extended samples. In shear flow not much molecular orientation was achieved. Also, annealing of oriented samples showed that all of the original structure produced during flow could be lost within thirty seconds at the melt temperature.

The results of the WAXS studies indicate a major failing of the Ericksen theory. It has been shown that Ericksen's theory predicts overshoot behavior based on the development of molecular orientation. It has also been shown that once the fluid is oriented no overshoot behavior is predicted by the theory. Actual measurements of the stress growth behavior of several liquid crystalline systems reveals that preshearing of these fluids affects the magnitude of the overshoot peak exhibited during

stress growth. In interrupted stress growth experiments it was found that even after three minutes of relaxation at the melt temperature, no overshoot peak was exhibited. These results are in apparent agreement with theory. However, the WAXS studies indicate that even if molecular orientation was produced, it would be lost within 30 seconds at the melt temperature. Therefore, if the overshoot peak exhibited was due to the development of molecular orientation, it should reappear after 30 seconds in the case of the 60 mole% PHB/PET system. The fact that no overshoot peak is exhibited even though the fluid is unoriented suggests that the peak is not due to the development of molecular orientation. It appears that Ericksen's theory predicts stress overshoot behavior for the wrong reason. In addition, Ericksen's theory predicts that once the fluid is oriented it should stay oriented. The results of the annealing experiments are not in agreement with the theoretical predictions. The results of jump strain measurements, and the comparison of dynamic to steady shear data support this conclusion. These results are discussed in more detail in the next section.

5.2 JUMP STRAIN MEASUREMENTS AND STRUCTURE REARRANGEMENT

Comparison of WAXS data to stress growth curves for the 60 mole% PHB/PET system indicates that Ericksen's theory is not entirely valid. The stress overshoot peak exhibited upon inception of shear appears to be due to some structure rearrangement other than the development of molecular orientation. The results of jump strain measurements and the compar-

ison of dynamic to steady shear data support this conslusion. These results are now analyzed.

5.2.1 JUMP STRAIN MEASUREMENTS

It has been shown that preshearing of liquid crystalline fluids can affect the magnitude of the stress overshoot peak exhibited upon inception of shear. Jump strain tests followed by inception of shear have shown that a step in strain can also affect the magnitude of the stress overshoot peak. It appears that the same structural reorganization is occuring as a result of preshearing or a step in strain.

In order to determine the nature of the structural change occuring during shear or with the application of strain, jump strain measurements were made. It was shown that for both the 60 mole% PHB/PET and the Kevlar systems, the relaxation modulus, G(t), was a strong function of applied strain. It was seen that G(t) relaxed verly quickly and did not exhibit a yield value. These results are in agreement with the stress relaxation behavior exhibited by the 60 mole% PHB and Kevlar systems. The jump strain and stress growth/relaxation experiments, therefore, indicate that the same type of structural change is occuring. The non-linearity of G(t) must be related to the structural change which causes a change in the stress overshoot behavior exhibited upon the inception of shear. For flexible chain polymers, such a change in structure would be related to the breaking up of entanglements during deformation. For liquid crystal-

line materials, however, such a break up of entanglements is not a valid mechanism as these materials are composed of semi-rigid rods. It is not expected, therefore, that a liquid crystalline system could possess a high density of chain entanglements. It is more probable that a break up of the domain structure exhibited by liquid crystalline fluids is taking place during deformation of the melt.

For the 60 mole% PHB/PET system it was found that the strain sweep and jump strain data did not agree. The results of the strain sweep measurements indicated that G(t) should remain independent of strain up to applied strains of 10 strain units. The jump strain measurements showed that G(t) was a strong function of strain at values of γ as low as 0.5 strain units. One reason for this difference may be associated with the deformation rates used in each experiment. In a strain sweep experiment, oscillatory frequencies of between 1 and 100 Hz are usually used. In a jump strain test, however, the fluid is subjected to a finite amount of strain instaneously. In such a test, the fluid experiences a very high deformation rate. The difference in deformation rates used in the jump strain and strain sweep experiments may have caused different degrees of rearrangement of the melt structure. A difference in the degree of rearrangement of melt structure would account for the difference in the jump strain and strain sweep data.

5.2.2 STEADY SHEAR VERSUS DYNAMIC DATA

Analysis of jump strain measurements shows that the same structure change which occurs during shear flow, may take place due to the application of finite amounts of strain. WAXS studies indicate that this structural reorganization is not that of molecular orientation. Comparison of steady shear to dynamic data supports this conclusion.

For flexible chain polymers, the dynamic mechanical properties (η^* and $2G'$) are usually comparable to the steady shear properties (η and N1) at low deformation rates. At higher deformation rates, the steady shear and dynamic properties deviate from each other. This deviation has been attributed to the break up of chain entanglements in shear flow which may not occur in oscillatory flow. For liquid crystalline fluids composed of rigid rods, such a break up of entanglements would not apply. Rather, a difference in dynamic and steady shear properties would be expected due to the development of molecular orientation in shear flow which may not occur in oscillatory flow. Miesowicz (4) has shown that liquid crystalline fluids can exhibit different values of viscosity based on the orientation of the fluid particles with respect to the flow direction. Therefore, for liquid crystalline fluids, if molecular orientation were occuring in shear flow but not in oscillatory flow a difference between η and η^* would be seen. For the 60 mole% PHB/PET copolymer system, it is seen that η and η^* tend to coincide. Proof of this result is shown in Figures 5.2 and 5.3 where η and η^* are plotted as functions of deformation rate at temperatures of 260 and 275°C. It should also be noted that

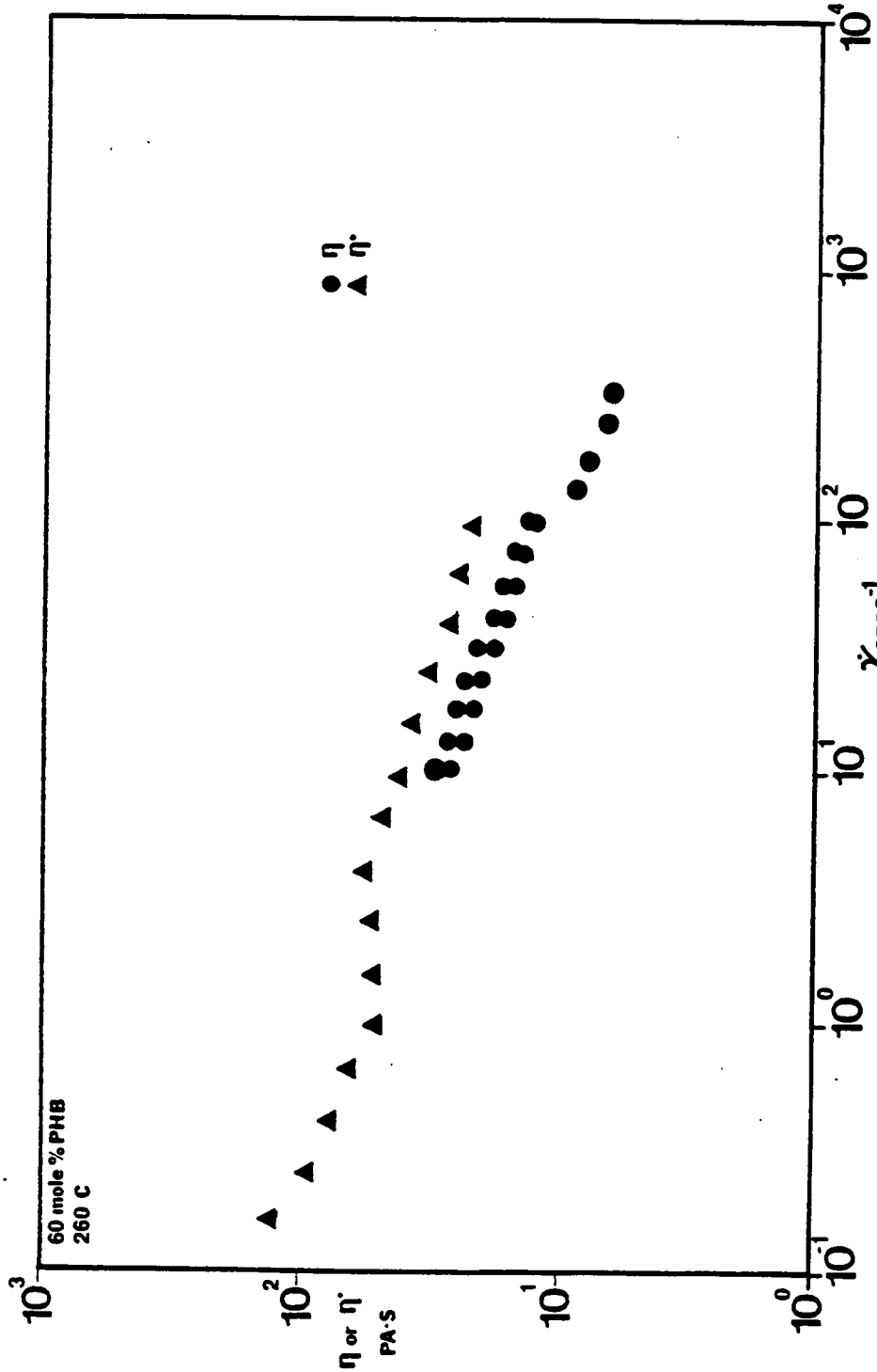

Figure 5.2 Steady Shear and Dynamic Data: η vs $\dot{\gamma}$, η^* vs ω.
60 mole% PHB/PET copolymer, 260°C.
50 mm C/P 0.04 rad.

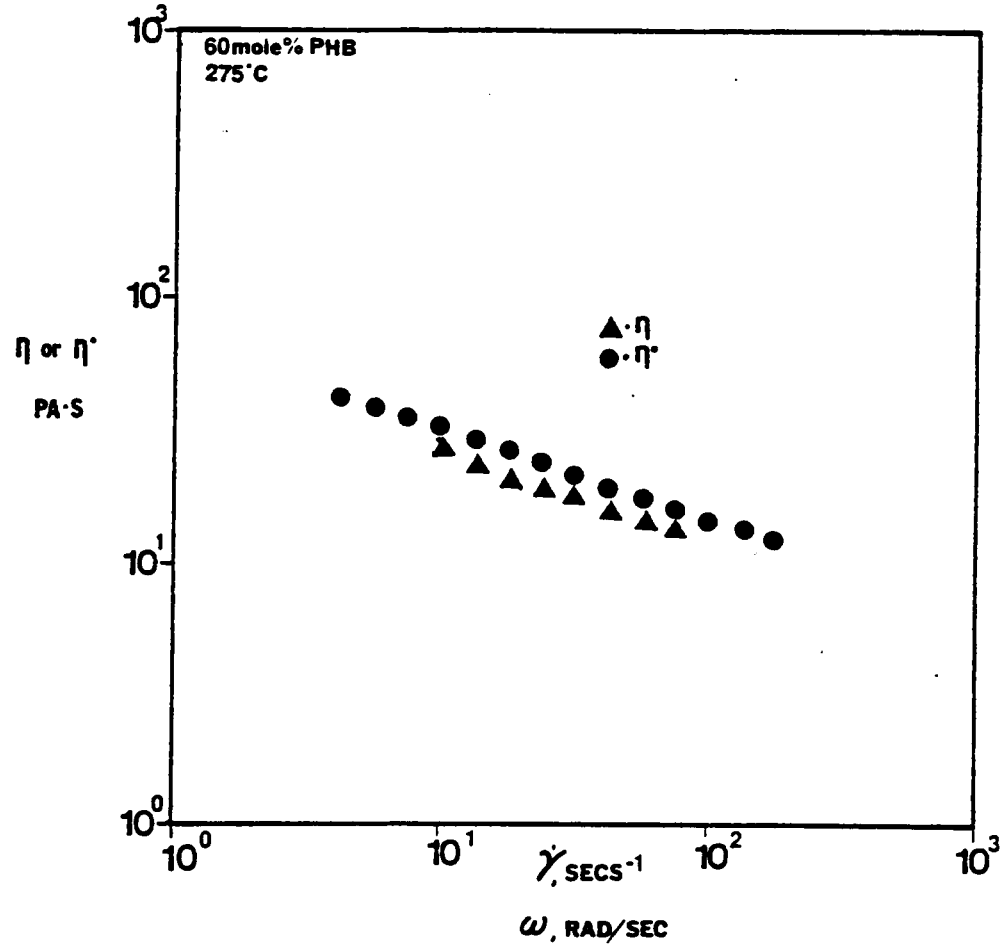

Figure 5.3 Steady Shear and Dynamic Data: η vs $\dot{\gamma}$, η^* vs ω
60 mole% PHB/PET copolymer, 275°C.
50 mm C/P 0.04 rad

Gotsis [123] has reported that η and η^* are of similar magnitude for the 80 mole% PHB/PET system.

One possible explanation for the similarity in magnitude of η and η^* is that molecular orientation is not developing in either flow. This conclusion is supported by the fact that WAXS measurements indicate very little affect of shear flow on the development of molecular orientation. In addition, any molecular orientation produced in the melt can be lost very quickly as the annealing experiments prove. Thus, η and η^* coincide because no moleclular orientation develops in either shear or oscillatory flow, and any orientation which does develop is quickly lost.

5.2.3 THE MODEL OF ZAREMBA, FROMM AND DEWHITT

One important objective of this study has been to determine the usefullness of Ericksen's theory to model the flow of liquid crystalline fluids. If molecular orientation is not developing in shear flow, then it may be possible to use a different constitutive equation which does not take the effects of molecular orientation into account. Based on the previous results of the similarity between η and η^*, an intelligent choice for such a constitutive equation may be made. It is known that constitutive equations based on a corrotating reference frame can predict a similarity between dynamic and steady shear properties ($\eta=\eta'$ and $2G'=N1$). (More information regarding such models is available elsewhere [120].) With these facts apparent, it was decided to test the constitu-

tive equation of Zaremba, Fromm, and DeWhitt (ZFD Model) [120] as it is a corrotational constitutive equation.

The major equations of the generalized ZFD model for prediction of the stresses are presented below:

(97) $$\tau = \sum_k \tau_k$$

(98) $$\tau_k + \lambda_k D\tau_k/Dt = -\eta_k \dot{\gamma}$$

or

(99) $$\tau = -\int_{-\infty}^{t} \sum_k \eta_k/\lambda_k \exp(-(t-t')/\lambda_k))\dot{\Gamma}' dt'$$

The ZFD equations are based on the superposition of maxwell models in a reference frame which translates and rotates with the fluid. Calculation of the predictions of the theory for simple shear and dynamic material properties is accomplished through the substitution of the correct form of the deformation and vorticity tensors into the above equations (see **reference [120]**). These calculations yield the following forms for the material parameters:

(100) $$\eta' = \eta = \sum_k \eta_k/(1+(\lambda_k \dot{\gamma})^2)$$

(101) $$2G' = N1 = \sum_k \eta_k \lambda /(1+(\lambda_k \dot{\gamma})^2)$$

Values of λ_k and η_k were calculated for the 60 mole% PHB/PET copolyester at 260 and 275°C. Only the first five terms of the series was used. Values of λ_k were chosen abitrarily, and the corresponding values of η_k were determined by fitting equation [100] to steady shear viscosity data. The results of these calculations are presented in Tables B.26 and B.27 in the appendix. The accuracy of the fit of the ZFD equation to the vis-

cosity can be seen in the plots in Figures 5.4 and 5.5. Using the values of material parameters calculated by fitting the steady shear viscosity, the predictions of the theory for N1, G', and transient behavior were investigated. The results of these calculations are presented in Figures 5.6 thru 5.11. It can be seen in the Figures that the predictions of the theory for the deformation rate dependence of G' and N1 are quite accurate. This result is interesting as it implies that the theory can accurately predict the elastic behavior (N1,G') of the 60 mole% PHB system by fitting the fluid's viscous behavior (η,η').

The predictions of the ZFD model for transient behavior are plotted against actual stress growth and stress relaxation curves for the 60 mole% PHB system at 275°C. It can be seen that in the case of stress growth, the ZFD model underestimates the magnitude of the stress overshoot peak. The stresses are also predicted to oscillate before reaching steady state. For stress relaxation, the theory predicts that the stresses relax much faster than observed, and again oscillate before reaching steady state.

5.2.4 SUMMARY

Analysis of rheological measurements and WAXS studies has revealed that the predictions of Ericksen's theory are not strictly valid for liquid crystalline fluids. The theory predicts stress overshoot behavior based solely on the development of molecular orientation during flow.

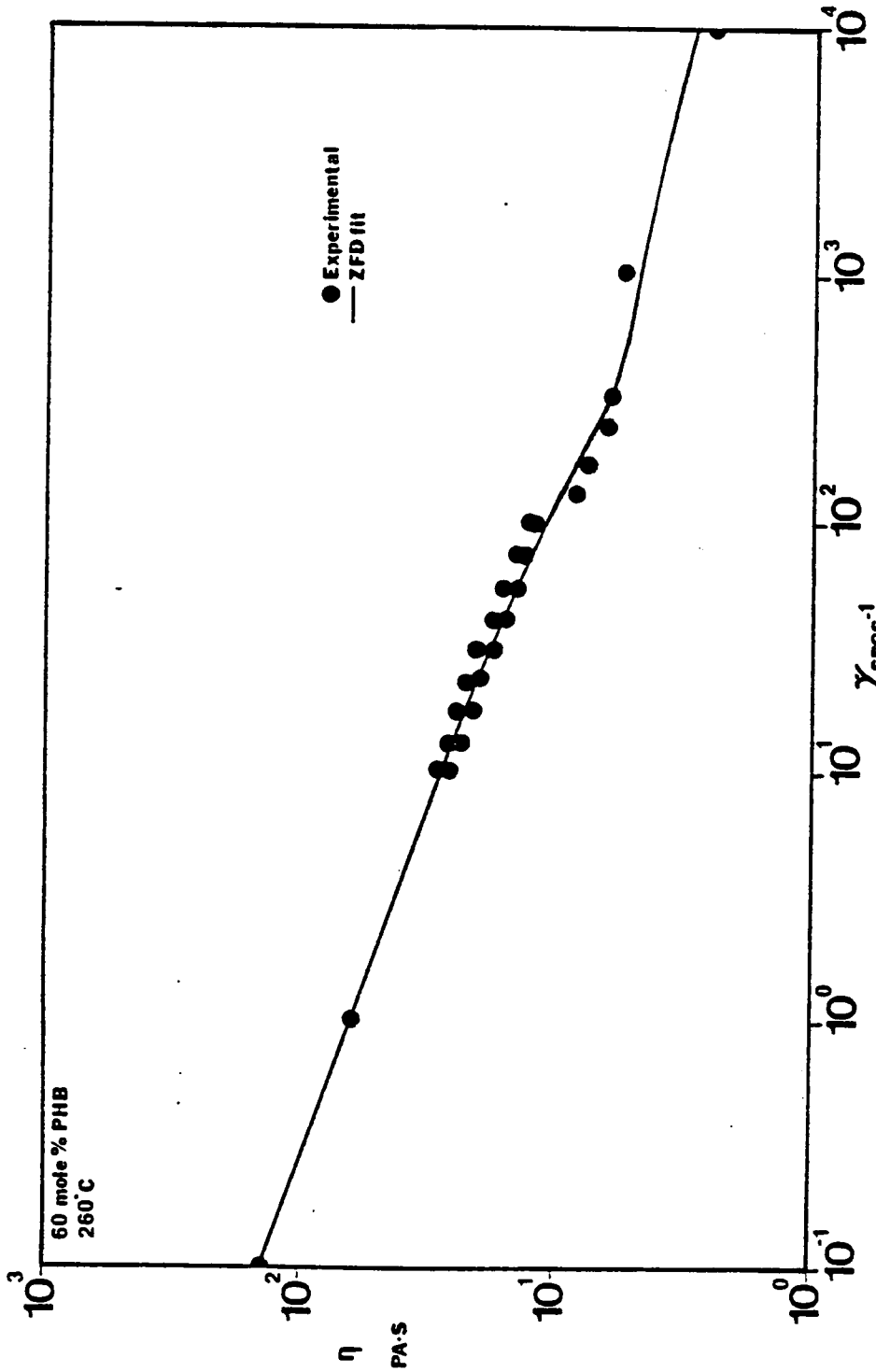

Figure 5.4 Fit of ZFD model: η vs $\dot{\gamma}$
60 mole% PHB/PET copolymer, 260°C.

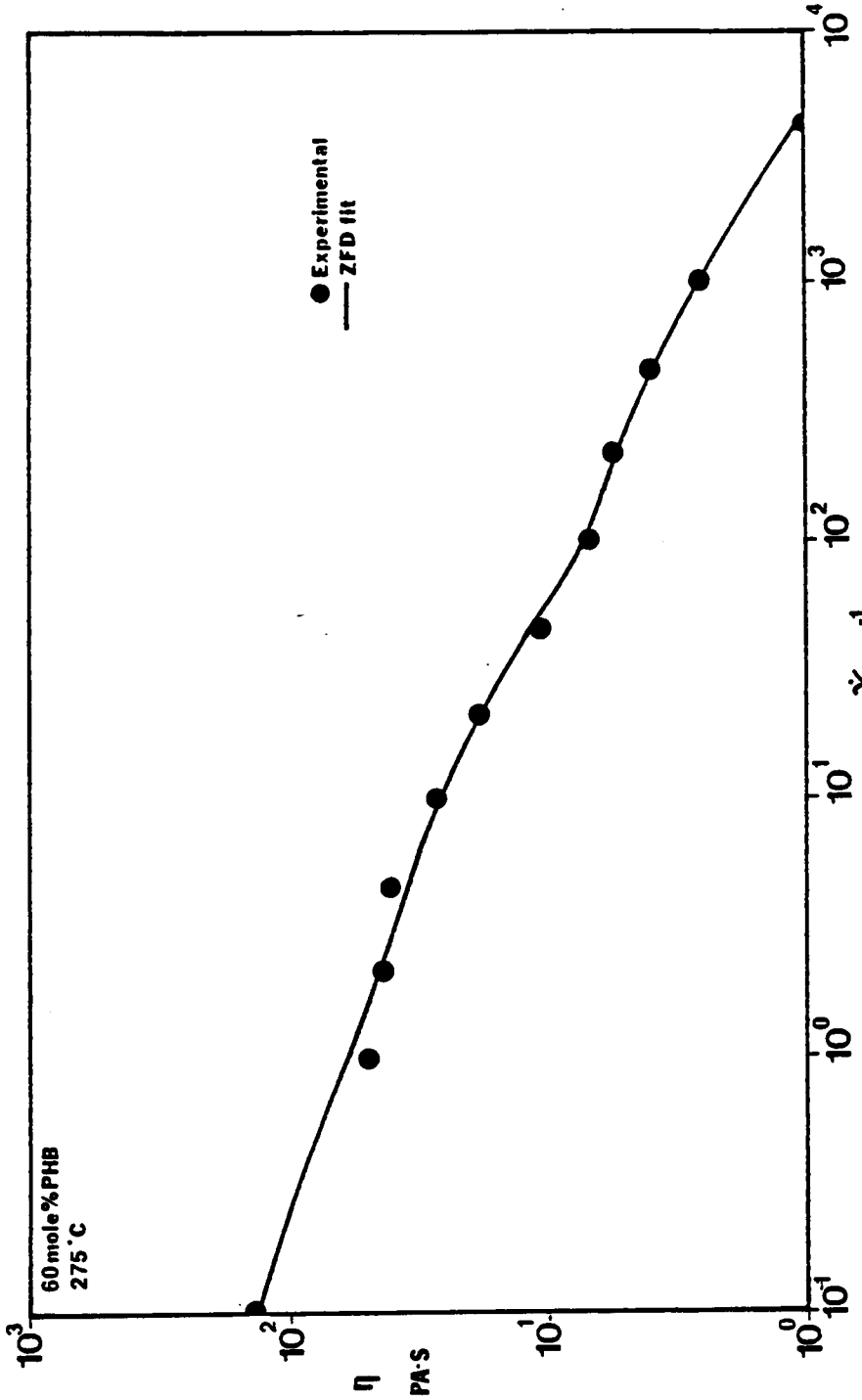

Figure 5.5 Fit of ZFD model: η vs $\dot{\gamma}$
60 mole% PHB/PET copolymer, 275°C.

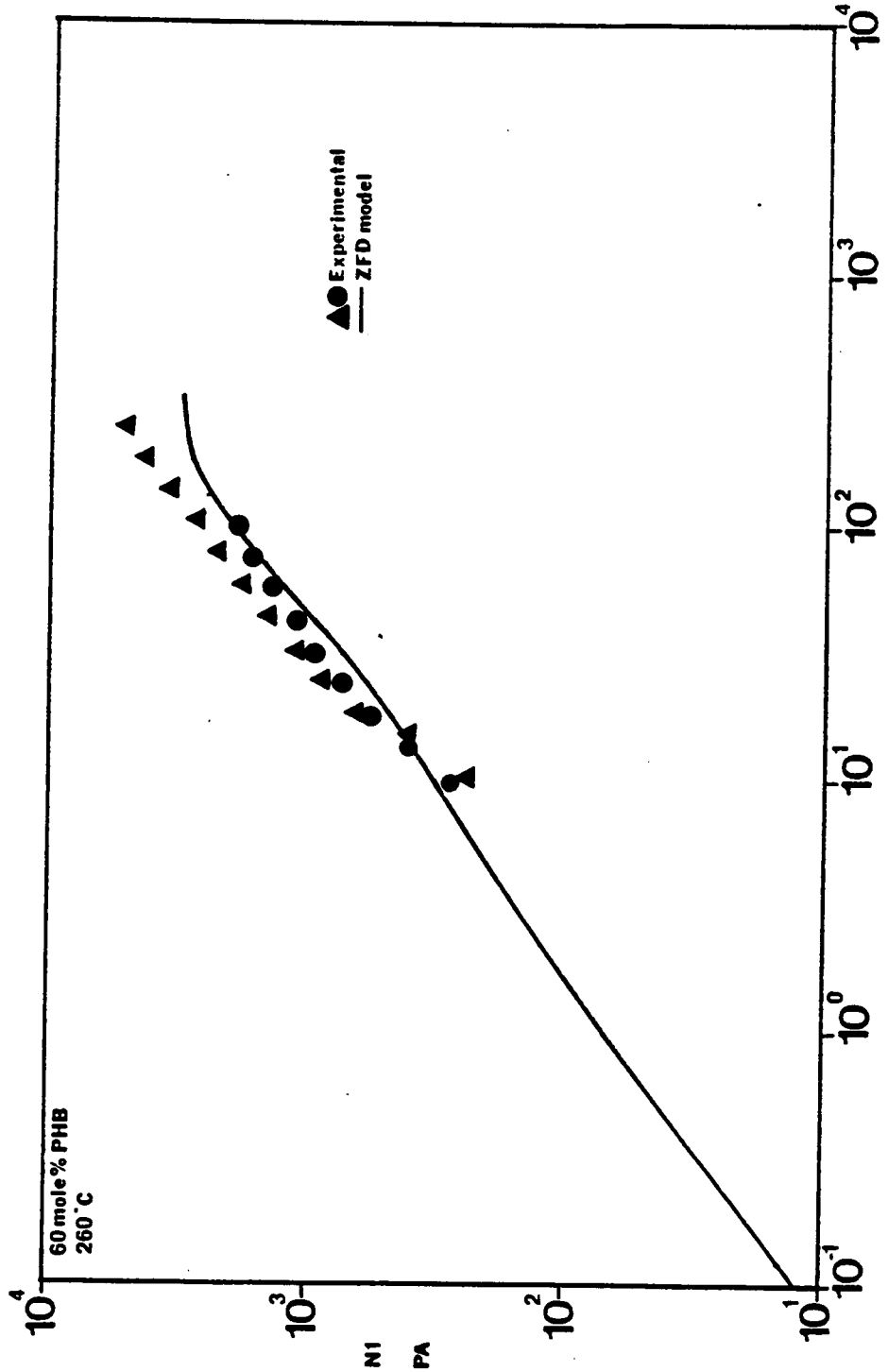

Figure 5.6 Fit of ZFD model: N1 vs $\dot{\gamma}$
60 mole% PHB/PET copolymer, 260°C.

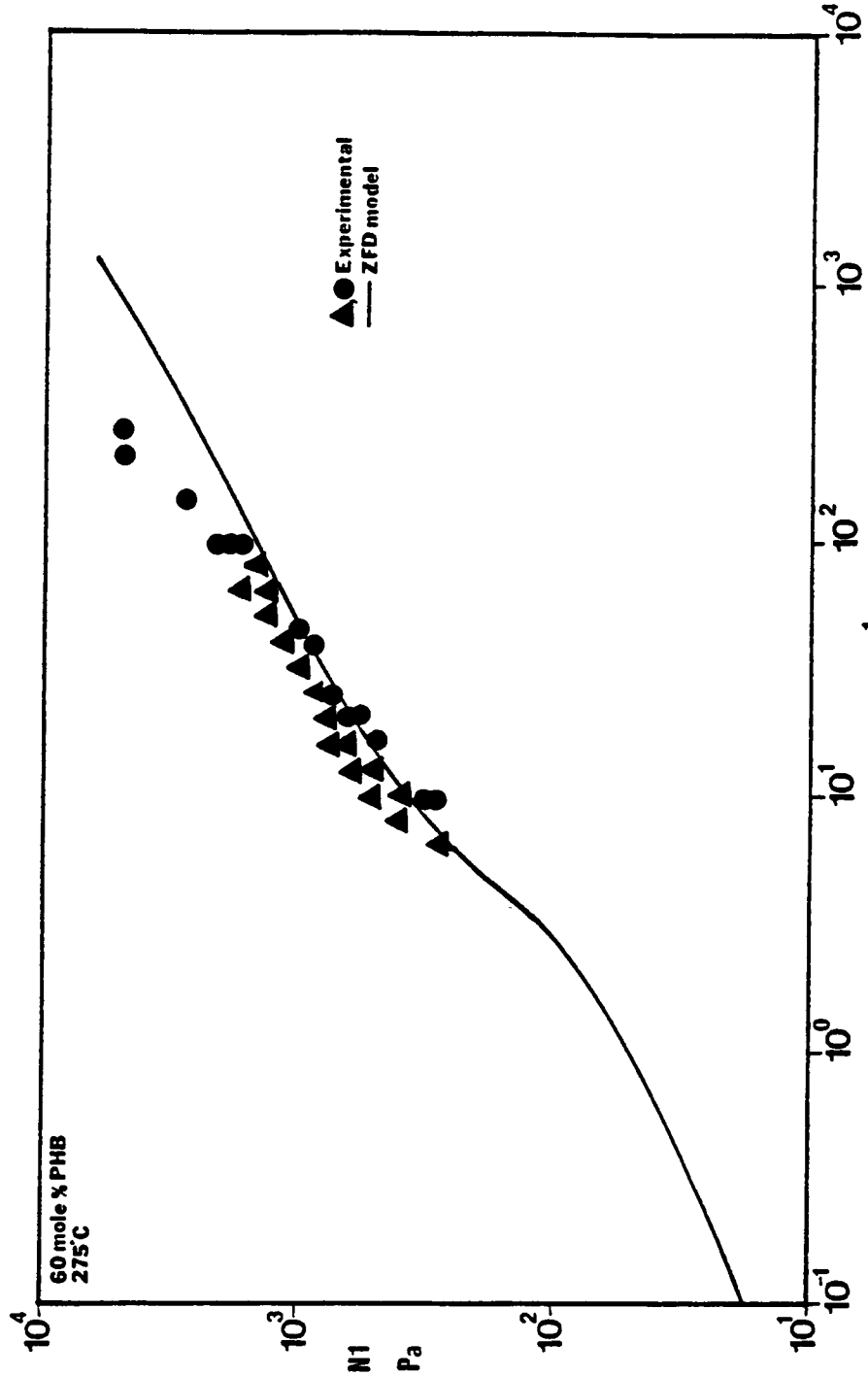

Figure 5.7 Fit of ZFD model: N1 vs $\dot{\gamma}$
60 mole% PHB/PET copolymer, 275°C.

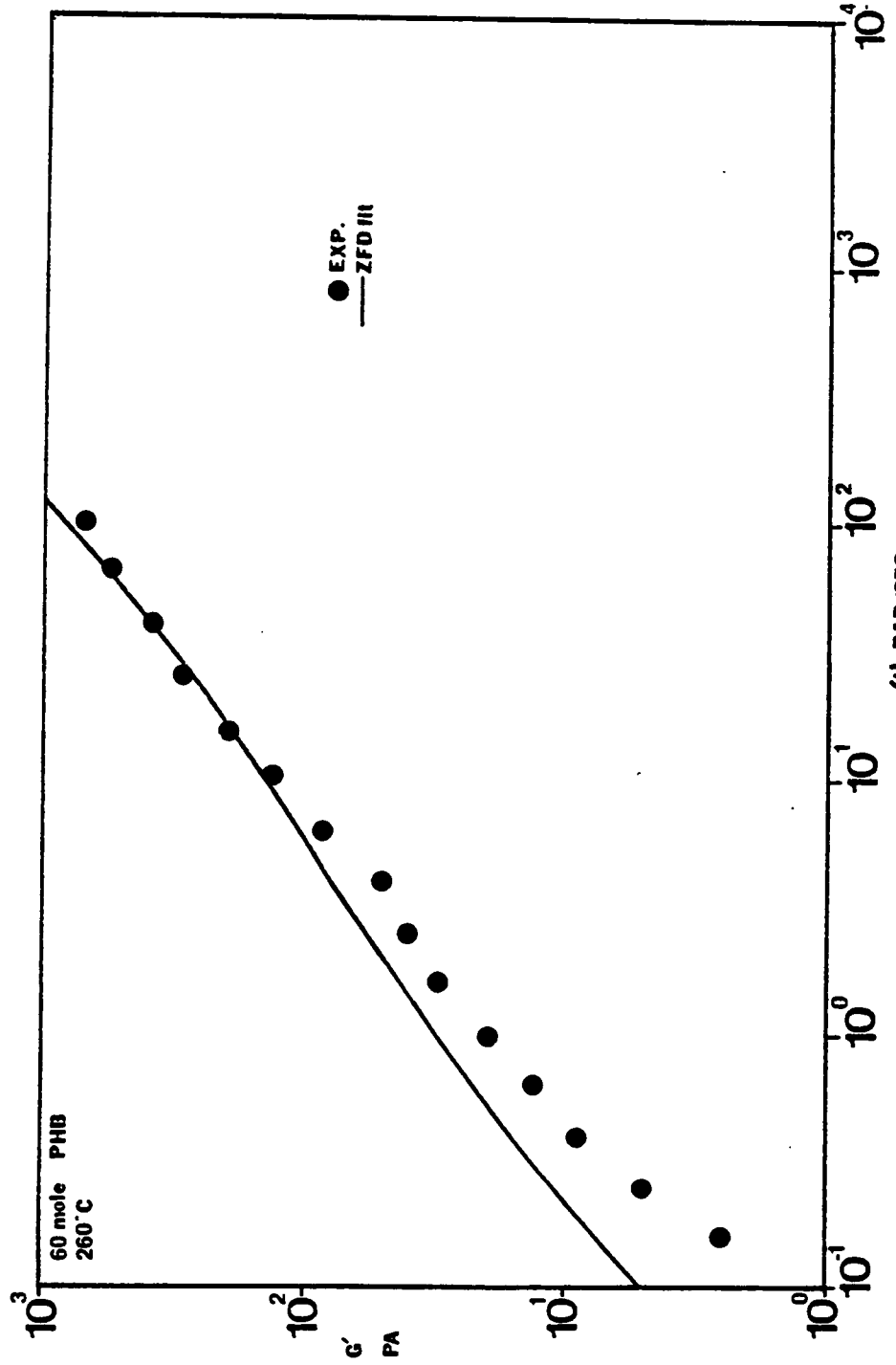

Figure 5.8 Fit of ZFD model: G' vs ω
60 mole% PHB/PET copolymer, 260°C.

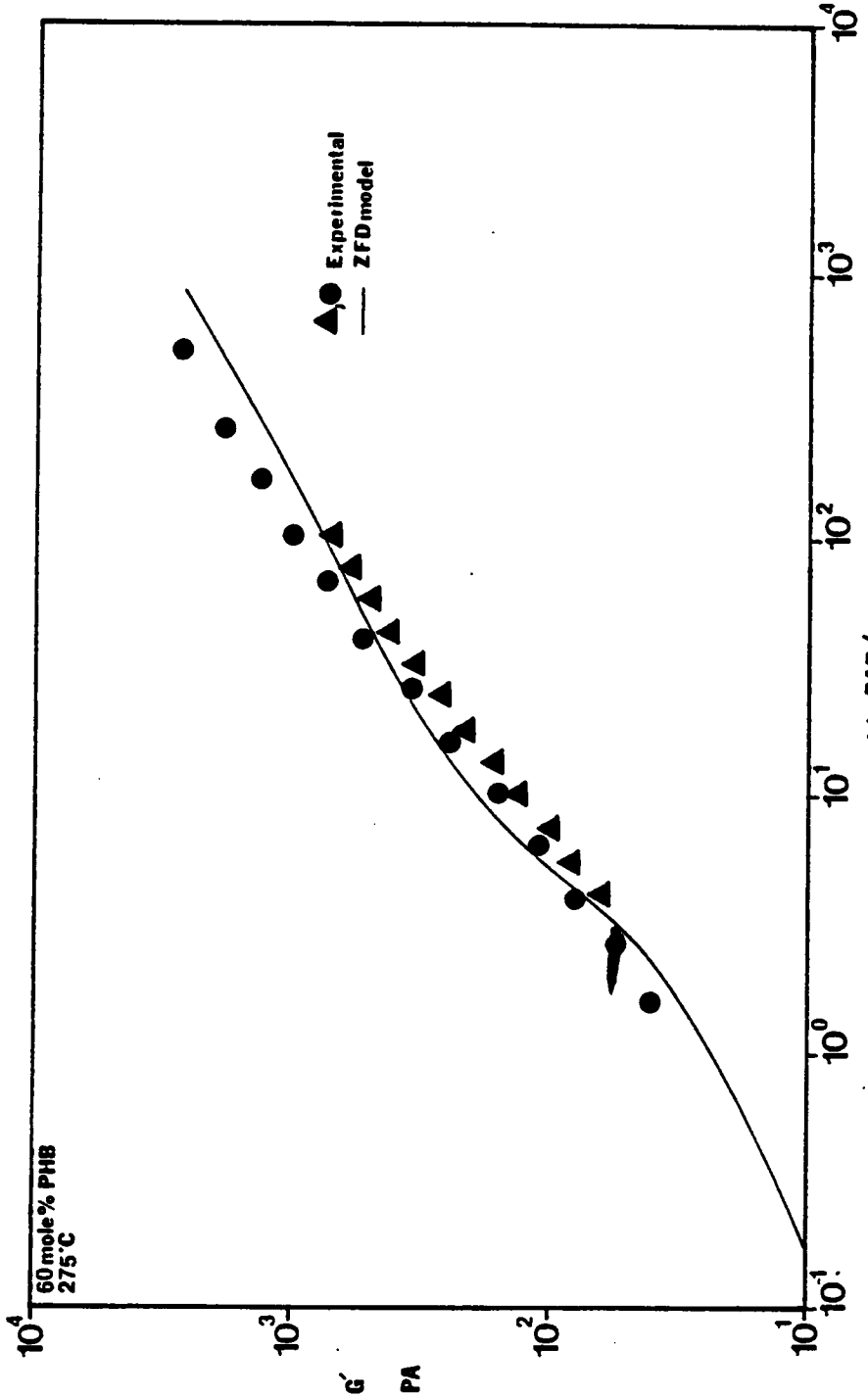

Figure 5.9 Fit of ZFD model: G' vs ω
60 mole% PHB/PET copolymer, 275°C.

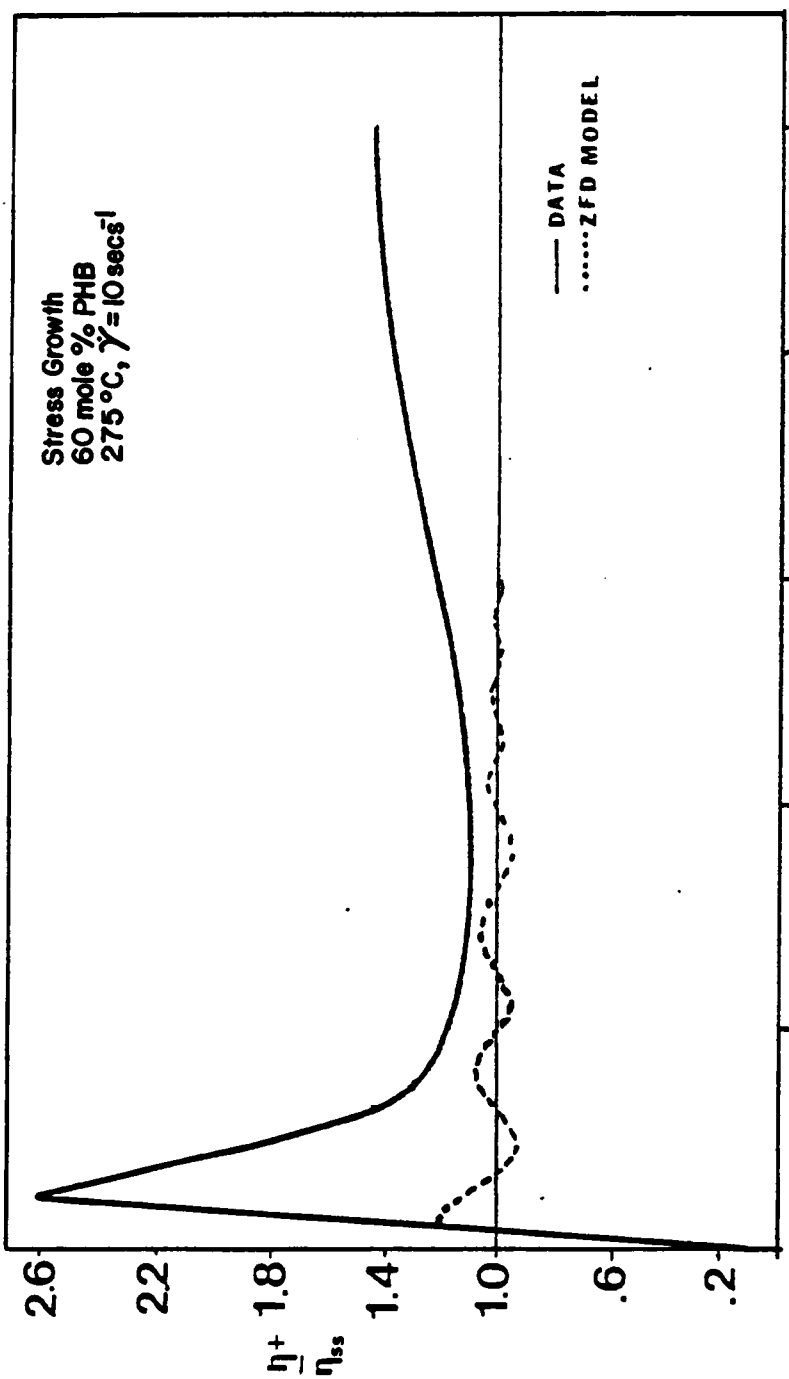

Figure 5.10 Fit of ZFD model: Stress Growth
60 mole% PHB/PET copolymer, 275°C.

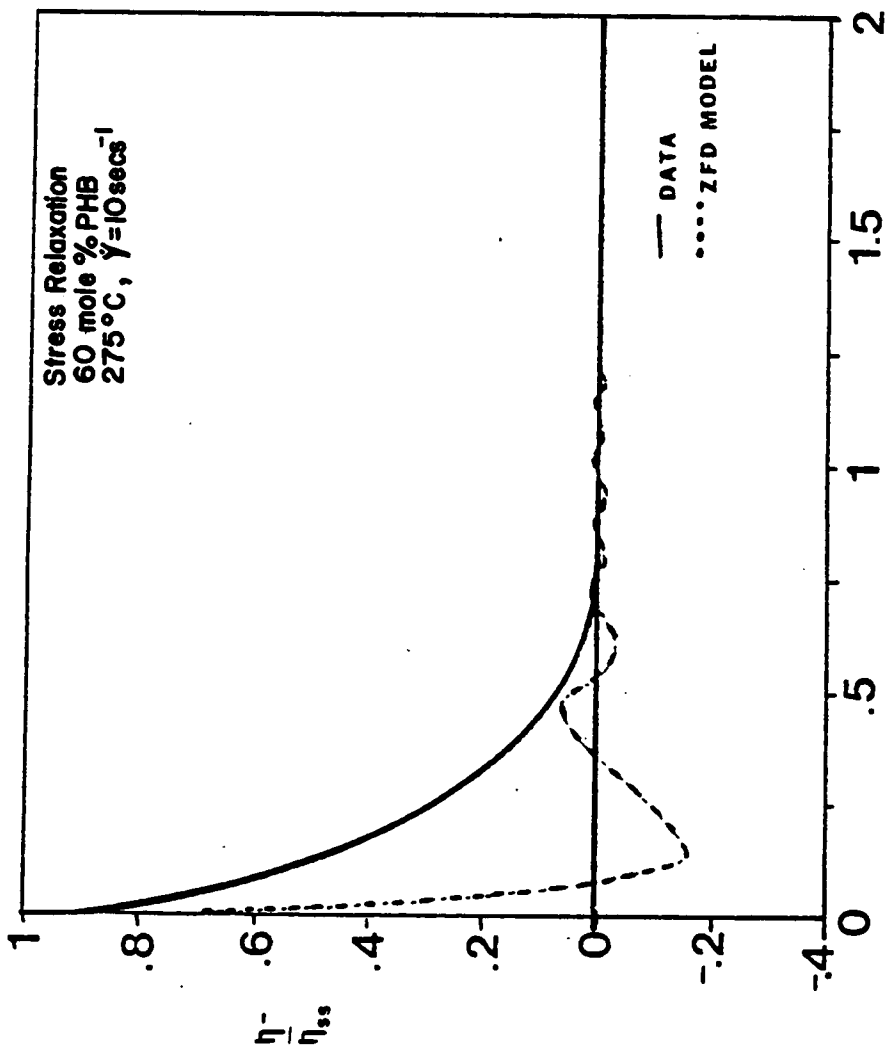

Figure 5.11 Fit of ZFD model: Stress Relaxation
60 mole% PHB/PET copolymer, 275°C.

WAXS studies show that this may not occur. Furthermore, the correlation between dynamic and steady shear data supports the conclusion that not much molecular orientation is achieved in shear flow. The success of the ZFD model in predicting the the steady shear and dynamic mechanical properties of the 60 mole% PHB/PET system suggests that the behavior of liquid crystalline fluids can be predicted to some extent with out taking molecular orientation effects into account. This is a significant result as it indicates that complicated theories such as Ericksen may not be needed to predict the flow behavior of liquid crystalline fluids.

It was mentioned that one possible mechanism causing the stress overshoot behavior exhibited by the PHB/PET and Kevlar systems could be due to the break up of the domain structure. In the next section, the WAXS and SEM results are analyzed in more detail. A structure change based on the break up of liquid crystalline domains is proposed to explain the behavior exhibited by the PHB/PET and Kevlar systems.

5.3 ANALYSIS OF WAXS AND SEM STUDIES

WAXS and SEM studies were performed to determine the effect of shear and extension on the development of molecular orientation and structure during flow. Such studies were designed to test the predictions of Ericksen's theory and to determine why injection molded plaques of the PHB/PET system exhibit anisotropic physical properties and a skin/core morphology. With respect to the predictions of Ericksen's theory, it has

been shown that the theory predicts a high degree of molecular orientation development in extensional flow. This prediction seems to be correct, but again, the method of preparation of the extended samples may have had an effect on the degree of molecular orientation seen in the extended samples. In shear flow the predictions of the theory are not consistent with WAXS results. Several questions still remain concerning the affect of different flow fields on the development of molecular orientation and structure. It is perhaps appropriate that these questions be restated:

1. Do liquid crystalline fluids actually orient in shear flow?
2. How long does molecular orientation remain in the melt state?
3. Does extensional flow orient liquid crystalline fluids more effectively than shear flow?
4. Are there any specific morphological textures associated with molecular orientation?

The WAXS and SEM studies which have been conducted provide answers to these questions and indicate the type of structural change which may occur during shear flow. These results are now analyzed.

5.3.1 THE AFFECT OF FLOW ON STRUCTURE DEVELOPMENT

According to the theory of Ericksen, in shear flow fluid particles will align at an angle to the flow direction determined by a fluid constant, λ. Actual determination of the degree of molecular orientation in sheared samples shows that very little orientation of the fluid particles occurs. This was shown to be true in Chapter Four. WAXS patterns exhib-

ited by sheared disks indicated very little presence of molecular orientation based on the azimuthal dependence of scattering intensity. On average, however, it was seen that the particles aligned at a zero angle with respect to the flow direction. Increasing the shear rate used in preparation of the samples sharpened the distribution of molecular orientation about the flow direction, but did not change the average angle of molecular orientation. Further evidence that the distribution of orientation may be dependent on the stress level experienced by the fluid is found by examining the cooled while sheared samples. In this case it was determined that a much higher degree of molecular orientation could be achieved as compared to samples prepared with no cooling during shear. Cooling the sample during shear causes an effective increase in viscosity. This increase in viscosity causes an increase in the magnitude of the stress field experienced by the fluid. The WAXS patterns exhibited by the cooled while sheared fluids indicated a high degree of molecular orientation with respect to the flow direction axis. Again, the average angle of molecular orientation did not change, just the distribution of orientation about the flow direction axis.

This last result indicates another possible flaw in Ericksen's theory. If the fluid particles align at an average angle of zero with respect to the flow direction, then a value of $\lambda=1$ should be used in the linear director equations. The theory has no provisions, however, for predicting the distribution of molecular orientation about the flow direction axis. The non-linear director equations might be used, but

these equations would only predict a shear rate dependence of the average angle of orientation with respect to the flow direction. The WAXS studies indicate that λ should be 1 and independent of shear rate, but that the distribution of orientation changes with the stress level experienced by the fluid.

With respect to the development of texture in sheared samples, it was seen that increasing the shear rate did not produce any change in the morphological texture exhibited. In all cases, an unoriented sponge-like texture was exhibited. Cooling the sample during shear, however, produced a fibrous texture oriented along the flow direction similar to the texture exhibted in extended samples. This result would tend to indicate that there may exist a correlation between molecular orientation and a fibrous texture. In an oriented sample, a fibrous texture exists as in the extended and sheared while cooled samples. In an unoriented sample, a sponge-like texture is exhibited, as in the sheared disks.

There are two possible explanations for the results just discussed. It may be that a minimum stress level exists for the development of molecular orientation and a fibrous texture. Such a minimum stress level could be related to the force necessary to align the fluid particles. Cooling the sample during shear increases the stress level experienced by the fluid and produces a high degree of molecular orientation and fibrous texture. Another possible explanation of the previous results involves

the relaxation of orientation in the melt state. It is conceivable that a high degree of molecular orientation is produced in shear flow, but this orientation relaxes quickly at the melt temperature. By cooling the sample during shear, the structure is "frozen" in. The annealing experiments support the later explanation. It was shown that annealing of highly structured samples could destroy the molecular orientation and fibrous texture exhibited within 30 seconds at the melt temperature. This result is suprising as liquid crystalline materials are thought to be composed of rigid molecules. The results of the annealing experiments indicate that these molecules may not be as rigid as previously thought.

In summary, it is seen that no obvious answer exists to the question of whether or not liquid crystalline fluids orient in shear flow. It is possible that such orientation does develop, but it is lost quickly in the melt state. It is also possible that high enough shear rates were not used in this study, implying the existence of a minimum stress level for the development of molecular orientation. In extensional flow, a high degree of molecular orientation develops and a fibrous texture is exhibited. In shear flow a low degree of molecular orientation is seen, and an unoriented sponge-like texture is exhibited. It appears that extensional flow is more effective than shear in structuring liquid crystalline fluids. It must be stated, however, that due to the method of preparation of the extended samples, some cooling during extension may have taken place. The fact that cooled while sheared samples exhibited the same structure as extended samples raises some question as to the

differences between the effect of shear and extensional flow on structure development.

It is seen that a correlation may exist between the presence of a fibrous texture and a high degree of molecular orientation. Such a correlation would tend to support the relationship between the skin/core morphology exhibited by injection molded plaques of the PHB/PET copolymer system, and the fountain flow effect. The skin layer would be due to the extensional flow at the advancing front, and the core region would be due to the shear flow in the core of the mold. Shear flow may be producing a high degree of molecular orientation within the core, but this orientation will be lost quickly due to longer cooling times in the core.

5.4 A POSSIBLE MECHANISM OF STRUCTURE REARRANGEMENT

Throughout the discussion it has been stated that some structural change other than the development of molecular orientation is taking place during shear flow. The rheological measurements, WAXS, and SEM studies indicate the type of structural change which may be taking place. A proposed mechanism to explain all of the rheological data and WAXS measurements is now discussed.

One of the important features of liquid crystalline materials is their ability to exist in well ordered domains in the fluid state. Onogi and Asada (55) have termed this structure a "polydomain structure."

These authors have proposed that all liquid crystalline materials should exhibit a three region viscosity curve based on destructuion of the polydomain structure. This has already been discussed to some extent in the Literature Review in Chapter Two. Experimental evidence for the destruction of the polydomain structure exists, and has already been mentioned. Investigators working with the Kevlar system have shown, through the use of rheo-optical methods, that in shear flow the polymain structure can be broken up into smaller domains which rotate during flow (Horio). In extensional flow, however, the polydomain structure remains intact.

A schematic representation of what is meant by the destruction of the polydomain structure is given in Figure 5.12. At rest, a structure exists which is made up of a number of large liquid crystalline domains. The material surrounding the domains is made up of unoriented liquid crystalline molecules. Upon deformation of the polydomain structure, several events may occur. If the deformation applied to the fluid is that of uniaxial extension, the polydomain structure may remain intact and deform elastically. If the deformation is one of shear flow, the domain structure may break up into smaller domains. Once the polydomain structure has been broken into smaller domains, other rearrangements of structure are possible. The smaller domains may coalesce, rotate, translate, or deform elastically. Depending on the size and action taken by the domains, differences in structure and molecular orientation will result. Such a destruction of the polydomain structure could also depend

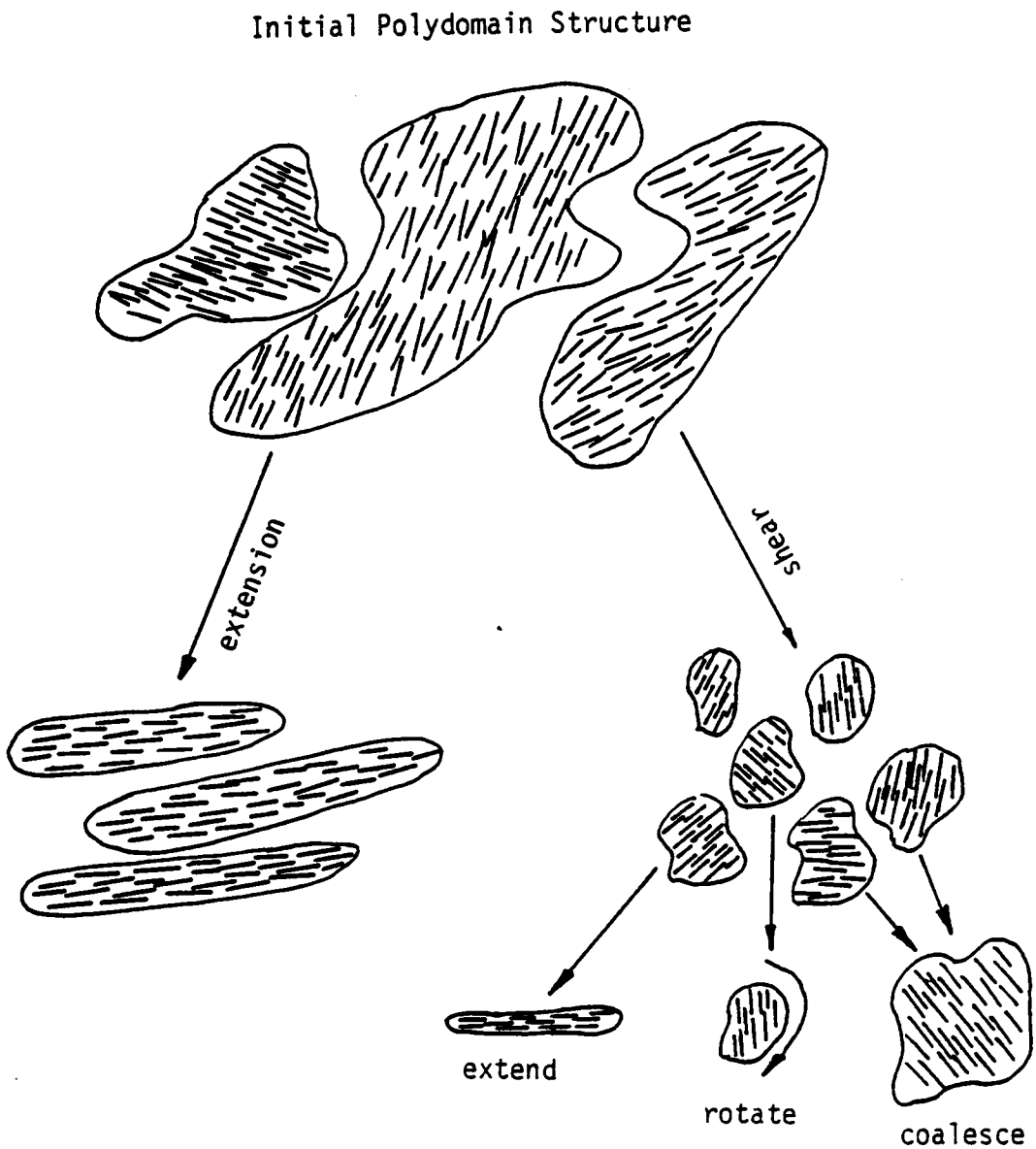

Figure 5.12 Schematic representation of the destruction of the polydomain structure.

on the application of some minimum stress level, and would be an irreversable change. At this point the mechanism described above will be used to explain the behavior of the PHB/PET and Kevlar systems.

5.4.1 VALIDITY OF THE POLYDOMAIN MECHANISM

In order to prove the validity of the mechanism of structure rearrengement discussed above, it will have to be shown that such an explanation is consistent with all of the experiment evidence. An examination of the rheological measurements will be conducted first, followed by an analysis of the WAXS and SEM data.

The stress overshoot peak exhibited upon inception of shear is consistent with the idea of a break up of the polydomain structure. Some minimum stress level would exist for such a phenomenon. The minimum stress level required to disrupt the polydomain structure would exhibit itself as a stress overshoot peak upon inception of shear. The destruction of the domain structure would be shear history sensitive and could be an irreversible change. All of the other tranient tests discussed, such as reversal of shear direction or interrupted stress growth, are in agreement with such an explanation. The stress relaxation behavior exhibited by the PHB/PET and Kevlar systems is also in agreement. If small isolated domains existed within the fluid, there would be no continuous structure to support any significant stresses upon cessation of shear. The stresses would, therefore, relax very quickly. The polydo-

main structure also allows the fluid to exhibit considerable elasticity due to the elasticity of the domains themselves.

The results of the jump strain measurements reinforce the validity of the polydomain structure mechanism. The jump strain measurements clearly demonstrate the destruction of some structure within the fluid with the application of strain. This is seen in the non-linearity of the relaxation modulus with respect to applied strain. The application of strain was also shown to affect the magnitude of the stress overshoot peak exhibited upon inception of shear.

The WAXS and SEM experiments provide the most convincing evidence for the validity of the structural change proposed. In shear flow, the domain structure would be disrupted. If the smaller domains rotated during flow, as seen in the case of the Kevlar system, then a low degree of molecular orientation would be seen. Increasing the shear rate, or cooling the sample during shear would increase the stress level experienced by the fluid. In such a case, the smaller domains may elongate rather than rotate thus producing a fibrous texture and a high degree of molecular orientation. In extensional flow, break up of the domains would not occur. The polydomain structure would just elongate while remaining intact.

Annealing of extended samples showed that the fibrous structure could degenerate into the same unoriented sponge-like texture exhibited in

shear flow. This would indicate that the domains may possess considerable elasticity. When subjected to the melt temperature, the elongated domains which comprise the fibrous texture, may relax into the sponge-like texture exhibited in shear flow. As a result of the change in shape of the domains, a decrease in the degree of molecular orientation occurs.

5.5 SUMMARY

An analysis of the predictions of the anisotropic fluid theory of Ericksen shows that the theory can qualitatively predict transient stress growth behavior. Such behavior is predicted solely on the basis of the development of molecular orientation during flow. WAXS studies, however, indicate that a high degree of molecular orientation does not develop in shear flow, and such structure does not remain in the melt state for long periods of time as predicted by the theory. A proposed mechanism based on the destruction of a polydomain structure within the melt is consistent with the rheological measurements and WAXS and SEM data.

The success of the ZFD model in correlating the steady shear properties 60 mole% PHB/PET system indicates that molecular orientation effects may not be as great a concern as previously imagined. However, the failure of the ZFD model to predict the transient behavior of the 60 mole% PHB system indicates other possibilities. The disruption of the

polydomian structure is a tranient phenomenon. Hand's theory may be a more suitable choice for modeling liquid crystalline fluids. This theory can describe anisotropic fluid behavior in terms of spherical particles which can deform as they flow. It appears that such a description is more valid for predicting the behavior of liquid crystalline fluids than the model of Ericksen.

CHAPTER SIX: CONCLUSIONS AND RECOMMENDATIONS

An investigation of the usefulness of Ericksen's anisotropic fluid theory has been conducted. The rheological behavior of several liquid crystalline materials has been investigated. The predictions of Ericksen's theory are in qualitative agreement with the experimentally measured behavior. However, WAXS and SEM analysis of specially prepared samples of the 60 mole% PHB/PET copolymer system reveals that the predictions of Ericksen's theory are not totally correct. With respect to the results and discussion presented in Chapters Four and Five, the following conclusions and recommendations are made.

6.1 ERICKSEN'S THEORY

1. Ericksen's theory has been shown to predict stress overshoot behavior upon inception of shear based on reorientation of the director. WAXS and SEM analysis reveals, however, that a high degree of molecular orientation is not developing in shear flow. In addition, any orientation produced during flow may be quickly lost. It appears that a disruption of texture is occuring which may be related to the break up of a polydomain structure.

2. Ericksen's theory predicts different stress overshoot behavior depending on the initial condtions and λ value specified. This is due to the fact that different choices of λ and initial conditions affect the

path taken by the director in order to achieve steady state. The value of λ directly determines the steady state position of the director.

3. Ericksen's linear director equations predict that fluids may orient in extensional flow, but not in shear flow. WAXS studies of specially prepared samples of the 60 mole% PHB/PET copolymer indicate that the molecules always orient at an average angle of zero with respect to the flow direction axis. This would indicate a λ value of 1 for this fluid. The WAXS studies also reveal, however, that the distribution of orientation about the flow direction axis is a function of the stress level experienced by the fluid. Ericksen's theory cannot account for such behavior. The non-linear director equations could predict a shear rate dependence in the angle of orientation, but not a stress level dependence in the distribution of orientation.

6.2 RHEOLOGICAL BEHAVIOR

1. Upon inception of shear, the liquid crystalline fluids tested in this study exhibit a stress overshoot peak. The magnitude of the shear stress overshoot peak is shear history dependent and can be completely removed by preshearing of the fluid. The stress overshoot peak appears to be related to the destruction of a polydomain structure within the fluid.

2. In interrupted stress growth tests it was found that once the stress overshoot peak had been destroyed, it would remain absent for at least

three minutes at the melt temperature. Such behavior indicates that the structural rearrangement occuring during start up of flow may be irreversible.

3. Upon cessation of shear flow, the liquid crystalline fluids tested exhibited very quick relaxation of the shear stresses, and no yield stress values. If a destruction of the polydomain structure within the fluid is occuring, then the stresses would relax quickly due to the existence of isolated domains which would not support stresses upon cessation of flow.

4. The non-linearity of G(t) determined with jump strain measurements indicates that a rearrangement of structure within the fluid takes place with the application of finite amounts of strain. Such experimental evidence supports the claim that a disruption of the polydomain structure may be occuring.

5. For the 60 mole% PHB/PET copolymer system, preshearing or a step in strain causes a decrease in the magnitude of the stress overshoot peak exhibited upon inception of shear flow. This indicates that the same disruption of texture is taking place due to both types of deformation.

6. The similarity in magnitude between the steady shear and dynamic mechanical properties ($\eta \simeq \eta^*$, $N1 \simeq 2G'$) of the 60 mole% PHB/PET copolymer system indicates that not much molecular orientation is developing in

shear flow. WAXS data support this conclusion. The ability of the ZFD model to correlate the steady shear and dynamic properties indicates that molecular orientation effects may not be as important as first thought for liquid crystalline fluids.

7. The failure of the ZFD model to accurately predict the transient behavior of the 60 mole% PHB/PET copolymer system may be because the disruption of texture is a transient phenomenon. Hand's theory may be more appropriate as it addresses the problem of elastic, spherical domains.

6.3 WAXS AND SEM STUDIES

1. In the case of the 60 mole% PHB/PET copolymer system, extensional flow produces a fibrous texture and high degree of molecular orientation. In shear flow, an unoriented sponge-like texture, and a low degree of molecular orientation developes. These results would tend to indicate a correlation between molecular orientation and a fibrous texture.

2. It appears that the fountain flow effect is responsible for the development of the skin/core morphologies exhibited by injection molded plaques of the 60 mole% PHB/PET copolymer system. The extensional flow at the front produces the highly ordered skin layer, while the shear flow in the core of the mold produces the unordered core layer. In addition, any orientation produced in shear flow is lost quickly as shown by the annealing experiments.

3. Any structure formed in the melt can be lost quickly at the melt temperature. It appears as if the liquid crystalline domains possess elasticity and relax quickly at the melt temperature. Any orientation produced in shear flow, therefore, may be lost due to such relaxation.

4. Cooling the sample during shear yields a high degree of molecular orientation and a fibrous texture. Results of annealing experiments indicate that this may be due to the freezing in of structure before relaxation occurs. It may be possible, however, that a minimum stress level exists for the production of a high degree of molecular orientation. Cooling the sample during shear increases the stress level experienced by the fluid.

5. The degree of molecular orientation and fibrous texture exhibited by the extended samples may not be due solely to the effects of extensional flow. Due to the method of sample preparation, cooling of the sample during extension may have taken place. The results seen for the cooled while sheared samples raise doubts as to the real effects of extensional flow on molecular orientation development.

6.4 RECOMMENDATIONS

1. It is seen that Ericksen's theory is not entirely valid for the description of liquid crystalline fluids. It is possible, however, that

Hand's theory could more accurately predict the behavior of such systems. To date, no detailed investigation of the predictions of Hand's theory for stress growth and extensional behavior has been conducted. It is recommended that such an investigation be performed to see if the predictions Hand's theory are in agreement with experimentally determined behavior.

2. In this study, the stress growth behavior of the PHB/PET and PPT/H_2SO_4 systems was investigated. The transient rheology of other liquid crystalline systems has not been investigated as throroughly. In order to determine the generality of the results found in this study, it is recommended that the transient rheological behavior of other liquid crystalline systems be investigated.

3. The results of jump strain measurements indicates a non-linearity of G(t) for the 60 mole% PHB/PET and Kevlar systems. It is recommended that an attempt be made to determine the forms of G(t) and the damping function, $H(\gamma)$, to be used in the generalized linear viscoelastic fluid model. It will then be possible to determine if the predictions of such a model are valid for transient behavior.

4. In this study, only the degree of molecular orientation, and textures exhibted by the PHB/PET systems was investigated. Other polymeric liquid crystalline systems should be investigated to determine the generality of the results of this investigation.

5. Due to the effects of cooling during shearing on the production of molecular orientation and texture, the results seen for extended ribbons is questionable. It is recommended that a method be found to produce extended ribbons of the PHB/PET copolymer under isothermal conditions. This is not an easy task as no oils exist with the correct density and temperature stability requirements. Therefore, extending the sample in an oil bath is not a practical operation.

A.0 REFERENCES

1. J. F. Wendorff, H. Finklemann, and H. Ringsdorf, J. of Polym. Sci., Polym. Symp., 63, 245 (1968).

2. O. Lehmann, Z. Phys. Chem., 5, 427 (1890).

3. R. S. Porter, and J. F. Johnson, "Rheology," Erich Ed., Vol. 4, Chapter 5, Academic Press, New York (1967).

4. M. Miesowicz, Nature, 158, 27 (1946).

5. J. A. Castellano, "Liquid crystals: The Fourth State of Matter," F. D. Saeva Ed., Marcel Dekker, Inc., New York (1979).

6. G. Oster, J. Gen. Physiology, 33, 445 (1950).

7. S. L. Kwolek, U. S. Patent No. 3,671,542 (1972).

8. A. Sloulios, G. Finoz, and J. Farrod, C: R. Acad. Sci., 251, 739 (1960).

9. Y. Bouligand, P. E. Cladis, L. Liebert, and L. Strzelecki, Mol. Cryst. Liq. Cryst., 25, 233 (1974).

10. R. K. Mishra, Mol. Cryst. Liq. Cryst., 29, 201 (1975).

11. J. R. Schaefgen, V. S. Foldi, F. M. Logullo, V. H. Good, L. W. Gulrich, and F. L. Killian, Polym. Prepr., Am. Chem. Soc., Div. Polym.Sci., 17, 69 (1976).

12. J. Preston, "Liquid Crystalline Order in Polymers," A. Blumstein Ed., Academic Press, New York (1978).

13. W. J. Jackson Jr., and H. F. Kuhfuss, J. Polym. Sci., Polym. Chem. Ed., 14, 2043 (1976).

14. Baird Wilkes Joseph, Submitted to Polymer (1982).

15. W. Rose, Nature, 191, 242 (1961)

16. Z. Tadmor, J. Appl. Polym. Sci., 18, 1753 (1974).

17. J. L. White, SPE Tech Papers, Woburn Mass., Sept 27-28 (1977)

18. Y. Ide, and Z. Ophir, Polym. Eng. and Sci., 23(5), 261 (1983).

19. C. W. Oseen, Trans. Farrady Soc., 29, 883 (1933).

20. F. C. Frank, Discuss. Farrady Soc., 25, 19 (1958).

21. J. L. Ericksen, Kolloid Z., 173, 117 (1960).

22. F. M. Leslie, Q. J. Mech. Appl. Math., 19, 265 (1966).

23. K. F. Wissbrun, Br. Polym. J., 12(4), 163 (1980).

24. G. L. Hand, J. Fluid Mech., 13, 33, (1962).

25. B. R. Duffy, J. Non-Newtonian Fluid Mech., 4, 177 (1978).

26. D. G. Baird, "Liquid Crystalline Order in Polymers,", A. Blumstein Ed., Chapter 7, Academic Press, New York (1978).

27. K. F. Wissbrun, J. of Rheology, 25(6), 619 (1981).

28. B. C. Benicewicz, J. F. Johnson, and M. T. Shaw, Mol. Cryst. Liq. Cryst.,(1980).

29. J. Hermans Jr., J. Polym. Sci., Part C2., 129, (1963).

30. W. G. Miller, C. C. Wu, E. L. Wee, G. L. Santee, J. H. Rai, and, K. G. Goebel, Pure Appl. Chem., 38, 25 (1974).

31. G. Kiss, and R. S. Porter, J. Polym. Sci., Polym. Symp., 65, 193 (1978).

32. G. Kiss, and R. S. Porter, J. Polym. Sci., Polym. Phys. Ed., 18, 361 (1980).

33. H. Aoki, J. L. White, and J. F. Fellers, J. Appl. Polym. Sci., 23, 2293 (1979).

34. E. Iizuka, Mol. Cryst. Liq. Cryst., 25, 287 (1974).

35. J. T. Yang, J. Am. Chem. Soc., 80, 1783 (1958).

36. J. T. Yang, J. Am. Chem. Soc., 81, 3902 (1959).

37. R. W. Duke, and L. L. Chapoy, Rheol. Acta, 15, 548 (1976).

38. J. F. Hutton, Rheol. Acta, 14, 979 (1975).

39. D. G. Baird, A. Gotsis, and G. G. Viola, Polym. Prepr., Am. Chem. Soc., Div. of Polym. Chem., 24(2), 292 (1983).

40. T. A. Huang, Ph.D., Univ. of Wisconsin, 1976 Dissert. Abs., 37, Ser. B, 5741 (1976).

41. A. Okagawa, R. G. Cox, and S. G. Mason, J. Colloid. Interface Sci., 45, 303 (1973).

42. P. K. Currie, Mol. Cryst. Liq. Cryst., 73, 1 (1981).

43. H. Boedtker, and P. Doty, J. Am. Chem. Soc., 78, 4267 (1956).

44. E. Fukada, and M. Date, Biorheology, 1, 101 (1963).

45. R. H. Marchessault, F. F. Moorehead, and N. M. Walters, Nature (London), 184, 632 (1959).

46. S. L. Kwolek, P. W. Morgan, J. R. Schaefgen, and L. W. Gulrich, Polym. Prepr., Am. Chem. Soc., Div. Polym. Chem., 17, 53 (1976).

47. S. L. Kwolek, P. W. Morgan, J. R. Schaefgen, and L. W. Gulrich, Macromolecules, 10(6), 1390 (1977).

48. S. P. Papkov, V. G. Kulichikhin, V. D. Kalmykova, and A. Y. Malkin, J. Polym. Sci., Polym. Chem. Ed., 12, 1953 (1953).

49. D. G. Baird, J. Appl. Poly. Sci., 22, 2701 (1978).

50. D. G. Baird, J. Rheology, 24(4), 465 (1980).

51. R. Jerman, and D. G. Baird, J. Rheology, 25(2), 275 (1981).

52. K. F. Wissbrun, and A. C. Griffin, J. Polym. Sci., Polym. Phys. Ed., 20, 1835 (1982).

53. W. J. Jackson Jr., Br. Polym. J., 12(4), 154, (1980)

54. C. P. Wong, and G. C. Berry, Polymer, 20, 229 (1979).

55. S. Onogi, and T. Asada. "RHEOLOGY", G. Astarita, G. Marucci, and L. Nicholais Eds., Vol. 3, Plenum Press, New York (1980).

56. M. W. Neufield, Phys. Z., 14, 645 (1913).

57. M. Miesowicz, Nature, 136, 261 (1935).

58. R. Porter, and J. Johnson, J. of Phys. Chem., 66, 1826, (1962).

59. H. Finkelman, D. Naegele, and H. Ringsdorf, Makromol. Chem., 180, 803 (1979).

60. G. Maret, and A. Blumstein, Mol. Cryst. Liq. Cryst., 88, 295, (1982).

61. G. Maret, F. Volino, R. B. Blumstein, A. F. Martins, and A. Blumstein, Proc. 27th Int. Symp. Macromol., Strausburg, Vol. II, 973 (1981).

62. L. Liebert, L, Strazelecki, D. van Luyen, and A. M. Levelut, Europ. Polymer J., 17, 71 (1981).

63. F. Volino, A. F. Martins, R. B. Blumstein, and A. Blumstein, C: R. Acad. Sci., Paris, 292, 829 (1981).

63. H. Kelker, R. Hatz, and C. Schumann," Handbook of Liquid Crystals", Verlag Chemie, Weinheim (1980).

65. P. G. DeGennes," The Physics of Liquid Crystals", Clarendon Press, Oxford (1974).

66. D. Ezernack, and E. Mclaughlin, J. Phys. E: Sci. Instrum., 14, 812 (1981).

67. J. D. Margerum, and L. J. Miller, J. Colloid Interface Sci., 58, 559 (1977).

68. H. Blades, U. S. Patent No. 3,869,430 (1974).

69. R. R. Luise, U. S. Patent No. 4,183,895 (1980).

70. G. Menges, and G. Wubken, Annual Tech. Conf., Soc. Plas. Eng., Preprints, Montreal Canada, 519 (1973).

71. C. Nguyen, MS Thesis, Virginia Polytechnic Institute and State University, (1982).

72. E. Joseph, PhD Dissertation, Virginia Polytechnic Institute and State University (1983).

73. Zachariades, Polym. Eng. and Sci., 23(15), 797 (1983).

74. D. G. Baird, E. Joseph, R. Pisipati, G. Viola, and G. L. Wilkes, Annual Tech. Con., Soc. Plas. Eng., Preprints, New Orleans, (1983).

75. M. Horio, Ann. Rep. Res. Inst. Chem. Fibers, Japan, 35, 87 (1978).

76. T. Asada, J. Soc. Rheology, Japan, 4, 102 (1976).

77. Y. Onogi, J. L. White, and J. F. Fellers, J. Non-Newt Fluid Mech., 7, 121 (1980).

78. J. A. Odell, E. D. T. Atkins, and A. Keller, J. Polym. Sci.: Polym. Letters Ed., 21, 289 (1983).

79. A. Azelius, Arsskr. Mat. Ach. Nat. p., 1 (1931).

80. J. L. Ericksen, Arch. Rat. Mech. Anal.,4, 231 (1959).

81. J. L. Ericksen, Trans. Soc. Rheol., 5, 23 (1961).

82. J. L. Ericksen, Arch. Rat. Mech. Anal., 9, 371 (1962a).

83. J. L. Ericksen, Arch. Rat. Mech. Anal., 10, 89 (1962b).

84. J. L. Ericksen, Phys. Fluids., 9, 1205, (1966a).

85. J. L. Ericksen, Arch. Rat. Mech. Anal., 23, 266 (1966b).

86. J. L. Ericksen, Trans. Soc. Rheol., 11, 5 (1967).

87. J. L. Ericksen, Trans. Soc. Rheol., 13, 1,9 (1969a).

88. J. L. Ericksen, Mol. Cryst. Liq. Cryst., 7, 153 (1969b).

89. J. L. Ericksen, "Liq. Cryst. Ordered Fluids, 181, New York-London (1970).

90. F. M. Leslie, Arch. Rat. Mech. Anal., 28, 265 (1968a).

91. F. M. Leslie, Proc. Roy. Soc., SerA, 307, 359 (1968b).

92. F. M. Leslie, Mol. Cryst. Liq. Cryst., 7, 407 (1971).

93. F. M. Leslie, Rheol. Acta, 10, 91 (1971).

94. L. Davison, Phys. Fluids, 10, 2333 (1967).

95. L. Davison, Phys. Review, 180, 232 (1969).

96. L. Davison, and D. E. Amos, Phys. Review, 183, 288 (1969)

97. P. C. Martin, D. S. Pershan, and J. Swift, Phys. Review, 25, 844 (1970).

98. E. L. Aero, and A. N. Bulygin, Izv. Akad. Nauk. SSSR. MZLG 3

99. W. Helfrich, J. Chem Phys., 50, 100 (1969a).

100. W. Helfrich, J. Chem. Phys., 51, 4092 (1969b).

101. W. Helfrich, J. Chem. Phys., 53, 2267 (1970).

102. W. Helfrich, J. Chem. Phys., 56, 3187 (1972).

103. J. D. Lee, and A. C. Eringen, J. Chem. Phys., 54, 5027 (1971a).

104. J. D. Lee, and A. C. Eringen, J. Chem. Phys., 55, 4504 (1971b).

105. J. D. Lee, and A. C. Eringen, J. Chem. Phys., 55, 4509 (1971c).

106. A. C. Eringen, and J. D. Lee, Liq. Cryst. Ordered Fluids, 2, 315 (1973).

107. F. Jahnig, and H. Schmidt, Ann. Phys. (U.S.A.), 71, 129 (1972).

108. M. Shainpoor, Rheol. Acta, 15, 99 (1976).

109. J. Wahl, and F. Fisher, Mol. Cryst. Liq. Cryst., 22, 359 (1973).

110. B. R. Duffy, J. Non-Newt. Fluid Mech, 7, 107 (1980a).

111. B. R. Duffy, J. Non-Newt. Fluid Mech, 7, 359 (1980b).

112. B. R. Duffy, J. Non-Newt. Fluid Mech, 8, 213 (1981a).

113. B. R. Duffy, J. Non-Newt. Fluid Mech, 9, 1 (1981b).

114. J. G. Oldroyd, Proc. R. Soc., London SerA, 200, 523 (1950).

115. R. S. Rivlin, J. Rat. Mech. Anal., 4, 681 (1955).

116. W. Noll, J. Rat. Mech. Anal., 4, 3 (1955).

117. M. J. Stephen, and J. P. Straley, Rev. Mod. Phys, 46, 617 (1974).

118. A. E. Green, and R. S. Rivlin, Arch. Rat. Mech. Anal., 1, 1 (1957).

119. Rhemoetrics Mechanical Spectrometer Operations Manual

120. R. B. Bird, R. C. Armstrong, and L. Hassager, Dynamics Of Polymeric Fluids, Vol. 1, John Wiley Pub., New York (1977).

121. M. E. Davis, Numerical Methods and Modeling for Chemical Engineers, John Wiley Pub., New York (1984).

122. F. E. McFairlane, V. A. Nicely, and T. G. Davis, Comtemporary Topics in Polymer Science, Vol. 2, E. M. Pearce, and J. R. Schaefgen Ed., Plenum Press (1977).

123. A. D. Gotsis, M.S. Thesis, Virginia Polytechnic Institute and State University, (1984).

124. T. Asada, H. Muramatsu, R. Watanabe, and S. Onogi, Marcromolecules, 13, 876, (1980).

125. K. Shimamura, J. L. White, and J. F. Fellers, J. Appl. Polym. Sci., 26, 2165 (1981).

B.0 DATA TABLES

B.1 STEADY SHEAR DATA

60 mole% PHB/PET Copolyester
275°C, 50 mm C/P .04 rad

Shear rate $secs^{-1}$	Viscosity Pa-S
1.00	33.00
1.49	36.50
2.46	21.10
4.26	18.10
4.50	19.38
6.05	14.10
13.34	16.76
23.70	14.54
42.20	12.39
75.00	10.57
133.40	8.56
4.5	19.38
7.91	17.28
14.10	15.02
25.00	13.68
44.50	11.51
79.10	10.09
140.60	8.03
7.03	16.90
22.30	11.37
39.50	9.09
70.30	9.52
125.00	7.60
222.30	6.20

B.2 STEADY SHEAR DATA

60 mole% PHB/PET Copolyester
275°C , 50 mm C/P .04 rad

Shear rate $secs^{-1}$	Normal Stress Difference Pa			
10.00	360	359	352	357
12.59	475	486	—	—
15.85	586	606	591	491
19.95	731	712	—	—
21.55	—	—	624	618
25.15	818	808	741	—
31.63	960	926	—	—
39.81	1060	872	884	—
46.42	—	—	1022	1024
50.12	1259	1250	—	—
63.10	1231	1552	—	964
79.44	1081	1387	—	—
100.00	—	—	2105	2179
158.50	—	—	2878	—
215.50	—	—	4605	4859
251.70	—	—	4683	—

B.3 STEADY SHEAR DATA

60 mole% PHB/PET Copolyester
275°C , 50 mm P/P 1.0 mm gap

Shear rate $secs^{-1}$	Viscosity Pa·S		
1.00	65.40	56.70	50.00
2.16	55.00	53.50	44.20
4.64	38.60	46.30	41.30
10.00	18.90	17.13	16.32
12.59	16.10	14.94	16.32
15.85	14.00	13.00	14.64
19.95	13.00	12.05	13.61
21.55	13.20	11.90	———
25.12	12.14	11.50	12.93
31.63	11.61	11.00	12.17
39.81	10.90	10.23	11.43
46.42	9.40	9.80	10.20
50.12	10.00	9.36	10.63
63.10	8.93	8.26	9.76
79.44	———	7.86	8.68
100.00	———	7.15	6.76
215.50	6.60	5.70	5.60
464.20	4.30	5.10	3.90

B.4 STEADY SHEAR DATA

60 mole% PHB/PET Copolyester
275°C , 50 mm P/P 1.0 mm gap

Shear rate $secs^{-1}$	Normal Stress Difference Pa				
10.00	295	297	273	265	505
12.59	445	438	446	—	—
15.85	639	636	641	—	—
19.95	821	805	851	—	—
21.55	—	—	—	660	750
25.12	1029	1027	1024	—	—
31.63	1296	1286	1374	—	—
39.81	1060	872	884	—	—
46.42	—	—	—	1043	1407
50.12	1836	1806	1911	—	—
63.10	1958	1924	2100	—	—
79.44	—	2184	2548	—	—
100.00	—	2558	3006	1884	1752
215.50	—	—	—	5031	5066
464.20	—	—	—	8715	9970

B.5 STEADY SHEAR DATA

60 mole% PHB/PET Copolyester
275°C , 50 mm P/P 0.7 mm gap

Shear rate secs^{-1}	Viscosity Pa·S			
0.50	20.90	—	—	—
0.70	22.50	—	—	—
0.97	16.40	—	—	—
1.34	16.40	—	—	—
1.86	13.50	—	—	—
2.60	13.30	—	—	—
3.60	11.53	—	—	—
5.00	10.97	16.12	14.90	16.17
6.95	9.34	11.61	12.70	12.81
9.65	9.30	11.14	10.90	11.19
13.41	9.78	9.70	8.94	9.60
18.64	9.53	9.04	9.05	8.87
25.90	8.19	8.50	8.61	8.32
35.99	7.85	8.24	8.30	7.94
50.00	7.18	7.43	8.02	7.50
69.48	6.89	7.05	6.06	4.05
96.54	6.55	6.72	—	—
131.41	—	6.14	—	—
186.40	—	5.47	—	—
259.00	—	4.99	—	—

B.6 STEADY SHEAR DATA

60 mole% PHB/PET Copolyester
275°C , 50 mm P/P 0.7 mm gap

Shear rate $secs^{-1}$	Normal Stress Difference Pa			
5.00	—	—	19	—
6.95	42	—	39	—
9.65	—	39	64	49
13.41	42	85	121	35
18.64	97	148	131	95
25.90	154	247	239	159
35.99	367	414	394	297
50.00	880	1038	599	541
69.48	1374	1500	——	——
96.54	2012	2070	——	——
131.41	——	2664	——	——
186.40	——	3374	——	——
259.00	——	4350	——	——

B.7 STEADY SHEAR DATA

60 mole% PHB/PET Copolyester
275°C , 50 mm P/P 0.5 mm gap

Shear rate secs^{-1}	Viscosity Pa·S		
2.00	18.19	—	—
3.56	12.58	—	—
6.33	10.81	—	—
10.00	9.36	—	—
11.25	9.05	8.88	—
12.59	8.69	—	—
15.83	8.32	—	—
20.00	8.20	7.79	7.95
25.12	7.71	—	—
28.12	7.27	—	—
31.63	7.45	—	—
35.60	7.48	7.89	7.15
39.81	7.05	—	—
50.00	6.80	6.77	—
63.25	6.68	6.80	6.36
79.44	6.06	—	—
88.92	4.20	—	—
215.50	3.90	4.90	—
464.20	3.10	—	—

B.8 STEADY SHEAR DATA

60 mole% PHB/PET Copolyester
275°C , 50 mm P/P 0.5 mm gap

Shear rate $secs^{-1}$	Normal Stress Difference Pa		
2.00	34	—	—
3.56	43	—	—
6.33	130	77	—
10.00	194	—	—
11.25	182	95	—
12.59	225	—	—
15.83	228	—	—
20.00	281	194	262
25.12	271	—	—
28.12	196	—	—
31.63	311	—	—
35.60	386	263	335
39.81	436	—	—
50.00	429	612	—
63.25	1249	1105	1063
79.44	1250	—	—
88.92	878	—	—
100.00	1915	1615	—
215.50	3079	3233	—
464.20	5993	5924	—

B.9 STEADY SHEAR DATA

60 mole% PHB/PET Copolyester
275°C , 50 mm P/P 0.3 mm gap

Shear rate $secs^{-1}$	Viscosity Pa·S		
5.00	17.75	——	——
10.00	13.62	——	——
15.00	12.90	12.73	12.32
20.00	11.41	11.90	11.64
25.00	10.85	10.78	11.00
30.00	10.02	10.09	9.92
40.00	10.06	10.58	9.87
50.00	9.83	9.87	9.32
60.00	9.28	9.15	——
70.00	9.40	9.46	9.44
80.00	7.81	7.66	8.84
100.00	8.67	9.18	——

B.10 STEADY SHEAR DATA

60 mole% PHB/PET Copolyester
275°C , 50 mm P/P 0.3 mm gap

Shear rate $secs^{-1}$	Normal Stress Difference Pa		
5.00	128	—	—
10.00	198	—	—
15.00	152	136	—
20.00	168	179	240
25.00	238	203	277
30.00	373	299	312
40.00	424	397	—
50.00	516	521	498
60.00	475	459	—
70.00	541	507	489
80.00	704	898	505
100.00	531	522	—

B.11 STEADY SHEAR DATA

60 mole% PHB/PET Copolyester
260°C , 50 mm C/P 0.04 rad

Shear rate $secs^{-1}$	Viscosity Pa·S			
1.00	160.4	—	—	—
1.59	123.0	—	—	—
2.16	106.0	116.0	—	—
2.24	89.0	—	—	—
3.98	66.0	—	—	—
4.64	70.3	77.4	—	—
6.31	50.0	—	—	—
10.00	28.2	31.3	26.3	25.3
13.34	25.6	26.8	22.3	20.0
17.78	23.8	24.9	20.5	18.8
23.72	22.5	22.8	18.9	17.8
31.62	20.8	20.7	—	17.3
42.17	17.8	18.3	14.4	16.6
56.24	8.4	16.1	14.6	14.1
74.99	15.1	13.4	12.9	12.8
100.00	11.8	9.5	12.2	11.4

B.12 STEADY SHEAR DATA

60 mole% PHB/PET Copolyester
260°C , 50 mm C/P 0.04 rad

Shear rate $secs^{-1}$	Normal Stress Difference Pa			
1.00	145	—	—	—
1.59	137	—	—	—
2.24	167	—	—	—
3.98	241	—	—	—
4.64	186	—	—	—
6.31	373	—	—	—
10.00	215	348	175	244
13.34	446	557	345	422
17.78	624	737	515	637
23.72	811	961	665	774
31.62	1010	1147	947	1087
42.17	949	1271	1290	1245
56.24	1538	1472	1290	1604
74.99	2032	1933	1526	1778
100.00	1790	1920	1943	2046

B.13 STEADY SHEAR DATA

60 mole% PHB/PET Copolyester
260°C , 50 mm P/P 1.0 mm gap

Shear rate secs^{-1}	Viscosity Pa·S		
1.00	65.6	56.7	50.0
2.16	55.0	53.5	44.2
4.64	38.6	46.0	41.0
10.00	16.7	14.8	22.6
13.34	14.0	13.2	17.1
17.78	11.9	11.8	15.2
21.55	13.2	11.9	18.7
23.72	10.8	10.7	13.8
31.62	9.9	9.9	12.8
42.17	9.2	7.6	11.7
46.42	9.4	9.8	10.2
56.24	8.7	9.1	10.9
74.99	8.1	8.6	10.0
100.00	7.5	7.1	7.7
133.40	6.9	—	8.3
177.80	6.6	6.1	6.5
215.50	6.3	5.7	5.6
237.20	4.5	6.3	—
316.20	5.8	4.9	—
464.40	4.3	5.1	3.9

B.14 STEADY SHEAR DATA

60 mole% PHB/PET Copolyester
260°C , 50 mm P/P 1.0 mm gap

Shear rate $secs^{-1}$	Normal Stress Difference Pa		
1.00	107	—	—
2.16	197	264	—
4.64	278	381	—
10.00	613	628	278
13.34	312	420	399
17.78	483	658	674
21.55	989	860	—
23.72	703	880	948
31.62	968	1167	1250
42.17	1276	1567	1499
46.42	1476	—	—
56.24	1664	1970	2009
74.99	2128	2534	2612
100.00	2692	2628	2996
133.40	3440	4144	—
177.80	4144	4415	4848
215.50	4812	—	—
237.20	4112	5576	—
316.20	5317	6022	—
464.40	9839	—	—

B.15 STRAIN SWEEP DATA

60 mole% PHB/PET Copolyester
50 mm P/P 0.3 mm gap, ω=50 HZ

	Storage and Loss Moduli (Pa)					
	250°C		260°C		275°C	
Strain Units	G'	G''	G'	G''	G'	G''
1.25	649	1594	485	1292	564	1276
2.08	623	1571	452	2667	513	1214
2.92	612	1567	442	1235	486	1193
3.75	597	1541	438	1223	491	1175
4.58	604	1522	432	1211	493	1180
5.42	616	1521	440	1204	473	1157
6.25	613	1513	444	1196	461	1143
7.08	611	1497	446	1178	465	1131
7.92	602	1475	442	1160	459	1110
8.75	588	1442	433	1132	439	1056
9.58	577	1412	419	1100	426	1016
10.42	562	1375	406	1107	408	976

B.16 STRAIN SWEEP DATA

60 mole% PHB/PET Copolyester
50 mm P/P 0.3 mm gap, ω=5 HZ

	Storage and Loss Moduli (Pa)					
	250°C		260°C		275°C	
Strain Units	G'	G''	G'	G''	G'	G''
1.25	127	306	70	223	73	216
2.08	117	301	67	214	68	205
2.92	117	299	66	213	71	206
3.75	118	299	65	210	69	205
4.58	119	298	66	209	68	204
5.42	119	296	66	206	67	202
6.25	119	293	65	206	67	200
7.08	119	290	64	204	65	198
7.92	118	288	64	203	64	196
8.75	117	288	63	200	63	194
9.58	117	283	61	197	60	190
10.42	113	278	59	195	58	187

B.17 DYNAMIC MECHANICAL PROPERTIES

60 mole% PHB/PET Copolyester
50 mm C/P 0.04 rad, Strain=5%

Frequency rad/sec	Complex Viscosity Pa·S 250°C	260°C	275°C
0.10	315.0	220.0	—
0.16	245.0	131.7	—
0.25	208.4	91.2	—
0.39	176.6	74.4	—
0.63	153.0	67.8	—
1.00	122.0	48.8	61.1
1.59	118.0	50.0	58.5
2.51	98.6	52.8	52.9
3.98	82.6	48.9	47.1
6.31	69.2	45.1	43.7
10.00	58.6	39.7	39.0
15.85	48.8	36.4	35.4
25.12	40.9	31.5	30.5
39.81	34.7	26.8	26.5
63.10	30.1	22.9	22.8
100.00	26.3	20.5	19.7

B.18 DYNAMIC MECHANICAL PROPERTIES

60 mole% PHB/PET Copolyester
50 mm C/P 0.04 rad, Strain=5%

Frequency rad/sec	Storage Modulus Pa 250°C	260°C	275°C
0.10	21.4	4.1	—
0.16	18.9	2.5	—
0.25	26.6	5.3	—
0.39	35.6	9.0	—
0.63	47.0	13.0	—
1.00	62.9	2.9	24.8
1.59	88.5	18.4	27.7
2.51	134.0	38.5	35.4
3.98	173.0	54.2	50.8
6.31	233.0	83.6	76.9
10.00	309.0	135.0	121.0
15.85	401.0	211.0	201.0
25.12	525.0	306.0	300.0
39.81	677.0	427.0	420.0
63.10	879.0	570.0	558.0
100.00	1100.0	730.0	681.0

B.19 DYNAMIC MECHANICAL PROPERTIES

60 mole% PHB/PET Copolyester
50 mm C/P 0.04 rad, Strain=5%

Frequency rad/sec	Loss Modulus Pa 250°C	260°C	275°C
0.10	23.1	21.7	—
0.16	33.9	20.7	—
0.25	45.1	22.3	—
0.39	60.7	28.2	—
0.63	84.3	40.8	—
1.00	105.0	48.7	55.9
1.59	164.0	77.2	88.5
2.51	209.0	127.0	128.0
3.98	280.0	187.0	181.0
6.31	369.0	272.0	265.0
10.00	498.0	374.0	370.0
15.85	662.0	537.0	524.0
25.12	884.0	729.0	795.0
39.81	1202.0	978.0	966.0
63.10	1682.0	1326.0	1323.0
100.00	2383.0	1914.0	1852.0

B.20 JUMP STRAIN

60 mole% PHB/PET Copolyester
250°C , 50 mm C/P 0.04 rad

Relaxation Modulus (Pa)

Time	Strain Value				
secs	0.1	0.5	1.0	5.0	10.0
0.01	1080	1270	2400	875	599
0.02	839	479	839	456	420
0.03	659	360	509	240	348
0.04	569	264	390	204	264
0.05	509	216	330	156	180
0.06	450	180	300	132	120
0.07	390	156	270	120	89
0.08	345	144	228	108	59
0.09	300	139	192	99	54
0.10	270	129	186	94	50
0.20	105	72	120	59	26
0.30	75	62	102	46	22
0.40	66	48	72	36	16
0.50	59	38	66	26	13
0.60	57	38	59	24	12
0.70	48	36	59	23	12
0.80	42	31	54	22	10
0.90	33	26	54	18	10
1.00	30	24	42	16	10

B.21 JUMP STRAIN

60 mole% PHB/PET Copolyester
260°C , 50 mm C/P 0.04 rad

Relaxation Modulus (Pa)

Time	Strain Value				
secs	0.1	0.5	1.0	5.0	10.0
0.01	1440	1650	1350	599	360
0.02	899	839	600	360	300
0.03	659	479	390	240	240
0.04	539	330	300	120	186
0.05	450	285	210	96	144
0.06	360	225	168	74	90
0.07	306	180	138	66	60
0.08	270	165	120	58	51
0.09	240	135	99	50	39
0.10	210	120	90	48	34
0.20	96	54	36	24	16
0.30	63	30	30	18	10
0.40	60	15	24	12	—
0.50	60	15	18	12	—
0.60	54	12	15	10	—
0.70	54	9	—	—	—
0.80	48	—	—	—	—
0.90	42	—	—	—	—
1.00	36	—	—	—	—

B.22 JUMP STRAIN

60 mole% PHB/PET Copolyester
275°C , 50 mm C/P 0.04 rad

Relaxation Modulus (Pa)

Time	Strain Value				
secs	0.1	0.5	1.0	5.0	10.0
0.01	2100	815	1530	1030	600
0.02	1200	408	840	767	479
0.03	899	312	540	456	348
0.04	599	252	360	300	276
0.05	599	192	300	156	199
0.06	539	156	240	120	144
0.07	479	132	210	96	66
0.08	420	120	195	84	54
0.09	390	96	165	82	48
0.10	300	84	150	70	40
0.20	240	55	105	48	28
0.30	210	48	75	47	25
0.40	132	43	75	34	22
0.50	60	24	60	22	12
0.60	60	19	45	14	10
0.70	—	14	30	12	—

B.23 STRAIN SWEEP

12 wt% PPT/H_2SO_4 Solution
60°C, 25 mm C/P 0.1 rad, ω=10 HZ

Strain Units	Storage and Loss Moduli (Pa) G'	G''
0.10	1836	2547
0.20	1869	2462
0.30	1806	2510
0.40	1769	2423
0.50	1737	2400
0.60	1685	2346
0.70	1576	2301
0.80	1515	2199
0.90	1382	2045
1.00	1310	1974
1.10	1275	1903
1.20	1221	1834
1.30	1186	1735
1.40	1112	1692

B.24 DYNAMIC MECHANICAL PROPERTIES

12wt% PPT/H_2SO_4 Solution
60°C , 25 mm C/P 0.04 rad, Strain=5%

Frequency rad/sec	Dynamic Mechanical Properties G' Pa	G'' Pa	η* Pa·S
0.10	268	426	5032
0.16	330	618	4420
0.25	539	732	3599
0.39	732	985	3082
0.63	1008	1248	2543
1.00	1253	1564	2004
1.59	1744	1919	1636
2.51	2336	2298	1304
3.98	2986	2769	1023
6.31	3736	3315	792
10.00	4604	3904	604
15.85	5774	4632	467
25.12	7065	5410	354
39.81	8532	6261	266
63.10	10400	7330	202
100.00	12300	8515	149

B.25 JUMP STRAIN

12 wt% PPT/H_2SO_4 Solution
60°C , 25 mm C/P 0.04 rad

Relaxation Modulus (Pa)

Time	Strain Value					
secs	0.1	0.5	1.0	5.0	10.0	20.0
0.01	11300	9590	7650	3360	2060	1030
0.02	11000	6900	6250	2400	1340	671
0.03	10100	5750	5100	1680	1100	611
0.04	8630	5370	4320	1100	1010	587
0.05	8150	4790	3650	863	767	551
0.06	6830	4320	3170	767	575	527
0.07	6710	3840	2880	671	408	503
0.08	5750	3640	2690	573	336	479
0.09	5630	3450	2500	527	288	384
0.10	5270	3260	2300	479	240	240
0.20	3600	2110	1440	312	134	72
0.30	2520	1630	1110	230	96	50
0.40	2160	1340	910	187	72	38
0.50	1920	1110	765	153	72	31
0.60	1560	1050	670	139	58	24
0.70	1440	921	595	120	48	—
0.80	1320	767	555	105	38	—
0.90	1200	729	480	101	—	—
1.00	1200	671	470	101	—	—
2.00	719	575	307	53	—	—
3.00	599	422	240	43	—	—
4.00	479	364	182	38	—	—
5.00	360	288	135	—	—	—
6.00	240	230	115	—	—	—
7.00	—	211	106	—	—	—
8.00	—	192	96	—	—	—

B.26 ZFD FIT

60 mole% PHB/PET copolymer, 260°C

Final Approximate Solution

i	1	2	3	4	5
η_i (Pa·S)	188.83	43.03	18.13	16.21	6.19
λ_i (secs)	0.0001	0.001	0.01	0.10	10.0

Data		Calculated Parameters		
$\dot{\gamma}$ secs	η Pa·S	η Pa·S	N1 Pa	G' Pa
0.10	140.0	140.0	13	6
1.00	60.5	60.5	71	35
10.00	29.0	29.2	322	161
17.78	23.8	23.9	483	242
23.72	22.5	21.8	588	294
31.62	20.8	20.1	730	365
42.17	17.9	18.4	936	468
56.24	16.0	16.6	1228	614
75.00	15.1	14.4	1612	806
100.00	11.8	12.0	2052	1078
133.40	8.2	9.6	2480	1240
177.80	7.5	7.7	2818	1410
237.20	6.3	6.3	3025	1513
316.30	6.2	5.4	3083	1542

B.27 ZFD FIT

60 mole% PHB/PET copolymer, 275°C

Final Approximate Solution

i	1	2	3	4	5
η (Pa·S)	173.00	0.65	6.67	2.90	1.13
λ (secs)	0.0001	0.001	0.05	0.01	0.1

Data		Calculated Parameters		
$\dot{\gamma}$ secs	η Pa·S	η Pa·S	N1 Pa	G' Pa
0.10	138.1	138.1	18	9
1.00	50.0	49.6	47	24
2.10	44.0	45.3	75	38
4.60	41.0	39.7	171	85
10.00	27.5	28.3	405	203
21.50	18.7	16.9	680	340
46.40	10.2	11.3	970	485
100.00	6.9	7.8	1500	750
215.50	5.6	5.1	2178	1090
464.40	3.9	3.7	3193	1600

C.0 LISTING OF ERICKSEN'S PROGRAM

```
C*********************************************************************
C   THIS PROGRAM USES THE IMSL ROUTINE DGEAR TO SOLVE A SERIES OF
C   COUPLED LINEAR DIFFERENTIAL EQUATIONS.  THE ADAMS PREDICTOR
C   CORRECTOR METHOD IS USED TO SATISFY THE INITIAL CONDITIONS, AND
C   FINITE DIFFERENCES ARE USED TO APPROXIMATE THE JACOBIAN MATRIX.
C   THIS PROGRAM IS BEING USED TO EVALUATE ERICKSEN,S ANISOTROPIC
C   FLUID THEORY.  THE PROGRAM CALCULATES THE TRANSIENT NORMAL AND
C   SHEAR STRESSES USING MATERIAL PARAMETERS CALCULATED FROM DATA
C   OBTAINED FOR 60 MOLE% PHB/PET COPOLYESTER.  THE VERSATEC PLOTTER
C   IS THEN USED TO PLOT OUT THE RESULTS.
C
C   THE FOLLOWING VARIABLES ARE USED FOR THE IMSL ROUTINES:
C        N       NUMBER OF DIFFERENTIAL EQUATIONS
C        FCN     USER SUPPLIED SUBROUTINE TO DEFINE DIFFERENTIAL
C                EQUATIONS
C        FCNJ    USER SUPPLIED SUBROUTINE TO DEFINE JACOBIAN MATRIX
C                (A DUMMY SUBROUTINE IS USED HERE)
C        X       INDEPENDENT VARIABLE, HERE X REPRESENTS TIME
C        H       STEP SIZE IN ADAMS METHOD
C        Y       DEPENDENT VARIABLE VECTOR OF LENGTH N, HERE Y(I)-Y(N)
C                ARE THE THREE VECTORS DESCRIBING THE DIRECTOR
C        XEND    VALUE OF X AT WHICH SOLUTION IS DESIRED
C        TOL     TOLERANCE ON CALCULATIONS
C        METH    DESIRED METHOD: METH=1 ADAMS METHOD
C                                METH=2 GEAR METHOD
C        MITER   INPUT ITERATION METHOD INDICATOR (SEE IMSL MANUAL)
C        INDEX   INPUT AND OUTPUT PARAMETER       (SEE IMSL MANUAL)
C        IWK     INTEGER WORK VECTOR              (SEE IMSL MANUAL)
C        WK      WORK VECTOR                      (SEE IMSL MANUAL)
C        IER     ERROR VECTOR ON OUTPUT           (SEE IMSL MANUAL)
C
C        A DESCRIPTION OF VERSATEC PLOTTER ROUTINES WILL BE GIVEN
C        FURTHER DOWN IN THE PROGRAM.
C*********************************************************************

      DIMENSION Y(10),YPRIME(10),PD(10,10),T12(100),TN1(100),WK(100),
     &IWK(10),TIME(100)
      EXTERNAL FCN,FCNJ
C---------------------------------------------------------------------
C----SET VALUES FOR ERICKSENS THEORY, AND DGEAR
C----WHERE:      GAMA            SHEAR RATE
C----            DLAM            LAMBDA IN ERICKSEN THEORY
C----            Y(1)-Y(3)       INITIAL CONDITIONS ON VECTORS
C----            T12(1),TN1(1)   INITIAL CONDITIONS ON STRESSES
C----            ALP1-ALP5       ERICKSEN MATERIAL PARAMETERS
```

```
      GAMA=10.
      DLAM=1.0
      N=3
      Y(1)=0.001
      Y(2)=0.001
      Y(3)=1.0
      T12(1)=0.0
      TN1(1)=0.0
      TIME(1)=0.0
      ALP1=0.0
      ALP2=48.0*GAMA**(-0.46)+116.8
      ALP3=0.0
      ALP4=72.0*GAMA**(-0.46)-116.8
      ALP5=72.0/GAMA
      TOL=0.00001
      H=0.00001
      METH=1
      MITER=2
      INDEX=1
C-----------------------------------------------------------------------
C----STEP DEFINES TIMES AT WHICH SOLUTION IS DESIRED
C----THE FOLLOWING WRITE STATEMENTS PUT COLUMN HEADINGS ON OUTPUT
C-----------------------------------------------------------------------
      STEP=0.01
      WRITE(6,5)
 5    FORMAT(1H1)
      WRITE(6,10)
 10   FORMAT(5X,'TIME',15X,'N1',15X,'N2',15X,'N3')
      WRITE(6,15)X,Y(1),Y(2),Y(3)
 15   FORMAT(1X,4(2X,F14.7))
      KOUNT=2
C-----------------------------------------------------------------------
C----KOUNT IS A COUNTER USED TO SEQUENCE THE STRESS VECTORS T12 AND TN1.
C----THE FOLLOWING NESTED LOOPS PERFORM THE CALLS TO DGEAR SUCH THAT
C----SOLUTIONS ARE CALCULATED AT XEND.  THRU USE OF STEP, XEND RANGES
C----FROM 0.01 TO 10 SECONDS LINEARLY.
C-----------------------------------------------------------------------
      DO 25 I=1,5
      DO 20 J=1,9
       XEND=FLOAT(J)*STEP
       CALL DGEAR(N,FCN,FCNJ,X,H,Y,XEND,TOL,METH,MITER,INDEX,IWK,
     * WK,IER)
       IF(IER.GT.128)GO TO 40
       TIME(KOUNT)=XEND
       T12(KOUNT)=ALP1*Y(1)*Y(2)+ALP2*GAMA*0.5
     * +ALP4*(Y(1)**2+Y(2)**2)*GAMA*0.5+ALP5*Y(1)
     * *Y(2)*GAMA**2*0.5
       TN1(KOUNT)=ALP1*(Y(2)**2-Y(1)**2)+ALP5*(Y(2)**2-Y(1)**2)
     * *GAMA**2*0.5
       WRITE(6,15)XEND,Y(1),Y(2),Y(3)
       KOUNT=KOUNT+1
```

```
 20    CONTINUE
       STEP=STEP*10.0
 25    CONTINUE
C-----------------------------------------------------------------------
C----AT THIS POINT DEGEAR IS FINISHED.  THE STRESSES T12 AND TN1 ARE
C----NOW NORMALIZED WITH RESPECT TO THEIR STEADY STATE VALUES  AND THE
C----RESULTS ARE PRINTED OUT.
C-----------------------------------------------------------------------
      WRITE(6,5)
      KOUNT=KOUNT-1
      DO 35 I=1,KOUNT
       T12(I)=T12(I)/T12(KOUNT)
       TN1(I)=TN1(I)/TN1(KOUNT)
       WRITE(6,30)TIME(I),T12(I),TN1(I)
 30    FORMAT(1X,3(2X,F14.7))
 35    CONTINUE
 49    L1=KOUNT+1
       L2=KOUNT+2
C-----------------------------------------------------------------------
C----THIS PART OF THE PROGRAM USES THE VERSATEC PLOTTER TO PLOT OUT
C----THE STRESS T12 AND TN1 AS A FUNCTION OF TIME.  THE SUBROUTINES
C----USED HERE ARE ALL EXPLAINED IN THE VERSATEC MANUAL SUPPLIED BY
C----THE VIRGINIA TECH USER SERVICES.
C----THE FIRST SERIES OF SUBROUTINES PLOTS OUT T12, THE SECOND SERIES
C----PLOTS OUT TN1 AS A FUNCTION OF TIME.
C-----------------------------------------------------------------------
      TIME(L1)=-100.
      TIME(L2)=100.
      T12(L1)=0.0
      T12(L2)=0.5
      CALL PLOTS(0,0,50)
      CALL PLOT(1.0,2.0,-3)
      CALL FACTOR(0.50)
      CALL AXIS(0.0,0.0,2H   ,-2,11.0,0.0,TIME(L1),TIME(L2))
      CALL AXIS(0.0,0.0,2H   ,2,10.0,90.,T12(L1),T12(L2))
      CALL LINE(TIME,T12,KOUNT,1,0,11)
      CALL VPISYM(5.5,-0.9,.30,17H( T&τIME, SECSη ),0.,17)
      CALL VPISYM(-0.7,4.8,.30,16H( &?G+/&τ?GSSη ),90.,16)
      CALL VPISYM(6.0,10.,.15,17HERICKSEN'S THEORY,0.0,17)
      CALL VPISYM(6.0,9.7,.15,17HSTRESS GROWTH:    ,0.0,17)
      CALL VPISYM(6.0,9.4,.15,17H&?C=1  &?K=1      ,0.0,17)
      CALL VPISYM(6.0,9.1,.15,17HINIT COND N2=1    ,0.0,17)
      CALL FACTOR(1.0)
      CALL PLOT(13.0,0.0,-3)
C-----------------------------------------------------------------------
C----NOW TN1 WILL BE PLOTTED OUT
C-----------------------------------------------------------------------
      TN1(L1)=0.00
      TN1(L2)=0.20
      CALL FACTOR(0.50)
      CALL AXIS(0.0,0.0,2H   ,-2,11.0,0.0,TIME(L1),TIME(L2))
```

```
      CALL AXIS(0.0,0.0,2H  ,2,10.0,90.,TN1(L1),TN1(L2))
      CALL LINE(TIME,TN1,KOUNT,1,0,11)
      CALL VPISYM(5.5,-0.9,.30,17H( T&τIME, SECSη ),0.,17)
      CALL VPISYM(-0.7,4.8,.30,15H( N1+/N1&τSSη ),90.,15)
      CALL VPISYM(6.0,10.,.15,17HERICKSEN'S THEORY,0.0,17)
      CALL VPISYM(6.0,9.7,.15,17HSTRESS GROWTH:    ,0.0,17)
      CALL VPISYM(6.0,9.4,.15,17H&?C=1  &?K=1      ,0.0,17)
      CALL VPISYM(6.0,9.1,.15,17HINIT COND N2=1    ,0.0,17)
      CALL FACTOR(1.0)
      CALL PLOT(2.0,-1.5,999)
      STOP
40    WRITE(6,45)IER,XEND
45    FORMAT(1X,'IER=',I5,'XEND=',F14.7)
      DO 55 I=1,N
       WRITE(6,50)N,Y(I),YPRIME(I)
50     FORMAT(1X,I4,2X,2(2X,F14.7))
55    CONTINUE
      STOP
      END
      SUBROUTINE FCN(N,X,Y,YPRIME)
      DIMENSION Y(N),YPRIME(N)
      GAMA=10.0
      DLAM=1.0
      YPRIME(1)=0.5*GAMA*Y(2)*(DLAM+1.0-2.0*DLAM*Y(1)**2)
      YPRIME(2)=0.5*GAMA*Y(1)*(DLAM-1.0-2.0*DLAM*Y(2)**2)
      YPRIME(3)=-1.0*DLAM*GAMA*Y(1)*Y(2)*Y(3)
      RETURN
      END
      SUBROUTINE FCNJ(N,X,Y,PD)
      DIMENSION Y(N),PD(N,N)
      RETURN
      END
```

The vita has been removed from the scanned document